University of Alberta

Multi-Failure Network Restorability Design in Survivable Transport Networks

By

Jude Chukwuelozonam Akpuh

A thesis submitted to the Faculty of Graduate Studies and Research
in partial fulfillment of the requirements for the degree of

Master of Science
In
Engineering Management

Mechanical Engineering

Fall 2009
Edmonton, Alberta

Examining Committee

1. Dr. John Doucette, Engineering Management, Department of Mechanical Engineering

2. Dr. Amit Kumar, Engineering Management, Department of Mechanical Engineering

3. Dr. Raymond Patterson, Accounting and Management Information Systems (AMIS)

Abstract

The Dual Failure Restorability (DFR) problems involve the design of network topology to be restorable in the event of single failure events, as well as dual failure events. We developed new *integer linear programming* (ILP) models to optimally design mesh topology networks with various survivability schemes, including span restoration, *p*-cycle, DSP and path restoration to achieve specified levels of dual failure restorability sought in the networks. The ILP models consist of two variations; the first model simply applies the limit of dual failure restorability sought in the network to each pair of spans in the network, and the second applies the limit of dual failure restorability to the average of dual failure restorability in the entire network. We performed the design experiments with about 137 test case networks, made up of four different network families, 10-node, 12-node, 15-node, and 18-node network families. The results shows that the capacity cost increases as the specified levels of dual failure restorability sought in the network increases and that the relative increase in capacity cost in sparsely connected networks is much higher than the highly connected networks.

Acknowledgements

I thank God for the opportunity and the strength He gave to me to do this work. My sincere appreciation goes to the following individuals who devoted their priceless time and resources to this work. First to my supervisor, Dr. John Doucette, thank you for your tireless support, the funding, exceptional guidance, and your encouragement throughout this program. To my dearest and loving wife, Ada and our beautiful kids; Shalom and Chibunnam, thank you, I could not have done this work without your unwavering support. I also want to thank my mother, Teresa Akpuh for her prayers and support. My appreciation also goes to my colleagues at the department of mechanical engineering and TRLabs; Chris Iyawe, Brody Todd, Brian Forst, Diane Onguetou, Aden Grue, Adil Kodian, Md Noor-E-Alam, Ahmed Kasem, Dimitri Baloukov, and, Ye Tang. To the entire staff of TRLabs, special thanks to Chris Hagen, Dave Clegg, Luke Chong, Rhoda Hayes and Linda Richens for the welcoming atmosphere at TRLabs. Finally I would like to say thank you to the department of Mechanical Engineering, TRLabs and NSERC for the scholarship awards I received towards this research project.

Table of Contents

List of Tables

List of Figures

Chapter 1

Introduction

1. Telecommunications Network Systems

A typical telecommunication network consists of interconnected nodes (routing and switching facilities), and a collection of links or physical connections (such as cables, twisted wires, fibre optics, etc.) over which traffic of various sources and types flows from origin nodes to destination nodes. The traffic may include voice, video, and data combined into packages often referred to as *demands* [1]-[6]. Telecommunication networks are categorized into *private networks* and *public networks*.

1.1. Private Networks

Private networks are privately owned networks, operated and managed by individual owners such as private organizations, companies, and schools (university campuses). In private networks, each workstation located in the network uses an allocated IP address within the private IP address spaces in their domain to gain access into the network. The use of facilities within such networks is highly restricted to users within the organization that owns the network; otherwise permission is required for access. An example of such a network is *local area networks* (LAN) [7]-[8]. A good example of LAN is the university campus LAN, operated within the university campus where access is restricted to university staff, students, and other guests permitted to use it. Other examples of private networks include *wide area networks* (WANs) [9]-[10], used to connect several LANs owned by one organization that are geographically separated. *Metropolitan area networks* (MANs) [11]-[12] can also be classified into the private network group, especially in the case where it is owned and operated by the same organization to connect various sites that operate in a large city.

1.2. Public Networks

Public networks are owned, operated, and managed by telecommunication carrier companies, (commonly referred to as service providers). They provide services to private networks and to the public on purely commercial terms. Public networks can be mapped geographically into three different parts; *long-haul networks*, *metro networks,* and *access networks* [13]-[15]. Long-haul networks (also known as inter-exchange networks) have trunk lines usually of much higher capacity, spanning over a much longer distance than other networks. Metro networks are also known as *metropolitan inter-office* networks; they are networks connected by what is generally known as *central offices* (COs) [16]-[17]. The COs are individually linked to various blocks of access networks. Metro networks usually have ring-like (cyclic) topologies and provide points of access between the long-haul networks and the access networks. Access networks, on the other hand, provide connections from private networks and residential subscribers to the COs. They usually have tree-like topology and are relatively sparse with a number of single node terminations and a large number of commercially based private subscribers. Figure 1.2.1, similar to the illustration in [17], shows the relationships between the various parts of public and private networks and their line of communication indicated by the arrow on top of the diagram.

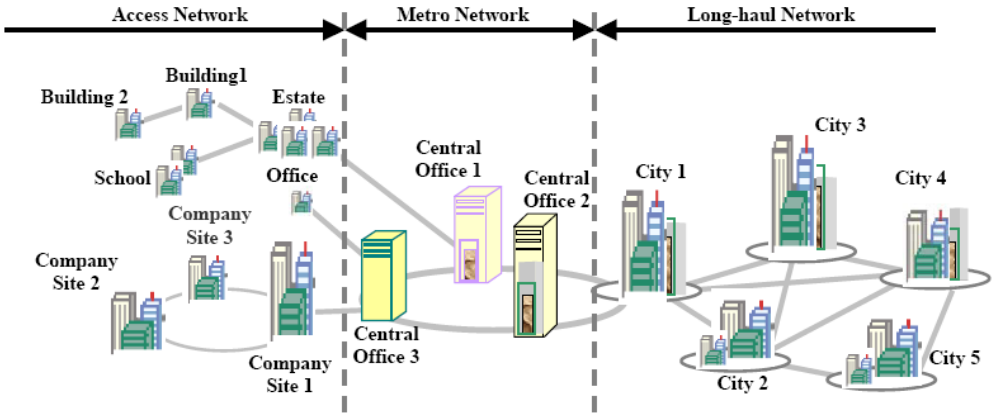

Figure 1.2.1-Various partitions of a public network and their line of communication.

The relationship between the three blocks shows that public networks provide long haul service paths for private networks through access networks. The primary role of the long-haul network is to provide means of transporting traffic

such as voice, data, and video from users (clients) in some private networks to other users in another geographical location; as such it is often referred to as a transport network.

A metro-network serves both access and long-haul networks. Traffic from various access networks merges at various COs at peering points known as *points of presence* (POPs) [17] which connect the sub-regions to the long-haul network (back-bone network). Similarly, long-haul networks of various countries access each other at peering points or *network access points* (NAPs) [17]-[18]. Communication lines between various cities are established through long-haul networks and, in the same manner, local areas and sub-regions communicate through metro networks. Traffic flows from access networks through metro networks into the long-haul networks and back to access networks in the same fashion. In this thesis, the discussion on telecommunication network systems is limited. Section 1.3 will briefly discuss the transport network architecture and its infrastructure, which is the core area of this work.

1.3. Transport Networks

A transport network is often referred to as the *backbone network* of the public telecommunication networks. Operated by telecom providers, transport networks are made up of nodal equipment comprised of multiplexing, switching, and routing devices such as IP routers, switches, *digital cross-connect systems* (DCS), *add-drop multiplexers* (ADMs) [19], etc., connected by a collection of optic fibre cables over which aggregated traffic types flow from origin nodes to destination nodes. These traffic types as indicated earlier may include voice, video, data, etc., and are often groomed to be transported through fibre optics to various destination nodes. The infrastructure and the framework of a transport network will depend largely on the transport technology or standard being deployed as well as the network type or function. However, the essential and the most basic function is to provide means of transmission for the different services at various layers of the network regardless of what technology is being deployed.

The earliest transport network was made up of twisted copper wires and was first invented as analog telephone, known as the *public switched telephone network* (PSTN) [19]. The copper cables were specifically dedicated to one voice channel, spanning over a long distance for transmitting the analog voice signal from one point to another. Over the past years, transport networks have undergone a number of evolutionary processes resulting in more sophisticated and intelligent transport networks. They have developed to form the framework for the next generation network. Some of this advancement is driven by the need to satisfy the growing demands for telecommunication network services such as the Internet, enormous multi-media applications transmissions, and even voice and other data connections. In surveys conducted in 1993 and 2000 by the Internet Software Consortium (ISC), the numbers of host computers were 1,313,000 and 72,398,098 respectively. By July 2008, this figure had jumped to 570,937,778 [20]. It is partly the transport network system that has expanded the potential for sustaining the growth, for example through the development of fibre optic cable. This has led to many advances that enable transport networks to address some of the bandwidth issues and availability problems.

Frequency division multiplexing (FDM) [21]-[22] systems were first ushered in during the era of digital transmission services. With FDM, multiple voice signals are combined by assigning each to a different signal frequency within a particular bandwidth and transmitting them over a single line or channel. Digital transmission mechanisms were an important development in the transport network system. They provided more capabilities to users and improved the quality of transmission as analogue signals degraded over a long distance due to signal-to-noise ratio problems during amplification [22]**.** Other significant developments include switching, routing, network control technologies, and broadband architectures such as *synchronous optical networking* (SONET)/*synchronous digital hierarchy* (SDH), IP, *multi-protocol label switching* (MPLS), and *asynchronous transfer mode* ATM [18]-[19] have been instrumental to the enhancement of the transport network system. In general, a transport network can be partitioned into 2 layers, the physical layer and the logical layer (virtual layer).

In section 1.3.1 the two parts and their relationship in terms of function is discussed.

1.3.1. Physical and Logical Layers of Transport Networks

The nodes (buildings containing the nodal equipment such as the routers, switches, etc.) and the actual fibre conduit connections (the ducts) represent the physical layer of the transport network. In the logical layer, there are no actual connections between some of the nodes; rather, connections are logically established through the switching devices in the physical network. The number of logical layer connections in the entire network can be expressed as $c = n(n-1)/2$ [18], where c is the number of logical connections and n is the number of nodes in the network. Figure 1.3.1 shows typical connections in both layers and the mapping of logical layer on physical layer. The links between nodes in the physical layer are the actual fibre optic cable infrastructure and are represented by solid dark lines as shown in Figure 1.3.1(*a*), while the logical layer paths on the same network are indicated by dashed gray lines in Figure 1.3.1(*b*). Figure 1.3.1(*c*) shows how logical links are mapped on physical connections.

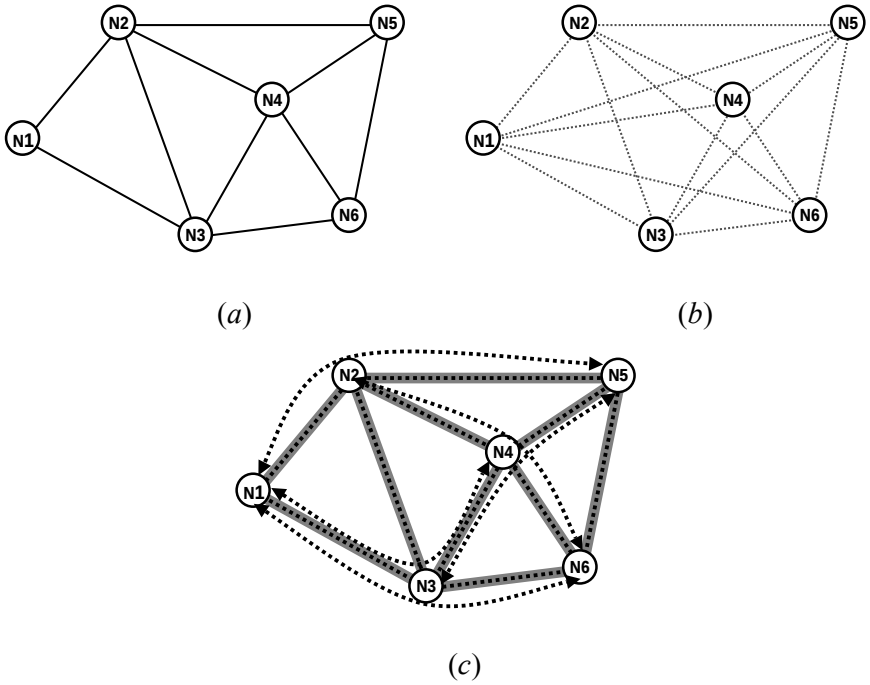

Figure 1.3.1-Physical and logical layers of a transport network.

In the logical layers, the logical connections appear to be directly linked between each pair of nodes but in reality these links are actually established through physical links in the physical layer. The physical layer is dedicated to network transport operations by performing cross connections, switching, and multiplexing services at this layer. This layer links the service network layer to the actual physical media layer. The concept of network survivability by rerouting failed spans and network protection is actually implemented at the layer. This thesis focuses on network restoration and survivability in the event of multi-failure scenarios. In the service network, various types of services can be aggregated into what is referred to as the *demands* to be served by the physical network. A demand unit translates to the actual transmission capacity (lightpath) requirement between a pair of nodes in the network. Each service network depends on the function and type of services provided. However, regardless of the type of service, the traffic is groomed and served by the transport network layer.

1.3.2. Transport Network Framework and Infrastructure

As mentioned in the previous section, there exist several layers in the service network and the transport network and each of the layers in the service network could offer a different type of service and in turn be served by another layer in the network. The types of services offered by a particular layer depends on the network functions and the technologies deployed within the transport network; for example, IP networks serving data, ATM networks used to serve voice and data through packet-switching networks, SONET applies to standardize incompatible optical networking technologies, to create a level of compatibility necessary for various transport network applications and equipment vendors to interface and function effectively, and *wavelength division multiplexing* (WDM) provides channels by multiplexing through which demands flow through the physical fibre. Several of these layers can be stacked upon each other where the layer on top is being served by the layer below and vice versa; for example, IP over ATM over SONET over WDM over Fibre [19] and [23]**.** In general, transport networks based on these technologies are classified into two main types: *packet-switched* transport

networks and the *circuit-switched* transport networks. In circuit-switched networks, a dedicated point-to-point connection is required to establish communication between users. This requires a fixed channel (bandwidth) connection between the users until the users terminate the communication line. These systems are predominantly used to serve public telephone systems and most recently are used to serve other types of digital data. Examples of transport network technologies based on circuit-switch networks are the *time-division multiplexing* (TDM) and the WDM. On the other hand, in packet switched networks, data traffic is split into small chunks called packets that are routed through various paths to the destination nodes. The packets are designated by labelling to specific destination nodes and upon arrival at these nodes; the packets are reassembled to the original form (sequence) as dispatched. This system is not very suitable for highly delay sensitive applications. Examples of packet switched transport networks technology are the ATM and MPLS.

1.4. Set Theory

This section describes some of the basic mathematical notations and concepts used in this thesis to implement the mathematical models. Details of these notations and concepts can also be found in [24]-[26]. We begin with set theory; a *set* is a group of unordered objects called *elements*. A set is considered special if all the elements in the set have unique ordered positions in the set. In most of this thesis, a set represents a group of unordered objects or elements. These elements often share common properties. A set S containing elements *s1*, *s2*, *s3, s4,* and *s5* can be written mathematically as $S = \{s1, s2, ..., s5\}$. To indicate that an element such as *s1* is a member of the set *S*, we use the notation $s1 \in S$. Similarly, $\notin$ indicates that and element is not a member of the set *S*, as in $s1 \notin S$. *S* can also be an empty set with no elements. If we index every element of the set *S* with *s* we can use the symbol $\forall$ to refer to every element of that set, such as $\forall s \in S$, which means "for each element *s* of the set *S*." This is often used to express mathematical operations applied to all members of the set. Two logical notations widely used in this thesis are | and:, both effectively meaning "such that." These

notations can be used to express logical or conditional value assignments to the elements in the set. For example, the expression $\forall s \in S \mid s \neq 1, s \geq 5, s = s^2$ is read as ''for all elements *s* of set *S*, such that *s* is not equal to 1, *s* is greater than or equal to 5, and *s* is equal to s^2. The cardinality $|S|$ of the set *S* represents the number of members in the set. For example, $S = \{s1, s2, ..., s5\}$ has cardinality $|S| = 5$; an empty set will have zero cardinality.

Some basic set operations can be performed on two or more sets; these include intersection, union, and complementation. Two sets are said to be equal if they contain the same and equal numbers of elements. The intersection (represented by $\cap$) of two equal sets is a set containing the elements that are common to both sets. For example sets X={2,4,6,8} and Y={8,6,2,4} are equal since the elements in these sets are the same and equal. This implies that X=Y. On the other hand, if two sets are not equal then $X \neq Y$. Other relationships between sets and common operations performed among them can be found in [25]. This discussion has been limited to the set theory used in the thesis, that is, the basics of set theory. More details on set theory and operations can be found in [1] [24]-[26].

1.5. Mathematical Programming and Optimization Notations

Mathematical programming and optimization methods have long been decision-making tools applied in systems design, including the design and optimization of telecommunication networks. In the case of network design, the primary objective is to invest minimal resources to achieve optimal design. *Linear programming* (LP) is a mathematical programming method used to solve network optimization problems. *Integer linear programming* (ILP) and *mixed integer programming* (MIP) [1] are classes of LP. We used ILP optimization to solve our network problems. The problems are formulated by building a *mathematical model* using *a mathematical programming language* (AMPL) [19], and then the model is applied to individual network topology. Typical LP problem formulations are made up of a set of linear equations with two distinct parts, the objective function and the

constraints. A general representation of a linear programming model similar to the expressions in [17] and [19] is as follows:

Maximize (or Minimize): $f(x_1, x_2, ..., x_n)$ (1.5.1)

Subject to:

$f_i(x_1, x_2, ..., x_n) \le c_i \qquad \forall i = \{1, 2, ..., m\}$ (1.5.2)

The expression above can also be written in algebraic form as shown below:

Maximize (or Minimize): $\sum_{\forall i \in \{1,2,...,n\}} a_i \cdot x_i$ (1.5.3)

Subject to:

$\sum_{\forall i \in \{1,2,...,n\}} b_{i,j} \cdot x_i \le c_j \qquad \forall j = \{1, 2, ..., m\}$ (1.5.4)

$0 \le x_i \ge d_i \qquad \forall i = \{1, 2, ..., n\}$ (1.5.5)

Equation (1.5.1) and (1.5.3) represent objective functions, maximized or minimized as the case may be. The variables are represented by $\{x_1, x_2, ..., x_n\}$. Equations (1.5.2) and (1.5.4) represent constraints. The constants are a_i, $b_{i,j}$, c_j, and d_i. Equation (1.5.5) indicates the bounds set for each variable if required. Typically in ILP problems, all the decision variables are restricted to integer values and in MIP problems the decision variables are a mixture of integers and real numbers. For more details on LP, the reader is referred to [1].

1.6. Network Graphs

As defined in section 1.1, a typical network comprises a set of nodes and spans through which demands flow from the origin node to the destination node(s). A transport network is a type of graph where the vertex is a node and the span (edge) is a link or channel between two nodes. In simple terms, a graph G, is made up of a set of vertices V, and a set of edges E, and is denoted by $G = (V, E)$, where $V = \{v_1, v_2, ..., v_{|v|}\}$ and $E = \{e_1, e_2, ..., e_{|E|}\}$. The edges of a graph are often weighted and the weight could be cost, lengths, or demands (the amount of flow) on an

edge [27] [28]. In this thesis, the weight on each span is expressed in terms of cost and capacity. The unit cost on each edge is proportional to the length (Euclidean distance) of the span and the capacity represents both working and spare capacities. Figure 1.6.1 shows a simple graph with $|V|=6$ and $|E|=10$.

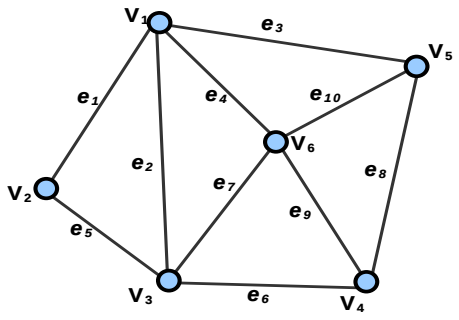

Figure 1.6.1-A simple network graph.

In Figure 1.6.1, the vertices are $V=\{v_1,v_2,...,v_6\}$ and the edges are $E=\{e_1,e_2,...,e_{10}\}$. In transport network terms, if an edge $e=\{(v_1,v_2)\}$, v_1 denotes the origin node often known as the *source* and v_2 represents the destination node also known as the *sink* [1] or vice visa. A directed graph means that an edge can also be represented by a set of two ordered vertices adjacent to it in the graph. Some transport networks are considered directed simply because the edge is specially weighted and flows (commodities) between a pair of nodes that can only be unidirectional. However, in the context of this work, the network graphs are considered to be undirected, meaning that any set of the two vertices are not necessarily ordered A vertex (node) can be connected to more than one edge (span). The degree of a node, denoted by d is the number of edges connected to it; for example, the degree of node i is d_i. The average of all the node degrees of individual nodes in the network is known as the *average nodal degree*, $\bar{d}$ of the network. Average nodal degree is an important parameter in determining how densely or sparsely connected a network is and some of the behaviours of the network in terms of capacity efficiency can be predicted using this metric.

1.7. Thesis Outline

In chapter 1 the basics of telecommunication networks is discussed, with a brief description of the framework and the infrastructure of transport networks. Brief definitions of some of the network terms and concepts, such as set theory, graph theory, and network optimization methods are presented.

The concept of network survivability, single failure scenarios, and different classes and types of survivability schemes that can be deployed in a typical transport network are discussed in chapter 2. *Automatic protection switching* (APS) is described, including 1+1 APS, 1:1 APS, and 1:N APS. Two types of survivable rings are described: *unidirectional path-switch rings* (UPSR) and *bi-directional line-switch rings* (BLSR). Regarding mesh restorable networks, we discuss *span and path restoration mechanisms*, *demand-wise shared protection* (DSP), and *p*-cycles. A literature review of the topics covered in the thesis, and the motivation for and objectives of this work are also presented in chapter 2.

Chapter 3 covers part of the core subject of the thesis, dual failure restorability design in a survivable transport network. Dual failure restorability as applied to some the different survivability schemes is discussed in chapter 3. A brief introduction to dual failure categories with illustrations and an example within each survivability scheme is presented and the network ILP design models developed for some of the mechanisms are described.

In chapter 4 we discuss the experimental set-up, simulation, and the results that are presented. We also briefly discuss how our network topologies are formed, limitations of the size of eligible routes enumerated for each demand pair in the network, and demand matrix. In chapter 5 we discuss the how results obtained from various restoration mechanisms are compared and the validation of results from span and path restoration, *p*-cycles, and DSP is explained.

A comparative analysis of dual failure restorability results in the four restoration mechanisms are discussed in chapter 6. These include side-by-side comparison of span restoration, and *p*-cycle networks as span-based restoration mechanisms, and path restoration and DSP networks as path-based restoration mechanisms.

In chapter 7 we draw the conclusions and highlight some of our contributions. We also discuss our findings, the limitations of this work and the future directions.

Chapter 2

Network Survivability

2. Concept of Network Survivability

This chapter briefly reviews the concepts of network survivability and how the restoration mechanisms of the different survivability schemes function. This may be important to readers who are not familiar with this subject area. This chapter provides a basic understanding of the fundamentals of restoration or protection mechanisms of the schemes before ILP model formulations are introduced in chapter 3. The overview focuses only on the survivability schemes of interest in this work.

Network survivability is the ability of a network to continue to function in the event of failure, by using restoration or protection mechanisms to restore demands that are affected by the failure [29]. Survivability in transport networks is one of the most important considerations in the design of a transport network. In recent years, the number of subscribers to telecommunication services provided by transport networks has more than quadrupled [20]. Telephone, the Internet, video, and other data transmission vehicles have experienced an unprecedented increase in the number of user applications, thus the impact of service disruption has become more significant. To reduce or eliminate the impact of failure, networks are designed with restoration mechanisms. Network failures may include software failures, node failures, and span failures. In this thesis, single span failures and dual span failures in the physical layer are considered. Single span failure occurs when only one span fails at a time. In dual failure, failures of two spans occur in an overlapping time frame, that is, a second span failure occurs before a first failed span is repaired, resulting in two simultaneous failures. In the absence of active survivability mechanisms in place to restore demands across failed spans, single and dual failures often result in network outages. In this chapter, restoration mechanisms for single span failures are considered; in chapter 3 dual span failure

restorability design models are discussed. Triple failures will not be discussed, as such failures are considered uncommon. The probability of triple failure is relatively very low compared to dual failure and single failure scenarios [17]. Some of the mechanisms typically used for single failure survivability are introduced in section 2.1.

2.1. Classification of Network Survivability Schemes

There are two classes of network survivability mechanism; *pre-connected, or pre-configured*, *survivability mechanism*, and *restoration mechanism* [18]. A pre-planned or pre-configured survivability mechanism, or *protection mechanism*, consists of a dedicated spare capacity already in place that will direct routing of demands flow over a failed span. Pre-connected backup channels specifically provide for restoring specific primary working channels before the actual failure occurs. In the event of failure, the dedicated backup channels are immediately activated or switched on to restore flows on the failed link. In a *restoration mechanism*, enough spare capacity is available at any point in time to dynamically accommodate any request for backup channels in the event of failure. Single or multiple backup channels can be shared by numerous primary working channels depending on the order and time of failure, which working routes are affected, and which backup channels are available for use. A restoration mechanism requires a little more time than a protection mechanism to determine which backup channels are available for restoration of a failed link. Hence, a restoration mechanism usually requires a longer restoration time than a pre-configured protection mechanism, and the difference in restoration times can be significant [18]. Activation of protection and restoration mechanisms can be managed in a centralized controlled system or within the locality of the specific span failure. Local management allows a shorter restoration time. After restoration, the system updates the entire network with the reconfigured routing protocols.

Some of the survivability schemes developed to date include *automatic protection switching* (APS) 1+1, 1:1, 1:N, and M:N APS as in [18] [29] [30], *survivable rings* [18] and [31]-[35], and others deployed in a mesh restorable network such

as *span restoration*, *path restoration*, *shared backup protection path* (SBPP) *demand-wise shared protection* (DSP) and *p*-cycles [18]. APS systems and survivable rings are considered briefly in sections 2.2 and 2.3, respectively, while mesh restorable network survivability schemes are discussed in more detail in section 2.4.

2.2. Automatic Protection Switching (APS)

1+1 APS is one of the earliest and the simplest forms of protection mechanism. It is made up of two disjoint paths, one serves as the primary working channel and the other serves as a dedicated backup channel [29] [30]. Both channels carry live signals in a bridged state ready to be switched when failure occurs. APS is considered to be one of fastest switching mechanisms in terms of restoration time [18] [36] but requires at least 100% capacity redundancy. 1:1 APS is similar to 1+1 APS but the backup channel for 1:1 APS does not transmit live signal in a bridge state. Also, 1:1 APS can be used to carry lower priority signals when not in use for restoration of the working channel [18]. This means that in the event of failure, the working channel has to be switched to the backup channel. Hence restoration is slightly slower for 1:1 APS compared to 1+1 APS.

1:N APS is a protection arrangement closely related to 1:1 APS. In this case a single backup channel is provided for a number of primary working channels. In other words, any of the working channels reserves the right to use the backup capacity (single spare channel) in the event of failure. Upon a span failure in any of the primary working channels, the receiving end signals the transmitting end with a request for a head-end-bridge of the failed working channel to the backup channel. Finally, M:N APS is similar to 1:N APS, but in this case M backup channels are shared by N working channels. In M:N APS, the number of backup channels is typically less than or equal to the number of working channels (i.e., $M \leq N$).

APS systems are limited to restoring single failure situations, except in some configurations with M:N APS.

2.3. Survivable Ring Networks

Survivable rings are a more advanced form of restoration mechanism compared to the APS mechanisms described above. They are pre-connected cyclic structures of two types: *unidirectional path switched rings* (UPSR) and *bi-directional line switched rings* (BLSR) [18] and [31]. In the UPSR, two disjoint and equally capacitated paths are required between each pair of nodes; one path serves as primary working channel and the other as the spare capacity channel. The working signal is transmitted in one direction while a copy of the signal is transmitted in the opposite direction by the protection path. The BLSR is a more efficient type of survivable ring than the UPSR. In the BLSR, there are two pairs of bi-directional links between each pair of nodes. One pair is designated working channels and the other pair is used as protection channels. Upon failure of a link, signals from the working channels are looped back into the protection channels at the adjacent nodes of the surviving portion of the ring through the use of *add/drop multiplexers* (ADM) at the nodes. The BLSR has an advantage over the UPSR in the sense that the channels in the BLSR can be reused around the ring while that of the UPSR cannot. Survivable rings are typically used in metro area networks that are dominated by nodal equipment such as ADMs. For more details on survivable ring networks the reader is referred to [18] and [31][36].

2.4. Survivable Mesh Networks

In a mesh restorable network, the physical topology (the distribution of nodes and links) and the degree of connectivity between adjacent nodes make it possible for diverse routing alternatives between each pair of nodes. This advantage enhances the cost effectiveness of both working and spare capacity placement in the network, and as a result, the network routing is more efficient and redundant. The survivability schemes that can be implemented in a mesh network include span restoration, path restoration, demand-wise shared protection (DSP), *p*-cycles, shared backup path protection (SBBP), and quite a few more that are beyond the scope of this thesis.

2.4.1. Span Restoration

In span restoration (SR), restoration routes are optimally distributed between the end nodes of each span bearing working capacity. Upon failure of a span, the restoration mechanism uses the spare channels provided for that span to restore the demands on the failed span [19] [37] [38]. Figure 2.4.1 illustrates how the span restoration mechanism works. As shown in Figure 2.4.1(*a*), upon failure of span (N3-N4), the restoration mechanism uses the available restoration channels for the span (N3-N4) to restore the demands on it. In this case, as shown in Figure 2.4.1(*b*), the demands on the failed span (N3-N4) are rerouted through the available spare channels (N3-N2-N4 and N3-N5-N4) between the end nodes of the failed span.

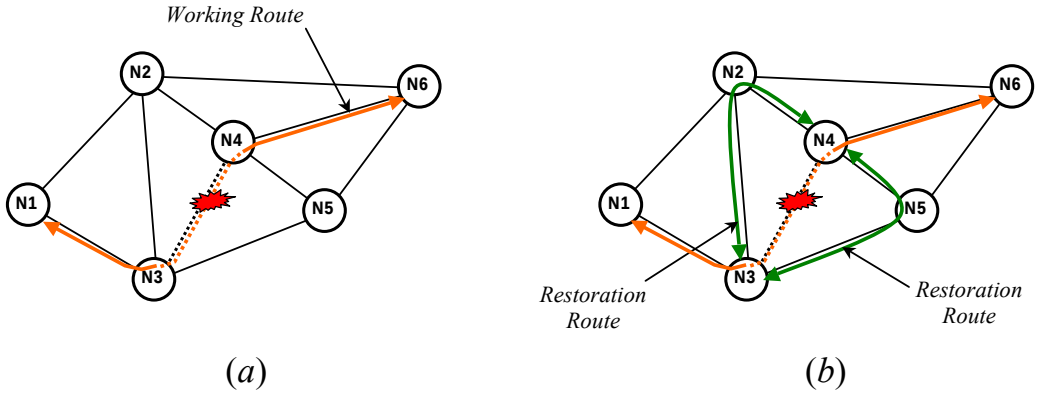

Figure 2.4.1-Span restoration mechanism.

As mentioned in section 2.1, the restoration mechanism can be controlled via a centralized management system or by a distributed local control system. The centralized control system requires less resources and regular updates of network protocol system but has longer restoration time. While in the distributed control, the restoration process is managed locally [19], the mechanism benefits from faster restoration time but requires more resources and regular updates of the entire network system protocols.

2.4.2. Path Restoration

Path restoration (PR) is an end-to-end path restoration mechanism. Restoration is achieved through complete rerouting of the failure-affected lightpaths. The

restoration paths used for each failed lightpath are routed between the origin and destination (O-D) nodes of the lightpath. The restoration paths formed isolates the failed span. The path restoration mechanism is also called *failure-dependent path protection* (FDPP) [39] [40]. The basic design of a path restorable network is similar to the *multi-commodity maximum flow* (MCMF) type of transport network where numerous end-to-end (O-D) primary paths bear the total demand units [19]. Figure 2.4.2 illustrates the path restoration mechanism. In Figure 2.4.2(*a*), failure of the span (N3-N4) results in failure of the entire lightpath (N1-N3-N4-N6). Figure 2.4.2(*b*) shows the restoration paths (N1-N2-N4-N6) and (N1-N3-N5-N6) used for restoring the primary working route (N1-N3-N4-N6).

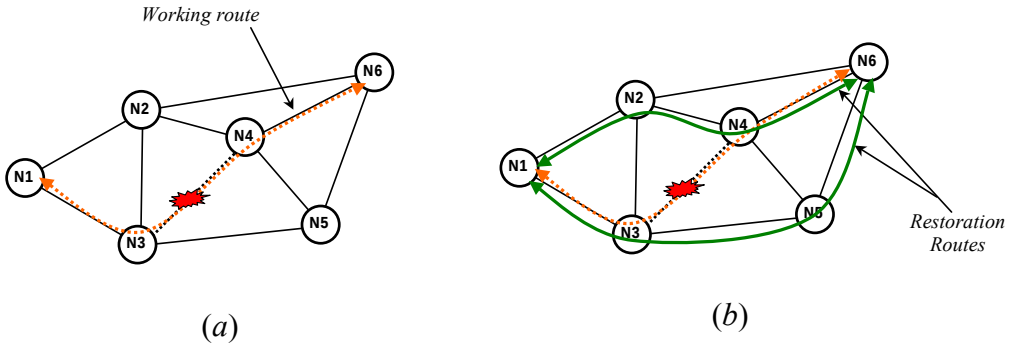

(*a*) (*b*)

Figure 2.4.2-Path restoration mechanism.

As seen in Figure 2.4.2(*b*), portions of the surviving stub (N1-N3) and (N4-N6) are reused as part of the restoration paths for the failed span by (N1-N2-N4-N6) and (N1-N3-N5-N6), respectively. The reuse of the surviving stubs in the affected working channel is enabled by a mechanism called *stub-release*. For more information on path restoration and stub release the reader is referred to [18] and [19].

2.4.3. *p*-Cycles

p-cycles are ring-like cyclic structures of spare capacity placed within the network to provide restoration routes for failed spans [18]. *p*-cycles are similar to survivable rings but different in that they have some features and capability that the rings do not possess. First, *p*-cycles combine the capacity and efficiency for restoration of mesh restorable networks and the switching speed of survivable

rings; second, the configuration of *p*-cycles enables them to provide restoration paths for *on-cycle spans* (spans that are on the *p*-cycles), as well as providing two restoration paths for the *straddling spans* (spans whose end nodes are on the cycles). While restoration in rings is limited to the spans on the rings, the *p*-cycle is capable of providing two units of capacity for the failed straddling span without the straddling span itself bearing any spare capacity. Figure 2.4.3 illustrates a typical restoration process in a *p*-cycle network. Figure 2.4.3(*a*) shows two *p*-cycles, (*p*-cycle 1: N1-N2-N3-N4-N5-N6-N7 and *p*-cycle 2: N4-N5-N6-N7-N8-N9) used to protect the network from failure. When an on-cycle span (N1-N7) fails, affecting any lightpath through the span and *p*-cycle 1 as shown in Figure 2.4.3(*b*), a restoration path is formed by the surviving part of the *p*-cycle 1. Affected lightpaths are inserted into the surviving portion of the *p*-cycle through the end nodes of the failed span, rerouting the demands the nodes of the failed span.

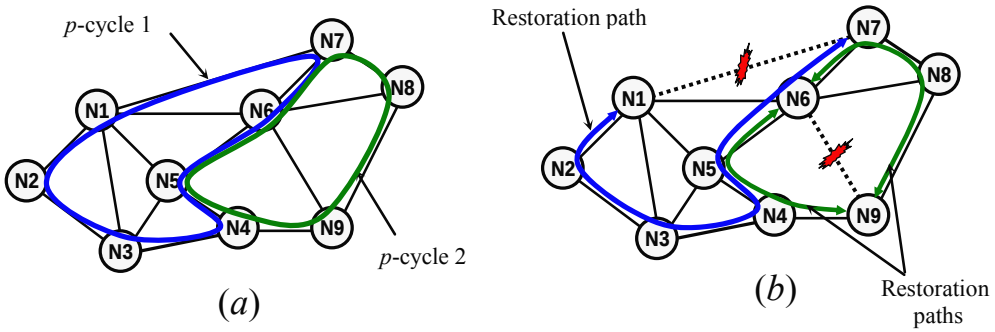

Figure 2.4.3-An illustration of *p*-cycle restoration mechanism.

When the straddling span (N6-N9) relating to *p*-cycle 2 as shown in Figure 2.4.3(*b*) fails, two (2) restoration routes, (N9-N4-N5-N6) and (N6-N7-N8-N9), are formed between the end nodes of the failed span, each capable of restoring a unit capacity of the demands on the failed span. This feature provides the *p*-cycles with the advantage of achieving better capacity redundancy of less than 100% in mesh restorable networks [18].

2.4.4. Demand-Wise Shared Protection (DSP)

Demand-wise shared protection is a pre-configured protection mechanism in which a single backup route is designated solely for restoring a number of diverse

working routes of a particular demand relation [41]-[43]. The primary working routes as well as the backup route for each demand relation are required to be completely span-disjoint routes. DSP is very similar to the design of 1:N APS or M:N APS systems, except that the term 1:N APS is used for single-hop routes while DSP can apply to multi-hop routing between the O-D nodes [42]. Figure 2.4.4 illustrates a typical DSP network. Figure 2.4.4(*a*) and Figure 2.4.4(*b*) show 9 and 10 demand units, respectively, exchanged between O-D nodes (N1-N9). Three working routes (N1-N2-N7-N9), (N1-N6-N9), and (N1-N4-N5-N9), and a backup route (N1-N3-N8-N9) are used to route and protect the demand units in each network. In DSP network design, a minimum of 1 and a maximum of $\overline{d}$ -1 disjoint working routes plus a single disjoint backup route is required for 100% single failure restorability. In the Figure 2.4.4(*a*), three ligthpaths are routed on each of the three working routes to serve the nine demand units. In Figure 2.4.4(*b*), four lightpaths are routed on one of the three working routes and three lightpaths are routed on the other two working routes.

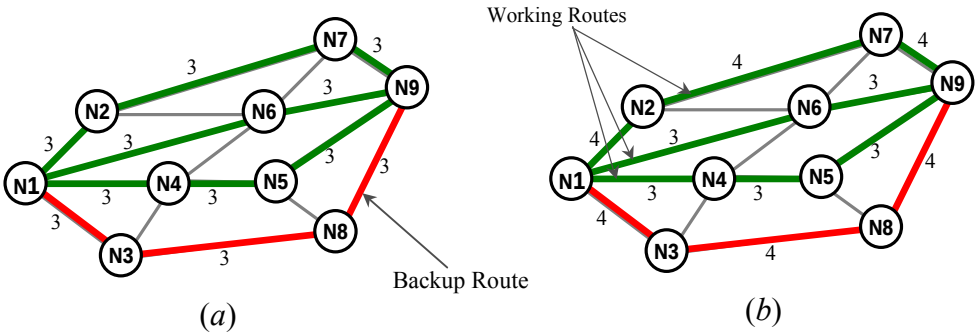

Figure 2.4.4-DSP protection mechanism.

The backup route is strictly reserved for any of the working routes in a particular O-D demand pair, so that when a working route fails, the backup route switches on to restore the demands on the failed working route. The backup route must be assigned sufficient capacity to restore the maximum flow on any of the working routes. DSP is more efficient in networks with higher connectivity than in the lower connectivity networks, since the number of disjoint routes between O-D pairs depends on the nodal degree of each node along various OD paths.

2.5. Prior Work on Dual Failure Restoration

Most of the earlier work on network survivability, particularly in the physical layer, focused on single failure survivability. Later work on restoration mechanisms included node failure protection and other multi-layer protection mechanisms, and some of the restoration mechanisms described earlier in this chapter. Others include those in [44]-[47]. Even with advances in the design of single failure survivable networks, there is still a lot of work to be done to address other types of failure such as dual failures. Very few reports have been published to date in the area of dual failure restorability. Most of these works focused on span-restorable networks and on *p*-cycle networks; one of the earliest is [48]. This work proposed a design formulation for a span restorable network based on an ILP method to provide sufficient spare capacity placement for dual failure restorability. But detailed work was required to determine the extent of spare capacity savings relative to single failure design based on the same ILP method. Other more extensive work on dual failure restorability in span-restorable networks is found in [49]-[51]. This work examines the capacity requirement for complete dual failure restorability using a number of variations in the design formulations. It found that the cost of fully protecting a network from dual failure could be three times the cost of single failure protection. In [49] a specified limited budget is used to determine the maximum value of dual failure restorability, R_2, achievable with the available budget. Another variation of the model finds the minimum cost of spare capacity on demand basis for different classes of services which range from "best-effort-only" for any failure to 100% dual failure restorability. The work was implemented on a span-restorable network and R_2 is defined as dual failure restorability on a given pair of spans i and j when both spans fail and is expressed as: $R_2(i,j) = 1 - \frac{N(i,j)}{w_i + w_j}$, where $N(i,j)$ is the number of non-restorable working capacities under the dual failure of spans i and j; w_i and w_j represent the working capacity on span i and span j, respectively. However, our approach defines dual failure restorability according to [52].

In [53], another work based on span-restorable networks is an extension of [54] and [55]. This work studied the performance of *active restoration* (AR) and *path-based protection* (PBP) schemes by presenting the blocking and the restoration behaviours of the two schemes. From the findings, the proactive protection and the active restoration schemes do not guarantee 100% dual failure restorability. In comparison, the active restoration scheme results in higher restorability with the advantage that the method significantly reduces the probability of blocking. In [56] [57], the sub-graph routing method is used to improve dual failure restorability, and a model is developed for 100% single failure restorability while maximizing dual failure restorability up to 95-99%. The work evaluated a mesh-restorable WDM network using sub-graph routing in the event of dual failure scenarios, and found that the network can withstand a complete dual failure event and that the sub-graph routing can achieve inherent dual failure restorability up to 72%-81% with this method. But this does not guarantee 100% dual failure restorability for all the pairs of spans affected by a dual span failure in the network. Neither of the two approaches used in [56] [57] (*the proactive sub graph fault tolerance* and the *reactive sub-graph fault tolerance*) can provide 100% dual failure restorability. It is recommended that complete dual failure restorability can best be achieved by a combination of the two mechanisms.

With respect to demand-wise shared protection mechanisms, [58] is one of very few reports on DSP design for dual failure restorability. The work in [58] analyses the level of dual failure restorability inherent in a DSP network design for 100% single failure restorability. According to [58], DSP offers dual failure restorability up to about 86% when optimally designed for protection against a single failure scenario. The advantage may be attributed to diverse routing of the working channels over several disjoint paths in DSP such that failure affecting any given pair of spans would leave some working channel(s) surviving.

With respect to the *p*-cycle networks, a number of reports deal with dual failure restorability; one of the most recent is [59] and part of this thesis is based on this work. The design approach implemented in [59] suggests that high dual failure restorability can be achieved in a network optimally designed for 100% single

failure restorability, or at most minimal capacity can be added to assure 100% dual failure restorability. A similar approach was implemented in a span-restorable network [51]. This work considers two strategies, one with optimized *p*-cycles permanently placed in the network and the other with the *p*-cycles dynamically reconfigured after the first failure to generate a new set of *p*-cycles that can be used to protect other spans from subsequent dual failures. Both approaches show significant improvement in dual failure restorability, but still, up to 70% more capacity investment is required to guarantee 100% dual failure restorability. In [60] the model developed achieves the desired dual failure restorability class for individual demands in the network. The work follows the approach used in [51] but is implemented in the *p*-cycle network for a range of *quality of protection* (QoP) classes. The QoP classes include platinum, where working channels in the class are assured dual failure and single failure protection. Gold is assured a single failure, silver is best efforts only and bronze is not protected. While this classifies working channels in the QoP class, and provides different QoP services for the individual demands, the work in this thesis considers all working channels affected by failure in a pair of spans and guarantees the desired level of dual failure restorability. This ensures that a uniform level of R_2 is maintained across the networks over all the demand relations. Some of the new ILP design models, for example [52] and [61], consider a specific pair of spans for various dual failure protection relationships with the *p*-cycles. Optimal *p*-cycle assignments are then found to meet user specified minimum dual failure restorability. The primary difference between [52] and [61] is that dual failure restorability is defined differently. The difference is that a particular dual failure scenario, often considered non-restorable, can now be considered restorable under certain conditions where the spans affected by failure have common working channels and *p*-cycles crossing the spans. Both methods show a significant improvement in the dual failure restorability value using equivalent capacity investment for a network designed for 100% single failure restorability. Also, findings from these works show there is about 30% inherent dual failure restorability advantage in a network designed for 100% single failure

restorability. The work on *p*-cycles in this thesis is an extended version of the work in [52].

2.6. Motivation and Objectives

In the past, emphasis was placed on designing networks for single failure restorability, often denoted by R_1, with the assumption that the probability of dual failure occurrences was low. But with the recent and frequent occurrences of dual failure events across various networks, interest from the industry and recent publications suggests that awareness is growing of the importance of designing networks for dual failure protection. Over the years, the transport network system has become more sophisticated. But with the advent of new technologies and standards to make the networks more efficient and interfaces more compatible, and even with wide a range of new survivability schemes, network failures are still very frequent. As a result, outages are experienced from time to time. For example, in January 2008, a major failure on the fibre optics trunk line known as SeaMeWe-4, running across Europe from the Mediterranean to South-East Asia, caused major outages that affected a number of countries [62] and [63]. Here in Canada, the Canadian public CA*net 4 experienced more than a dozen major outages between February 2009 and May 2009 alone [64], averaging about three per month for single failure scenarios and a few dual failure events over the same period. Findings in the analysis of service path availability in a mesh restorable network [50], indicate that the major contributor to network unavailability is dual failure. This is an indication that designing a network to withstand dual failure events will result in significantly higher network availability values over time. Dual failure occurs when two spans fail simultaneously in an overlapping time frame. Other causes include scenarios such as maintenance operations on a span coinciding with a failure of another span [65] and *shared risk link groups* (SRLG), where failure of a physical span-duct shared between two or more separate spans (logically separated spans) can result in dual failure-like situation [66]. The cost of such failure can be enormous, ranging from severe disruptions in emergency services to huge economic losses in banking transactions. Because of the impact

of failure on critical network services, some network operators are required to meet a specified level of *network availability* and *quality of services* (QoS) as part of the *service level agreement* (SLA). The goal of this work is to design network models with optimal capacity investment that will be protected, or can be restored, from single or dual failure events. Such networks can be designed to provide specified levels of dual failure restorability for the network as a whole, thus providing assurance to network operators that certain levels of dual failure restorability are guaranteed in the network upon failure of any pair of spans at any point in time. The designs will also allow the operator to make decisions based on affordability. For example, if an operator cannot afford to invest in the total capacity required for 100% dual failure restorability, the operator could choose a capacity he can afford based on the cost of dual failure restorability. Since dual failure has direct impact on the availability of the network, the models will be designed to enhance the availability value of the networks. We will also review the general characteristics of different network sizes under dual failure scenarios and analyse how the cost of providing dual failure restorability will vary with each restoration scheme. We hope to determine which restoration mechanisms perform better in terms of total capacity efficiency (spare capacity relative to working capacity) in the network.

Chapter 3

Dual Failure Restorability[1]

3. Dual Failure Restorability Design

In this chapter there is a brief description of dual failure restorability design pertaining to the restoration mechanisms discussed in chapter 2. Dual failure scenarios in each of the restoration mechanisms and the formulation of the models are also discussed. Also, ILP models are introduced, notations for the models are described, and dual failure design models are formulated.

Efficient network dual failure restorability design ensures that sufficient and optimal spare capacities are distributed over the network to provide restoration channels for dual failure situations. Methods used to design dual failure restorable networks include linear programming (LP) [1] and pure *heuristics* and *meta-heuristics* algorithms such as the *simulated annealing* (SA) [67], *tabu search* (TS) [68], and *genetic algorithms* (GA) [69]. The design models used in this thesis are based on *integer linear programming* (ILP) methods using *arc-path* formulations [37] [73] that are designed only for *spare capacity placement* (SCP) models [37] [70]-[73]. In SCP optimization problems, individual working routes are often routed in advance by a shortest path algorithm before performing the optimization process for the spare capacity allocation.

3.1. Dual Failure Restorability Formulations

In this section the conventional definition of dual failure restorability R_2 is reviewed and formulation of the models in each of the survivability mechanisms is discussed. We review how dual failure restorability is used in the literature to justify the approach we adopted in this work. There are a number of ways to think of restoration quality or the measure of network survivability in a network beside the approach that we adopted in this work. Restoration quality can also be

[1] A substantially modified version of this chapter has been published in [74], and [86].

measure in terms of *network availability*. There are number of ways R_2 can be derived and different computational approaches can be used to calculate the overall network R_2.

In most of the literature, dual failure restorability is denoted by R_2 [17]-[18], [49]. $R_2 = 1$ when the overall network average dual failure restorability is 100%. This means that all the demands in the network are 100% restorable in the event of dual span failure. The design models guarantee sufficient spare capacity placement to restore 100% of the demands in the event of failure in a span pair. R_2 is usually derived from the cumulative average of individual pairs of spans in dual failure restorability. $R_2(i, j)$ represents the dual failure restorability of any pair of spans (i, j), where i and j are in the order of span failures. $R_2(i, j)$ is the fraction of the working capacity on the spans i and j that is restorable when both spans fail simultaneously. On the other hand, $R_2^r(i, j)$ is the dual failure restorability of a demand relation r on a pair of spans i and j when both spans fail. This is the fraction of total demand units that are restorable upon failure of spans i and j. $R_{2i}(j)$ is the dual failure restorability of span i, given that span j is also failed. With this approach the average R_2 of the network may vary when compared to the value of $R_2(i, j)$ if implemented on the same network with different survivability schemes. We formulated two models for each survivability scheme. Model 1 computes the *specific* dual failure restorability of each pair of spans in the network and ensures that it meets the minimum specified limit of dual failure restorability. Model 2 computes the *average* dual failure restorability of all pairs of spans in the network subject to the specified limit of dual failure restorability. In section 3.1.1 the variations in formulation of dual failure restorability for each survivability scheme is discussed.

3.1.1. Span-Based R_2 Calculations

The computation of R_2 of a pair of spans in a span-based restoration mechanism may vary, depending on how R_2 is defined. The $R_2(i, j)$ computation may yield a different numerical result when compared with the $R_{2i}(j)$ computation on the same network, except for 100% dual failure restorability. In the $R_2(i, j)$

computation, there are numerous ways to assign restoration flows to achieve required dual failure restorability. In this thesis, the notation $R_{2i}(j)$ defines the dual failure restorability of a pair of spans in the span-based restoration mechanism, whereas in some of the literature $R_2(i, j)$ is used [18] [49]. In this section we show a number of ways in which the value of $R_2(i, j)$ can be obtained by varying the assigned restoration flows.

In [18] [49], $R_2(i, j)$ is expressed as follows:

$$R_2(i,j) = 1 - \left(\frac{N(i,j)}{w_i + w_j} \right) \qquad \forall (i,j) \in S^2 \mid w_i + w_j \neq 0, \tag{3.1.1}$$

where $N(i,j) = N_i + N_j$ represents the non-restorable working capacity units on spans i and j. N_i and N_j are the non-restorable working capacities on spans i and j, respectively. w_i and w_j are the working capacities on spans i and j, respectively. Equation (3.1.1) can be rearranged such that $R_2(i,j)$ is expressed as:

$$R_2(i,j) = \frac{(w_i + w_j) - N(i,j)}{w_i + w_j} \qquad \forall (i,j) \in S^2 \mid w_i + w_j \neq 0. \tag{3.1.2}$$

If we define $Z(i,j) = Z_i + Z_j$ as the working capacity restorable on spans i and j (where Z_i and Z_j are the individual restorable working capacities on spans i and j, respectively), then $Z(i,j) = (w_i + w_j) - N(i,j)$ and equation (3.1.2) can be expressed as:

$$R_2(i,j) = \frac{Z(i,j)}{w_i + w_j} = \frac{Z_i + Z_j}{w_i + w_j} \qquad \forall (i,j) \in S^2 \mid w_i + w_j \neq 0. \tag{3.1.3}$$

The values of Z_i and Z_j are derived from the amount of unit flows assigned to the restoration routes used for restoring the working capacities on spans i and j. But from our analysis on a span-based restoration mechanism, the values of Z_i and Z_j can often be disproportionately allocated to the restoration routes of spans i and j in order to satisfy the required minimum R_2, particularly if the required specified level of dual failure restorability (R_2^* limit) is less than 100%. Figure 3.1.1

illustrates how restoration flows can be disproportionately assigned to different restoration routes to achieve the required level of dual failure restorability.

There are 8 demand lightpaths routed between O-D nodes (N1-N3) and another 2 demand lightpaths with O-D nodes (N3-N4) routed through (N3-N1-N4) in Figure 3.1.1(a). If span *i* represents (N1-N3), and span *j* represents (N1-N4), and they have working capacities of $w_i = w_{13} = 8$ and $w_i = w_{14} = 2$, respectively, the assignment of restoration flows to restoration routes (N1-N2-N3) and (N1-N2-N4) in Figure 3.1.1(b) can vary in a number of ways to achieve the specified level of dual failure restorability of less than 100%.

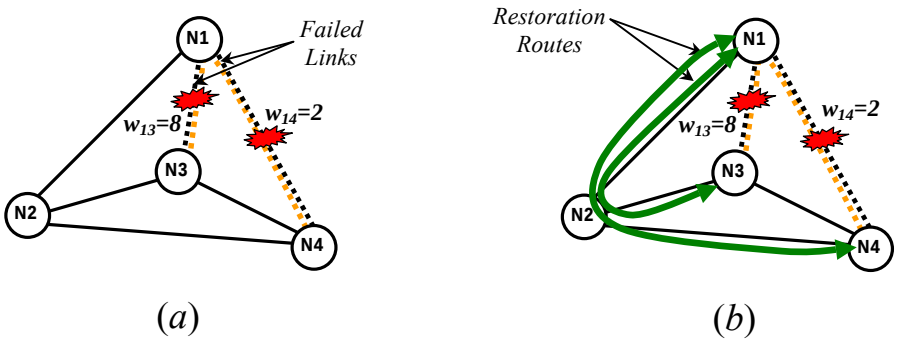

Figure 3.1.1-Illustration of different $R_2(i,j)$ computations in span restorable networks.

For example, if the required minimum dual failure restorability is 70%, upon failure of spans *i* and *j*, three restoration scenarios can be imagined. In scenario 1, 7 units of restoration flow is assigned to restore span *i*, and zero restoration flow is assigned to span *j*, resulting in $R_2(i, j) = 70\%$. Scenario 1 generally satisfies the required minimum dual failure restorability, but provides no restoration capacity at all for span *j*. If we considered a situation where one of the working routes has 2 demand lightpaths transversing both spans in this scenario, then the effective dual failure restorability would be only 50% while the actual numerical dual failure restorability value reads 70%. In scenario 2, 6 units of restoration flow is assigned to restore span *i*, and 1 unit of restoration flow is assigned to span *j,* resulting in $R_2(i, j) = 70\%$. The required specified dual failure restorability is achieved, but, effectively, only 50% of demands are restored if the same 2 demand lightpaths transverse both spans *i* and *j*. Computing dual failure

restorability using the $R_2(i,j)$ approach is further complicated if all the working routes affected by dual failure cross both spans *i* and *j*. In scenario 3, 6 and 1 units of restoration capacities are assigned to spans *i* and *j*, respectively. Using this approach to achieve 100% of $R_2(i,j)$ on each pair of spans is considered valid, since enough restoration capacity must be assigned to restore 100% of the demands on both failed spans *i* and *j*. Hence for 100% dual failure restorability, the *average* R_2 is computed using equation (3.1.4), where *S* represents the set of spans in the network.

$$R_2 = \frac{\sum_{\forall (i,j) \in S^2 | i \neq j} R_2(i,j)}{|S| \cdot (|S| - 1)} \tag{3.1.4}$$

With this approach, the effect on path oriented restoration and protection mechanisms would vary significantly when compared to span oriented restoration or protection mechanisms such as span restoration and *p*-cycle networks.

3.1.2. End-to-End R_2 Calculation

In path-based restoration mechanisms, the dual failure restorability for each demand relation *r* on any pair of spans *i* and *j* in the network is denoted by $R_2^r(i,j)$. And $R_2^r(i,j)$ is defined as the dual failure restorability of demand relation *r* on a given span pair *i* and *j* considering both spans failed simultaneously. It is the fraction of demand relation *r* that is restorable when spans *i* and *j* fail simultaneously. The value of the overall R_2 is derived by the average of $R_2^r(i,j)$ over all demand relations on the pair of spans *i* and *j*. Equation (3.1.5) shows how $R_2^r(i,j)$ is derived on a given pair of spans.

$$R_2^r(i,j) = \frac{N_2^r(i,j)}{d^r} \qquad \forall (i,j) \in S^2 \mid i \neq j \tag{3.1.5}$$

where $N_2^r(i,j)$ estimates the amount of restoration flows assigned to restore the demand units on spans *i* and *j*, d^r is the total demand units for the demand relation *r*, and $R_2^r(i,j)$ is expressed as the ratio of demands that are restorable to

total demand units in demand relation *r*. This approach is different from the approach discussed in section 3.1.1 where the working capacity on every span pair failure is considered. The approach in end-to-end path oriented protection mechanisms, such as DSP and path restoration, simplifies the need if necessary to pay particular attention to some critical or priority demand paths. For example, if some of the demand relations in the network are required to achieve at minimum 70% dual failure restorability, then the network is designed such that sufficient restoration paths are assigned to achieve 70% restorability of those demand relations. The average dual failure restorability of each demand relation *r* over all the span pairs (i, j) is expressed in equation (3.1.6).

$$R_2^r \le \frac{\sum_{\forall (i,j) \in S^2 | i \ne j} R_2^r(i,j)}{|S| \cdot (|S| - 1)} \qquad \forall r \in D \tag{3.1.6}$$

$$R_2 \le \frac{\sum_{\forall r \in D} R_2^r}{|D|} \tag{3.1.7}$$

Equation (3.1.7) calculates the average dual failure restorability R_2 of the entire network by averaging R_2^r of each demand over the cardinality of the demand relations in the network.

3.1.3. *p*-Cycle R_2 Calculations

The dual failure restorability for each span in span restoration and in *p*-cycles is defined differently following the approach used in [52]. $R_{2i}(j)$ is instead used to denote the dual failure restorability of a given span in span restorable and *p*-cycle networks. This approach evaluates the amount of working capacity that is restorable on span *i* given that span *j* has failed simultaneously. The required restoration capacities for span *i* are placed on other restoration routes except for those crossing span *j*. $R_{2i}(j)$ is expressed as:

$$R_{2i}(j) = \frac{N_{2i}(j)}{w_i} \qquad \forall (i,j) \in S^2 \mid i \ne j, \tag{3.1.8}$$

$$R_{2i} \le \frac{\sum_{\forall j \in S | i \neq j} R_{2i}(j)}{|S| - 1} \qquad \forall i \in S \ , \tag{3.1.9}$$

$$R_2 \le \frac{\sum_{\forall i \in S} R_{2i}}{|S|}, \tag{3.1.10}$$

where $N_{2i}(j)$ is the amount of working capacity restorable on span i. It is estimated by summation of the restoration flows assigned to each restoration route provided for restoring span i when span j has failed. The restoration routes considered in the estimate of the value of $R_{2i}(j)$ must not cross span j. w_i is the amount of working capacity on span i. Equation (3.1.9) estimates the average dual failure restorability of span i over all the other spans pairing with it, and in equation (3.1.10), the average dual failure restorability of the entire network is computed.

3.2. Dual Failure Restorability in Span Restorable Networks

In this section we discuss dual failure scenarios in span restoration and how the restoration mechanism can be designed with sufficient spare capacity to protect the network from dual failures. In span restoration, the type of configuration of the restoration mechanism can affect the spare capacity allocation in the network. For example, [18] describes a *pre-planned protection* type of configuration in span restoration where response to failures is predetermined for the first and second failure. In another configuration, the *distributed adaptive real-time restoration* can be a first event adaptive or fully adaptive restoration mechanism. The adaptive dual failure restoration type can be combined with the pre-planned protection type in a first failure protection, second failure restoration (1F*P*-2FR) concept [18]. In this thesis, the models are designed for the pre-planned protection type of configuration. The design formulation considers each pair of spans in a dual failure scenario and places sufficient capacity to ensure that the affected demand units are restored. The restoration routes of the first failed spans are pre-selected such that they do not cross the second failed span. This implies that when failure of spans i and j are considered, no restoration route used for span i should be routed through span i. So span restoration $R_{2i}(j)$ is used to define for spans i

and j the dual failure restorability of span i, given that span j has also failed. R_2 is then derived from the average of all $R_{2i}(j)$ values over the network. In the next section, the different dual failure scenarios are used to illustrate the effect of the restoration mechanism for any given pair of spans and to show how that relates to the dual failure restorability formulation in our design models.

3.2.1. Dual Failure Scenarios in Span Restoration

There are a number of dual failure scenarios that can affect the outcome of a restoration process of a span pair failure. Consider, for example, the first dual failure scenario involving two distant spans in a network in which restoration routes for the spans do not interact or share common restoration capacity. The dual failure restoration mechanism on this failure scenario would act as though there are two separate single span failures in the network, thereby requiring no additional capacity to achieve any specified level or full dual failure restorability. This means that a network that is optimally designed for 100% single failure restorability can withstand this particular kind of dual failure scenario without requiring additional capacity for the dual failure restorability. In a second important failure scenario, failure of a pair of spans in a 9-node network is illustrated in Figure 3.2.1(*a*) and Figure 3.2.1(*b*). Figure 3.2.1(*a*) shows a portion of the designated restoration route (N2-N4-N6-N7) of the first failed span (N2-N7) sharing spare capacities on span (N4-N6) with the restoration route (N5-N4-N6-N8) of the second failed span (N5-N8). This situation causes the restoration routes of both failed spans to contend for spare capacity on span (N4-N6). Additional resources are required on span (N4-N6) to ensure that there is sufficient restoration capacity for both failed spans to achieve the level of dual failure restorability required. A third major failure scenario involves a span pair failure where a restoration route of the first failed span is cut by the second span failure. Figure 3.2.1(*b*) shows one of the restoration routes of span (N2-N7) being cut by a span (N4-N6) failure. The surviving restoration route (N2-N6-N7) restores as much demand as the equivalent capacity that is placed on it. The situation will often result in an outage of the services routed on affected

restoration routes and complete outage of the demands affected by the failure if the only restoration route of the first failed span is hit by the second span failure.

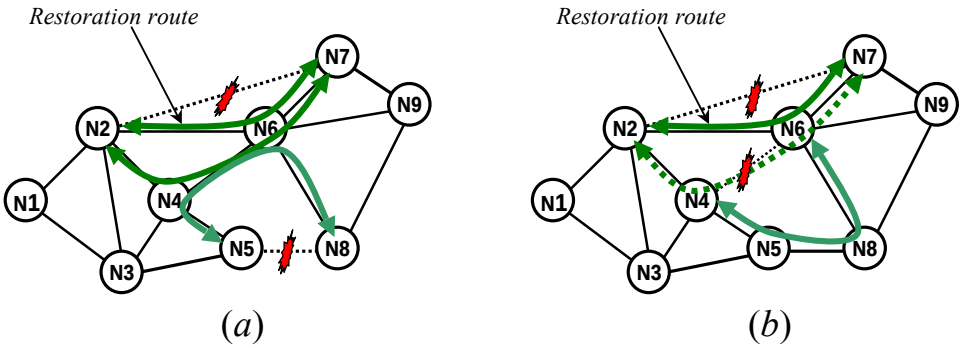

Figure 3.2.1-Illustration of dual failure scenarios in span restorable networks.

Sufficient restoration capacity must be provided to ensure that the desired level of dual failure restorability for the pair of spans in this scenario is achieved. This is what our design models are intended to do. The models ensure that adequate restoration capacity is provided such that a second span failure has enough spare capacity to restore the desired level of demands on the span and does not affect the restoration capacity of the first failed span. The last two failure scenarios outlined contribute substantially to a major increase in additional capacity requirement for dual failure restorability.

3.2.2. ILP Models for Dual Failure Restorability in Span Restoration

Before proceeding with the models we define the notations used in the formulations.

Sets:

S is the set of spans in the network indexed by i.

S^2 is the set of span pairs in the network indexed by (i, j).

P_i is the set of distinct eligible restoration routes for restoration of span i.

$P_{(i,j)}$ is the set of distinct eligible restoration routes for span i remaining when span j fails.

Input Parameters:

c_i is the cost of unit capacity on span i.

w_i is the working capacity on a span i.

$\delta_{i,j}^{p} \in \{0,1\}$ is 1 if the p^{th} restoration route for span i crosses span j, otherwise 0.

R_2^* is the specified minimum dual failure restorability limit.

Decision Variables:

f_i^p is the restoration flow assigned to the p^{th} restoration route for failure of span i.

$f_{i,j}^{p}$ is the restoration flow assigned to the p^{th} restoration route of span i, given that span j has also failed.

s_j is the spare capacity placed on span j.

$R_{2i}(j)$ is the dual failure restorability of span i given that span j has also failed.

The Models:

$$\text{Minimize} \sum_{\forall i \in S} c_i \cdot (s_i + w_i) \tag{3.2.1}$$

Subject to:

$$\sum_{p \in P_i} f_i^p \geq w_i \qquad \forall i \in S \tag{3.2.2}$$

$$\sum_{p \in P_i} f_i^p \cdot \delta_{i,j}^p \leq s_j \qquad \forall (i,j) \in S^2 \mid i \neq j \tag{3.2.3}$$

$$\sum_{p \in P_{i,j}} f_{i,j}^p \cdot \delta_{i,k}^p + \sum_{p \in P_{j,i}} f_{j,i}^p \cdot \delta_{j,k}^p \leq s_k \qquad \forall (i,j,k) \in S^3,\ i \neq j,\ i \neq k, j \neq k \tag{3.2.4}$$

$$R_{2i}(j) \leq \frac{\sum_{p \in P_i \mid \delta_{i,j}^p \neq 1} f_i^p}{w_i} \qquad \forall (i,j) \in S^2 \mid i \neq j \tag{3.2.5}$$

$$R_{2i}(j) \geq R_2^* \qquad \forall (i,j) \in S^2 \mid i \neq j \tag{3.2.6}$$

The objective function (3.2.1) and constraints (3.2.2) and (3.2.3) are derived from the conventional single failure restorability constraints [18] [19] [73]. The objective function (3.2.1) and constraints (3.2.2) through (3.2.6) make up model 1

of our dual failure restorability model. The objective function (3.2.1) minimizes the cost of spare and working capacity on any span *j*. It is important to note that working capacity in the objective function has no impact on the capacity optimization problem, since it is allocated in advance by the shortest path routing algorithm. However, the working capacity is included in the objective function to enable us to compute the total capacity cost for comparative analysis with other restoration mechanisms in subsequent chapters. Constraint (3.2.2) ensures that sufficient restoration flow is assigned to the restoration routes for the working capacity on span *i*. Constraint (3.2.3) computes the spare capacity allocated to span *j* as a result of restoration flows routed through span *j* upon failure of span *i*. The dual failure restorability constraints begin with constraint (3.2.4). It is similar to (3.2.3) but rather computes the spare capacity placed on span *k* in the event of failures of span *i* and span *j*. It sums up the amount of the restoration flows placed on the restoration routes for span *i* and span *j*, which crosses span *k*. Constraint (3.2.5) is the basic component of the dual failure restorability model and computes the dual failure restorability of individual span *i*, given that span *j* has also failed. It is the ratio of the sum of the restoration flows for span *i* which does not cross span *j* to the total working capacity w_i on span *i*. Finally, constraint (3.2.5) ensures that $R_{2i}(j)$ is at least equal to the specified level of dual failure restorability R_2^* required in the network. The additional constraints (3.2.7) through (3.2.9), shown below, simply replace constraint (3.2.6) to form *model 2*, the second dual failure restorability model. Constraints (3.2.7), (3.2.8), and (3.2.9) compute the average dual failure restorability for the entire network and ensure that the average dual failure restorability value is at least equal to the specified dual failure restorability limit.

Model 2 Components of Average Dual Failure Restorability:

$$R_{2i} \leq \frac{\sum_{j \in S | i \neq j} R_{2i}(j)}{(|S|-1)} \qquad \forall i \in S \qquad (3.2.7)$$

$$R_2 \leq \frac{\sum_{\forall i \in S} R_{2i}}{|S|} \tag{3.2.8}$$

$$R_2 \geq R_2^* \tag{3.2.9}$$

Constraint (3.2.7) uses the value of the average dual failure restorability of span *i* computed from constraint (3.2.5) to average over all spans *j* (pairing with span *i*). The average of the dual failure restorability of span *i* is subsequently averaged over all spans in the network with constraint (3.2.8); the average dual failure restorability for the entire network R_2 is required to be over R_2^* (specified R_2^* limit) in constraint (3.2.9). Detailed analyses of the results obtained from these models in different survivability mechanisms are presented in chapter 4.

3.3. Dual Failure Restorability in Path Restorable Networks

As mentioned in section 2.4.2, the path restoration mechanism uses specific end-to-end restoration paths to restore working routes that are affected by span failures in the network. More specifically, the choice of restoration path for any working lightpath in response to the failure depends on the specific span that fails. However, path restorable networks designed for 100% single failure restorability have limited capability to survive under dual failure events. For example, in a span pair failure where the second span failure damages the restoration path of the first failed span, outage would be caused by the first failed span. Therefore, extra capacity must be provided to ensure that the first failed working route is restorable upon second span failure. In section 3.3.1 we discuss dual failure scenarios that are likely to cause outage and show how we can provide capacity to protect the spans from failure. We also look at the formulation of new ILP models for dual failure restorability and some of the key features of path restoration such as stub release.

3.3.1. Dual Failure Scenarios in Path Restoration

The outcomes of dual span failures in a path restorable network depend on the path interactions, the order of span failures, and combinations of the failed pair of

spans. The outcome also depends on whether the failed spans are in primary working routes and/or in backup routes. The specific restoration path used to restore the affected working routes depends on which spans failed; that is, an individual restoration path is designated to restore the specific working path affected by a span failure. Compared to the number of failure scenarios in span restorations or *p*-cycles, there are fewer dual failure scenarios that can potentially cause an outage in path restoration.

The first scenario involves a span pair failure in which the restoration routes of the working routes affected by the first failure are hit by the second span failure. Another failure scenario happens when the first span failure damages the restoration route(s) designated for restoring the working routes affected by the second failure. These two scenarios would result in an outage in a network designed for 100% single failure restorability, since there is no extra restoration capacity available for the affected working routes after the second failure.

Figure 3.3.1 shows the failure of a single span *i*, (N4-N6) and the restoration path (N1-N4-N3-N6-N7-N10) used to restore the working route (N1-N4-N6-N7-N10). When span *i* fails, the restoration path (N1-N4-N3-N6-N7-N10) is used to restore the working route (N1-N4-N6-N7-N10) by rerouting the affected working route to isolate the failed span *i*.

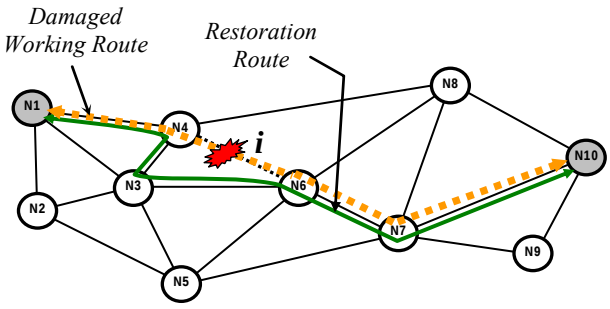

Figure 3.3.1-First failure response in path restorable network.

Following the first span failure, Figure 3.3.2 shows the failure of the second span *j*, (N7-N10) as it cuts the restoration route of the first failed working route. Any effort to restore the demands on the working route affected by the first failure would not be successful, due to the occurrence of the second failure. Similarly, in

the reverse order of the failure, the failure of span *i* will still result in an outage if the restoration routes of span *i* were already cut by failure of span *j*.

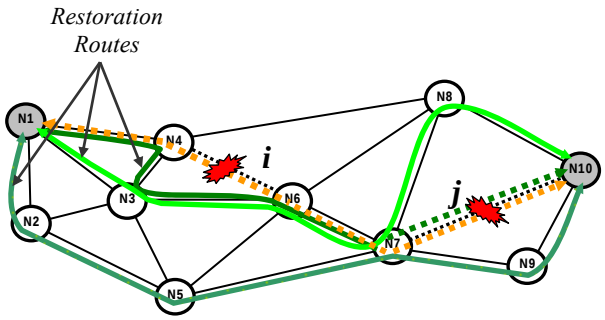

Figure 3.3.2-Second failure response in path restorable network.

Our new models ensure that sufficient restoration routes are provided for restoration of the affected working routes in the network. Similar to single span failure, stubs of all the working routes affected by both first and second failures are released prior to the restoration process. For example, in Figure 3.3.2 the restoration route (N1-N3-N6-N7-N8-N10) can reuse the stub on span (N6-N7) if it is specifically assigned to restore the demands on the working routes on both spans. In section 3.3.2 we define the notations, the sets used in the formulation, the input parameters, decision variables, and the formulation of a new ILP model for specified dual failure restorability.

3.3.2. ILP Models for Dual Failure Restorability in Path Restoration

In formulating the path restoration models, we first present the part that makes up model 1, and then present the part that makes up model 2. As mentioned earlier, model 1 calculates the dual failure restorability of each pair of spans, and model 2 computes the average dual failure restorability for all pairs of spans in the network. The model is shown below:

Sets:

S is the set of spans in the network indexed by i.

S^2 is the set of span pairs in the network indexed by (i, j).

D is the set of all the demand relations in the network indexed by r.

P^r is the set of eligible restoration routes for restoration of each demand relation r.

Q^r is set of all the working routes for demand r.

Q_i^r is the set of working routes for each demand relation r that is affected by failure of span i.

$Q_{i,j}^r$ is the set of working routes for each demand relation r that is affected by failure of span i.

$S^{r,p}$ is the set of spans contained in the restoration routes p for any demand relation r.

D_i is the set of demand relations affected by failure of span i.

$D_{i,j}$ is the set of demand relations affected by failure of span i and j.

$D'_{i,j}$ is the set of demand relations not affected by failure of span i and j, and $D = D_{i,j} + D'_{i,j}$.

Input Parameters:

c_j is the cost of unit capacity on span j.

d^r is the number of demand units for each demand relation r per node pair.

$w^{r,q}$ is the amount of working flow routed over working route q for demand relation r.

$s_{i,j}^{r*}$ is the amount of stub-release capacity on span j released in the event of failure of span i.

$s_{i,j,k}^{r*}$ is the stub-release capacity on span k upon failure of spans i and j.

R_2^* is the specified minimum dual failure restorability limit.

Decision Variables:

$f_i^{r,p}$ is the amount of restoration flow assigned to restoration route p for any demand relation r when span i fails.

$R_2^r(i,j)$ is the dual failure restorability of span i and span j when both spans fail.

R_2 is the average dual failure restorability of the entire network.

$f_{i,j}^p$ is the restoration flow assigned to the p^{th} restoration route of span i, given that span j has also failed.

s_j is the spare capacity assignment on a span j.

The Model:

$$\text{Minimize} \sum_{\forall j \in S} c_j \cdot (s_j + w_j) \tag{3.3.1}$$

Subject to:

$$\sum_{\forall p \in P^r | i \notin S^{r,p}} f_{i,q}^{r,p} \geq w^{r,q} \qquad \forall i \in S, \forall r \in D_i, \forall q \in Q_i^r \tag{3.3.2}$$

$$s_j + \sum_{\forall r \in D_i} s_{i,j}^{r*} \geq \sum_{\forall r \in D_i} \sum_{\forall p \in P^r | i \notin S^{r,p}} \sum_{\forall q \in Q_i^r} f_{i,q}^{r,p} \qquad \forall (i,j) \in S^2 \mid i \neq j \tag{3.3.3}$$

$$s_k + \sum_{\forall r \in D_{i,j}} s_{i,j,k}^{r*} \geq \sum_{\forall r \in D_{i,j}} \sum_{\forall p \in P^r | i,j \notin S^{r,p}, k \in S^{r,p}} \sum_{\forall q \in Q_{i,j}^r} f_{i,j,q}^{r,p} \quad \forall (i,j,k) \in S^3 \mid i \neq j, i \neq k, j \neq k \tag{3.3.4}$$

$$R_2^r(i,j) \leq \frac{\sum_{\forall q \in Q_{i,j}^r} \sum_{\forall p \in P^r | i,j \notin S^{r,p}} f_{i,j,q}^{r,p}}{d^r} \qquad \forall (i,j) \in S^2, \forall r \in D_{i,j} \mid i \neq j \tag{3.3.5}$$

$$R_2^r(i,j) = 1 \qquad \forall (i,j) \in S^2, \forall r \in D'_{i,j} \mid i \neq j \tag{3.3.6}$$

$$R_2^r(i,j) \geq R_2^* \qquad \forall (i,j) \in S^2, \forall r \in D_{i,j} \mid i \neq j \tag{3.3.7}$$

The objective function (3.3.1) and the first two constraints (3.3.2) and (3.3.3) make up the conventional ILP formulation for the 100% single failure

restorability design in the path restorable network [19]. The objective function simply minimizes the cost of the total capacity requirement in the network. Constraint (3.3.2) ensures that sufficient restoration capacity is assigned to the restoration routes assigned to restore the failed working routes of demand relation *r* on span *i*. Constraint (3.3.3) calculates the amount of spare capacity placed on each span *j* from all the restoration routes that cross span *j*. The dual failure constraints begin with constraint (3.3.4); similar to constraint (3.3.3), it computes the amount of spare capacity placed on each span *k* from all the restoration routes that cross span *k* when spans *i* and *j* fail. Both constraints implement the *stub release* mechanism to reduce the amount of additional spare capacity required in the network. Stub release is a process whereby the surviving portions of the failed working channel are freed to be reused for the restoration of the failed working channel [19]. The stub release $s_{i,j}^{r*}$ for single failure restorability and $s_{i,j,k}^{r*}$ for dual failure restorability compute the capacity yielded by the surviving stub portions of the failed working path on each span. Constraint (3.3.5) derives the dual failure restorability R_2 of each demand relation *r* for failure of a specific pair of spans *i* and *j*. It is the basic component of dual failure restorability for each demand considered for a span pair failure and can also be defined as the ratio of the sum of all the restoration flows of the demand relation to the total demand units. Constraint (3.3.6) assigns a value of 1 (i.e., 100% restorability) to dual failure restorability of the demands not affected by failure of the specific pair of spans *i* and *j*. A set of demand relations not affected by failure of spans *i* and *j* is denoted by $D'_{i,j}$, while the set of demand relations affected by failure of spans *i* and *j* is given by $D_{i,j}$. Constraint (3.3.7) enforces the minimum required dual failure restorability limit at the span pair level. The objective function (3.3.1) and constraints (3.3.2) through (3.3.7) make up *model 1* of the dual failure restorability model in the path restorable network. The second model, *model 2*, is obtained by replacing constraint (3.3.7) with constraints (3.3.8) through (3.3.10) and it averages the individual $R_2^r(i,j)$ values for all demand relations over the network.

Model 2 Component of Average Dual Failure Restorability:

$$R_2^r \le \frac{\sum_{\forall (i,j) \in S^2 | i \ne j} R_2^r(i,j)}{|S| \cdot (|S| - 1)} \qquad \forall r \in D_{i,j} \tag{3.3.8}$$

$$R_2 \le \frac{\sum_{\forall r \in D} R_2^r}{|D|} \tag{3.3.9}$$

$$R_2 \ge R_2^* \tag{3.3.10}$$

The average dual failure restorability for each demand relation over all pairs of spans in the network is computed in constraint (3.3.8). The overall network average dual failure restorability over all demands is computed by constraint (3.3.9), and constraint (3.3.10) ensures that the network average dual failure restorability is at least equal to the specified limit.

3.4. Dual Failure Restorability in DSP Networks

As mentioned in the introduction to DSP networks in chapter 2, DSP networks are routed on a per demand basis and the ILP model is formulated in the form of a joint capacity placement type of model. Dual failure in DSP networks requires a set of distinct disjoint routes for the primary working channels and up to two backup channels: a *primary backup* channel and a *secondary backup* channel. The routing of a typical node pair demand in a DSP network requires, at minimum, a nodal degree of 3 per each O-D node pair to satisfy the condition for dual failure protection. In the event of dual span failure affecting a primary working channel and the primary backup channel, the mechanism requires a secondary backup channel to act as a restoration channel of the two failed channels. The diversification of the primary working channels reduces by some fractions the demands that are affected by a dual failure occurrence. Thus the extra capacity required to protect a DSP network from dual failure largely depends on the network connectivity, how diverse the primary working channels are routed, and the level of dual failure restorability required. Two types of dual failure scenarios could potentially result in outages in a DSP network optimally designed for single

failure protection. These two types of failure scenarios and the ILP model are described in section 3.4.1.

3.4.1. Dual Failure Scenarios in DSP

An optimally designed DSP network for 100% single failure restorability has some level of inherent dual failure restorability advantage [58]. For example, failure of a pair of spans affecting only two disjoint working routes out of three existing working routes and a single backup route leaves the demands routed on the unaffected working routes and the backup route survivable. In other words, it would appear as though only one working route has failed. However, there are dual failure scenarios that will result in outage of services on the affected demand paths. One example involves a span pair failure where the first span failure cuts one of the primary working routes and the second span failure cuts another primary working route. In another example a span pair failure involves one of the primary working routes and the only backup route. This failure scenario could result in complete outage of the affected demand paths if O-D nodes have a node degree of 2, or if only a single working route and backup route were routed for the affected demands. Figure 3.4.1 illustrates how failure scenarios can affect a DSP network routed for 100% single failure and dual failure restorability. It shows a DSP network routing of the primary working channels and the backup channel(s) with 12 demand units exchanged between O-D node pair (N1-N9). Figure 3.4.1(*a*) shows the network routed to achieve 100% single failure restorability and in Figure 3.4.1(*b*) the network is routed for 100% dual failure restorability. Three out of the total four disjoint paths in Figure 3.4.1(*a*) are used as working channels (N1-N2-N7-N9), (N1-N6-N9), and (N1-N4-N5-N9); they bear 4 demand lightpaths each and the only backup channel (N1-N3-N8-N9) has 4 spare lightpaths to protect any of the working channels. Similarly in Figure 3.4.1(*b*), the same four disjoint paths are used, but in this case two working channels (N1-N2-N7-N9) and (N1-N6-N9) bear 6 demand lightpaths each and two backup channels (primary and secondary backup channels) have 6 spare lightpaths each.

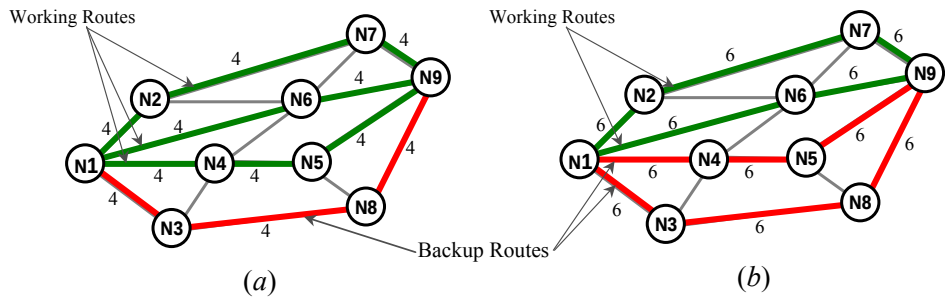

Figure 3.4.1-Illustration of routing of working and backup channels in DSP networks.

In scenario 1 a span pair failure occurs in two primary routes. For example, in Figure 3.4.2 (*a*) and (*b*), span failures occur between node pairs (N1-N6) and (N2-N7) cutting services on the two primary channels of each network.

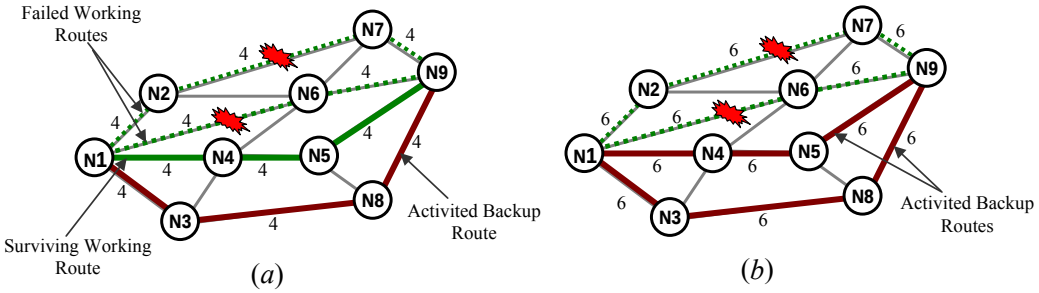

Figure 3.4.2-Illustration of dual failure scenario 1 in DSP networks.

For the network designed for 100% single failure restorability, Figure 3.4.2(*a*), one primary working channel survives the failures and the restoration mechanism switches to the backup channel to restore one of the failed working channels yielding about 66% dual failure restorability. On the other hand, the network designed for 100% dual failure restorability, Figure 3.4.2(*b*), has 100% of the demands restored by switching from the failed working channels to backup channels. The total spare capacity required for the dual failure restorability is about 33% more than the capacity required for the single failure restorability design.

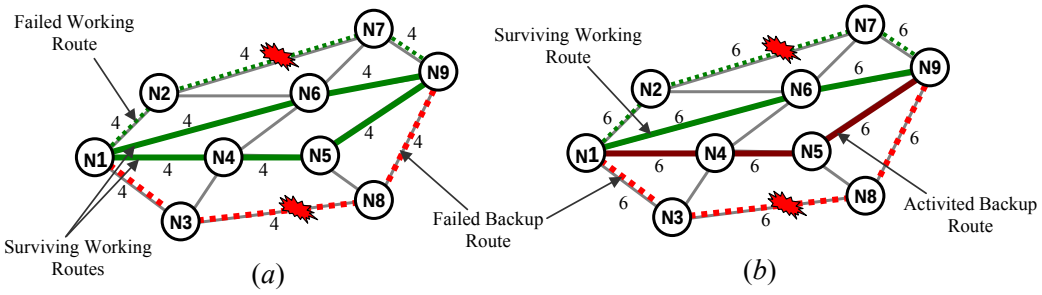

Figure 3.4.3-Illustration of dual failure scenario 2 in DSP networks.

Scenario 2, Figure 3.4.3(*a*) and (*b*), involves a span pair failure where a working channel and a backup channel are both hit by the span failures. Similar to scenario 1, 66% of the demands survive the dual failure and the 2 surviving working channels remain active. However, in the network designed for 100% dual failure restorability, the restoration mechanism switches to the primary backup channel to restore one of the failed working channels. The results may vary depending on the routing of the primary working channels and the backup channels.

3.4.2. ILP Models for Dual Failure Restorability in DSP

In this section, notations are defined for formulation of the models, the sets, the input parameters, and the decision variables. The models are presented thereafter.

Sets:

S is the set of all spans in the network indexed by i.

D is the set of O-D demand relations in the network indexed by r.

Q^r is the set of all eligible routes in demand relation r indexed by q. Q^r is indexed by $q1$ if q is used as working route or $q2$ if q is used as a backup route, so that $\forall q1, \forall q2 \in Q^r \,|\, q1 \neq q2$.

$S^{r,q}$ is the set of all spans crossed by route q in the demand relation r.

Input Parameters:

d^r is the amount of demand units for every O-D demand relation r.

$C^{r,q}$ is the unit cost of place demands on a route q between O-D of a demand relation r.

$\zeta_i^{r,q} \in \{0, 1\}$ equals 1 if route q of the demand relation r crosses span i, and is 0 otherwise.

R_2^* is the specified level of dual failure restorability required in the network.

Decision Variables:

$\alpha^{r,q} \in \{0, 1\}$ equals 1 if routes q of demand relation r is used as working route and is 0 otherwise.

$\beta^{r,q} \in \{0, 1\}$ equals 1 if route q of demand relation r is used as backup route and is 0 otherwise.

$g^{r,q}$ is the amount of flow assigned to working route q of demand relation r.

$f^{r,q}$ is the amount of restoration flow assigned to the route q for the restoration of demand relation r.

$R_2^r(i, j)$ is the dual failure restorability of demand relation r for failure of spans i and j.

R_2^r is the average dual failure restorability for the demand relation r.

R_2 is the average dual failure restorability for the entire network.

The Model:

Objective Function:

$$\text{Minimize} \sum_{\forall r \in D, \forall q \in Q^r} C^{r,q} \cdot (g^{r,q} + f^{r,q}) \tag{3.4.1}$$

Subject to:

$$\sum_{q \in Q^r} (\alpha^{r,q} + \beta^{r,q}) \cdot \zeta_i^{r,q} \leq 1 \qquad \forall r \in D, \forall i \in S \tag{3.4.2}$$

$$\sum_{\forall q \in Q^r} g^{r,q} = d^r \qquad \forall r \in D \tag{3.4.3}$$

$$\sum_{\forall q \in Q^r} \beta^{r,q} \leq 2 \qquad \forall r \in D \tag{3.4.4}$$

$$g^{r,q} \le \alpha^{r,q} \cdot d^r \qquad \forall r \in D, \forall q \in Q^r \qquad (3.4.5)$$

$$f^{r,q} \le \beta^{r,q} \cdot d^r \qquad \forall r \in D, \forall q \in Q^r \qquad (3.4.6)$$

$$\sum_{\forall q1 \in Q^r} f^{r,q1} \ge g^{r,q2} \qquad \forall r \in D, \forall q2 \in Q^r \qquad (3.4.7)$$

$$R_2^r(i,j) \le \frac{\sum_{\forall q \in Q^r | i,j \in S^{r,q}} (f^{r,q} + g^{r,q})}{d^r} \qquad \forall r \in D, \forall (i,j) \in S^2 \mid i \ne j \qquad (3.4.8)$$

$$R_2^r(i,j) \ge R_2^* \qquad \forall r \in D, \forall (i,j) \in S \mid i \ne j \qquad (3.4.9)$$

The objective function (3.4.1) and constraints (3.4.2) through (3.4.9) constitute model 1 of the DSP network model. The objective function (3.4.1) minimizes the total capacity cost (both working capacity and spare capacity cost) in the network. In DSP network design, the working capacity and the spare capacity are jointly optimized. Constraint (3.4.2) ensures that the individual working routes and the backup routes are completely span-disjoint. It also ensures that a certain route can be selected only as a working route or as a backup route in a demand relation. Constraint (3.4.3) ensures that all the demand units are served between O-D node pairs. Constraint (3.4.4) limits the number of backup channels required to 2 in the dual failure restorability design model. This constraint is not required in the single failure design model and should be excluded in the stand-alone single failure design model. Constraints (3.4.5) and (3.4.6) assign the amount of working flow and equivalent restoration flow to working routes and restoration routes, respectively. Both constraints (3.4.5) and (3.4.6) ensure that the amount of capacity assigned to each route does not exceed the total demand units d^r over O-D node pairs. Constraint (3.4.7) guarantees that there is enough restoration flow assigned to restore each working route for every demand relation *r*. Constraint (3.4.8) computes the dual failure restorability $R_2^r(i,j)$ of each pair of spans in the network. The formulation sums the total surviving restoration flows and the working flows over the total demand units considered for each span pair failure. Constraint (3.4.9) requires the dual failure restorability value $R_2^r(i,j)$ to be equal

to the specified dual failure restorability value. This is the basic component of model 1 formulation, it ensures that upon failure of any given pair of spans *i* and *j*, the minimum specified dual failure restorability value is guaranteed. Model 2 is obtained by replacing constraint (3.4.9) with constraints (3.4.10) through (3.4.13) as shown below.

Model 2 Component of Average Dual Failure Restorability:

$$R_2^r \le \frac{\sum_{\forall i,j \in S | i \ne j} R_2^r(i,j)}{|S| \times (|S| - 1)} \qquad \forall r \in D \tag{3.4.10}$$

$$R_2 \le \frac{\sum_{\forall r \in D} R_2^r}{|D|} \tag{3.4.11}$$

$$R_2 \le 1 \tag{3.4.12}$$

$$R_2 \ge R_2^* \tag{3.4.13}$$

Constraints (3.4.10) through (3.4.13) calculate the average dual failure restorability of the entire network and ensure that the average dual failure restorability is equal to the specified dual failure restorability. Constraint (3.4.10) calculates the average $R_2^r(i,j)$ value over all span pairs in the network. Constraint (3.4.11) computes the average of dual failure restorability over all demand relations *r,* to derive the average R_2 value for the network, which must not exceed unity in (3.4.12). Finally, constraint (3.4.13) ensures that the overall average R_2 value is at least the minimum specified limit of R_2^*.

3.5. Dual Failure Restorability in *p*-Cycle Networks

The dual failure restorability model design approach in *p*-cycle networks is similar to the approach used in the span restoration mechanism. The restoration of an on-cycle span in a *p*-cycle is performed by rerouting the demands on the failed span through the surviving portion of the *p*-cycle. The allocation of spare capacity for *p*-cycle restoration depends on whether two on-cycle spans fail or a

combination of an on-cycle and a straddling span fails, or two straddling spans fail. Another important factor to consider is the order of span failure. Unlike the other restoration mechanisms, the order of span pair failure in *p*-cycle networks has a more significant impact on the how the restoration is performed. For this reason, more detail is given in explaining the different failure scenarios and how the dual failure restorability value is derived in each case. We consider a number of dual failure scenarios and analyze the restoration capacity provided by *p*-cycles as affected by the failed span pairs and show how each component of the dual failure restorability value was formulated. The ILP formulation of *p*-cycle models in this work is an extended version of previous work in [52] and now in [74]. Therefore, in the next few sections we present almost verbatim some of the work in [74] and conclude with a detailed description of the models.

3.5.1. Dual Failure Scenarios in *p*-Cycle Networks

Some of the notations used in describing failure scenarios are also used in formulating the models; we define the complete set of notations before introducing the ILP model.

S is the set of all spans in the network, indexed by i. S^2 is the set of the entire span pairs indexed by i and j, where $i \neq j$. D is the set of O-D lightpath demands in the network indexed by r. P is the set of eligible p-cycles in the network indexed by p, and $P^{i,j}$ is the set of eligible p-cycles that cross spans i and j. Q^r is the set of all eligible working routes for the demand relation r indexed by q^r, and $Q^{r,i,j}$ is the set of working routes used by demand relation r that cross spans i and j, indexed by $q^{r,i,j}$. Input parameters include w_i, the amount working capacity on span I, and $x_{i,p} \in \{0, 1, 2\}$ are input parameters that describe whether span i cannot be protected by a particular cycle p ($x_{i,p} = 0$), i is an on-cycle span ($x_{i,p} = 1$), or i is a straddling span ($x_{i,p} = 2$). Decision variables include n_p, a non-negative decision variable representing the number of copies of p-cycle p used, and $n_{i,j,p}$ is a non-negative decision variable indicating the number of copies of p-cycle p used to restore span i if span j has also failed. $g^{r,q}$ is the amount of demand flow assigned to working route q of demand relation r. $R_{2i}(j)$ is the dual failure restorability of

span i given that span j has also failed. R_2 is the average dual failure restorability of the network.

An individual failure scenario for each pair of spans in a p-cycle network is represented by $R_{2i}^{x}(j)$, a non-negative decision variable computing the contribution of each scenario x, where $x \in \{1,2\ldots5\}$ for the dual failure restorability of span i in the event that span j has also failed. We begin by showing how the $R_{2i}^{x}(j)$ values are derived.

In dual failure scenario 1, $x_{i,p} = 1$ or 2 and $x_{j,p} = 0$ when one failed span i is either on a p-cycle p or a straddling span for p-cycle p, while the other failed span j is neither an on-cycle nor a straddling span for p-cycle p (failure order doesn't matter). Figure 3.5.1 shows the illustration of failure scenario 1. In Figure 3.5.1(a) the p-cycle (N1-N2-N3-N4-N5) is cut upon failure of span i, followed by the failure of span j. The failure of span j does not affect the restoration capacity of the p-cycle provided to span i. Hence in Figure 3.5.1(b), the restoration path is formed by the surviving portion of the p-cycle around the end nodes of the failed span i.

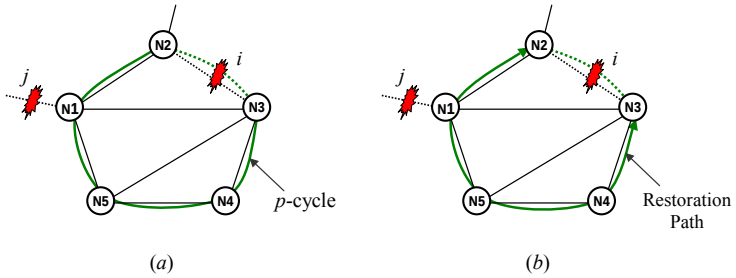

Figure 3.5.1-Illustration of dual failure scenario 1 in p-cycle networks.

In scenario 1, equation (3.5.1), the number of restoration routes available on p-cycle p to restore failed span i is the minimum of w_i (the working capacity of span i) and the product of $x_{i,p}$ and n_p (the number of copies of p-cycle p). $R_{2i}(j)$ will therefore be the sum of that minimum value for all p-cycle p divided by w_i.

$$R_{2i}^{1}(j) = \frac{\min\left(w_i, \sum_{\forall p \in P \mid x_{i,p} \neq 0, x_{j,p}=0} x_{i,p} \cdot n_p\right)}{w_i} \qquad \forall (i,j) \in S^2 \mid i \neq j \qquad (3.5.1)$$

Note that we don't use the $n_{i,j,p}$ variables since the working channels on span i will use all the restoration routes available to them while working channels on span j will use none (a p-cycle can't protect working channels on an off-cycle span).

In failure scenario 2, $x_{i,p} = 1$ and $x_{j,p} = 1$ meaning that both span failures involve on-cycle spans i and j to p-cycle p. This failure scenario is the key difference between the formulation presented here and the work in [52]. In the prior work [52], the equation was simply $R_{2i}^2(j) = 0$ because there would be no dual-failure restorability from a p-cycle struck by a pair of span failures. Figure 3.5.2 illustrates failure scenario 2. Figure 3.5.2(a) and Figure 3.5.2(b) show failure of two adjacent spans i and j, and the rerouting of the working route, respectively. Any working route through the O-D node pair (N1-N3), with the p-cycle (N1-N2-N3-N4-N5) which transverses both on-cycle spans i and j, can now be considered restorable when spans i and j fail. The working route transverses spans i and j can be restored through the restoration paths (N1-N5-N4-N3) formed around the end nodes (N1-N3) of the failed spans, as shown in Figure 3.5.2(b).

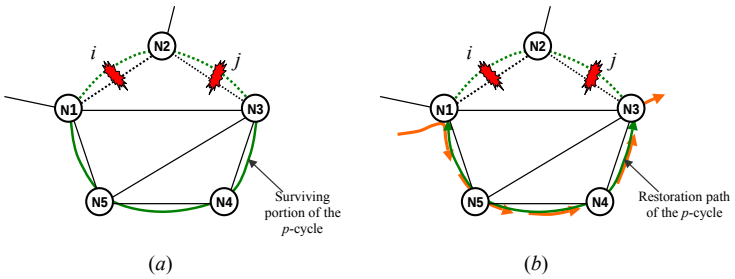

Figure 3.5.2-Illustration of dual failure scenario 2 in p-cycle networks.

The dual-failure restorability of span i from scenario 2, therefore, is the proportion of working lightpaths on span i that also pass through span j (which is itself also on the p-cycle), or the proportion of working channels on span i that can be protected by the p-cycle (one for each copy of the p-cycle), whichever is smaller. Equation (3.5.2) estimates the dual failure restorability value for this scenario.

$$R_{2i}^2(j) = \min\left(\frac{\sum_{\forall r \in D, \forall q \in Q^{r,i,j}} g^{r,q}, \sum_{\forall p \in P^{i,j}} n_p}{w_i} \right) \qquad \forall (i,j) \in S^2 \mid i \neq j \qquad (3.5.2)$$

From equation (3.5.2), $R_{2i}^{2}(j)$ is estimated as the minimum of the ratios of working flow on span *i* over the working capacity w_i and the number of available restoration units (*p*-cycle units) on span *i* over the working capacity w_i on span *i*.

In failure scenario 3, $x_{i,p} = 1$ and $x_{j,p} = 2$, where failed span *i* is on *p*-cycle *p* and failed span *j* is a straddling span of *p*-cycle *p*. Figure 3.5.3 illustrates this scenario. Figure 3.5.3(*a*) and (*b*) show both span failures, and the restoration routes formed to restore demands on the affected working routes on span *i*, when the second span *j* has also failed.

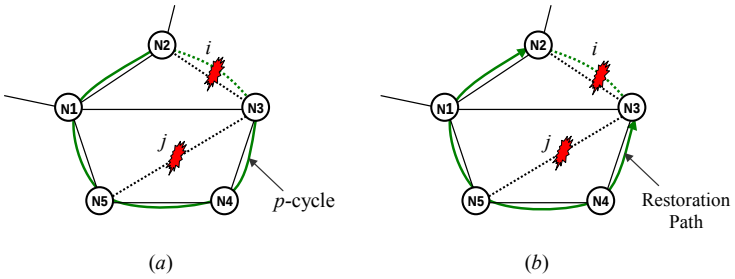

Figure 3.5.3-Illustration of dual failure scenario 3 in *p*-cycle networks.

Equation (3.5.4) applies to failure scenario 3 and here we use the $n_{i,j,p}$ variables (defined earlier) to properly assign restoration routes in the *p*-cycle to working channels on one of the failed spans. That exact assignment will be done within the overall ILP model, but we also need to include an equation to ensure that the restoration routes on *p*-cycle *p* used to restore working channels from span *i* when span *j* has also failed are not also used to restore working channels on span *j* when span *i* has also failed (which describes the same scenario but in the reverse order of failure). That is done by recognizing that in this particular scenario, the total of $n_{i,j,p}$ and $n_{j,i,p}$ cannot be any greater than n_p, the total number of copies of *p*-cycle *p*:

$$n_{i,j,p} + n_{j,i,p} \le n_p \qquad \forall p \in P,\ \forall (i,j) \in S^2 \mid i \neq j\,. \qquad (3.5.3)$$

Therefore, variables $n_{i,j,p}$ and $n_{j,i,p}$ represent the proportions of the total restoration capacity n_p of the *p*-cycle *p* available to restore spans *i* and *j,* respectively. The dual failure restorability of span *i* in the event of failure of span *j* is given in equation (3.5.4) as:

$$R_{2i}^{3}(j) = \frac{\sum_{\forall p \in P \mid x_{i,p}=1, x_{j,p}=2} n_{i,j,p}}{w_i} \qquad \forall (i,j) \in S^2 \mid i \neq j . \tag{3.5.4}$$

Dual failure scenario 4 is conceptually identical to failure scenario 3, except that failed span i is a straddling span for p-cycle p and failed span j is an on-cycle span (that is, $x_{i,p} = 2$ and $x_{j,p} = 1$). This manifests as a simple swap of the subscripts under the summation of equation (3.5.5).

$$R_{2i}^{4}(j) = \frac{\sum_{\forall p \in P \mid x_{i,p}=2, x_{j,p}=1} n_{i,j,p}}{w_i} \qquad \forall (i,j) \in S^2 \mid i \neq j . \tag{3.5.5}$$

The variables $n_{i,j,p}$ and $n_{j,i,p}$ in equation (3.5.3), introduced in scenario 3, are also required to assign the restoration capacity appropriately to the failed spans. Therefore equation (3.5.3) will be applied to this scenario.

In the final failure scenario (scenario 5), $x_{i,p} = 2$ and $x_{j,p} = 2$, where both failed spans are straddling spans for p-cycle p. Figure 3.5.4(a) and Figure 3.5.4(b) show the two failed spans and the restoration routes formed to provide restoration capacity for the failed spans, respectively.

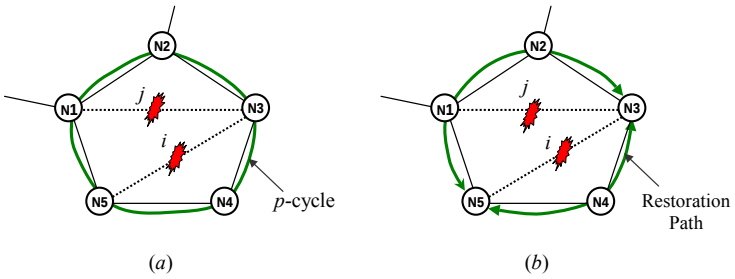

(a) (b)

Figure 3.5.4-Illustration of dual failure scenario 5 in p-cycle networks.

In this failure combination, we use the same $R_{2i}(j)$ calculation as the one in equations (3.5.4) and (3.5.5) for the previous two scenarios except that the subscript under the summation changes, as shown in equation (3.5.6).

$$R_{2i}^{5}(j) = \frac{\sum_{\forall p \in P \mid x_{i,p}=2, x_{j,p}=2} n_{i,j,p}}{w_i} \qquad \forall (i,j) \in S^2 \mid i \neq j . \tag{3.5.6}$$

A key difference, however, is how the $n_{i,j,p}$ variables are assigned. Recognizing that the two failed spans can individually or jointly make use of up to two restoration routes per copy of *p*-cycle *p*, we calculate the values of the $n_{i,j,p}$ variables as shown in equation (3.5.7).

$$2 \cdot n_p \geq n_{i,j,p} + n_{j,i,p} \qquad \forall p \in P,\ \forall (i,j) \in S^2 \mid i \neq j\,. \qquad (3.5.7)$$

We note that in some circumstances the failed spans in dual failure scenario 5 might actually cross each other. In other words, the protection path used to restore working channels on one failed straddling span must cross one of the end-nodes of the other failed straddling span. If that is the case, then a single copy of the p-cycle cannot provide a restoration route for both failed spans, though it can still provide two restoration routes for working channels on one of the spans. In these rare cases, equation (3.5.7) will not strictly hold, but our experience and a survey of a large number of eligible *p*-cycles in our test networks showed that these cases are so exceedingly rare that the error introduced in the R_2 calculations is negligible.

3.5.2. $R_{2i}(j)$ Contributions from Failure Scenarios

We define all of the above $R_{2i}(j)$ values individually but, in a real network, any pair of failed spans will likely meet the conditions for any or all of the dual-failure scenarios simultaneously for different *p*-cycles. We then combine all of these scenarios together in a single $R_{2i}(j)$ calculation:

$$R_{2i}(j) = \min\left(1, \sum_{\forall x \in 1\ldots5} R^x_{2i}(j)\right) \qquad \forall (i,j) \in S^2 \mid i \neq j\,. \qquad (3.5.8)$$

By definition, the maximum dual-failure restorability value can never be greater than 1.0, so we must also include the "minimum" function in the $R_{2i}(j)$ calculation as well as in the $R^1_{2i}(j)$ and $R^2_{2i}(j)$ calculations. Though the resulting equations in (3.5.1), (3.5.2), and (3.5.8) are non-linear, we can easily linearize them by using a pair of constraints for each. Since ILP in general seeks to make $R^1_{2i}(j)$, $R^2_{2i}(j)$,

and $R_{2i}(j)$ as large as needed, we can replace equations (3.5.1), (3.5.2), and (3.5.8) with the following six equations:

$$R_{2i}^{1}(j) \le 1 \qquad \forall (i,j) \in S^2 \mid i \ne j \tag{3.5.9}$$

$$R_{2i}^{1}(j) = \frac{\sum_{\forall p \in P \mid x_{i,p} \ne 0, x_{j,p} = 0} x_{i,p} \cdot n_p}{w_i} \qquad \forall (i,j) \in S^2 \mid i \ne j \tag{3.5.10}$$

$$R_{2i}^{2}(j) = \frac{\sum_{\forall r \in D, \forall q \in Q^{r,i,j}} g^{r,q}}{w_i} \qquad \forall (i,j) \in S^2 \mid i \ne j \tag{3.5.11}$$

$$R_{2i}^{2}(j) = \frac{\sum_{\forall p \in P^{i,j}} n_p}{w_i} \qquad \forall (i,j) \in S^2 \mid i \ne j \tag{3.5.12}$$

$$R_{2i}(j) \le 1 \qquad \forall (i,j) \in S^2 \mid i \ne j \tag{3.5.13}$$

3.5.3. ILP Models for Dual Failure Restorability in *p*-Cycles

Before presenting the ILP models, we define the complete set of notations used in the formulation of the models, including some others that have already been defined in earlier sections.

Notations:

Sets:

S is the set of all spans in the network indexed by i.

S^2 is the set of all the span pairs (i, j) in the network where $i \ne j$.

D is the set of O-D lightpath demands in the network indexed by r.

P is the set of enumerated eligible p-cycles in the network indexed by p.

$P^{i,j}$ is the set of eligible p-cycles that cross spans i and j.

Q^r is the set of all eligible working routes between O-D pairs for every demand relation r, indexed by q^r.

$Q^{r,i,j}$ is the set of working routes used by demand relation r that cross spans i and j, indexed by $q^{r,i,j}$.

$S^{r,q}$ is the set of all spans crossed by any route q in the demand relation r.

Input Parameters:

w_i is the amount working capacity on span i.

c_i is the unit cost of demands placed on a route q between O-D of a demand relation r.

$w_{x,i}^{r,q} \in \{0,1\}$ is an input parameter that defines whether a working route q for demand relation r crosses span i (i.e., $w_{x,i}^{r,q} = 1$ if working route q of demand relation r crosses span i, $w_{x,i}^{r,q} = 0$ otherwise).

$\delta_{i,p} \in \{0,1\}$ is an input parameter, $\delta_{i,p} = 1$ if span i is on p-cycle p, $\delta_{i,p} = 0$ otherwise (i.e., $\delta_{i,p} = 1$ if $x_{i,p} = 1$, and $\delta_{i,p} = 0$ if $x_{i,p} \neq 1$).

d^r is the amount of demand units between O-D of a demand relation r.

$x_{i,p} \in \{0, 1, 2\}$ is a input parameter, $x_{i,p} = 0$ indicates that span i is neither an on-cycle span nor a straddling span to p-cycle p, while $x_{i,p} = 1$ indicates that span i is an on-cycle span to p-cycle p and $x_{i,p} = 2$ indicates that span i is a straddling span to p-cycle p.

R_2^* is the specified level of dual failure restorability required in the network.

Decision Variables:

$g^{r,q}$ is the amount of demand flow assigned to working route q of demand relation r.

n_p is a non-negative decision variable representing the number of copies of p-cycle p used in the network.

$n_{i,j,p}$ is a non-negative decision variable representing the number of copies of p-cycle p used to restore span i if span j has also failed.

s_i is a non-negative decision variable representing the spare capacity on span i.

$R_{2i}(j)$ is the dual failure restorability of span i given that span j has also failed.

R_2 is the average dual failure restorability for the entire network.

It is important to note that the contribution of individual dual failure restorability in each scenario is summed up in equation (3.5.8), which is represented by constraint (3.5.17) in the model below.

The Model:

Minimize: $$\sum_{\forall i \in S} c_i \cdot (s_i + w_i) \qquad (3.5.14)$$

Subject to:

$$w_i \leq \sum_{\forall p \in P} x_{i,p} \cdot n_p \qquad \forall i \in S \qquad (3.5.15)$$

$$s_j = \sum_{\forall p \in P} \delta_{j,p} \cdot n_p \qquad \forall j \in S \qquad (3.5.16)$$

$$R_{2i}(j) \leq \sum_{\forall x \in 1...5} R^x_{2i}(j) \qquad \forall (i,j) \in S^2 \mid i \neq j \qquad (3.5.17)$$

$$R_{2i}(j) \geq R_2^* \qquad \forall (i,j) \in S^2 \qquad (3.5.18)$$

The objective function (3.5.14) minimizes the total capacity cost. Constraint (3.5.15) ensures that sufficient restoration capacity is provided in the p-cycles to fully protect all working channels on span i. Constraint (3.5.16) computes the spare capacity required on span j by summing up the total number of p-cycle copies on span j. The objective function (3.5.14) and constraints (3.5.16) and (3.5.16) form the conventional single failure restorability design model for p-cycle networks. Constraint (3.5.17), as mentioned earlier, is obtained by adding the individual dual failure restorability values computed in each failure scenario. Note that equation (3.5.17) no longer contains the "minimum function" as in equation (3.5.8). This is because linearization of the variables in the constraints eliminates the need to include the "minimum function." Constraint (3.5.18) ensures that the dual failure restorability value is at least equal to the specified minimum level of

dual failure restorability required. The objective function (3.5.14) and constraints (3.5.15) through (3.5.18) constitute model 1 of the dual failure restorability in this work. The remaining constraints (3.5.19) through (3.5.22) can replace constraint (3.5.18) to form model 2 of the dual failure restorability model. In the formulation, the model finds the average dual failure restorability of the *p*-cycle network. Constraint (3.5.19) computes the average dual failure restorability of span *i* given that span *j* has also failed. It sums the individual $R_{2i}^{x}(j) \mid x \in 1,...,5$ values over all span pairs (*i*, *j*) in the network. Constraint (3.5.20) restricts the upper bound of R_{2i} variables to unity (meaning that $0 \le R_{2i} \le 1$). Constraint (3.5.21) finds the overall network average dual failure restorability R_2 over all spans and constraint (3.5.22) ensures that the minimum requirement is met.

Model 2 Components of Average Dual Failure Restorability:

$$R_{2i} = \frac{\sum_{\forall j \in S \mid i \neq j} R_{2i}(j)}{|S| - 1} \qquad \forall i \in S \tag{3.5.19}$$

$$R_{2i} \le 1 \qquad \forall i \in S \tag{3.5.20}$$

$$R_2 = \frac{\sum_{\forall i \in S} R_{2i}}{|S|} \tag{3.5.21}$$

$$R_2 \ge R_2^* \tag{3.5.22}$$

The overall network dual failure restorability R_2 is calculated by averaging individual R_{2i} over the cardinality of spans in the network. Equation (3.5.22) specifies the minimum dual failure restorability R_2^* required. With this constraint, the network dual failure restorability is forced to be at least the specified value.

Chapter 4

Experimental Methods

4. Simulation Method and Test Networks

The ILP model was implemented in the AMPL 10.0 mathematical programming language and solved using the CPLEX 10.0 optimization software on a Sun UltraSparc III machine with 4-processors running at 900 MHz and with 16 GB of RAM (for the 10-node and 15-node networks) and a dual processor AMD Opteron 248 Windows 2000 desktop PC running at 2.19 GHz with 2 GB of RAM (for the 10-node and 25-node networks). We used a CPLEX mipgap setting of 0.0025, meaning our solutions are guaranteed to be within 0.25% of optimal.

4.1. Pre-solve Processing of Network Data

4.1.1. Network Topology

The network topology describes the physical layout of the nodes and the spans (links), i.e., the location of each node and the lengths of the spans connecting each node pair in the network. The length of each span is measured by the *Euclidean distance* of the 2-dimensional (2-D) points between the adjacent node pair of the span. For example, the length of span whose end nodes (O, D) are located at the points on a 2-D plane where $O = (O_x, O_y)$ and $D = (D_x, D_y)$ is expressed as $(O, D) = \sqrt{(O_x - D_x)^2 + (O_y - D_y)^2}$. We use the unit cost associated with capacity placement on each span in the network as equivalent to the length of the individual span. This means that unless otherwise specified, the cost of placing a unit capacity of demand lightpath or channel through that span is equal to the length of the span. In reality, the associated costs of designing a transport network will include fixed costs, such as right-of-way cost, leases, licensing, permits, and other "span establishment costs". In this work, we considered only incremental costs related to placing capacity to those spans, such as additional fibre,

wavelength terminations, line cards, amplifiers, etc. We assume that fixed costs will remain fairly constant with changes in capacity on the spans (and so we ignore them for our purposes), while the incremental costs will be directly proportional to the amount of capacity placed on a span. Also modularity and economies of scale are not considered. Therefore, each demand flow is assigned only to integer capacity units.

Each of our experimental network topologies is known in advance and each network family is headed by a master network with an average nodal degree $\bar{d}$ of 4.0. The master networks are 10, 12, 15, and 18 node networks. We named the networks in each network family according to the number of nodes and spans contained in each network. For example, the 10-node, 20-span network family is named *10n20s*, where *n* is the number of nodes, and *s* is the number of spans. For specific network connectivity we simply attach the number of spans to the name of the master network. For example, the $\bar{d}$ =2.6 network in the 10n20s network family contains only 13 spans, so we call it the *10n20s-13s* network. Figure 4.1.1 shows some of the master networks used in the experiments. Using the master networks of each network family, the sparser networks are generated by pseudo-randomly reducing the number of spans in the network. Each subsequent sparser network within the network family is identical to its next higher-degree network family member except that one or more spans have been removed from it. For example, in the 20-node, 40-span network, we randomly remove four spans to generate a lower average nodal degree network of $\bar{d} = 3.6$ and again randomly remove four more spans from the $\bar{d}$ =3.6 network to create the $\bar{d} = 3.2$ nodal degree network, and so on (see APPENDIX A for other network connectivities used).

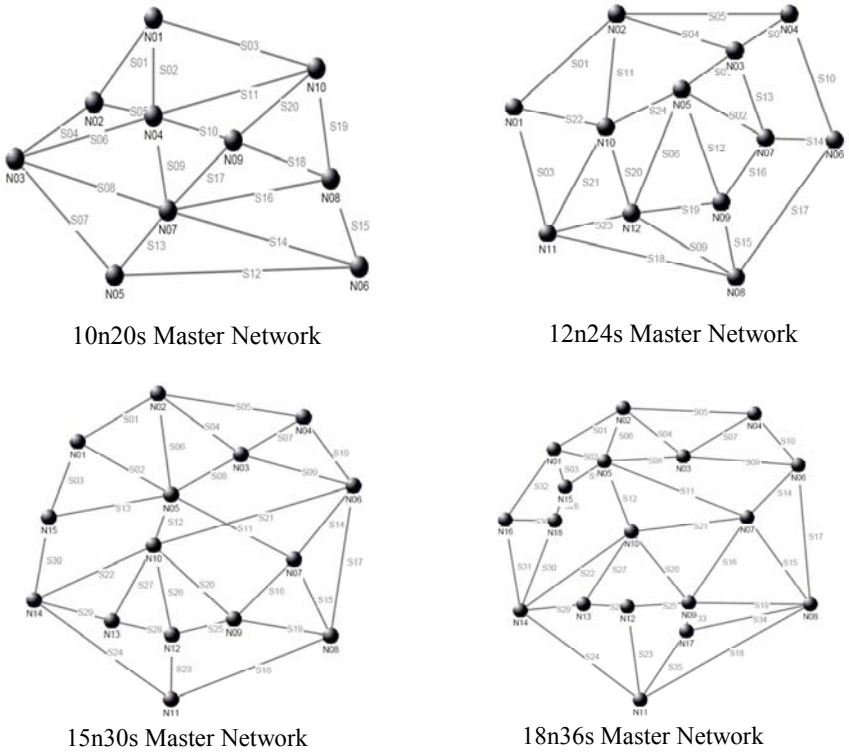

Figure 4.1.1-Master networks for network families.

In creating the lower degree networks we ensure that span removals are subject to bi-connectivity constraints, that is, we ensure that nodes are at least a degree of $\bar{d} \geq 2$. Other information about network topology is contained in the topology file of a network. This information includes the *mean time before failure* (MTBF) and *mean time to repair* (MTTR), which are parameters required for other computations in the network.

4.1.2. Demand Models

The number of integer lightpath demands, determine the number of lightpaths required to satisfy the demand flow between the O-D node pairs. In these simulations, integer demand units ranging from 1 to 10 units inclusive were randomly assigned to each node pair. In real transport network design and planning, assignment of lightpath capacity requires extensive study of the nature of demand patterns between the various points (cities) and other factors such as future expansion and over-subscription. Many models are used to establish the demand exchange pattern for various networks; some of these-*gravity-based*

model, *uniform random model*, *nondistance-weighted attraction model*, *bimodal uniform random model*, and *node size based model*-can be found in [37], [44], and [81]. A demand matrix table is often regenerated for entire networks and updated frequently if the demands are dynamically assigned. The demands exchanged between networks are used by all the network connectivities in the same network family, since the number of nodes in the network is not affected by the connectivity of the network. APPENDIX B shows the demand data and some samples of network topology data used in the experiments for various network families.

4.1.3. Enumeration of Eligible Routes

Some of the earliest works that describe the use of ILP methods for the design of survivable mesh networks are those of [37] and [73]. The method is an *arc-path* approach and uses the network's pre-processed topology and demand data to enumerate a set of distinct logical routes between various O-D nodes. Another type of approach, the *transhipment* or *network flow* type of model uses source and sink nodes for each lightpath demand, and all other nodes act as transhipment nodes or intermediaries where a conservation of demand flow into the node must correspond to flow out. The drawbacks with this approach are (1) that there is no explicit description of the restoration routes selected, meaning some other follow-up method will be needed to do so, and (2) there is no easy means of specifying any restrictions to the restoration routes for concerns such as length, and transmission loss [19]. In real network design problems, the size of the eligible routes enumerated for the ILP has a significant impact on the quality of the solution in terms of optimality. Unless all the eligible routes existing between each O-D node pair are enumerated for the solver to use, it cannot be guaranteed that the solution obtained is optimal. Too large an eligible route set results in excessive runtime, while too small an eligible route set results in design solutions that could be significantly sub-optimal. The theoretical estimate for the total number of all distinct routes possible in the network is given by $O(2^s)$ [37], where s is the number of spans in the network. Even though these problems are known to

be NP-hard [52], they prove to be difficult to solve and do not scale considerably well with increasing network sizes, connectivities, or numbers of eligible routes. Depending on the size of the network, this could mean hundreds of thousands or even millions of possible routes to enumerate and consider for each iteration, resulting in excessive runtimes. To reduce the size of the problem and make it solvable in a reasonably short time, we limited the required size of eligible restoration routes to 100 in span restoration, the eligible restoration routes to 100 in DSP and path restoration, and the eligible *p*-cycles to 500 for the entire *p*-cycle networks. The actual number of eligible routes used may vary with the survivability schemes and the network connectivity. Some of the smaller networks might not contain the specified amount, and the size of eligible restoration routes indicated is specific to each span in span restorable networks, and to each demand for DSP and path restoration.

4.1.4. Design Optimization

There are approximately 164 test case networks used in this study. All the networks are solved using CPLEX, which is developed by ILOG CPLEX. It uses a number of mathematical algorithms such as the *simplex algorithm* for LPs, the *barrier algorithm* for QPs and the *branch-and-bound algorithm* for MIPs [83]. CPLEX optimization runtimes for the networks ranged from minutes to several hours depending on the size of the networks. Typically, the higher the specified dual failure restorability level required and the more richly connected the network is, the more optimization time is needed. The very large networks in most cases took a day or two to solve, depending on the survivability mechanism. The network data is pre-processed before routing the working routes and generating eligible restoration route sets and other parameters for the optimization process. Some of the AMPL programs are shown in APPENDIX C.

Chapter 5

Experimental Results[2]

5. Results and Analysis

The solutions obtained from the test-case networks for the different survivability schemes are separated into two categories, each category corresponding to the different ILP model in each survivability scheme. The first ILP formulation is referred to as "model 1" and the second ILP formulation, a variation of model 1, is referred to as "model 2." The primary difference between these two models is explained in section 3.1. In order to keep the analysis concise and clear, we show one pair of charts only for each model. These charts contain the most sparsely and the most densely connected networks from each of the 10n20s and 18n36s master network families. The charts from other nodal degree networks are presented in APPENDIX D. The charts in APPENDIX D are identical to the charts shown in the sections of this chapter. However, slight variations in trends may be noticeable where there are some unique topographical differences within the network family. In the model 1 charts, we show only networks with average nodal degrees ($\overline{d}$) from 3.0 to 4.0 $\overline{d}$, since dual failure restorability for every pair of spans requires at minimum $\overline{d} \geq 3$ for dual failure restorability to be feasible. Only network sizes above the threshold of $\overline{d} \geq 3$ can have dual failure restorability for each pair of spans. Model 1 implements the dual failure restorability of each pair of spans. The average dual failure restorability for the entire network is formulated in model 2, where individual nodes with $\overline{d} = 2.0$ are considered exclusively for single failure restorability. For example, in the 15-node network family, the dual failure restorability on each pair of spans is guaranteed if and only if the total number of spans is over 23. Otherwise, we consider the *average* dual failure restorability of all the pairs of spans in the networks using model 2 of the ILP design models. There are basically two types of charts presented in this chapter. The first chart

[2] Some of the data and charts presented in this chapter have been published in [74],[82], and [86].

(example Figure 5.1.1 and Figure 5.1.2) simply shows capacity cost obtained at various levels of dual failure restorability in all network connectivities normalized to the capacity cost of $\overline{d}$ =4.0 network and at R_2=0. Normalizing capacity costs data across all network connectivities in the same network family shows where each node degree network stands in terms of capacity cost. For example, in the 10-node network family, we obtained various capacity cost data of the $\overline{d}$ =3.2, $\overline{d}$ =3.4, $\overline{d}$ =3.6, $\overline{d}$ =3.8, and $\overline{d}$ =4.0 networks at R_2^*=0, R_2^*=0.1, R_2^*=0.2,…, R_2^*=1.0, (50 capacity cost data points), and then normalized to the least capacity cost data point in the network family, which is at R_2^*=0 of the $\overline{d}$ =4.0 network. We then plot the normalized capacity costs on the *y*-axis and corresponding levels of dual failure restorability on the *x*-axis. Similarly, the second charts (example Figure 5.1.3) shows capacity cost data that is normalized in individual network connectivity instead of the network family. For example, for $\overline{d}$ =3.2 network at R_2^*=0, R_2^*=0.1, R_2^*=0.2,…, R_2^*=1.0, (10 capacity cost data points), are normalized to capacity cost data at R_2^*=0. This enables us to also compare the increase in capacity cost at various levels of dual failure restorability in individual network connectivity.

5.1. Span Restoration Results

5.1.1. Model 1 of Span Restoration

Model 1 of the ILP models in span restoration computes the dual failure restorability of each pair of spans and requires the solution to be at minimum equal to the specified dual failure restorability limit. This means that every node pair in the network has to have at least $\overline{d} \geq 3$ for dual failure restorability of the particular pair of spans to be feasible. Otherwise, the network dual failure restorability is measured as an average of the dual failure restorability of the entire span pairs in the network. This is discussed in section 5.1.2 of the model 2 designs.

Figure 5.1.1 and Figure 5.1.2 show the normalized total capacity cost versus the specified dual failure restorability limit R_2^* for different network connectivities of the 10n20s and the 18n36s network families.

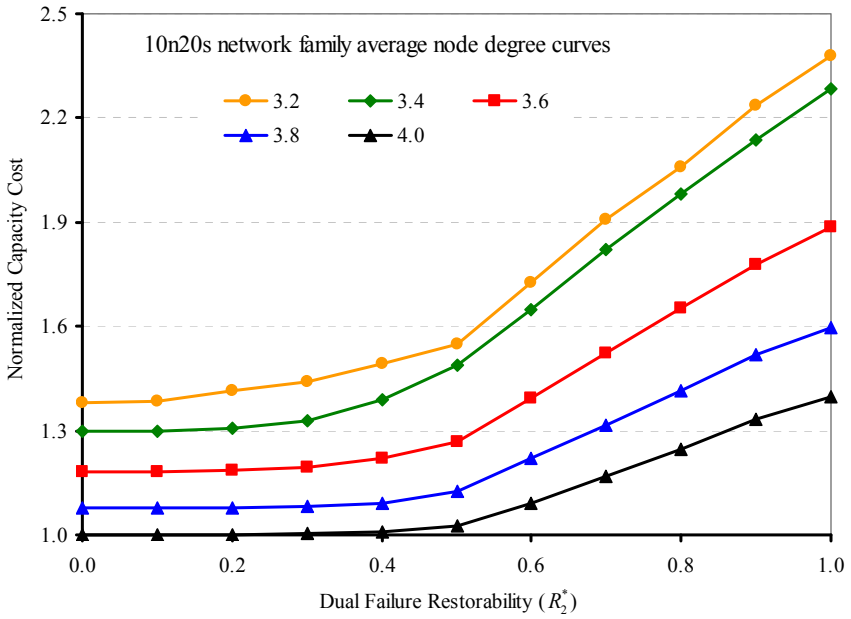

Figure 5.1.1-Dual failure restorability curves in model 1 of 10n20s span restorable network family.

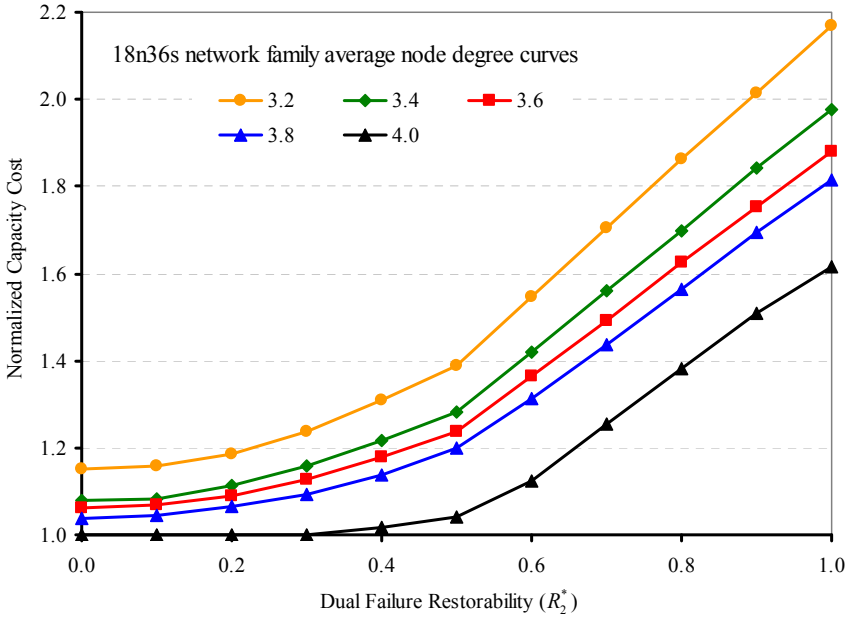

Figure 5.1.2-Dual failure restorability curves in model 1 of 18n36s span restorable network family.

The total capacity cost of each node degree network in the charts is normalized to the least capacity cost network within the network family. The least capacity cost

networks for the 10n20s and the 18n36s network families happen to be the node degree 4.0 $R_2^* = 0$. Each curve represents a particular network connectivity ranging from nodal degrees of 3.0 to 4.0. The total capacity cost of each network curve increases as the specified dual failure restorability limit approaches 100%. For networks with a lower average nodal degree we find the total capacity cost increases even more sharply as the specified dual failure restorability limit tends toward 100%. On the other hand, the total capacity cost of the highly connected networks tend to show much less increase in capacity cost, and in some cases the capacity cost remains significantly flat until the specified dual failure restorability limit reaches 40%. As expected, this shows the ability of a typical survivable mesh network optimally designed for single failure protection to achieve some level of dual failure restorability. This is similar to the findings from previous work on dual failure restorability design in [17] and [51]. Another important observation is the degree of capacity increase as compared to various network families in each survivability scheme. The rapid increase in capacity cost is significantly higher in sparsely connected networks when compared to densely connected networks. For example, in Figure 5.1.1 on the 3.2 $\bar{d}$ network, total capacity cost increases at an average of about 7.6% as the dual failure restorability limit increases by 10% compared to 4.1% for the 4.0 $\bar{d}$ network. The 18n36s network family shows a trend similar to the 10n20s network family. The 3.2 $\bar{d}$ network increases at an average rate of 5.6% in total capacity cost compared to 3.6% for the 4.0 $\bar{d}$ node network when the specified dual failure limit is increased by 10%.

Figure 5.1.3 and Figure 5.1.4 show the 10n20s and 18n36s network families, respectively, with plots of normalized total capacity cost against the specified dual failure restorability limit. In these charts normalization of the total capacity cost is performed on individual network size; the total capacity cost at various levels of specified dual failure restorability in the network is normalized to the least capacity cost (equivalent to the capacity cost at $R_2^* = 0$ of individual network connectivities). These charts show the rate of increase in capacity cost for specific

network sizes over a unit increase in dual failure restorability. The cost increase is noticeably higher for smaller sized networks (lower node degree networks) than for larger networks. For example, in Figure 5.1.3, the capacity cost of the 3.2 $\bar{d}$ network in the 10n20s network family increases more rapidly between 0.0% and 0.5% of specified dual failure restorability limit compared to the 4.0 $\bar{d}$ network that remains almost significantly flat up to the 0.4% mark. On the other hand, the individual curves in the 18n36s network family (Figure 5.1.4) respond slightly differently relative to the network sizes than the curves in the 10n20s network family. Looking closely at Figure 5.1.3, we can observe that the $\bar{d}$ =3.2 and $\bar{d}$ =4.0 network curves for the 10-node network cross paths at about $R_2^* = 0.4$. This effect is simply a result of normalizing each capacity cost data to the capacity cost at $R_2^* = 0$ for individual network connectivity curves. This means that each connectivity curve does not reflect the normalized capacity cost relative to other network connectivities in the network family. It is not unusual to find minor topological changes in one of the various network sizes that may result in slight deviation from the slopes seen in the other curves, but the general trend still holds.

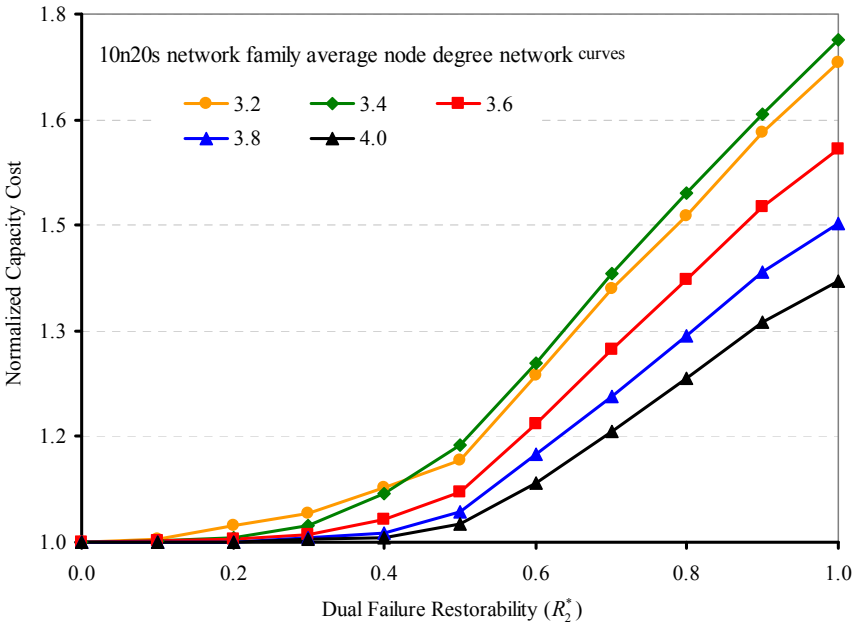

Figure 5.1.3-Rate of capacity cost increase in 10n20s span restorable network family over specified dual failure restorability limits in model 1.

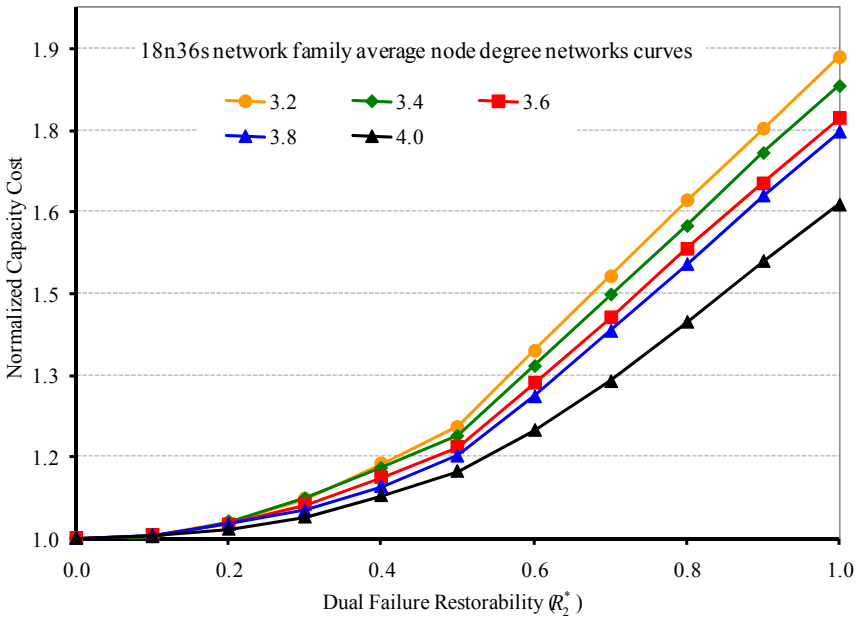

Figure 5.1.4-Rate of capacity cost increase in 18n36s span restorable network family over specified dual failure restorability limits in model 1.

We rearranged the data from the 10n20s network family to show the normalized capacity cost plotted against the average nodal degrees (various network connectivities) in Figure 5.1.5.

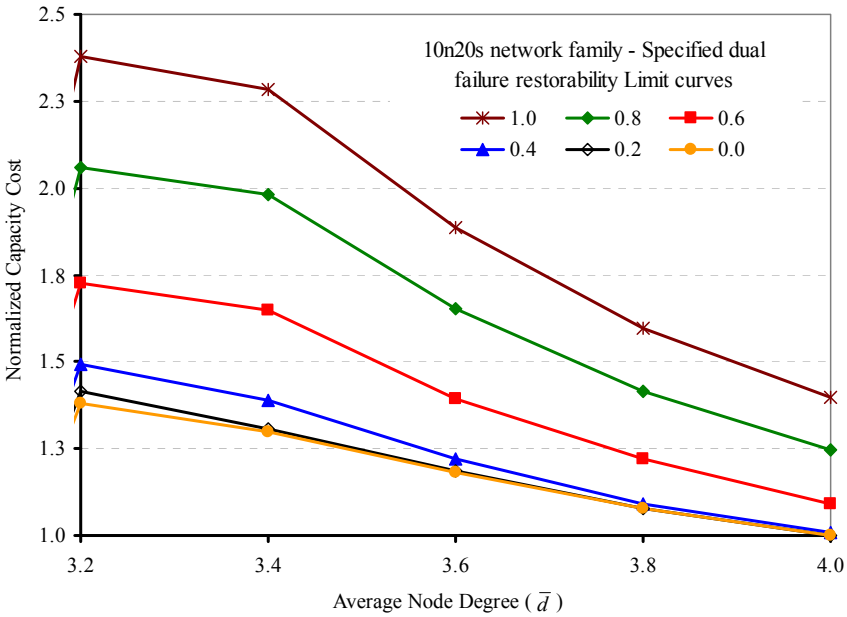

Figure 5.1.5-Capacity cost variations in different network connectivities in 10n20s network family.

Figure 5.1.5 shows that smaller networks require more capacity investments to achieve the same level as larger networks of specified dual failure restorability in the all the survivability schemes. For example, comparing the curves of $\bar{d}$ =3.2 and $\bar{d}$ =4.0 networks, the capacity cost of the $\bar{d}$ =3.2 network is nearly 40% more than that of the $\bar{d}$ =4.0 network if at least 20% of demands are restorable in the event of dual failure. In section 5.1.2 we discuss a variation of model 1 and contrast the capacity efficiency in both models.

5.1.2. Model 2 of Span Restoration

Model 2 computes the dual failure restorability of each pair of spans, averages it over the entire network, and ensures that sufficient capacity is placed to meet the average specified dual failure restorability limit. Model 2 simply requires the network *average* of dual failure restorability to satisfy the specified level, while model 1 requires that the dual failure restorability of each pair of spans meets the specified minimum. Figure 5.1.6 and Figure 5.1.7 depict data for model 2 equivalent to the data in model 1 that is shown in Figure 5.1.1 and Figure 5.1.2. Figure 5.1.6 and Figure 5.1.7 plot normalized total capacity cost against the specified dual failure restorability limit.

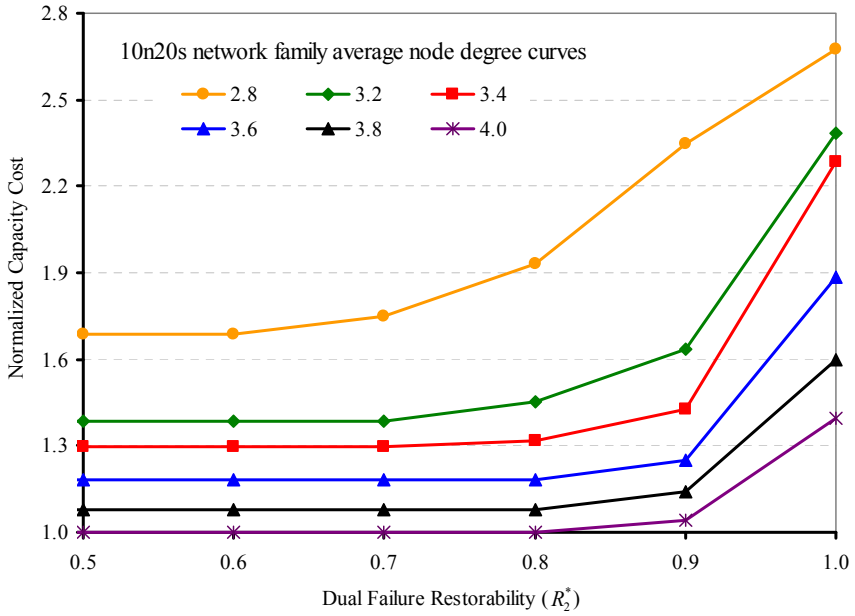

Figure 5.1.6-Dual failure restorability curves in model 2 of 10n20s span restorable network.

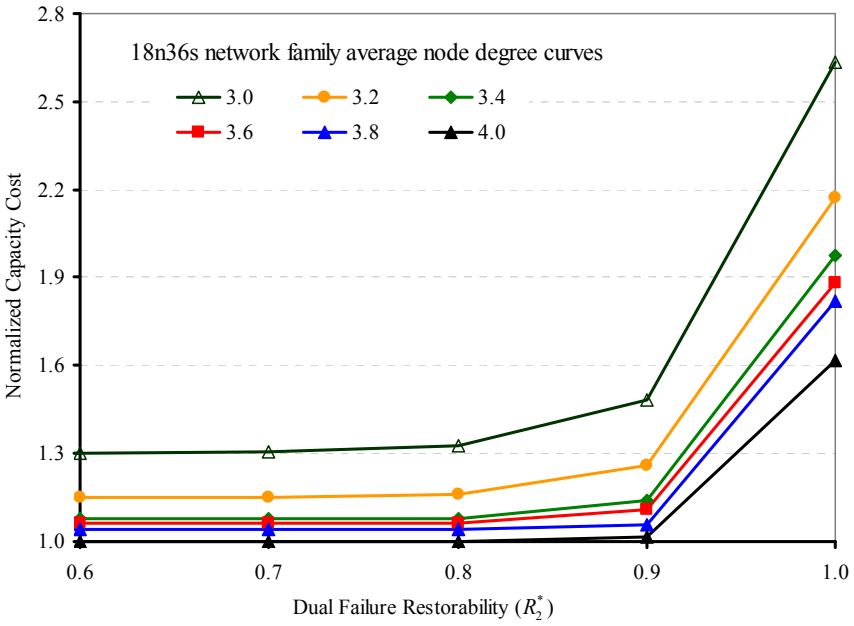

Figure 5.1.7-Dual failure restorability curves in model 2 of 18n36s span restorable network.

The trends for model 2 are similar to those for model 1; that is, as the specified dual failure restorability limit approaches 100%, the capacity cost increases significantly. The charts are truncated at $R_2^* = 0.5$ and $R_2^* = 0.6$ on the x-axis of the 10n20s and the 18n36s network families, respectively, as there is no noticeable increase in capacity cost from $R_2^* = 0$ to $R_2^* = 0.6$. The difference in the total capacity requirement in model 1 is much greater than the capacity requirement in the model 2 to provide an equivalent level of dual failure restorability. The quantitative difference between these two models and other restoration mechanisms is discussed in chapter 5.

The rate at which the total capacity requirement increases at higher levels of specified dual failure restorability limit in the sparsely connected networks is also higher, as they have lower capacity efficiency compared to the densely connected networks. Figure 5.1.8 and Figure 5.1.9 plot normalized capacity cost against the specified dual failure restorability limit for 10n20s and 18n36s network families, respectively; in this case, the capacity cost corresponding to the specified level of dual failure restorability is normalized to the least capacity cost within the individual network.

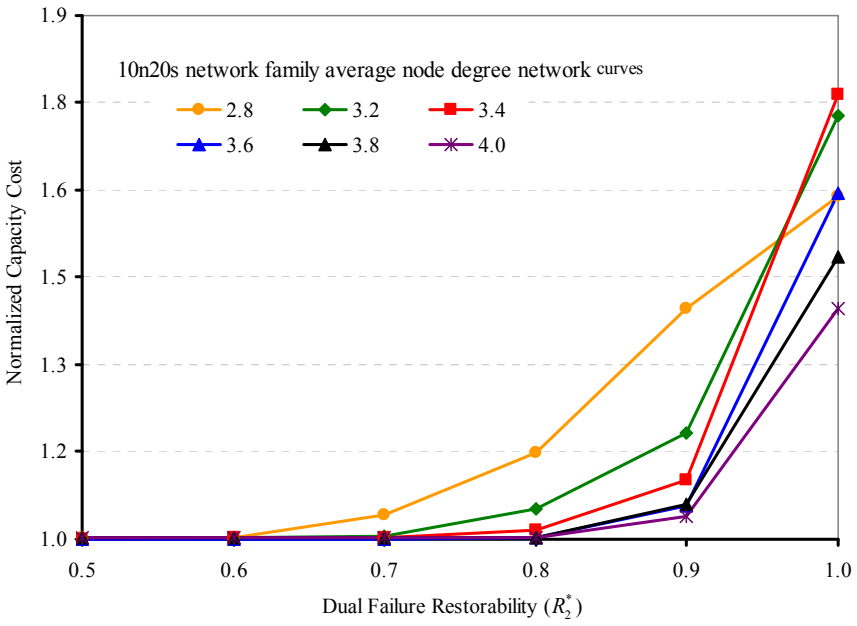

Figure 5.1.8-Rate of capacity cost increase in 10n20s span restorable network family over specified dual failure restorability limits in model 2.

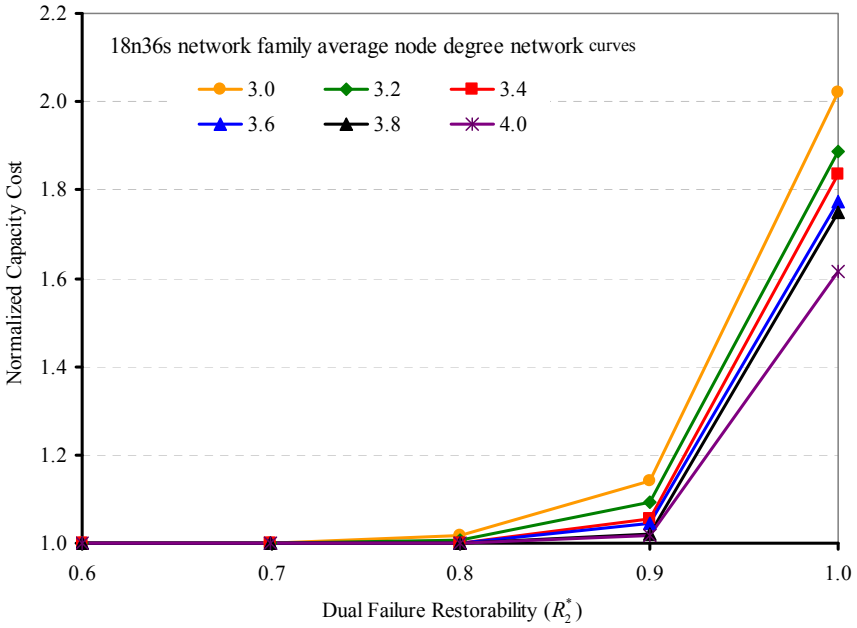

Figure 5.1.9-Rate of capacity cost increase in 18n36s span restorable network family over specified dual failure restorability limits in model 2.

Normalized capacity cost remains significantly flat in the 10-node network family up to about 50% of specified dual failure restorability. Capacity cost begins to increase from $R_2^* = 0.6$ in the 18-node network, cost is flat up to R = 0.8, then begins to rise, particularly for the most sparsely connected networks. This is in

line with the observations that no additional capacity is required in order to provide up to 40% and 50% dual failure restorability for the 10-node network and 18-node network families, respectively.

5.2. *p*-Cycle Restoration Results

5.2.1. Model 1 of *p*-Cycle Restoration

The formulation of model 1 for *p*-cycle restoration is similar to the formulation of model 1 for span restoration. Model 1 for *p*-cycle restoration also considers the capacity placement for strictly restoring a specified amount of demands on any given pair of spans that fail simultaneously. As mentioned in section 3.5 we followed the formulation approach used in [52], with an additional constraint to enhance the dual failure restorability values. Figure 5.2.1 and Figure 5.2.2 show normalized total capacity cost plotted against the minimum specified dual failure restorability R_2^*, for different network connectivities in 10n20s and 18n36s *p*-cycle networks, respectively. The curves from this model behave very much like the corresponding curves in span restoration and the curves generated in [52].

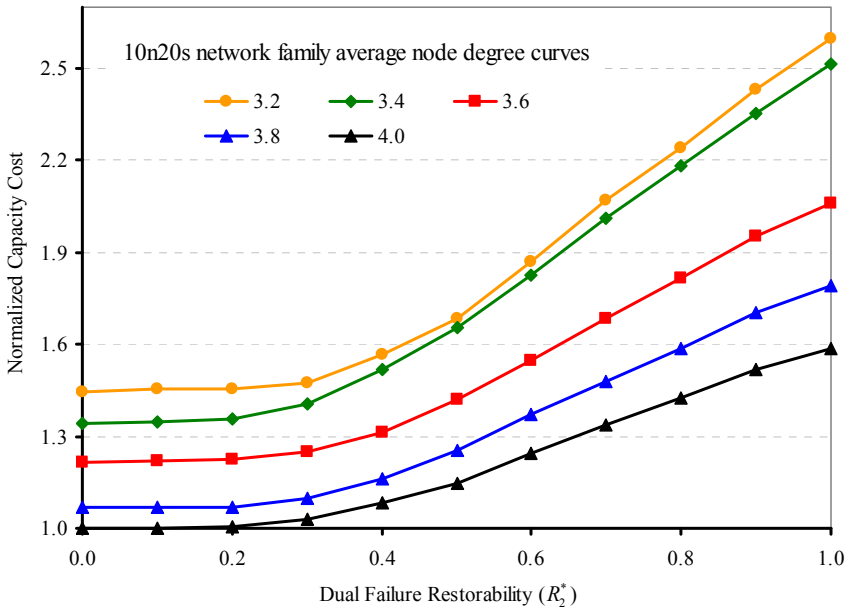

Figure 5.2.1-Dual failure restorability curves in model 1 of 10n20s *p*-cycle restorable network family.

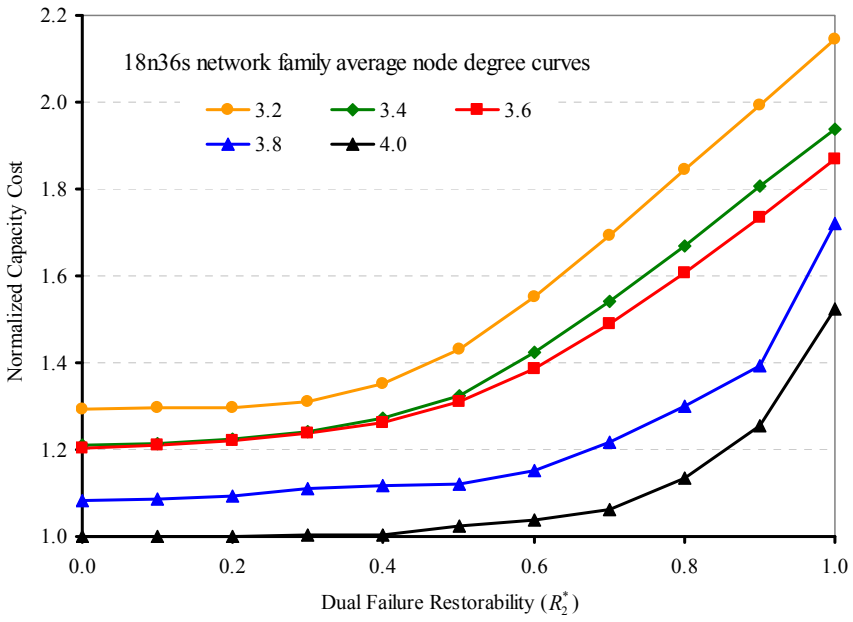

Figure 5.2.2-Dual failure restorability curves in model 1 of 18n36s *p*-cycle restorable network family.

The capacity requirement generally increases with increasing R_2^*. But our results show that much more additional capacity is required to provide the same level of dual failure restorability for each pair of spans failure in the networks compared to the previous work in [52]. The sparsely connected networks in the 10n20s network family (Figure 5.2.1) require more capacity for the same level of dual failure restorability obtainable in relatively denser networks.

Trends in model 1 of *p*-cycle restoration are typical for span restorable networks and resemble those published previously [52]. But in this model, we see a higher level of inherent dual failure restorability advantage in the fully connected network (4.0 average nodal degree network) when compared to lower nodal degree networks. For example, the 4.0 $\bar{d}$ network has about 70% inherent dual failure restorability advantage compared to about 50% advantage in the 3.8 $\bar{d}$ network and 30% advantage in the 3.6 $\bar{d}$ network. This means that no additional capacity is required to achieve dual failure restoration of 70% of the demands if any given pair of spans fails in the 4.0 $\bar{d}$ network. A look at the 3.2 average node degree network in the 10n20s network family shows that the network requires about 42.5% more capacity than the 4.0 average nodal degree network to achieve

100% single failure restorability. Also, up to about 100% more increase in capacity is required to provide 100% dual failure restorability for the 3.2 $\bar{d}$ network compared to the 4.0 $\bar{d}$ network. In the 18n36s network family, the proportion of extra capacity required in the network is much less than the capacity required for the 10n20s network family. The 4.0 $\bar{d}$ network curves in both network families also show that a larger proportion of additional capacity is required in smaller networks than in larger networks to protect the network from same level of dual failure. In the 18n36s network, no additional capacity investment is required to restore up to 70% of the demands on every pair of spans that fails, while in the 3.2 $\bar{d}$ network, the inherent dual failure restorability is slightly less than 25%. Figure 5.2.3 (the 10n20s network family) and Figure 5.2.4 (the 18n36s network family) show how the individual *p*-cycle network connectivity curves increase in capacity cost relative to the total capacity cost at 100% single failure restorability. The network capacity costs are normalized to the least capacity cost network at $R_2^* = 0$ with single failure restorability. In the 10n20s network family, nearly all the curves (3.2, 3.4, 3.6, 3.8, and 4.0) showed no increase up until about 20% specified dual failure restorability.

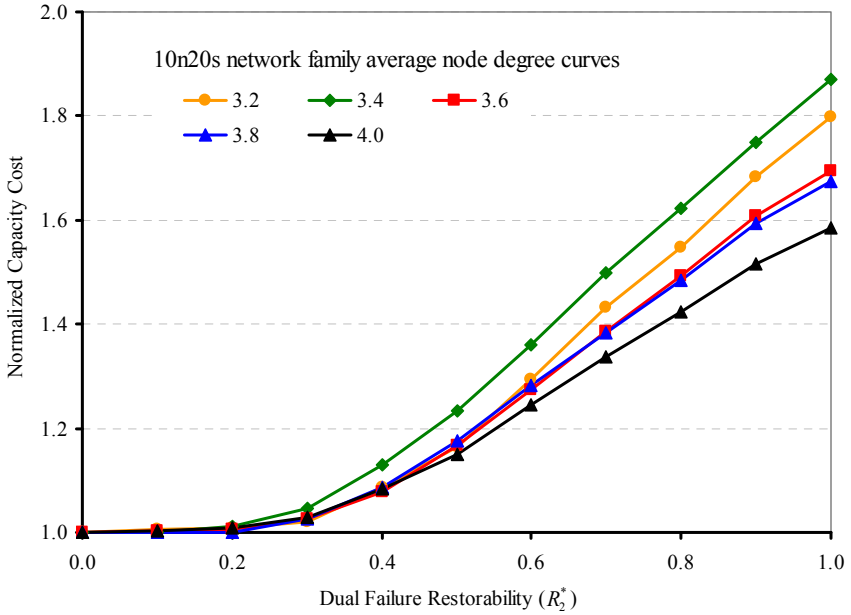

Figure 5.2.3-Rate of capacity cost increase in 10n20s *p*-cycle restorable network family over specified dual failure restorability limits in model 1.

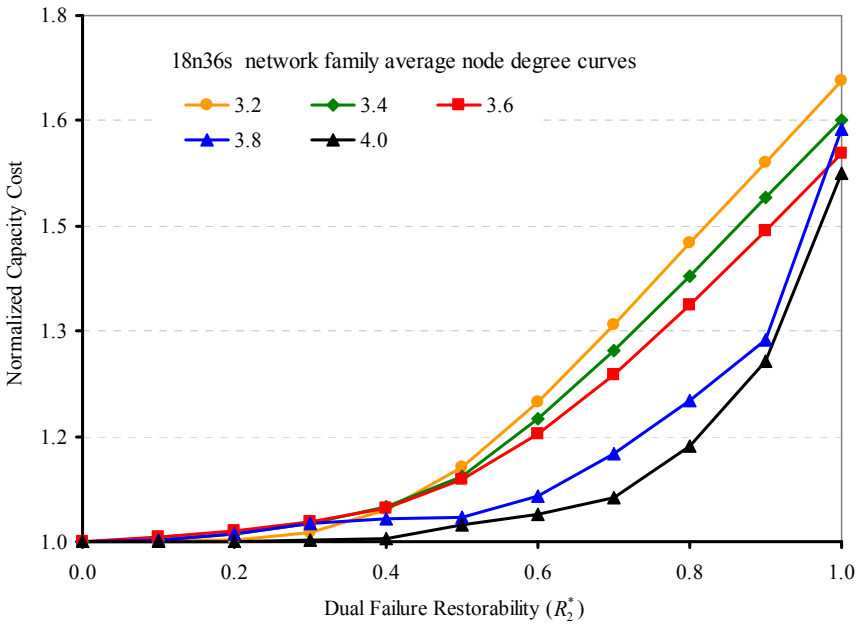

Figure 5.2.4-Rate of capacity cost increase in 18n36s *p*-cycle restorable network family over specified dual failure restorability limits in model 1

In the 18n36s network family (Figure 5.2.4) cost versus R_2^* varies slightly depending on network size. At 80% specified dual failure degree restorability level, the 3.2 $\bar{d}$ network requires about 42% more capacity than is required for 100% single failure restorability, the 3.8 $\bar{d}$ network requires about 20% more capacity than is required for 100% single failure restorability, and the 4.0 $\bar{d}$ network requires about 4% more capacity than is required for 100% single failure restorability. Similar plots for the other network connectivities are shown in APPENDIX C.

5.2.2. Model 2 of *p*-Cycle Restoration

The charts generated from model 2 are similar to the charts shown in model 1 except that there is a much higher capacity savings between $R_2^* = 0$ and $R_2^* = 0.8$. Figure 5.2.5 shows the 10n20s network family chart from model 2 with a normalized capacity cost plotted on the *y*-axis and a specified dual failure restorability limit plotted on the *x*-axis for the various network curves. Similarly, Figure 5.2.6 shows the same normalized capacity cost plot against the specified dual failure restorability limit chart for the 18n36s network family. The charts are

truncated on the *x*-axis at $R_2^* = 0.4$ as there are no changes in capacity cost until at least $R_2^* = 0.6$ Both the 10n20s and 18n36s network family curves are significantly flat until about 60% and 70% R_2^*, respectively.

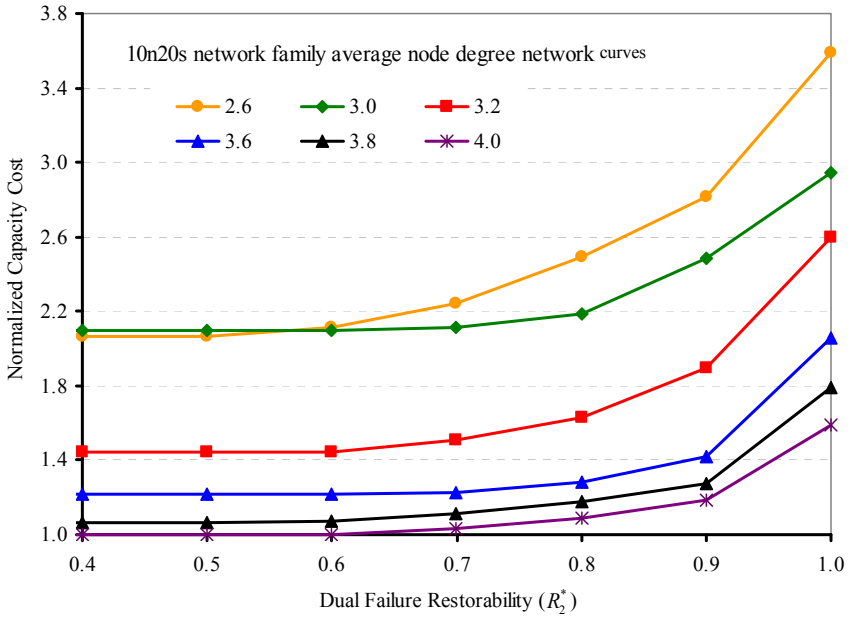

Figure 5.2.5-Dual failure restorability curves in model 2 of 10n20s *p*-cycle restorable network family.

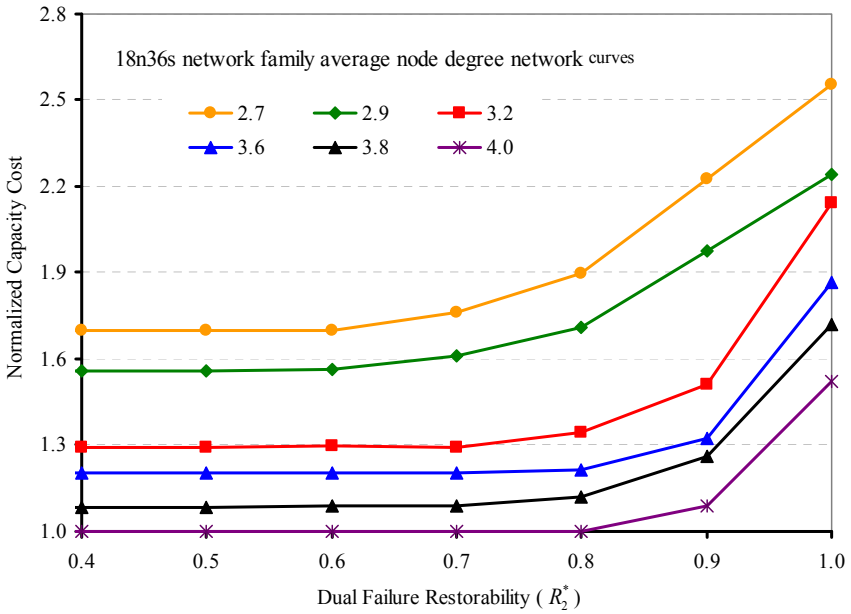

Figure 5.2.6-Dual failure restorability curves in model 2 of 18n36s *p*-cycle restorable network family.

The implication is that, on average, no additional capacity is required to protect the *p*-cycle network for $R_2^* \leq 0.6$ using model 2 *p*-cycle restoration. The 60% dual failure restorability value for this model at $R_2^* \leq 0.6$ therefore marks the degree of inherent dual failure restorability obtainable in a network optimally designed for 100% single failure restorability. This inherent dual failure restorability advantage is even higher in more densely connected networks. For example, in the 18n36s network family (Figure 5.2.6), the 4.0 $\overline{d}$ and 3.8 $\overline{d}$ curves show that, on average, about 80% of the demands can be restored in the event of a dual failure scenario with the single failure network design. Similarly in the 10n20s network family (Figure 5.2.5), there is a very insignificant increase in capacity cost corresponding to the 70% mark on the dual failure restorability limit scale for the 4.0 $\overline{d}$, 3.8 $\overline{d}$, and 3.6 $\overline{d}$ networks. In the 10n20s network family, the 2.6 $\overline{d}$ and 3.0 $\overline{d}$ curves practically overlap in capacity cost until the corresponding value of dual failure restorability reaches 60%. This is not an anomaly in the 2.6 $\overline{d}$ network, the resulting capacity cost for networks whose $\overline{d} \leq 2.9$ happen to have reduced cost for dual failure restorability due the fact that some of the nodes are $\overline{d} = 2.0$, and as such only factor in the single failure protection cost. Network nodes whose $\overline{d} \leq 2.0$ typically return the cost of single failure protection for some node pairs, thereby reducing the overall average cost of dual failure restorability for the entire network. A detailed analysis of the data and a comparative study of the models are presented in section 6.5.

Figure 5.2.7 and Figure 5.2.8 show the relative change in capacity cost with respect to the 100% single failure restorability cost (that is, at specified dual failure restorability $R_2^* = 0$). These charts express in a different way the same data shown above with the inherent dual failure restorability advantage in the networks. In Figure 5.2.7 and Figure 5.2.8 there is no increase in capacity cost until about 60% dual failure restorability. The charts are truncated at $R_2^* = 0.4$ as there is no significant increase is capacity cost up to that point. The clustering of

the curves in the charts shows that almost all the network connectivities increase capacity cost at the same rate per unit increase in dual failure restorability.

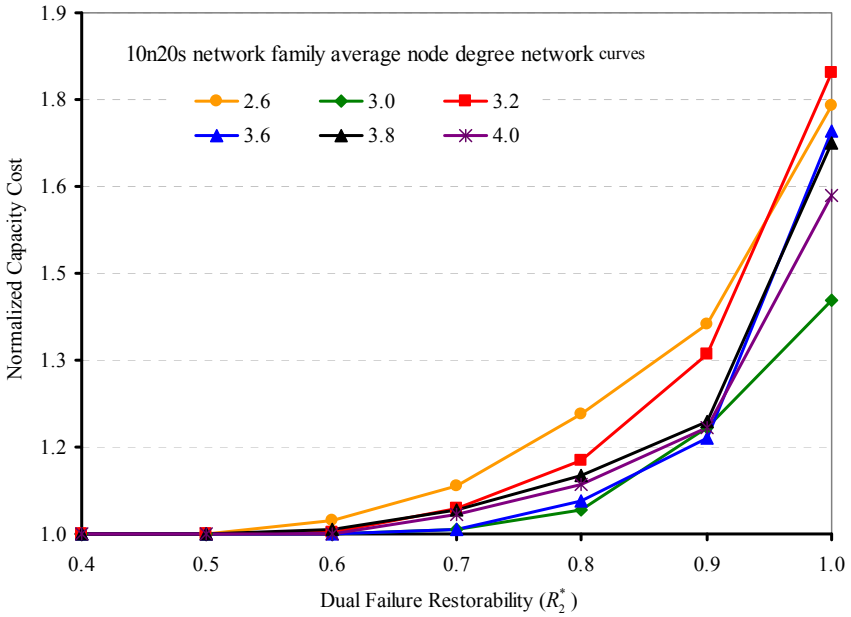

Figure 5.2.7-Rate of capacity cost increase in 10n20s *p*-cycle restorable network family over specified dual failure restorability limits in model 2.

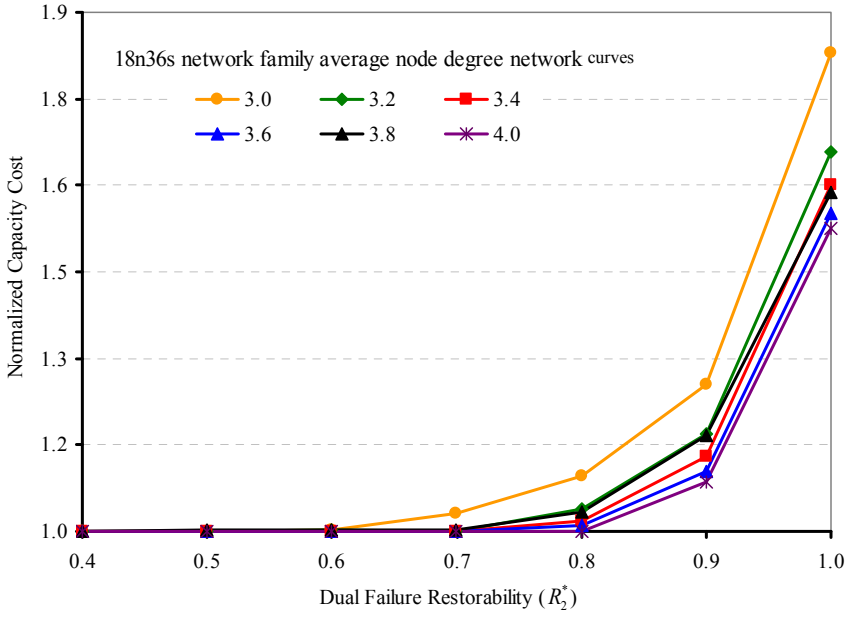

Figure 5.2.8-Rate of capacity cost increase in 18n36s *p*-cycle restorable network family over specified dual failure restorability limits in model 2.

An observation from model 2 data, also noticed in other restoration mechanisms, is that the larger the network size, the more the capacity savings when

approaching 100% specified dual failure restorability. The effect of averaging the individual dual failure restorability over a number of spans whose demands are neither affected by the failure nor require extra capacity may be the major contributor of the apparent savings in capacity cost.

5.3. Path Restoration Results

5.3.1. Model 1 of Path Restoration

Path restoration models may differ slightly from span restoration models and *p*-cycle models in that they depict path-based restoration mechanisms, while span restoration and *p*-cycle models represent span localized restoration mechanisms. However, path restoration model trends in capacity cost versus specified dual failure restorability do not differ much from the models described in sections 5.3.1 and 5.4.1. In the *p*-cycle and span restoration mechanisms seen so far, capacity cost increases as the level of dual failure restorability increases toward 100%. The major interest in using a path restoration model is to find the extent of capacity increase relative to the amount of capacity required for 100% single failure restorability. In [19], path restoration was the most efficient restoration mechanism in the single failure restorability design compared to other restoration mechanisms such as *p*-cycle, span restoration, and *shared backup path protection* (SBPP). In chapter 5 the difference in capacity cost with respect to dual failure restorability for all the restoration mechanisms is discussed. But for now attention is focused on path restoration models 1 and 2. Due to excessive runtimes for 18n36s network family processing, data from this network family is incomplete. Data for the 15n30s network family is presented in the format of earlier sections.

Figure 5.3.1 and Figure 5.3.2 plot the normalized capacity cost (*y*-axis) of network sizes ranging from $\overline{d} = 3.0$ to $\overline{d} = 4.0$ against the specified dual failure restorability limit (*x*-axis) sought in the network for 10 node and 15 node family networks, respectively. The total capacity cost of each network curve is normalized to the least cost capacity network curve at $R_2^* = 0$.

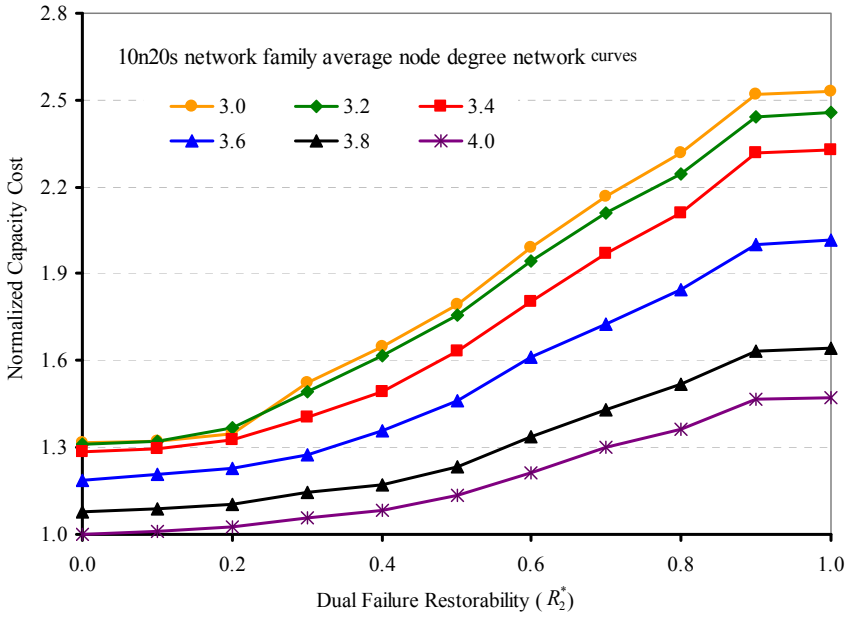

Figure 5.3.1-Dual failure restorability curves in model 1 of 10n20s path restorable network family.

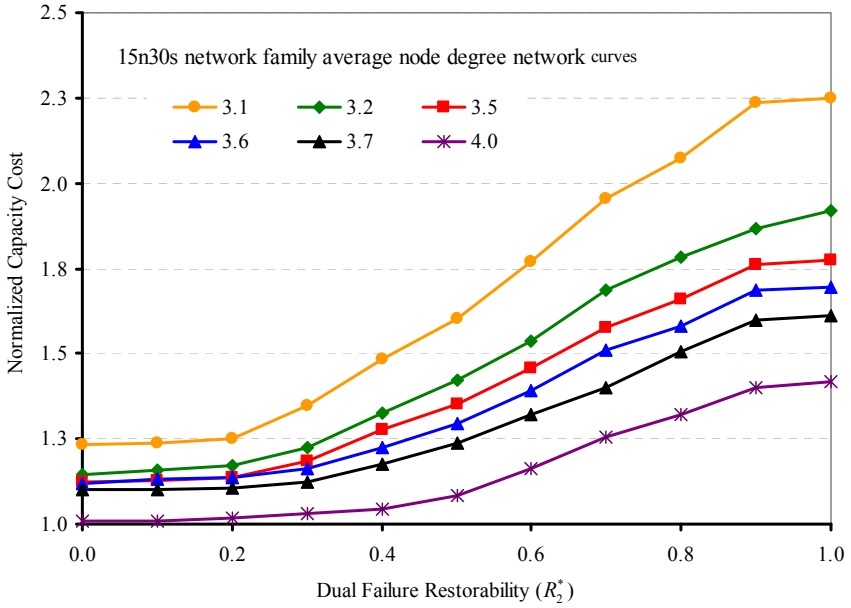

Figure 5.3.2-Dual failure restorability curves in model 1 of 15n30s path restorable network family.

Figure 5.3.1 shows that the 3.0 $\bar{d}$ network of the 10n20s network family incurs the highest capacity cost with respect to the 4.0 $\bar{d}$ network at $R_2^* = 0$, and requires about 92% increase in additional capacity to protect the network from a complete dual failure scenario. The 3.2, 3.4, 3.6, 3.8, and 4.0 $\bar{d}$ networks require an additional 87.6%, 81.1%, 69.4%, 52.7%, and 47.7% increase in capacity,

respectively, to provide the same 100% dual failure restorability relative to the single failure cost. As expected, the 4.0 $\bar{d}$ networks require much less capacity investment for complete dual failure protection than the lower network connectivities. In the 15n30s network family (Figure 5.3.2) there is a significant reduction in capacity cost for various levels of dual failure restorability compared to the 10n20s network family. The 3.2, 3.5, 3.6, 3.7, and 4.0 $\bar{d}$ networks require 66.0%, 57.7%, 51.1%, 46.4%, and 40.6% increase in capacity, respectively, to provide full dual failure restorability. The 15n30s network uses slightly less capacity for equivalent nodal degrees than the 10n20s network.

Figure 5.3.3 and Figure 5.3.4, based on path restoration model 1, show the increase in capacity cost relative to the cost of single failure restorability design for 10n20s and 15n30s network families, respectively. The capacity cost on each network curve is normalized to the $\bar{d} = 4.0$ network cost at single failure design, that is, capacity cost at $R_2^* = 0$. In the 10n20s (Figure 5.3.3) and the 15n30s (Figure 5.3.4) network families, a significant increase in capacity cost begins rising at $R_2^* = 0.2$, re-enforcing the validity of the findings from restoration mechanisms previously discussed. The 4.0 $\bar{d}$ networks of the 10 node and 15 node network families, respectively, require less capacity compared to the 3.2 $\bar{d}$ or 3.3 $\bar{d}$ networks. As the network size increases, the capacity utilization in both network families improves and the amount of capacity required for dual failure protection is reduced accordingly. The richly connected networks (average nodal degree of 3.7 and 4.0) have lower capacity costs compared to the more sparsely connected networks (average nodal degree of 3.1 and 3.2).

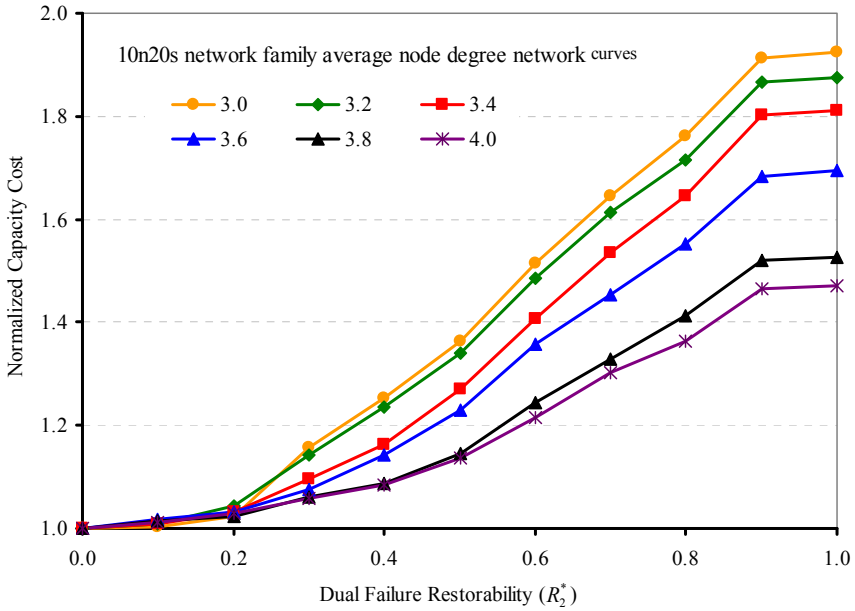

Figure 5.3.3-Rate of capacity cost increase in 10n20s path restorable network family over specified dual failure restorability limits in model 1.

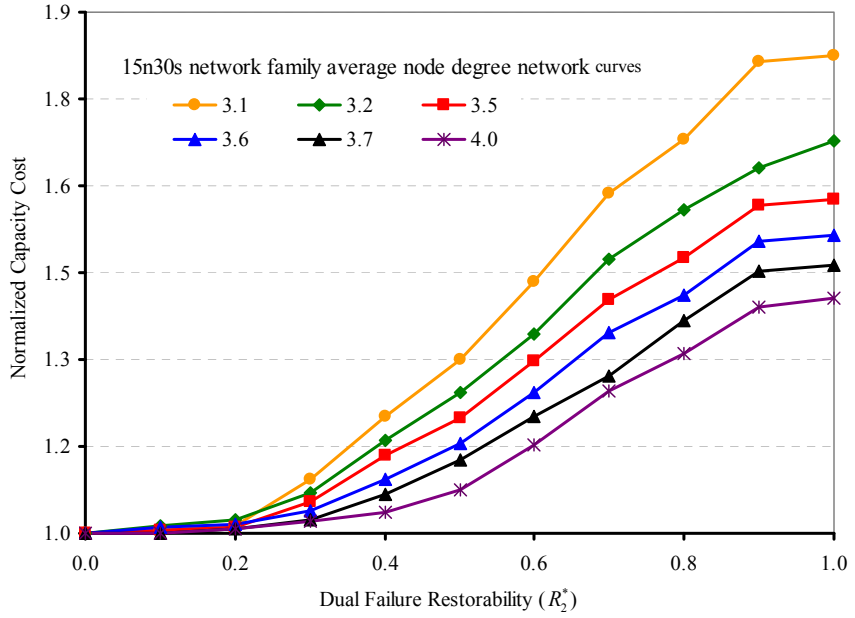

Figure 5.3.4-Rate of capacity cost increase in 15n30s path restorable network family over specified dual failure restorability limits in model 1.

The cost of the dual failure restorability in both network families generally decreases as the connectivity of the network increases. Other network charts generated from model 1 are shown in APPENDIX D.

5.3.2. Model 2 of Path Restoration

In model 2 there are much more significant savings in the total capacity cost compared to the capacity cost obtained for the same level of dual failure restorability in model 1. As shown in previous models of span restoration and *p*-cycle networks, the savings are even more significant with richly connected networks. The savings in some of these networks approach almost 55% of the total capacity cost. Figure 5.3.5 and Figure 5.3.6 show the normalized capacity cost plotted against the specified dual failure restorability R_2^* for 10n20s and 15n30s network families, respectively. In Figure 5.3.6 (15n30s network family), the normalized capacity cost of the network connectivity (3.1, 3.2, 3.5, 3.6, 3.7, and 4.0) is plotted on the *y*-axis while the specified dual failure restorability is plotted on the *x*-axis.

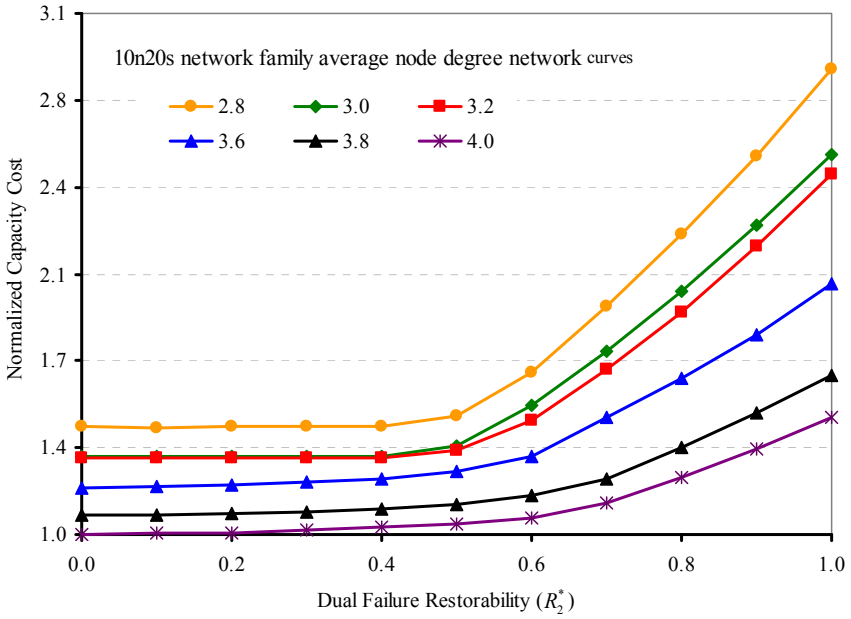

Figure 5.3.5-Dual failure restorability curves in model 2 of 10n20s path restorable network family.

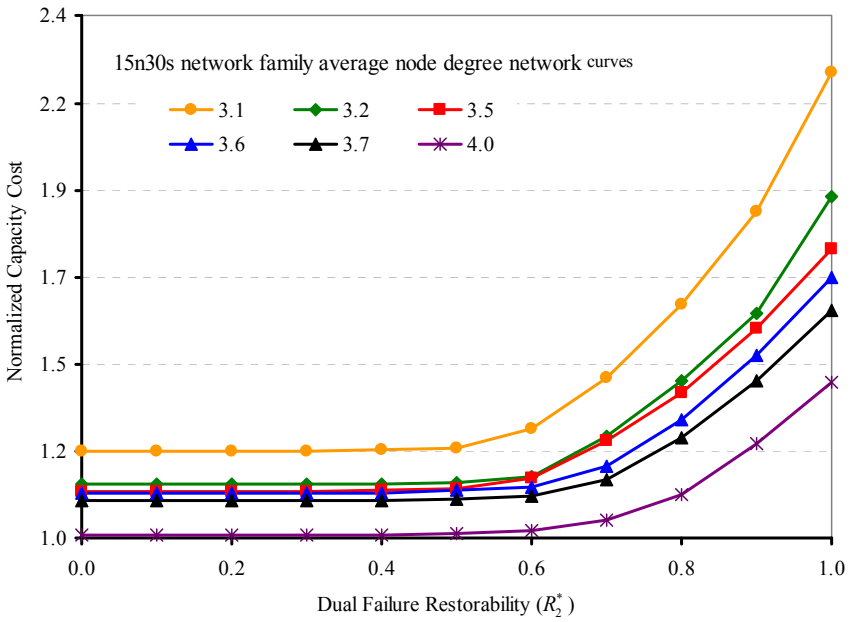

Figure 5.3.6-Dual failure restorability curves in model 2 of 15n30s path restorable network family

Figure 5.3.5 (10n20s network family) and Figure 5.3.6 (15n30s network family) indicate that, in almost all the network sizes, very little or no extra capacity is required to protect, on average, 50% of the demands on the network. This means that if any given pair of spans fails simultaneously, on average, 50% of the demands can be restored without additional backup capacity. Furthermore, up to 60% of the demands are restorable in fully connected networks. But from $R_2^* > 0.6$ there is a sharp increase in additional spare capacity required to protect the network from corresponding levels of dual failure restorability. As usual, the capacity cost of each network curve increases as the level of dual failure restorability increases. For example, on the 10n20s network family (Figure 5.3.5), there is a capacity cost increase of about 20% and 40% for the 4.0 $\bar{d}$ network at $R_2^* = 0.8$ and $R_2^* = 1.0$, respectively. And as network sizes become smaller, there is a sharper increase in capacity cost. The 2.8 $\bar{d}$ networks show capacity cost increases of 32%, 50.8%, 70.8%, and 92.6% at R_2^* = 0.7, 0.8, 0.9, and 1.0, respectively. Similarly, in the 15n30s network family (Figure 5.3.6) the capacity cost of the 4.0 $\bar{d}$ network curve rises by 10.8%, 24.2%, and 40.5% for R_2^* = 0.7,

0.8, 0.9, and 1.0, while the 2.9 $\bar{d}$ capacity cost goes up by 80% for complete dual failure restorability.

Figure 5.3.7 and Figure 5.3.8 show plots of normalized capacity cost (y-axis) against specified dual failure restorability levels (x-axis) in 10n20s and 15n30s network families respectively. The 10n20s network family chart (Figure 5.3.7) shows the normalized capacity cost of network connectivities with average node degrees of 2.8, 3.0, 3.2, 3.6, 3.8, and 4.0, while the 15n30s network family chart (Figure 5.3.8) shows the normalized capacity cost of network connectivities with average node degrees of 3.1, 3.2, 3.5, 3.6, 3.7, and 4.0. Each network connectivity curve in the respective network family shows how the increase in capacity cost on various dual failure restorability levels is compared to the capacity cost at $R_2^* = 0$. As in the previous restoration mechanisms, a sharper increase in capacity cost is more significant in sparsely connected networks compared to more richly connected networks, and smaller networks tend to incur more capacity cost than larger networks.

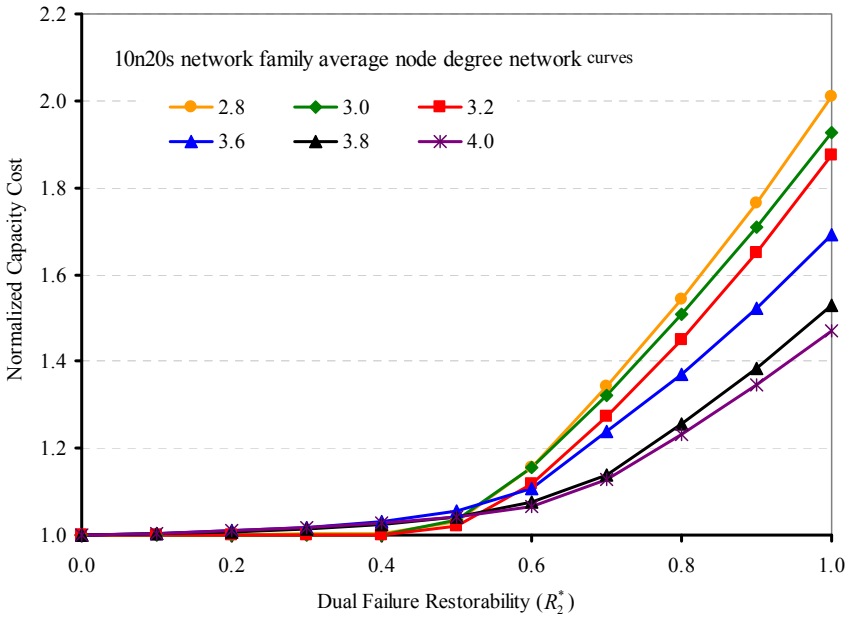

Figure 5.3.7-Rate of capacity cost increase in 10n20s path restorable network family over specified dual failure restorability limits in model 2.

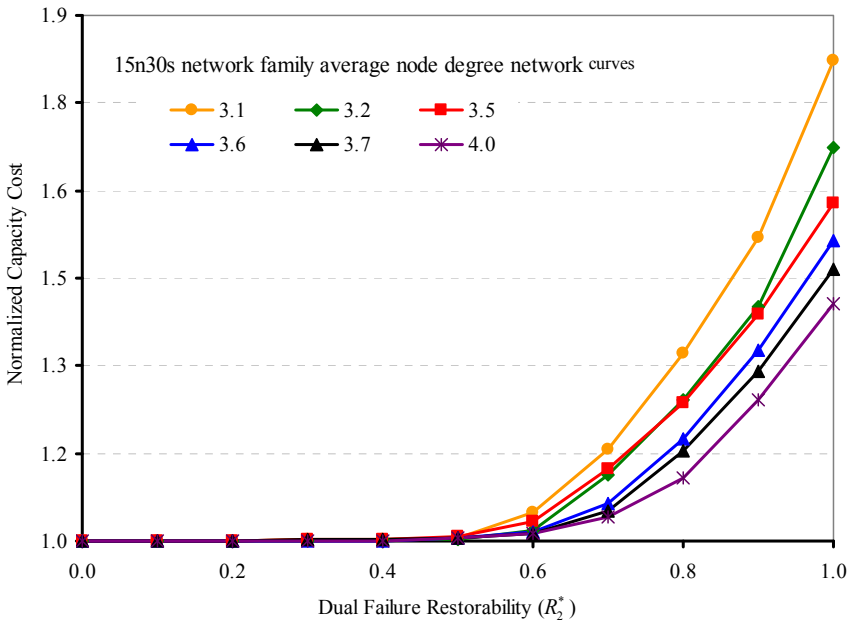

Figure 5.3.8-Rate of capacity cost increase in 15n30s path restorable network family over specified dual failure restorability limits in model 2.

For example in Figure 5.3.7 (10n20s network family) a significant increase in capacity cost on some of the network connectivity curves begins at $R_2^* = 0.3$, compared to $R_2^* = 0.5$ in Figure 5.3.8 (15n30s network family). The effect of averaging the dual failure restorability in model 2 coupled with the capacity utilization efficiency advantage inherent in path restoration makes path restoration an attractive choice for the dual failure restorability design model. The total capacity required is reduced by averaging the dual failure restorability within the network rather than finding the amount of capacity that is strictly required to protect every pair of spans in the network.

5.4. Demand-Wise Shared Protection Results

5.4.1. Model 1 of Demand-Wise Shared Protection

Figure 5.4.1 and Figure 5.4.2 show normalized capacity cost (*y*-axis) plotted against specified dual failure restorability levels (*x*-axis) for several network connectivities of the 10n20s and 18n36s network families, respectively as described by model 1 of demand-wise shared protection (DSP). Data from model 1 DSP shows almost the same trend as data from model 1 of path restoration, but

in DSP the curves seem to rise much more sharply over $R_2^* = 0.4$. Figure 5.4.1 and Figure 5.4.2 were chosen as representatives of all of the test case networks studied under this restoration mechanism. Each data point represents the cost of the total amount of capacity needed to provide the specified dual failure restorability level in the networks. The data points are divided into six separate curves, one for each level of network connectivity ($\bar{d}$ = 3.0, 3.2, 3.4, 3.6, 3.8, 4.0). All data points were normalized to the capacity cost of the $\bar{d} = 4.0$ network at $R_2^* = 0$. As the specified level of dual failure restorability sought in the network increases toward 100%, the total capacity cost increases more rapidly relative to the capacity cost at $R_2^* = 0$; that is, at 100% single failure restorability on a fully connected network. It is important to note that in model 1, the dual failure restorability is formulated to ensure that enough capacity is allocated in the network to strictly restore a specific amount of demands on every pair of spans that are affected by failure.

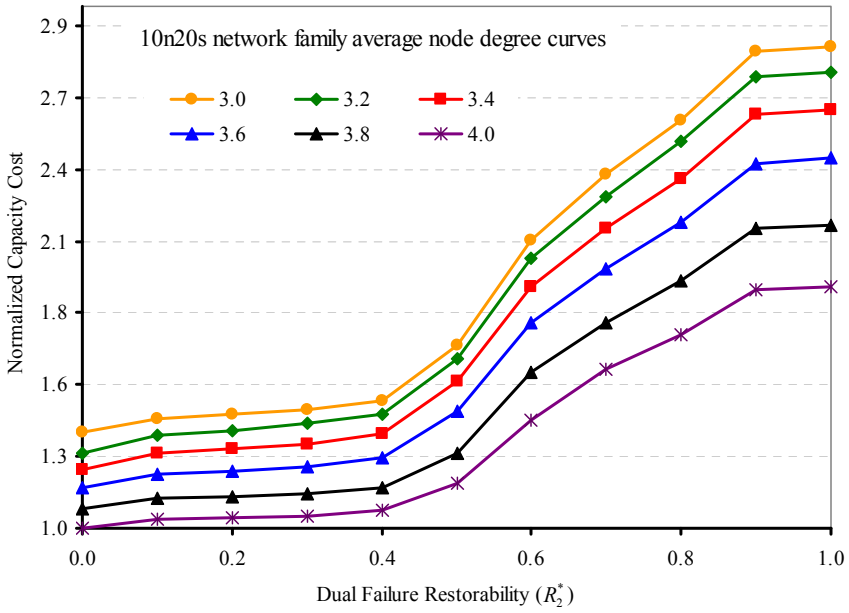

Figure 5.4.1-Dual failure restorability curves in model 1 of 10n20s DSP restorable network family.

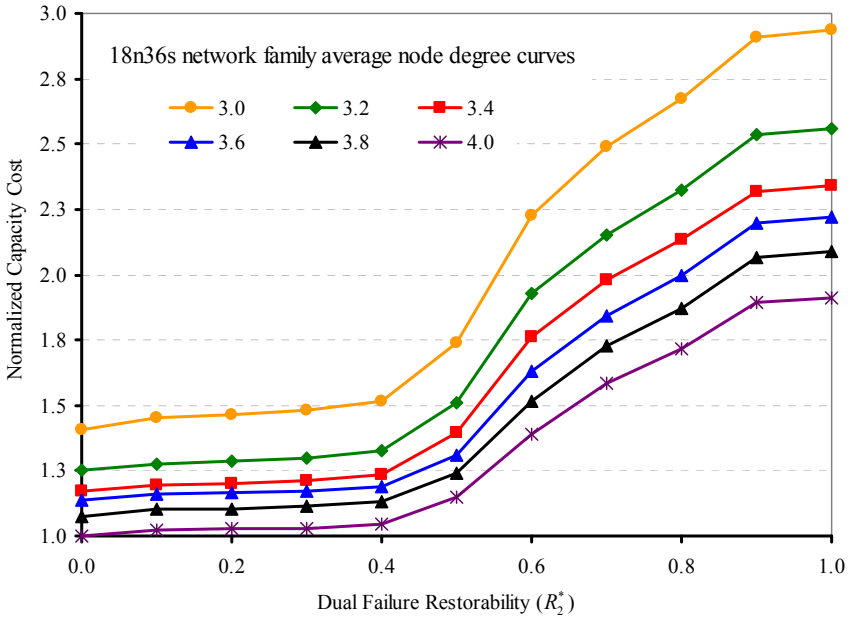

Figure 5.4.2-Dual failure restorability curves in model 1 of 18n36s DSP restorable network family.

Network connectivity curves in network families 10n20s (Figure 5.4.1) and 18n36s (Figure 5.4.2) remained significantly flat and only a slight increase in capacity cost appears between $R_2^* = 0$ and $R_2^* = 0.4$. This means that an insignificant amount of extra capacity would be required to provide dual failure restorability to the specified levels of R_2^*. This suggests that there is a significant amount of inherent dual failure restorability advantage provided by the 100% single failure restorability design network in DSP. For example, in the 10n20s and 18n36s network families, 7.6% and 5.6% more capacity is required, respectively, to provide 40% dual failure restorability (i.e., $R_2^* = 0.4$) in the $\bar{d} = 4.0$ network as compared to $R_2^* = 0$ (i.e., required for single-failure restorability). From $R_2^* = 0.4$ upwards, there is a sharp increase in the capacity cost, which indicates that, much more additional capacity is required to provide dual failure protection at specified level of each network connectivity. The richly connected networks have better capacity efficiency compared to the poorly connected networks.

Figure 5.4.3 and Figure 5.4.4 show the capacity cost increase relative to the capacity cost of the $\bar{d} = 4.0$ network at $R_2^* = 0$ for the 10n20s and 18n36s network families, respectively.

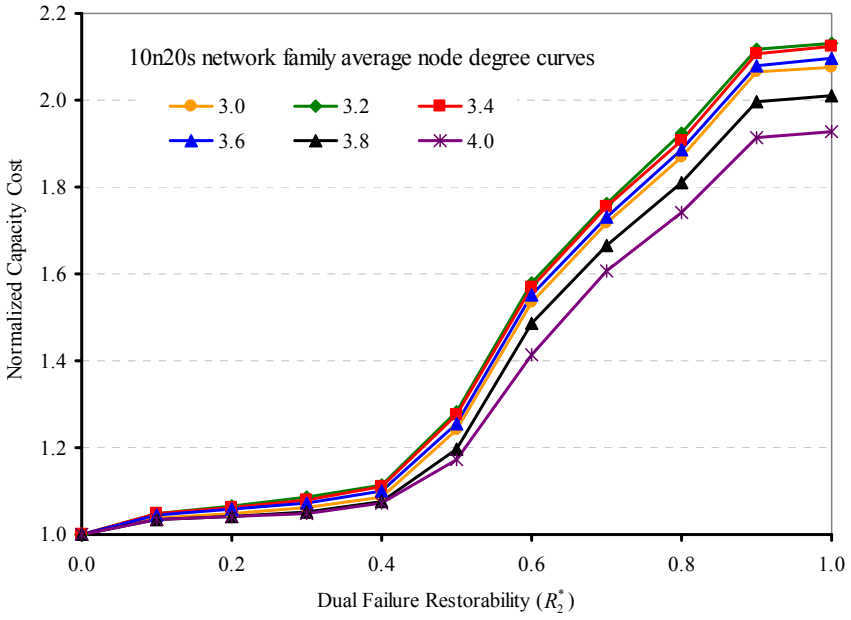

Figure 5.4.3-Rate of capacity cost increase in 10n20s DSP restorable network family over specified dual failure restorability limits in model 1.

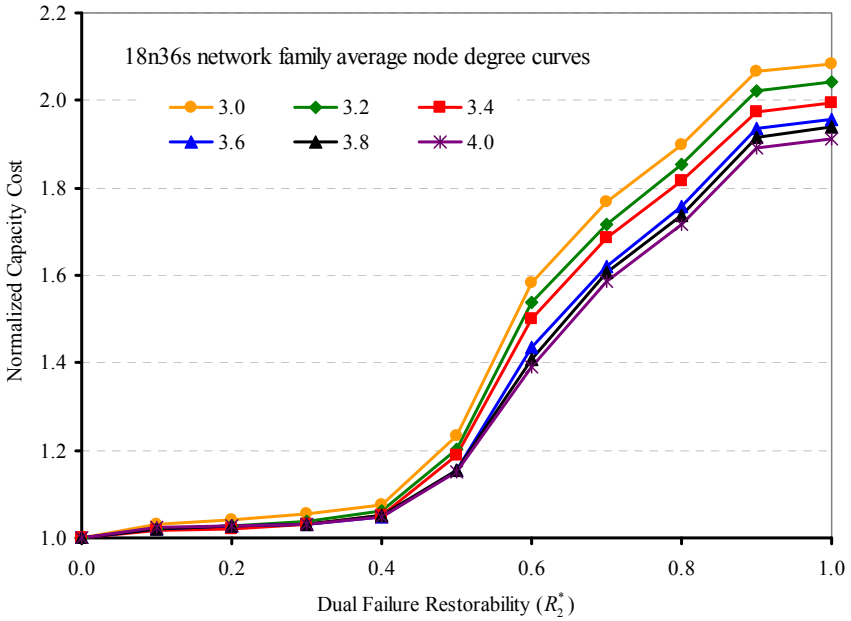

Figure 5.4.4-Rate of capacity cost increase in 18n36s DSP restorable network family over specified dual failure restorability limits in model 1.

Clustering of the network connectivity curves in Figure 5.4.3 and Figure 5.4.4 indicates that the network curves behave similarly in terms of capacity requirement for dual failure restorability. However, the marginal increase in capacity costs relative to the single failure restorability cost is more significant in

the lower degree networks. As we have seen in the previous restoration mechanisms, this shows that the lower average nodal degree networks in DSP require more capacity investment than the more richly connected networks to provide an equivalent level of dual failure protection. For example, in the 10n20s network family, we considered the 3.0 nodal degree network and the 4.0 nodal degree network at specified dual failure restorability limits of $R_2^* = 0.4$ and $R_2^* = 0.5$, respectively. We find that the margin of additional capacity required relative to the previous level of dual failure restorability increases by 14.3% in the 3.0 $\bar{d}$ network, while the additional capacity of the 4.0 $\bar{d}$ network increases only by about 9.4% at the corresponding level. The remaining charts from model 1 of DSP networks, including the 12n24s and the 15n30s network family charts are shown in APPENDIX D.

5.4.2. Model 2 of Demand-Wise Shared Protection

For model 2 DSP we present charts equivalent to the charts shown for model 1 DSP. As mentioned earlier, the difference between model 1 and model 2 is that the latter computes the *average* dual failure restorability limit sought in the network. The formulation averages the dual failure restorability of a specific pair of spans over the entire span pairs in the network. Similar to the charts shown in the previous restoration mechanisms discussed, Figure 5.4.5 and Figure 5.4.6 show plots of normalized capacity cost (*y*-axis) for different network connectivities against specified dual failure restorability (*x*-axis) for the 10n20s and 18n36s network families, respectively. The *x*-axis of the 10n20s network family is truncated at $R_2^* = 0.5$ and the *x*-axis of the 18n36s network family is truncated at $R_2^* = 0.7$, as there is no increase in capacity cost for any network connectivity up to $R_2^* = 0.7$ on the 10n20s network family and $R_2^* = 0.8$ on the 18n36s network family curves.

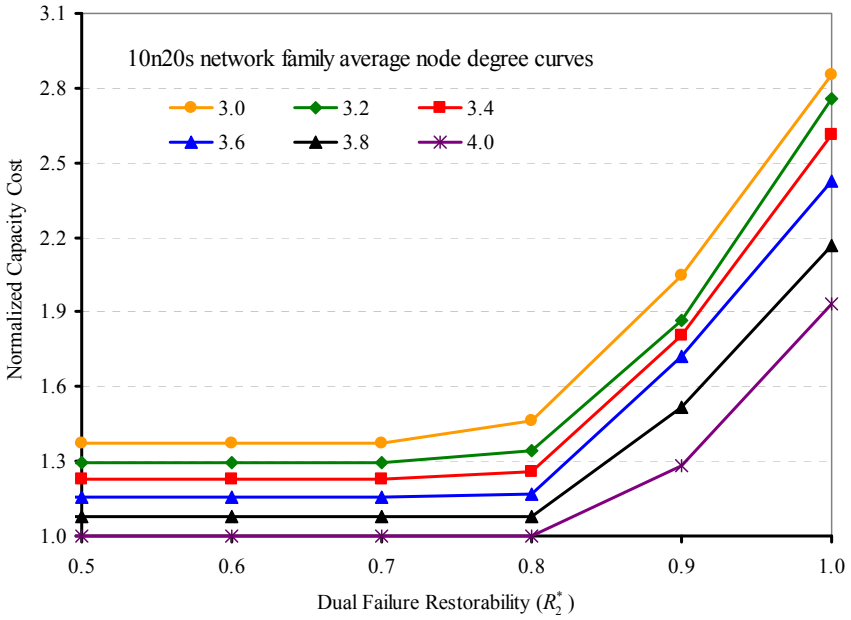

Figure 5.4.5-Dual failure restorability curves in model 2 of 10n20s DSP restorable network family.

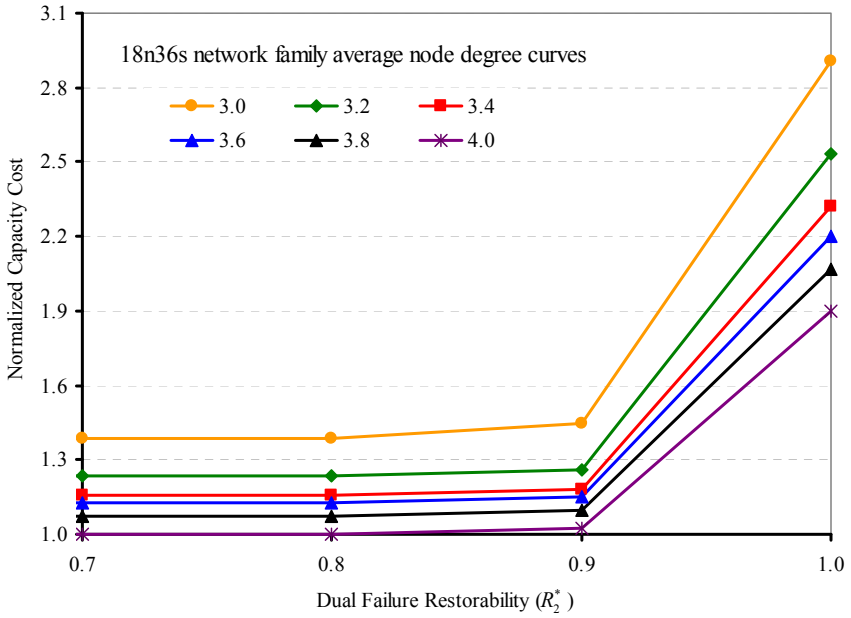

Figure 5.4.6-Dual failure restorability curves in model 2 of 18n36s DSP restorable network family.

The results of model 2 in DSP suggest that we can achieve average dual failure restorability values near 70% in 10n20s network families (Figure 5.4.5) and up to 80% in the 18n36s network families (Figure 5.4.6), and that this can be achieved without adding extra capacity in an optimally designed DSP network for 100% single failure restorability. For example, the capacity cost of the 3.6, 3.8, and 4.0

$\bar{d}$ networks remained flat up until $R_2^* = 0.8$ and the capacity cost of the 3.0, 3.2, and 3.4 $\bar{d}$ networks remained flat until $R_2^* = 0.7$ of the 10n20s network family chart. This implies that no extra capacity is required to restore up to 80% of the demands in the 3.6, 3.8, and 4.0 $\bar{d}$ networks when dual failure occurs and that no extra capacity is required to restore 70% of the demands in 3.0, 3.2, and 3.4 $\bar{d}$ networks optimally designed for full single failure restorability. This is in line with the findings in [58] which suggest that there is about 86% average dual failure restorability inherent in DSP networks that are optimally designed for 100% single failure restorability. The contrast in the capacity cost savings between model 1 and model 2 indicates how much effect averaging the dual failure restorability values may have on the overall dual failure restorability value. The effect of averaging the dual failure restorability value is investigated in section 5.5.

In Figure 5.4.7 and Figure 5.4.8, the individual network connectivity capacity cost is normalized to the capacity cost of the $\bar{d} = 4.0$ network at $R_2^* = 0$ for the 10n20s and 18n36s network families, respectively. These charts indicate how the capacity cost of each individual network connectivity rises with respect to increasing levels of specified dual failure restorability. In Figure 5.4.7 and Figure 5.4.8 the network curves are held together tightly, indicating that the increase in capacity cost with an increase in dual failure restorability occurs at similar rates for all the network connetivities. However, the increase in capacity cost is sharper in smaller networks with lower average node degrees. For example, comparing the 10n20s network curves (Figure 5.4.7) with the 18n36s network curves (Figure 5.4.8), we find that the 3.0, 3.2, and 3.4 $\bar{d}$ networks tied together in the 10n20s network family appear to have steeper capacity cost gradients compared to their counterparts in the 18n36s network family.

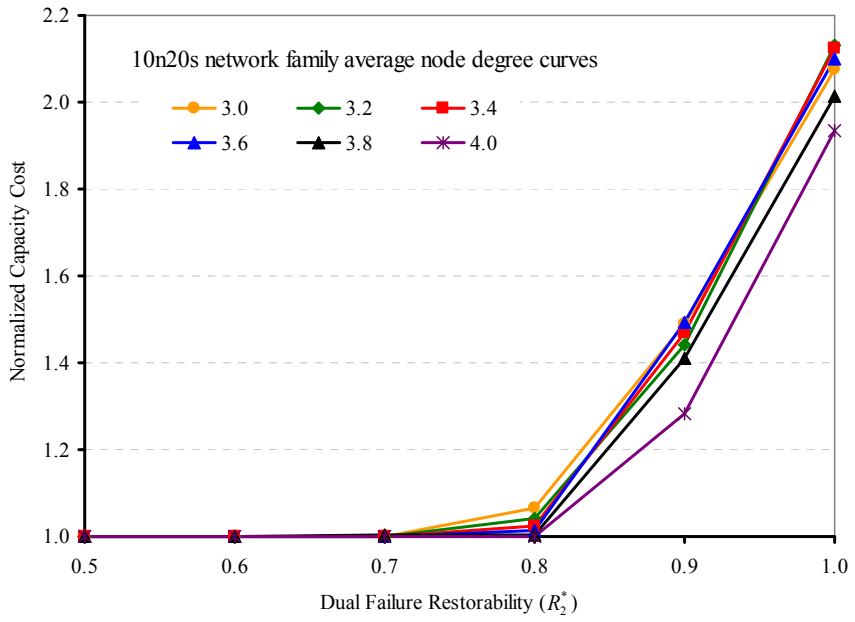

Figure 5.4.7-Rate of capacity cost increase in 10n20s DSP restorable network family over specified dual failure restorability limits in model 2.

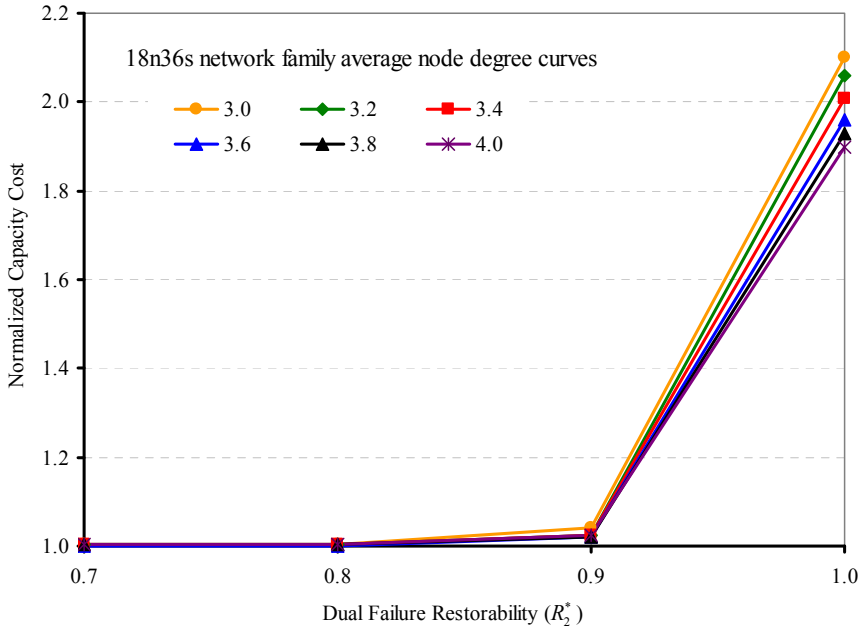

Figure 5.4.8-Rate of capacity cost increase in 18n36s DSP restorable network family over specified dual failure restorability limits in model 2.

The 18n36s network family also appears to show more dramatic capacity savings in DSP model 2 versus DSP model 1. In Figure 5.4.8, which represents the 18n36s network family, the only significant and noticeable increase in capacity cost occurs about $R_2^* = 0.8$ toward 100% dual failure restorability. This reiterates

observations made for model 2 of other restoration mechanisms where a large capacity savings is obtained by averaging the dual failure restorability over all the span pairs. Still, the cost of single failure design and dual failure restorability for DSP networks relative to other restoration mechanisms remains significantly higher. DSP networks will be compared with other restoration mechanisms in chapter 5 where we use a few simple networks to compare the values of dual failure restorability computed by models 1 and 2.

5.5. Validation of Models and Data

A number of methods were used to validate the results obtained from the experiments in this work. First, we compared the results of our 100% single failure restorability (i.e., at $R_2^* = 0$) to the benchmark data obtained from the 100% single failure restorability design models in [19]. With our design models, we used the same network data, parameters, and solver settings as used in [19] to solve a few network sizes in the 15 node and 20 node network families. The results in span, path and *p*-cycle restoration mechanisms show a negligible difference in the total capacity cost. For example, the in the 10-node network family, Table 5-1 below shows the percentage difference in total capacity cost for each restoration mechanisms obtained in our models, and the models in [19] which we referred to as the *reference model*.

Table 5-1-Percentage difference in total capacity cost of validation models over reference models.

	Restoration Mechanisms		
Networks	Span	*p*-Cycle	Path
10n20s-15s	0.0136%	0.0100%	N/A
10n20s-20s	0.0061%	0.0085%	N/A
15n30s-25s	0.0096%	0.0018%	0.0002%
15n30s-30s	0.0010%	0.0178%	0.0181%
20n40s-35s	0.0047%	0.0101%	0.0001%
20n40s-40s	0.0167%	0.0051%	0.0001%

Note that the mipgap use to solve these networks is 0.01%. As we can see from Table 5-1, only a few data points exceed the 0.01% migap by an insignificant margin. We also compared 100% single and dual failure restorability results of 15-node network from our DSP models and the models developed in [84]. The total capacity costs obtained in both models are the same for the 100% single and

with very insignificant difference in dual failure restorability models. The table below shows the results for both models.

Table 5-2-100% single and dual failure validation results in DSP networks

DSP Networks Validation Results						
	Single Failure			Dual Failure		
Test network	Validation Network Capacity Cost	Reference Network Capacity Cost	Percentage(%) Difference	Validation Network Capacity Cost	Reference Network Capacity Cost	Percentage(%) Difference
15n30s-25s	542348	542348	0.0000%	1113970	1113967	0.0003%
15n30s-30s	407689	407689	0.0000%	773889	773885	0.0005%
20n40s-35s	780390	780385	0.0006%	1445469	1445458	0.0008%
20n40s-40s	649292	649290	0.0003%	1230124	1230101	0.0019%

As we can see from Table 5-2 that the percentage difference in the capacity cost for both the single and dual failure restorability results are within 0.01% of the mipgap value applied to the solver. The highest percentage difference in capacity cost for these networks is 0.0008% for the dual failure restorability of 20n40s-35s network.

Lastly, we used a small sized network that we worked out manually to compare to the results of the design models obtained by the solver. The total capacity costs results obtained in the all the validation test network cases were within 0.001% of the network solved manually. We also used same network to attempt to explain why the average dual failure restorability model, model 2 tend to achieve more capacity cost savings when compared to model 1. We used a typical routing of demand lightpaths in DSP networks (Figure 5.5.1) to demonstrate that there is substantial capacity costs savings in model 2 networks when compared to model 1 networks. Figure 5.5.1(*a*) shows a DSP network with a single working route and two restoration routes. In Figure 5.5.1(*b*), we simply added three more spans without routing any working or restoration routes through them.

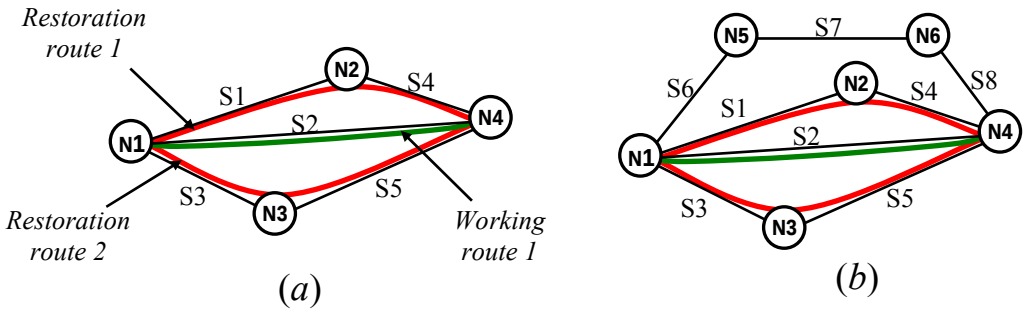

Figure 5.5.1-Averaging dual failure restorability effect on DSP networks.

We found that by adding these three spans, any dual failure scenarios affecting a combination of the newly added spans will result to 100% dual failure restorability values for the pair of spans since no demand lightpaths are affected by their failures. Consequently by averaging the individual pair of spans dual failure restorability values over the entire network, the 100% dual failure restorability values resulting from the newly added spans contribute to higher overall capacity cost savings in the network. This effect is more prevalent in large networks where a sizeable number of span pairs do not bear any demand lightpaths and more significant in path based restoration mechanisms.

Chapter 6

Comparative Analysis

6. Introduction

Two models were considered for each restoration mechanism in the survivability schemes discussed in chapter 4. In this chapter, these models are compared, first by looking into differences in total capacity costs for specified levels of dual failure restorability in each of the restoration mechanisms. Span restoration and *p*-cycle networks will be compared next. As mentioned in chapter 4, span restoration and *p*-cycle restoration mechanisms have similarities in their formulations and we consider how dual failure restorability is defined relative to each pair of spans in the respective networks. Path restoration and DSP, both path-based restoration mechanisms, are compared to determine why they differ in terms of total capacity cost. Finally, we put the four restoration mechanisms on the same chart to determine the benefits one might have over the other. Based on trends of the charts and the data we obtained in chapter 4, we look at only three node degree network curves when comparing the models. Also, we use only the 10n20s and the 18n36s network families to analyze the findings, adding other network sizes where appropriate to make the illustrations more understandable. Due to the limited data acquired on the 18n36s network family of path restorable networks, only the 10n20s and the 15n30s network families are used when comparing various restoration mechanisms. Analysis of the work done in [19], shows that path restoration appears to be the most efficient restoration mechanism in terms of capacity utilization. The next most efficient restoration mechanisms are *shared backup path protection* (SBPP), followed *p*-cycle, and, finally, span restoration in the mesh restorable networks. SBPP is not included in our experiments due to the excessive runtimes encountered with SBPP networks. The difference in the work presented here is that formulations of dual failure restoration models focus on restoring demands on span pair failure rather than single span failure. The failure of two separate spans occurring in an overlapping

time frame has a wide range of scenarios, and could affect the outcome of dual failure restorability according to the restoration mechanisms being deployed. But regardless of how the dual failure restorability processes differ and how they are defined in these restoration mechanisms, it is necessary to put all the mechanisms on the same scale to determine which survivability schemes offer more advantages in terms of capacity utilization in dual failure restorability.

6.1. Comparison of Dual Failure Restorability Models in Span Restoration

In order to present a concise and understandable discussion of the comparison of model 1 and model 2 of dual failure restorability design in span restoration, we compared only one pair of network families (10n20s and 18n36s) and only three selected node degree networks as representative of the curves seen in chapter 4. We compare the networks within an average nodal degree of 3.0 to 4.0. The feasibility of model 1 in dual failure restorability computation lies within $\bar{d} \geq 3.0$.

Figure 6.1.1 and Figure 6.1.3 show plots of normalized capacity costs against specified dual failure restorability limits of the 10n20s and 18n36s network families, respectively, based on models 1 and 2. The dashed curves represent the networks in model 1 and the solid curves represent model 2 networks. Figure 6.1.2 and Figure 6.1.4 compare the network connectivity curves of model 1 and model 2 in the 10n20s and 18n36s network family curves, respectively, showing the relative increase in capacity cost of model 1 networks over model 2 networks. These curves indicate the amount of percentage increase in capacity required by a model network 1 over the capacity used to design an equivalent level of dual failure restorability in model 2 networks.

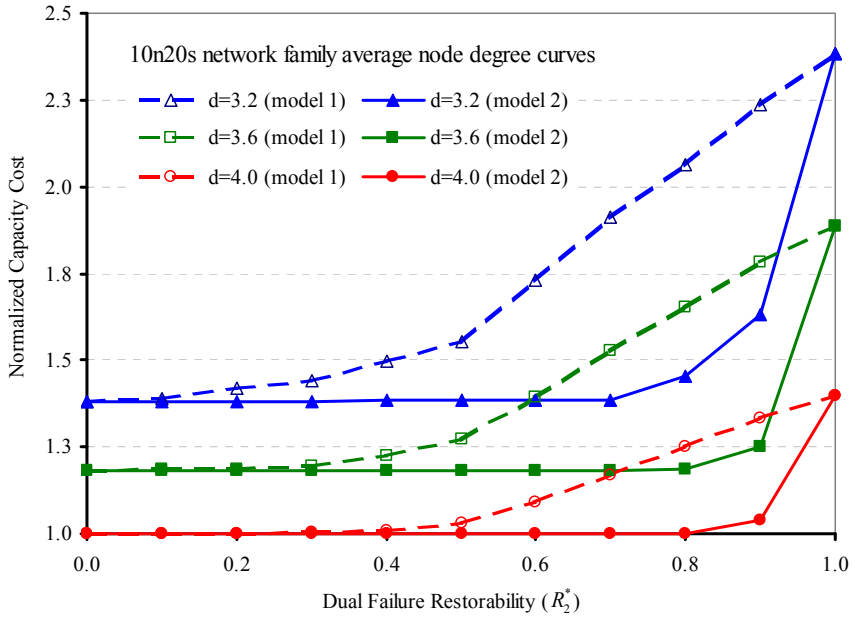

Figure 6.1.1-Dual failure restorability limit curves of model 1 and model 2 in 10n20s span restorable network.

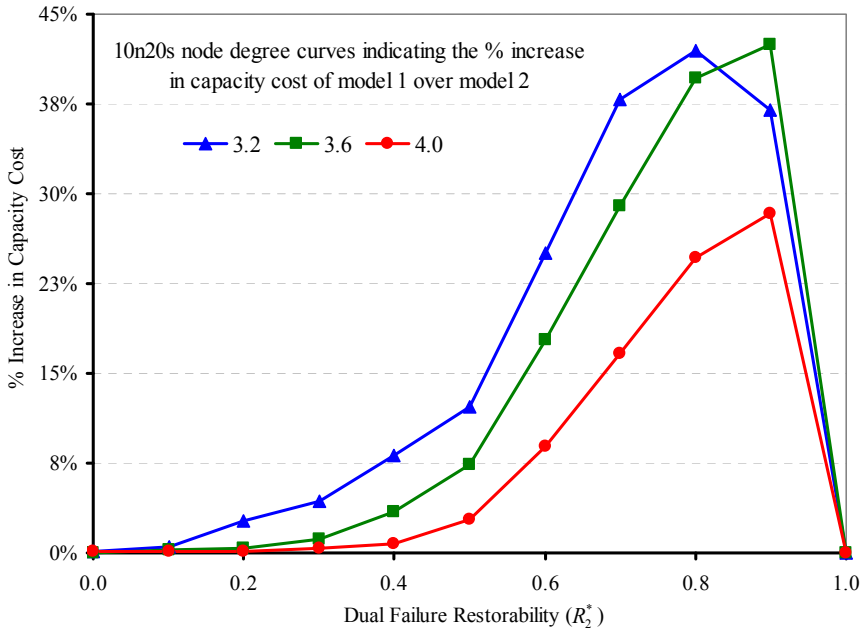

Figure 6.1.2-Relative increase in capacity cost of model 1 over capacity cost of model 2 in 10n20s span restorable network.

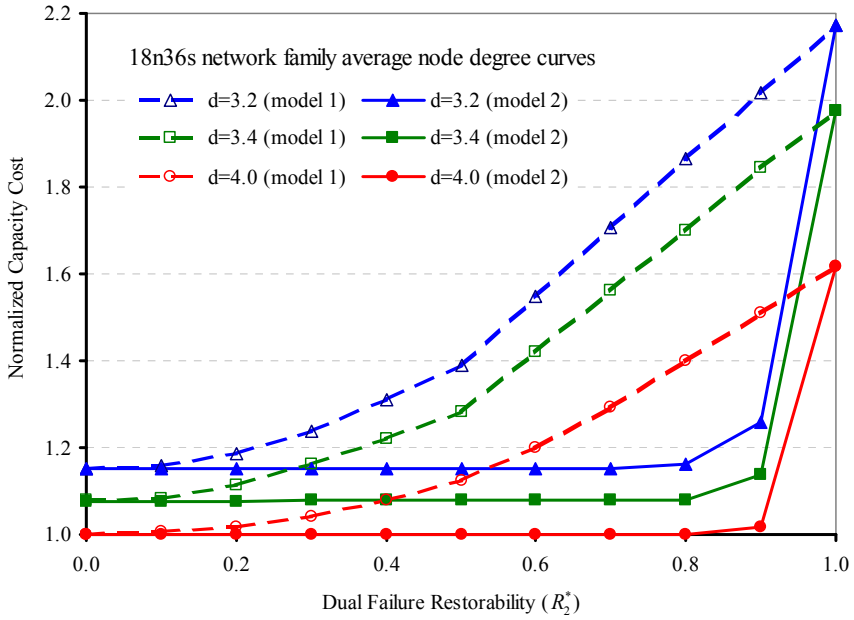

Figure 6.1.3-Dual failure restorability limit curves of model 1 and model 2 in 18n36s span restorable network.

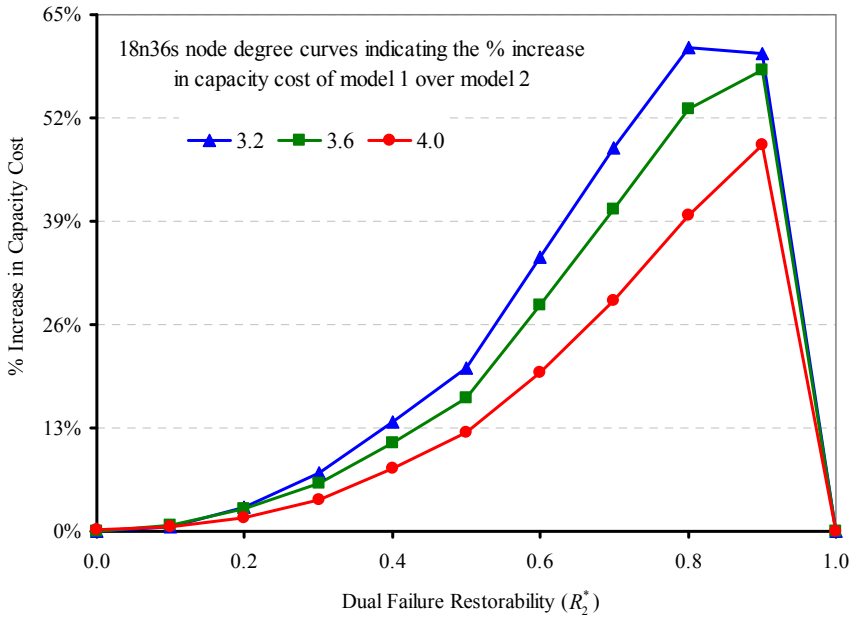

Figure 6.1.4-Relative increase in capacity cost of model 1 over the capacity cost of model 2 in 18n36s span restorable network.

Figure 6.1.1 and Figure 6.1.3 show network curves of 10n20s and 18n36s network families discussed in chapter 4. The capacity costs in model 1 of both networks increase as the specified dual failure restorability levels increase. Model 2 networks do not show an increase in capacity costs until $R_2^* = 0.7$ in the 10n20s

and $R_2^* = 0.8$ in the 18n36s network family, respectively. The increase in capacity cost of model 1 networks is proportional to network size. The highest percentage increase in capacity required by model 1 networks over model 2 networks occurs between $R_2^* = 0.7$ and $R_2^* = 0.9$ as shown in Figure 6.1.2 and Figure 6.1.4. In both models the capacity costs at $R_2^* = 0$ and at $R_2^* = 1.0$ remain basically the same. A larger gap in capacity cost is evident on the lower average node degree networks compared to the higher average node degree networks. In the 10n20s network family, the capacity cost of 3.2, 3.4, and 4.0 $\bar{d}$ networks of model 1, began to increase from $R_2^* = 0.1$, $R_2^* = 0.2$, and $R_2^* = 0.4$, respectively, while the capacity cost on the same networks in model 2 began to increase from $R_2^* = 0.6$, $R_2^* = 0.7$ and $R_2^* = 0.8$, respectively. This means that model 1 network design begins to incur a significant increase in capacity cost as soon as the dual failure restorability level is increased by a tenth of a percentage point.

Similarly in the 18n36s network family shown in Figure 6.1.3, the capacity cost increase begins at $R_2^* = 0.1$ for the 3.2, 3.4, and 3.6 $\bar{d}$ networks of model 1; the capacity cost of corresponding node degree networks of model 2 do not see any increase until $R_2^* = 0.8$. The same conclusion can be drawn from Figure 6.1.4, a 18n36s network family, where there is relative increase in capacity cost from $R_2^* = 0.1$ for model 1 and from $R_2^* = 0.8$ for model 2. It is important to note that even though model 2 averages the dual failure restorability of each pair of spans, the resulting total capacity cost of networks with $\bar{d} < 3.0$ does not reflect the actual total capacity cost required for protecting the network from dual failure restorability. Some nodes with $\bar{d} = 2.0$ cannot be protected against dual failure and the dual failure restorability cost of such nodes is not reflected in the total capacity cost, as only single failure capacity cost is factored in.

6.2. Comparison of Dual Failure Restorability Models in *p*-Cycle Restoration

Models of *p*-cycle restoration reflect the trends in equivalent networks based on span restoration models. Figure 6.2.1 and Figure 6.2.3 show the average node degree network curves for both models in the 10n20s and the 18n36s network families, respectively. Each data point represents the plot of normalized capacity cost against a specified dual failure restorability limit. The dash curves in Figure 6.2.1 and Figure 6.2.3 represent model 1 networks and the solid curves represent model 2 networks. The capacity cost of each data point on the network curves is normalized to the least capacity cost network at $R_2^* = 0$ and $\bar{d} = 4.0$. In the model 1 networks, the specified the capacity cost begins to increase as soon as the dual failure restorability level increases, while in model 1 networks the curves tend to remain flat until about $R_2^* = 0.6$. This means there is much more capacity savings in a model 2 network design compared to a model 1 network design, with savings occurring mostly between $R_2^* = 0.2$ and $R_2^* = 0.9$ in both network families. Figure 6.2.2 and Figure 6.2.4 show the percentage increase in capacity cost of model 1 networks relative to the capacity cost used to design corresponding levels of dual failure restorability networks using model 2 for the 10n20s and 18n36s network families. In Figure 6.2.2 the capacity cost for model 1 rises continuously with dual failure restorability (R_2^*). The sparser networks require more capacity than the denser networks for the same level of dual failure restorability in model 2. At $R_2^* = 0.8$ we find the highest percentage gap in capacity requirement between same network size designed with model 1 and model 2. About 38%, 41%, and 31% more capacity is required by model 1 over model 2 in 3.2, 3.6, and 4.0 $\bar{d}$ networks designed to provide the same level of R_2.

Similarly in Figure 6.2.4 the highest capacity cost increase of model 1 over model 2 is between $R_2^* = 0.8$ and $R_2^* = 0.9$, with average node degree curves of 3.2, 3.6, and 4.0 requiring about 36%, 32%, and 16%, respectively, more capacity in model 1 versus model 2.

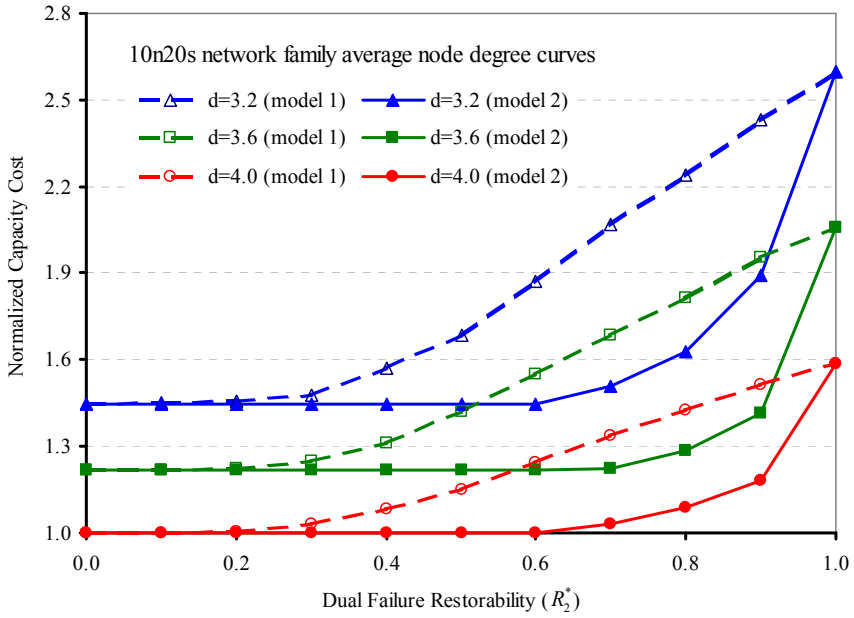

Figure 6.2.1-Dual failure restorability limit curves of model 1 and model 2 in 10n20s *p*-cycle restorable network.

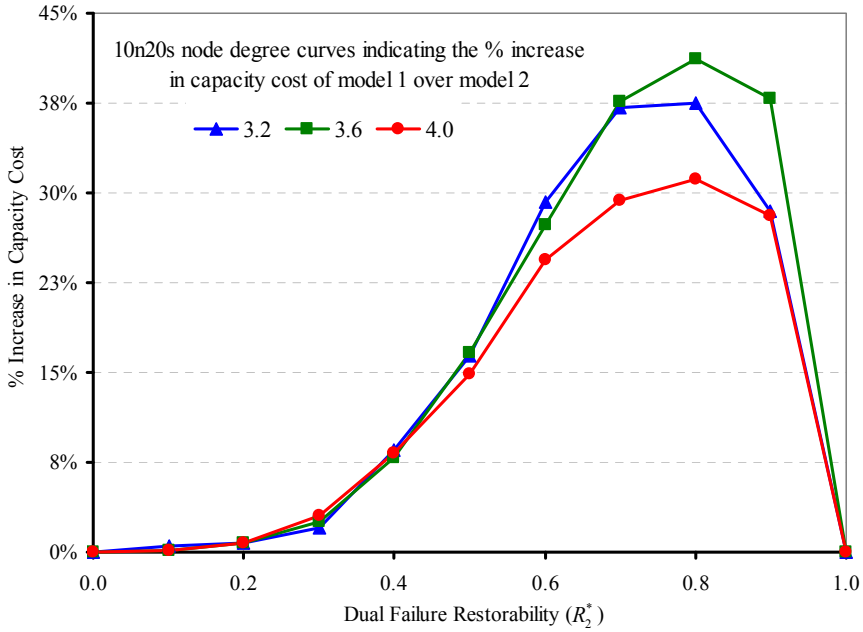

Figure 6.2.2-Relative increase in capacity cost of model 1 over the capacity cost of model 2 in 10n20s *p*-cycle restorable network family.

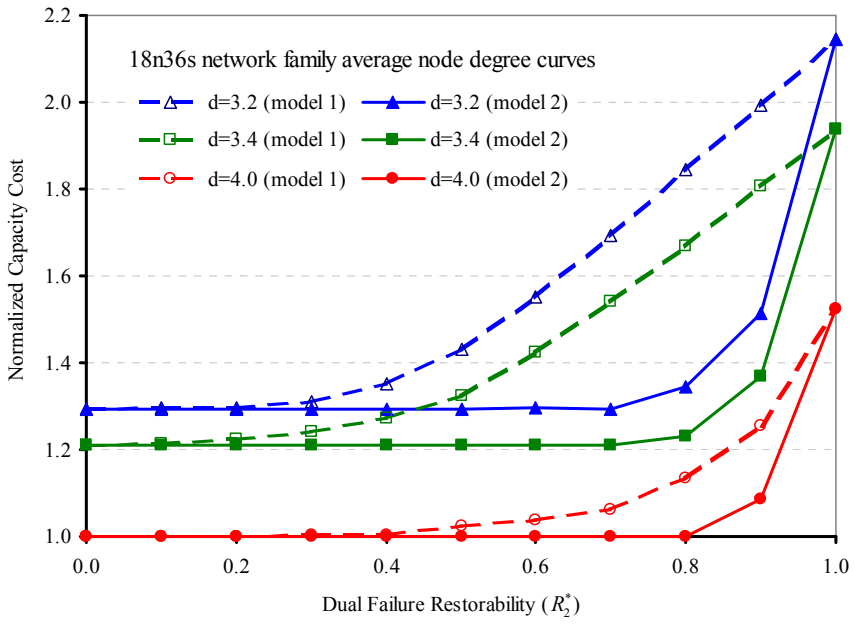

Figure 6.2.3-Dual failure restorability limit curves of model 1 and model 2 in 18n36s *p*-cycle restorable network.

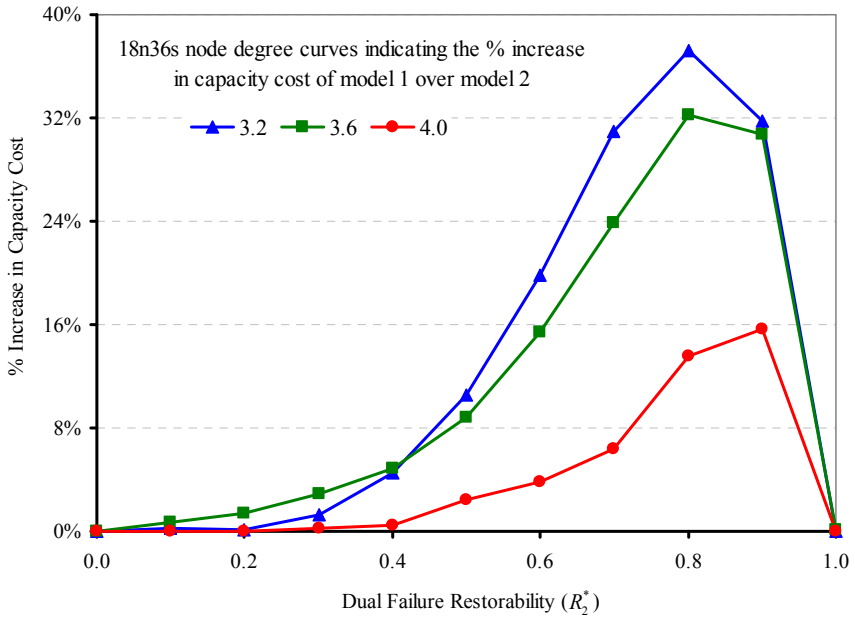

Figure 6.2.4-Relative increase in capacity cost of model 1 over the capacity cost of model 2 in 10n20s *p*-cycle restorable network family.

The larger gap in capacity cost between model 1 and model 2 over the range of $R_2^* = 0.2$ and $R_2^* = 0.9$ reaffirms observations made in chapter 4 regarding the effect of averaging the dual failure restorability values over the entire network in model 2. The inherent dual failure restorability advantage is even greater in the

model 2 expression of the 4.0 $\bar{d}$ network in the 18n36s network family, where a significant increase in capacity cost occurs from $R_2^* = 0.8$. Figure 6.2.2 clearly shows in the 10n20s network, that the model 1 networks require insignificant additional capacity compared to model 2 networks up to $R_2^* = 0.2$. From Figure 6.2.2 we can determine the amount of increased capacity required by model 1 to design the same size of network as in model 2. Model 2 networks need extra capacity only from $R_2^* = 0.7$ (10n20s, Figure 6.2.1) or R_2^*=0.8 (18n36s, Figure 6.2.3), while both 10n20s and 18n36s model 1 networks need extra capacity from $R_2^* = 0.2$. Densely connected networks have more inherent dual failure restorability advantage that sparsely connected networks.

6.3. Comparison of Dual Failure Restorability Models in Path Restoration

In this section dual failure restorability curves for different network connectivities in model 1 and model 2 of the 10n20s and 15n30s network families are presented. Excessive runtimes encountered in the 18n36s network family of path restorable networks prevented the generation of sufficient data for comparison with the 18n36s node networks of other restoration mechanisms.

Figure 6.3.1 and Figure 6.3.3 show the dual failure restorability curves of model 1 and model 2 in the 10n20s and 15n30s network families. The charts show the average node degree network curves plotted with the normalized capacity cost on the *y*-axis, against the specified dual failure restorability limit on the *x*-axis. For the 10n20s network family (Figure 6.3.1), we compare model 1 and model 2 of the networks of average node degrees 3.2, 3.6, and 4.0, while for the 15n30s network family (Figure 6.3.3), model 1 and model 2 of the 3.3, 3.7, and the 4.0 $\bar{d}$ networks are compared. Figure 6.3.2 and Figure 6.3.4 show how model 1 curves increase in capacity cost relative to model 2 in the 10n20s and 15n30s network families, respectively. The total capacity cost at various levels of dual failure restorability limit R_2^* is normalized to the total capacity cost at $R_2^* = 0$. The dashed curves represent model 1 networks, while solid curves represent model 2 networks.

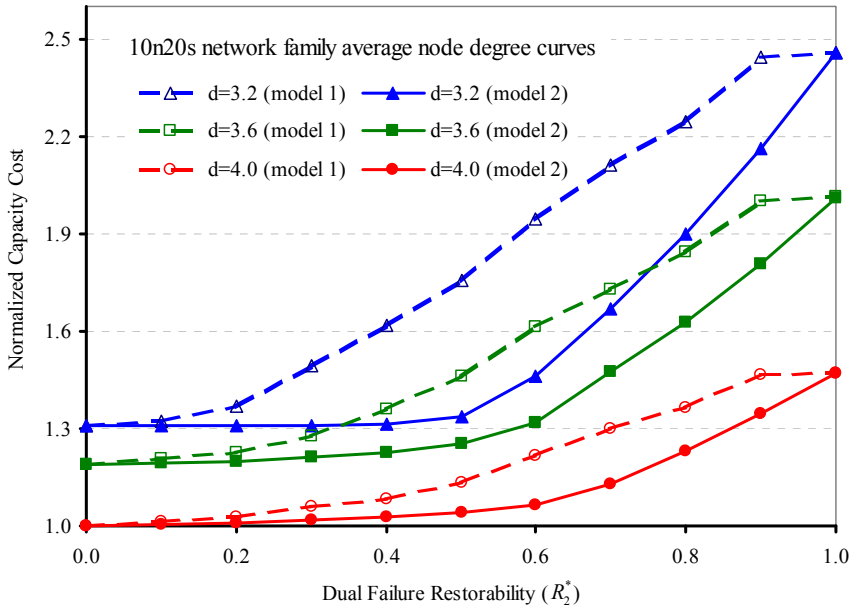

Figure 6.3.1-Dual failure restorability limit curves of model 1 and model 2 in 10n20s path restorable network.

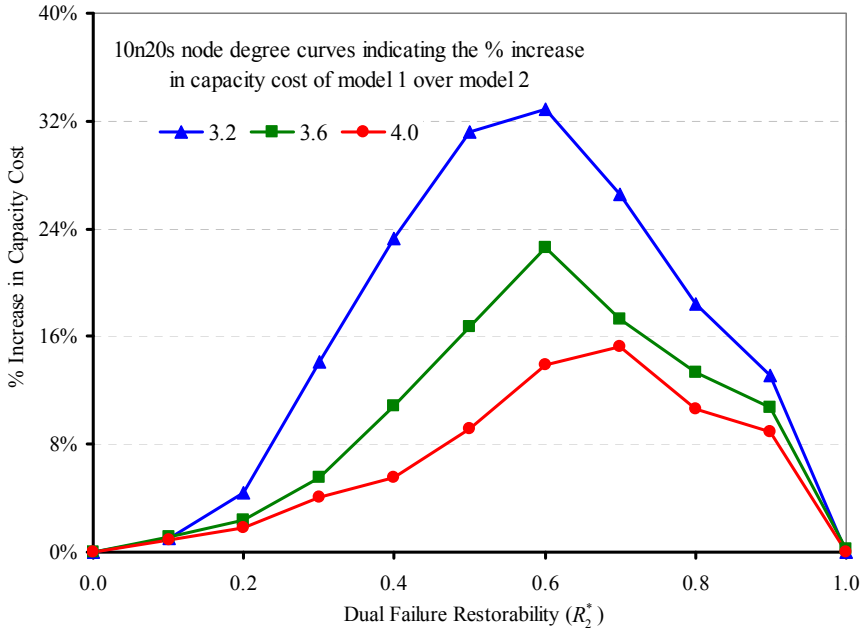

Figure 6.3.2-Relative increase in capacity cost of model 1 over the capacity cost of model 2 in 10n20s path restorable network family.

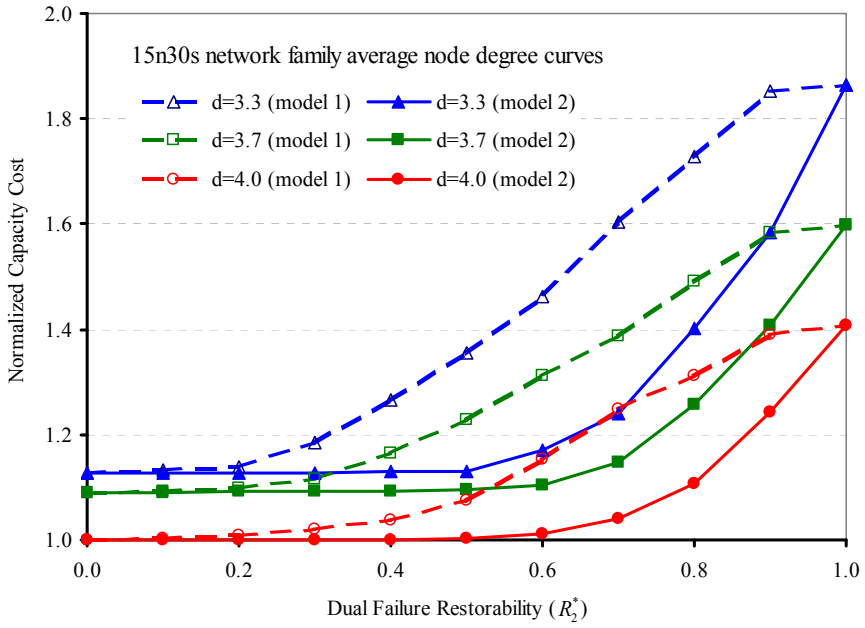

Figure 6.3.3-Dual failure restorability limit curves of model 1 and model 2 in 15n30s path restorable network.

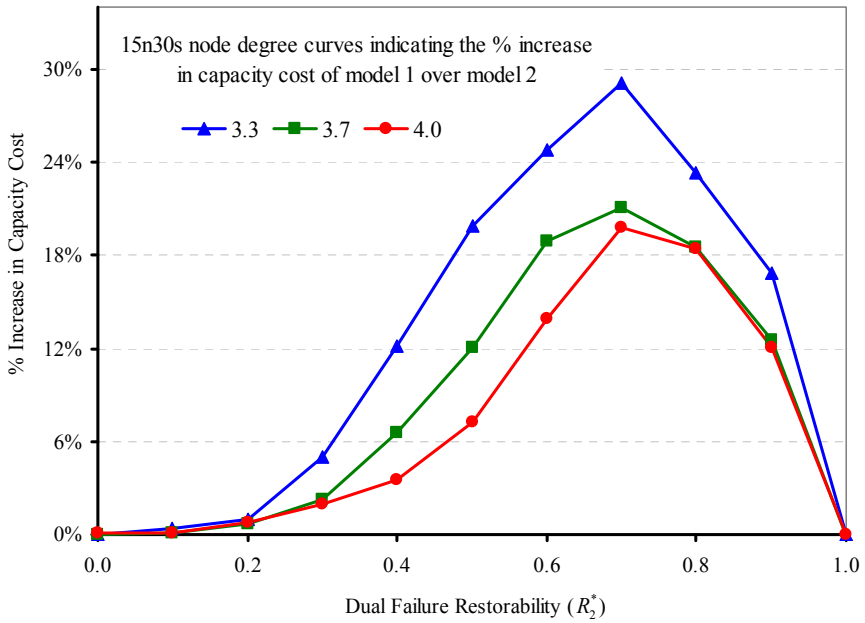

Figure 6.3.4-Relative increase in capacity cost of model 1 over the capacity cost of model 2 in 15n30s path restorable network family.

As expected, both models compared similarly to other restoration mechanisms discussed earlier. In the 10n20s network families in Figure 6.3.1, capacity cost increases rapidly as the required dual failure restorability level increases in model 1 networks compared to model 2 networks. Figure 6.3.1 suggests that, on average,

the percentage increase in capacity cost between $R_2^* = 0.2$ and $R_2^* = 0.9$ is 8.0%, 6.6%, and 4.8% for the 3.2, 3.6, and 4.0 $\bar{d}$ network curves, respectively, for model 1 networks, compared to 6.6%, 5.4%, and 3.8% for the 3.2, 3.6, and 4.0 $\bar{d}$ networks, respectively, in model 2. Similarly, the 15n30s network family in Figure 6.3.3 shows an average increase in capacity cost between $R_2^* = 0.2$ and $R_2^* = 0.9$ to increase by 6.4%, 4.2%, and 4.8% in the 3.3, 3.7, and the 4.0 $\bar{d}$ networks, respectively, for model 1, while an increase of 4.5%, 3.3%, and 2.8% in the $\bar{d}$ =3.3, $\bar{d}$ =3.7, and $\bar{d}$ =4.0 networks, respectively, is shown for model 2. This additional capacity required by model 1 over model 2 is indicated by the curves representing the networks in Figure 6.3.2 and Figure 6.2.4. These charts show the percent of additional capacity needed by model 1 networks to achieve the same level of dual failure restorability inherent in model 2 networks. For model 1 network designs, the capacity costs at $R_2^* = 0.9$ and $R_2^* = 1.0$ remain almost unchanged in model 1 networks, indicating that it would incur nearly equivalent capacity costs to design for dual failure restorability of 90% and 100%. As in networks of other survivability schemes analysed previously, the highly connected networks exhibit higher capacity efficiency than the less connected networks. For example, in the 15n30s network family, the $\bar{d}$ =4.0 network provides an inherent dual failure restorability level of about 60% compared to about 30% in the 10n20s network family. Overall, between $R_2^* = 0.2$ and $R_2^* = 1.0$, we expect more capacity cost savings for networks based on model 2 than those based on model 1.

6.4. Comparison of Dual Failure Restorability Models in DSP Networks

To investigate DSP networks, we use the 10n20s and 18n36s network family charts in Figure 6.4.1 through Figure 6.4.4, showing the average node degree network curves of networks designed by models 1 and 2. The charts in Figure 6.4.1 and Figure 6.4.3 plot the normalized capacity cost (*y*-axis) against the specified dual failure restorability limit (*x*-axis) for the 10n20s and 18n36s

network families, respectively. Figure 6.4.2 and Figure 6.4.4 show the percentage increase in total capacity cost of model 1 over model 2 for various node degree networks in the 10n20s and 18n36s network families, respectively.

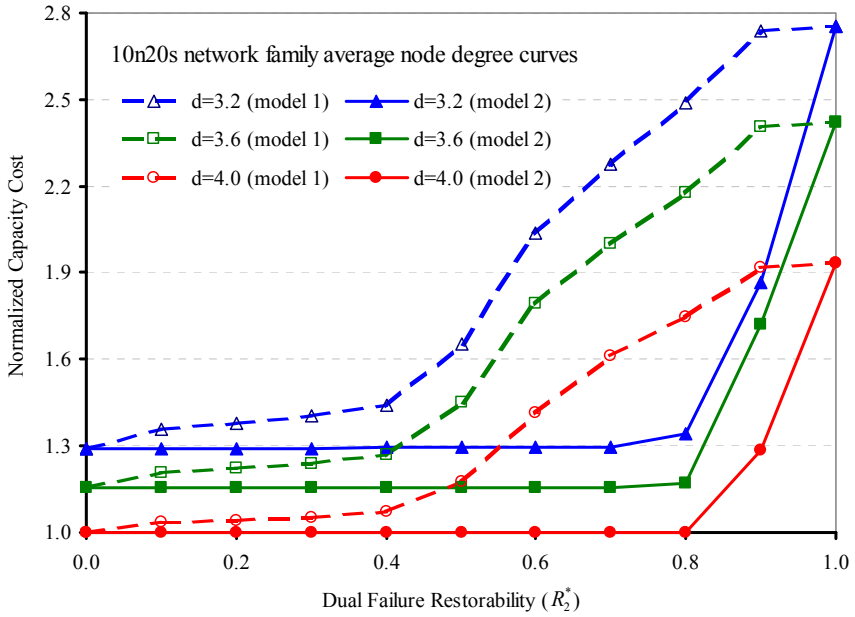

Figure 6.4.1-Dual failure restorability limit curves of model 1 and model 2 in 10n20s DSP restorable network.

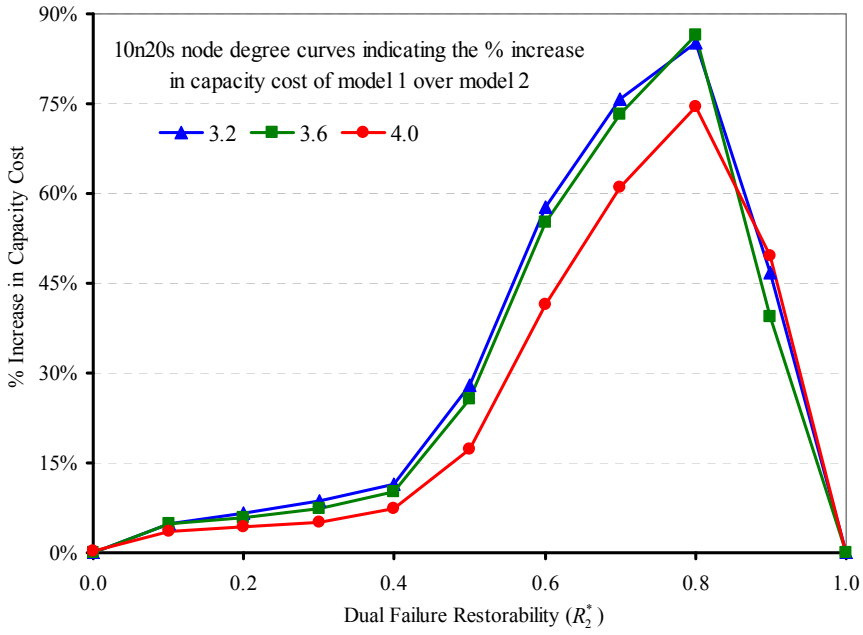

Figure 6.4.2-Relative increase in capacity cost of model 1 over the capacity cost of model 2 in 10n20s DSP restorable network family.

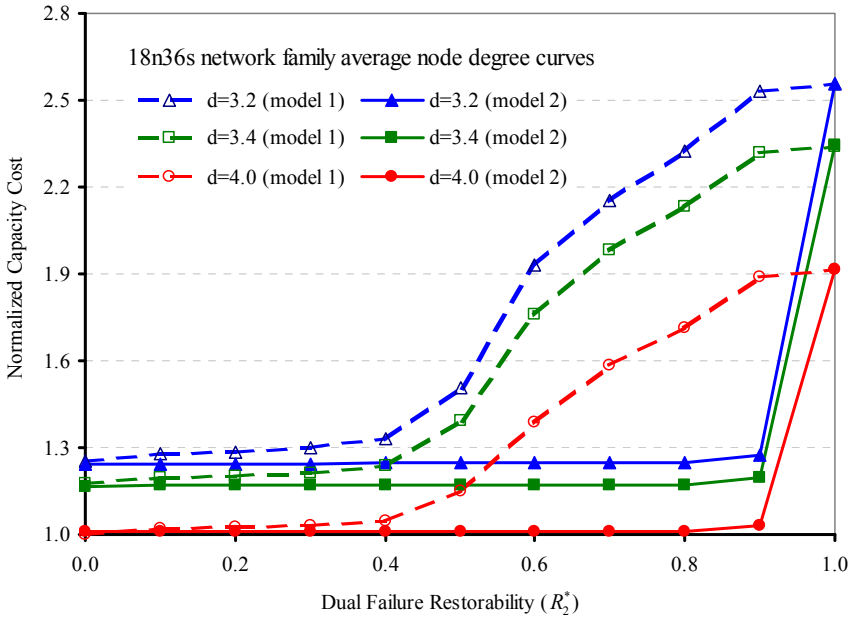

Figure 6.4.3-Dual failure restorability limit curves of model 1 and model 2 in 18n36s DSP restorable network.

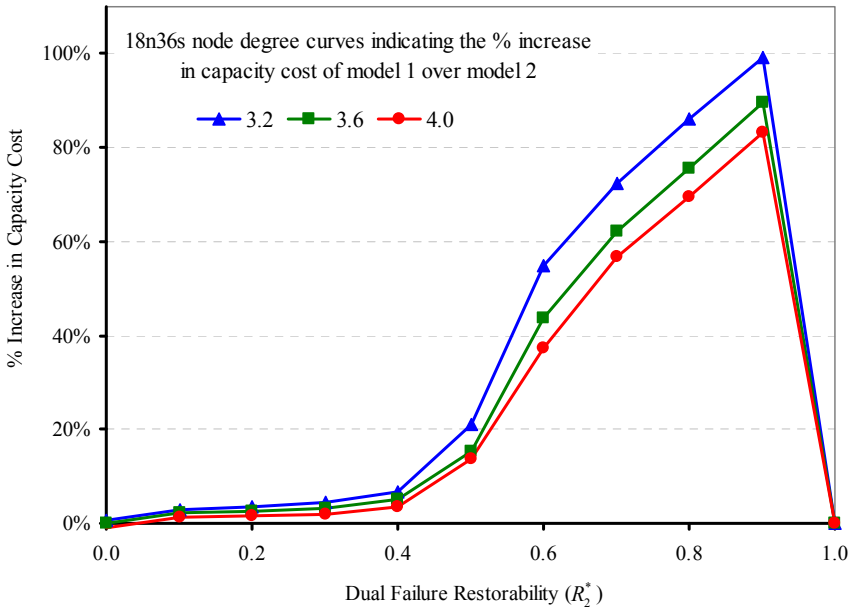

Figure 6.4.4-Relative increase in capacity cost of model 1 over the capacity cost of model 2 in 18n36s DSP restorable network family.

In Figure 6.4.1 and Figure 6.4.3 the data points are normalized to the least capacity cost at $R_2^* = 0$ in the 4.0 $\bar{d}$ network. Figure 6.4.2 shows the percentage more capacity required by model 1 over model 2 to design the same network for a 10n20s network family. From the 10n20s and 18n36s network family charts, the

average percentage point difference between model 1 and model 2 is about 1.9% up to $R_2^* = 0.4$, indicating that the gap in capacity requirement between the two models at $R_2^* \leq 0.4$ is not very significant. We also notice that there is a sharper increase in capacity cost in model 1 networks compared to model 2 networks. Network curves in model 2 do not show any increase in capacity cost until certain specified dual failure restorability level. For example, in model 2 the capacity cost of the 3.2, 3.6, and the 4.0 $\bar{d}$ networks remain flat until $R_2^* = 0.8$ in the 10n20s network family (Figure 6.4.1) and up to $R_2^* = 0.85$ in the 18n36s network family (Figure 6.4.3). This indicates that in these network sizes, no extra capacity is required to protect 80% of the demands from a dual failure scenario if optimally designed for 100% single failure restorability. The largest percentage difference in capacity cost for both models compared at different levels of dual failure restorability occurs at $R_2^* = 0.8$ for the 10n20s network family and at $R_2^* = 0.9$ for the 18n36s network family. Figure 6.4.2 shows the individual network connectivity capacity cost increase in model 1 relative to the capacity cost increase in model 2 at various levels of dual failure restorability.

6.5. Comparison of Dual Failure Restorability in *p*-Cycle and Span Restoration

Dual failure restorability as it relates to this work in both *p*-cycle and span restoration is defined in the same context and follows the same approach to formulating the design models. Though there are fundamental differences between the span and *p*-cycle restoration models, the methods of restoration for both mechanisms are very similar in that they operate by restoring specific spans. This makes it interesting to compare the two restoration mechanisms to see how they differ in terms of capacity efficiency. Both restoration mechanisms are compared with respect to model 1 in section 6.5.1 and to model 2 in section 6.5.2.

6.5.1. Comparison of *p*-Cycle and Span Restoration Mechanisms Based on Model 1

In Figure 6.5.1 and Figure 6.5.3, we show the respective node degree network curves of 10n20s and 18n36s network families on a plot of normalized capacity cost against specified dual failure restorability levels. Dashed lines represent span restoration curves and solid lines represent *p*-cycle network curves. Figure 6.5.2 and Figure 6.5.4 show the percentage increase in capacity cost of span restoration networks relative to *p*-cycle networks for the node degree networks shown in Figure 6.5.1 and Figure 6.5.3. In other words, Figure 6.5.2 shows the increase (in percentage) of capacity required by a span restoration network to provide the same level of dual failure restorability as a *p*-cycle restoration mechanism on the same network. Our findings indicate that in both the 10n20s and the 18n36s network families the *p*-cycle networks perform better in terms of capacity utilization than the span restoration mechanism. The findings in [19] suggest a similar trend in the case of single failure restorability design. In some cases, such as in Figure 6.5.2, the difference in capacity cost of the $\bar{d}$ =3.2 network curve shows a sharp increase and decrease of percentage difference in capacity cost between span restoration and *p*-cycle within the range of $R_2^* = 0.1$ and $R_2^* = 0.4$, and a fundamental change in shape of that curve relative to the others. The reason is simply a function of how those curves were generated. Recall that these curves represent the relative difference between capacity *p*-cycle and span restoration curves in Figure 6.5.1.

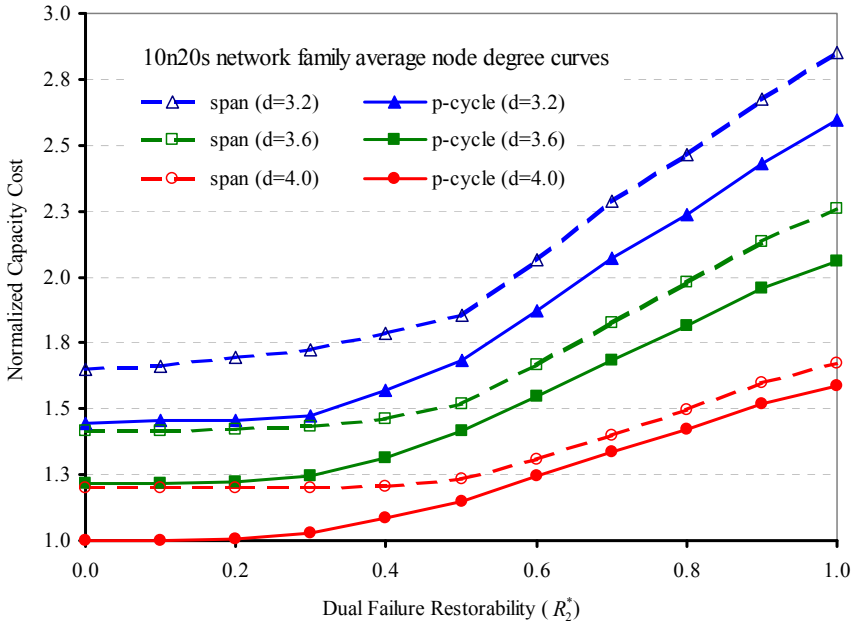

Figure 6.5.1-Comparison of dual failure restorability in model 1 of *p*-cycle and span restoration in 10n20s network family.

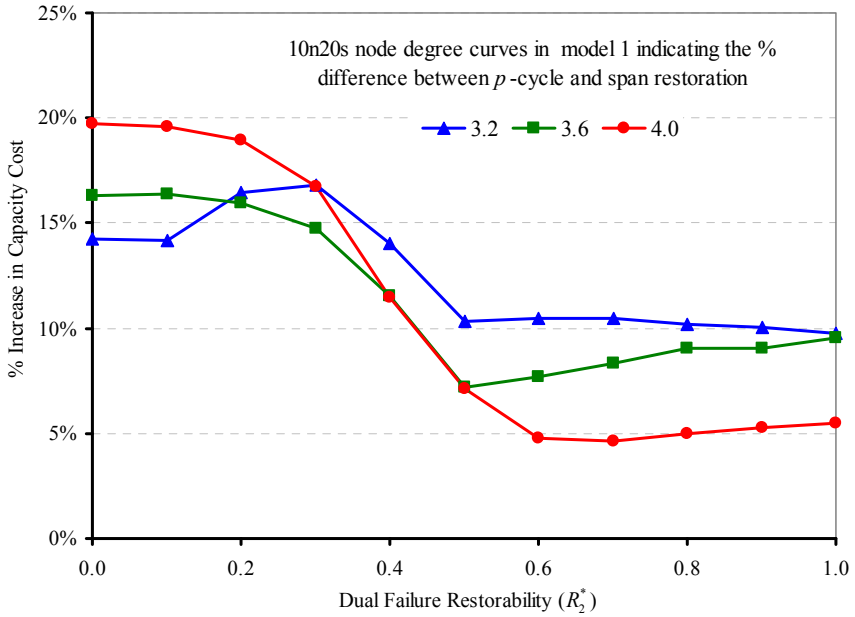

Figure 6.5.2-Percent increase in dual failure restorability cost between *p*-cycle and span restoration mechanisms in model 1 of 10n20s network family.

In the case of the $\bar{d}$ =3.2 data in Figure 6.5.1, topological consideration, sets of eligible routes, etc., conspire to cause the *p*-cycle and span restoration curves to get a little further apart between $R_2^* = 0.1$ and $R_2^* = 0.4$ than in the case of the other curves.

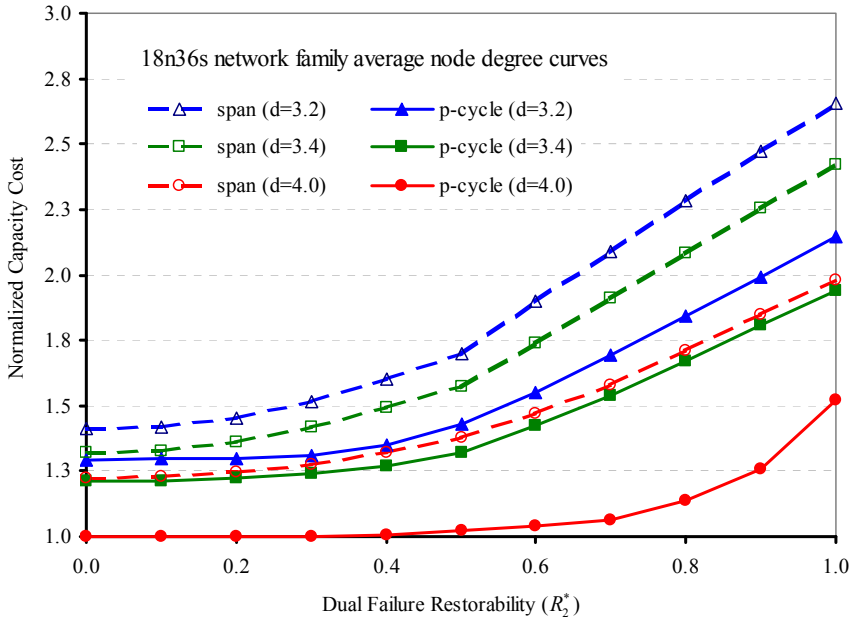

Figure 6.5.3-Comparison of dual failure restorability in model 1 of *p*-cycle and span restoration in 18n36s network family.

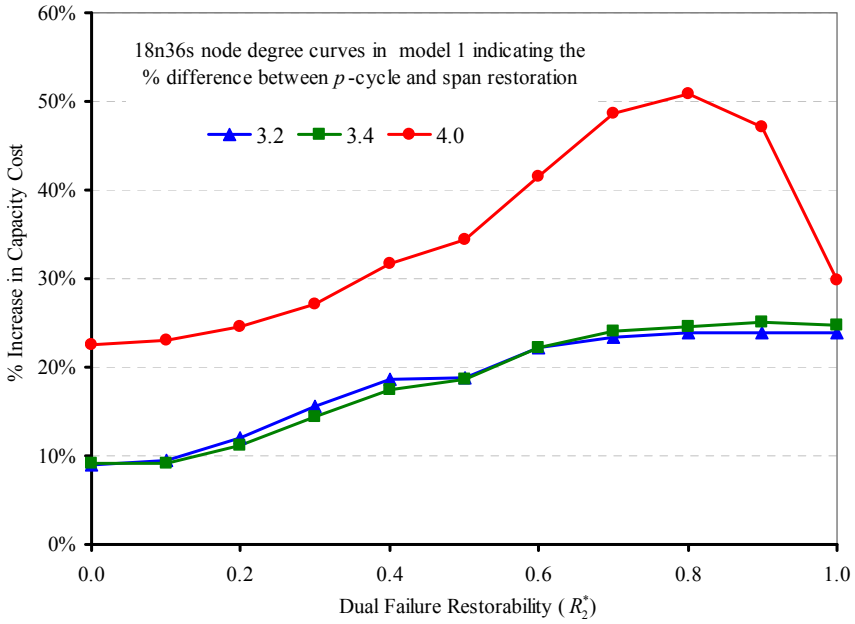

Figure 6.5.4-Percent increase in dual failure restorability cost between *p*-cycle and span restoration mechanisms in model 1 of 18n36s network family.

We can see from Figure 6.5.1 and Figure 6.5.3 that span restoration networks incur significantly more capacity cost at various levels of dual failure restorability than the *p*-cycle networks. In the 10n20s network family (Figure 6.5.2), as much as 19.7% more capacity is required for the 4.0 $\overline{d}$ network in the span restoration

mechanism than in *p*-cycle networks. Similarly, up to about 16.8% more capacity is required in the 3.2 $\bar{d}$ network for span restoration than is required for *p*-cycle restoration. In the 18n36s network family (Figure 6.5.4), the 4.0 $\bar{d}$ network requires about 50.9% more capacity for span restoration than is required for *p*-cycle restoration. This suggests that the amount of capacity required to protect a certain network from a dual failure scenario in a span restorable network is greater by a significant amount than the capacity required to protect the same network using *p*-cycle restoration.

6.5.2. Comparison of *p*-Cycle and Span Restoration Mechanisms Based on Model 2

Figure 6.5.5 and Figure 6.5.7 show the increase in capacity cost versus specified dual failure restorability levels for span restoration and *p*-cycle restoration in 10n20s and 18n36s networks, respectively, based on model 2. Span restoration curves are indicated by dashed lines, while the *p*-cycle network curves are shown in solid lines. Figure 6.5.6 and Figure 6.5.8 show the percentage increase in capacity cost of span restoration networks over *p*-cycle restoration networks for 10n20s and 18n36s networks, respectively, based on model 2.

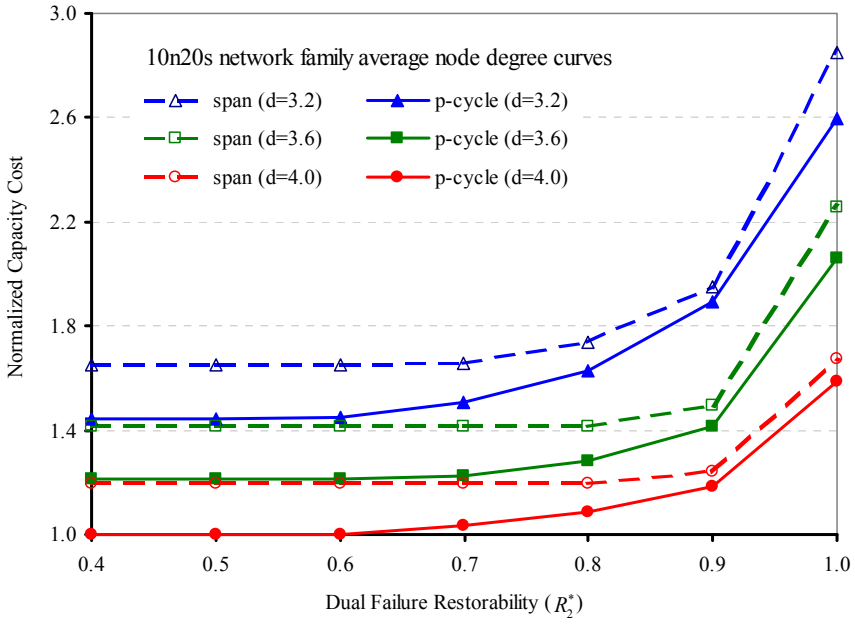

Figure 6.5.5-Comparison of dual failure restorability in model 2 of *p*-cycle and span restoration in 10n20s network family.

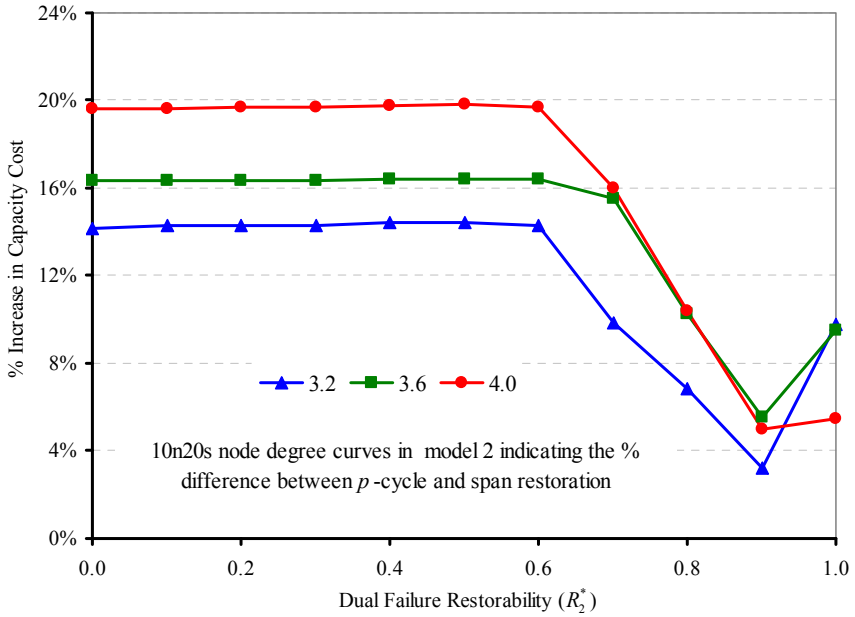

Figure 6.5.6-Percent increase in dual failure restorability cost between *p*-cycle and span restoration mechanisms in model 2 of 10n20s network family.

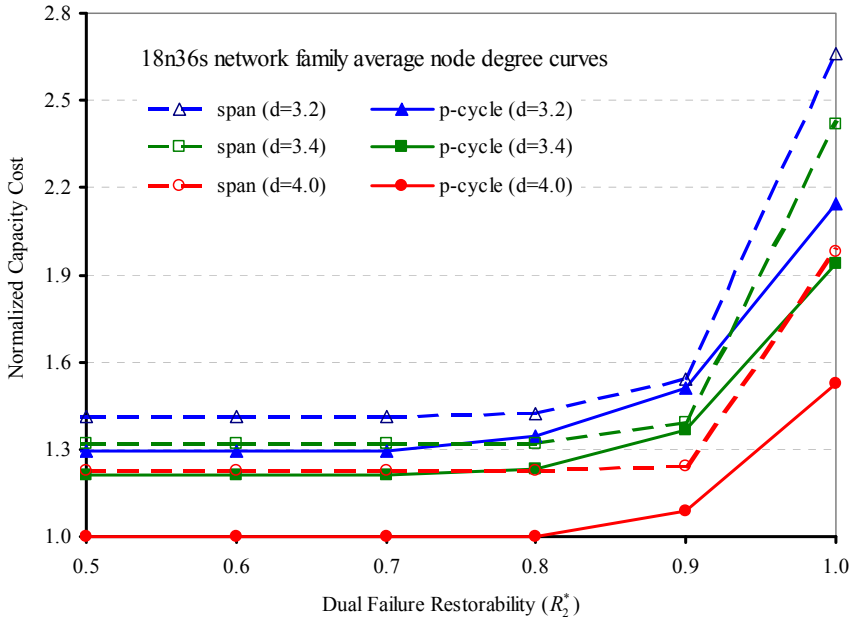

Figure 6.5.7-Comparison of dual failure restorability in model 2 of *p*-cycle and span restoration in 18n36s network family.

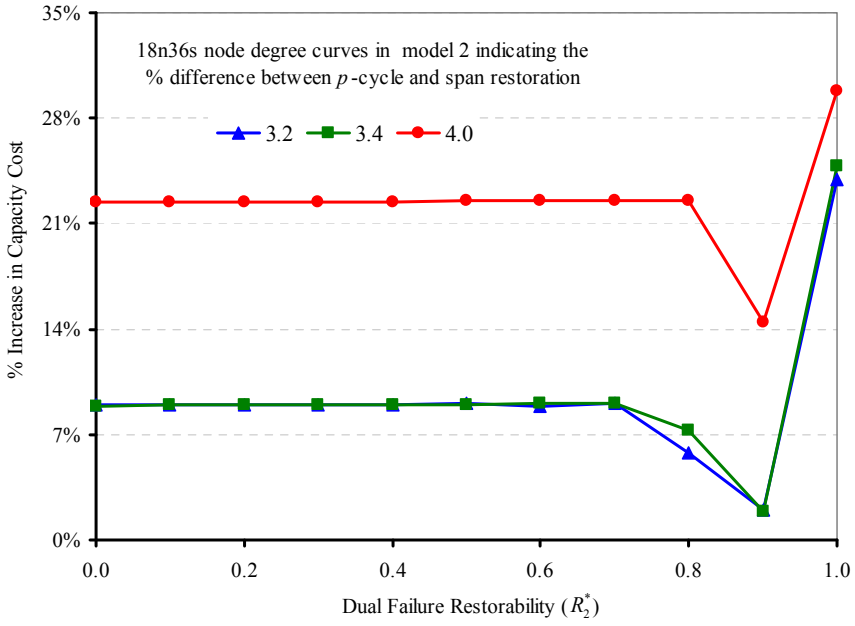

Figure 6.5.8-Percent increase in dual failure restorability cost between *p*-cycle and span restoration mechanisms in model 2 of 18n36s network family.

As observed in chapter 5, the network connectivity curves remain flat until about $R_2^* = 0.6$ for in the 10n20s network family and about $R_2^* = 0.7$ in the 18n36s network family (Figure 6.5.5 and Figure 6.5.7, respectively). The span restoration design model 2 incurs more capacity cost than the *p*-cycle restoration model 2 to

provide the same level of dual failure protection for the same size network. Figure 6.5.6 and Figure 6.5.8 show that in the 10n20s and 18n36s network families, respectively, the percentage increase in capacity cost is almost 20% more for the span restoration mechanism than *p*-cycle restoration to protect an equivalent network. Span restoration requires much higher capacity than *p*-cycle restoration at lower levels of dual failure restorability and begins to narrow down from $R_2^* = 0.6$ as the dual failure restorability approaches $R_2^* = 1.0$. For example, in Figure 6.5.6, in the 10n20s network family the capacity required for span restoration in the 4.0 $\bar{d}$ network is about 19.6% more than the capacity required for *p*-cycle restoration between $R_2^* = 0$ and $R_2^* = 0.6$. At $R_2^* = 0.9$ and $R_2^* = 1.0$ the difference in capacity cost between span and *p*-cycle restoration is narrowed to 5.0% and 5.5%, respectively. In the 18n36s network family (Figure 6.5.8), about 22.4% more capacity is needed for span restoration compared to *p*-cycle restoration of the 4.0 $\bar{d}$ network between $R_2^* = 0$ and $R_2^* = 0.7$. In conclusion, we find that irrespective of the models used, the *p*-cycle restoration mechanism appears to show better capacity utilization than the span restoration mechanism in network connectivities. At the same time, the higher cost of dual failure restorability of span restoration is balanced by its higher inherent dual failure restorability advantage compared to *p*-cycle restoration.

6.6. Comparison of Dual Failure Restorability in DSP and Path Restoration Mechanisms

Path restoration and DSP are both path-based restoration mechanisms, this means that restoration for any given pair of spans failure, is performed by completely rerouting the affected paths. We expressed the dual failure restorability for each pair of spans in both mechanisms in terms of specific dual failure restorability for each demand on the individual pair of spans. In other words, the dual failure restorability of each pair of spans is related to every demand unit in the network. Therefore, formulations of the dual failure restorability model in DSP and path restoration mechanisms follow the same fundamental approach of ensuring that

sufficient capacity is placed in the network to restore any specified proportion of demands affected by failure. With this similarity it is important to examine how DSP performs in terms of capacity efficiency relative to path restoration. Model 1 and model 2 are compared for both restoration mechanisms. Finally, data for all the restoration mechanisms-span restoration, *p*-cycle, DSP, and path restoration-are combined to provide a side-by-side comparison of all the restoration mechanisms considered in this work. In comparing the DSP and path restoration mechanisms, the 15n30s network family is used in place of the 18n36s network family as long runtimes resulted in an incomplete data set for the latter.

6.6.1. Comparison of DSP and Path Restoration Mechanisms Based on Model 1

Figure 6.6.1 through Figure 6.6.4 show various node degree networks of design model 1 in both DSP and path restoration in 10n20s and 15n30s network families. Figure 6.6.1 and Figure 6.6.3 show the normalized capacity cost (*y*-axis) plotted against the specified dual failure restorability levels (*x*-axis) for DSP and path restoration in 10n20s and 15n30s network families, respectively. The dashed curves represent the DSP networks and the solid curves represent the path restorable networks. In all figures capacity cost is normalized to the least capacity cost 4.0 $\bar{d}$ network at $R_2^* = 0$. Figure 6.6.1 and Figure 6.6.3 show the 3.2, 3.6, and 4.0 $\bar{d}$ networks curves in the 10n20s network family and 3.3, 3.7, and 4.0 $\bar{d}$ network curves in the 15n30s network family, respectively. As in the previous charts, the lower connectivity networks consistently incur more capacity cost than the higher connectivity networks in both restoration mechanisms. A significant increase in capacity cost begins about $R_2^* = 0.2$ for node degree curves in path restoration networks, while in DSP networks an increase in capacity cost starts at about $R_2^* = 0.1$. Figure 6.6.2 and Figure 6.6.4 show the percentage increase in capacity cost for 10n20s and 15n30s network families, respectively, required by various DSP network curves to provide the level of dual failure restorability obtainable in a path restoration mechanism on the same sized network. For

example, in the 10n20s network family, to provide 100% dual failure restorability, the 4.0 $\overline{d}$ network would require about 110% more capacity with a DSP mechanism than is required by path restoration.

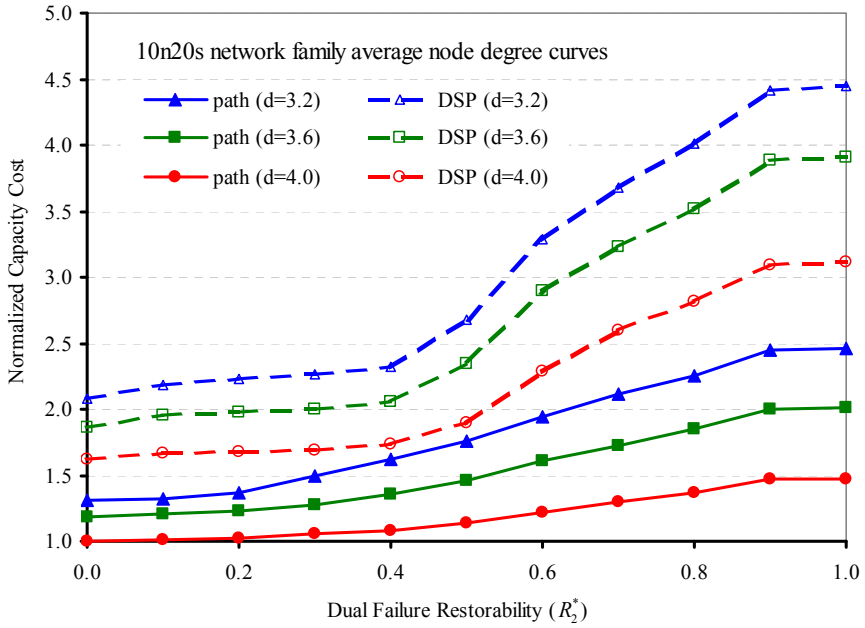

Figure 6.6.1-Comparison of dual failure restorability in model 1 of DSP and path restoration in a 10n20s network family.

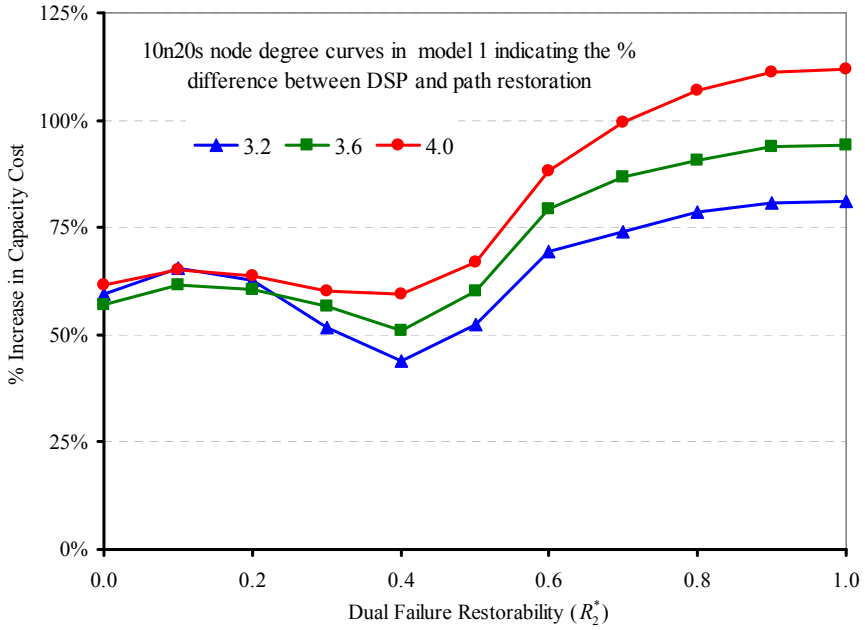

Figure 6.6.2-Percentage increase in dual failure restorability cost required by DSP over path restoration in model 1 of 10n20s network family.

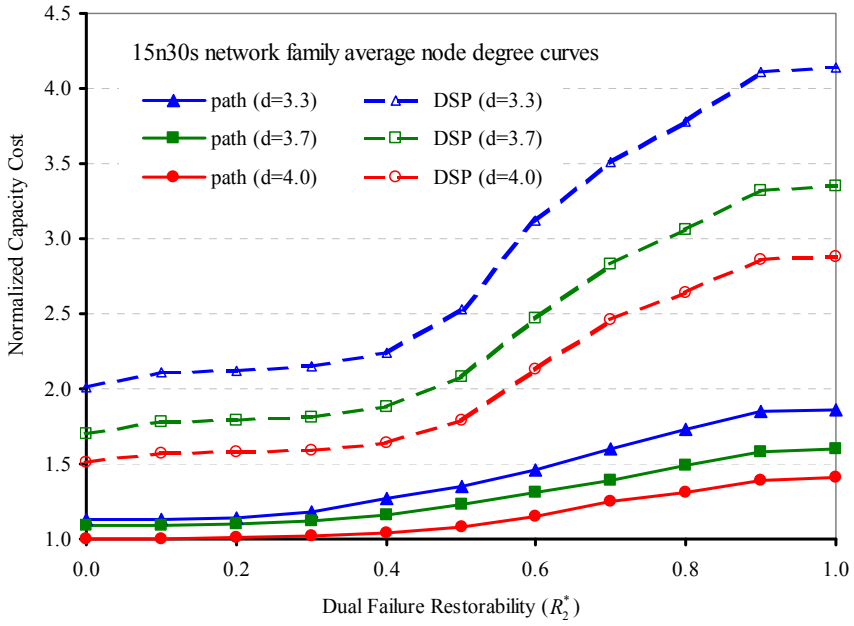

Figure 6.6.3-Comparison of dual failure restorability in model 1 of DSP and path restoration in 15n30s network family.

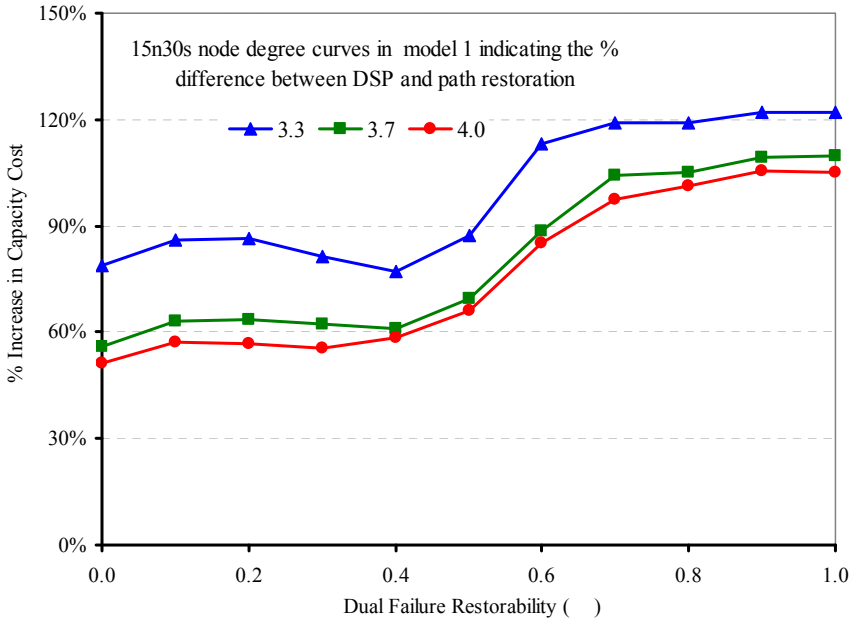

Figure 6.6.4-Percentage increase in dual failure restorability cost required by DSP over path restoration in model 1 of 15n30s network family.

Figure 6.6.1 to Figure 6.6.4 show that, based on model 1, for both network families, the capacity cost of a path restorable network is lower than the capacity cost of a DSP network. In most instances, DSP restoration requires as much as 120% more capacity than path restoration to provide an equivalent level of dual

failure restorability for the same network size. The highest percentage differences in capacity cost occur between the lowest nodal degree networks of both restoration mechanisms.

6.6.2. Comparison of DSP and Path Restoration Mechanisms Based on Model 2

Figure 6.6.5 and Figure 6.6.7 show capacity cost versus dual failure restorability for network connectivities 3.2, 3.6, and 4.0 $\bar{d}$ for the 10n20s network family and 3.3, 3.7, and 4.0 $\bar{d}$ for the 15n30s network family, respectively, for DSP and path restoration based on model 2. The charts plot the capacity cost on the *y*-axis against specified dual failure restorability levels on the *x*-axis. The dashed curves represent DSP networks and solid curves represent path restorable networks. The capacity cost data is normalized to the least capacity cost, that is, the 4.0 $\bar{d}$ connection of the path restorable network at $R_2^* = 0$. Figure 6.6.6 and Figure 6.6.8 show the percentage increase in capacity required by various DSP networks to provide a level of dual failure restorability equal to the path restoration mechanism for the same network size, based on model 2.

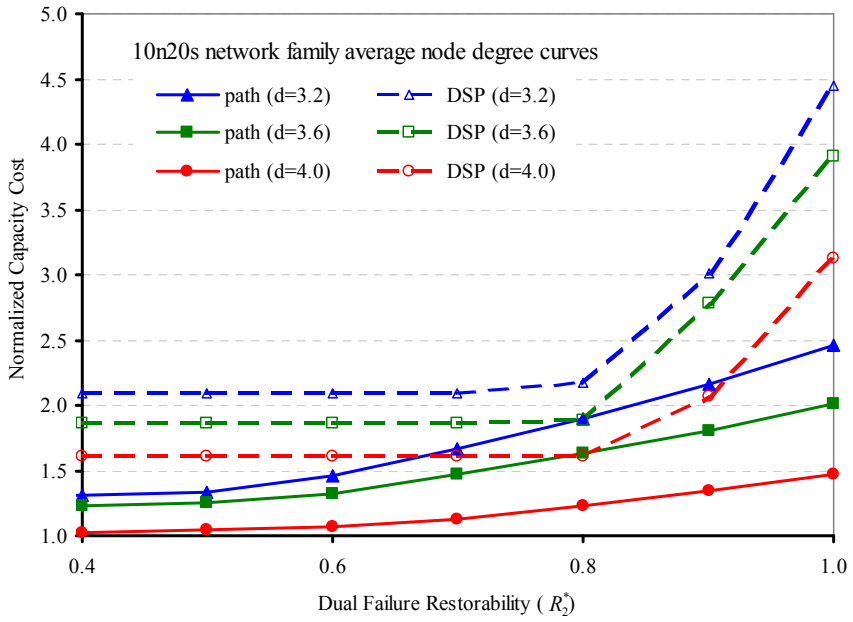

Figure 6.6.5-Comparison of dual failure restorability in model 2 of DSP and path restoration in 10n20s network family.

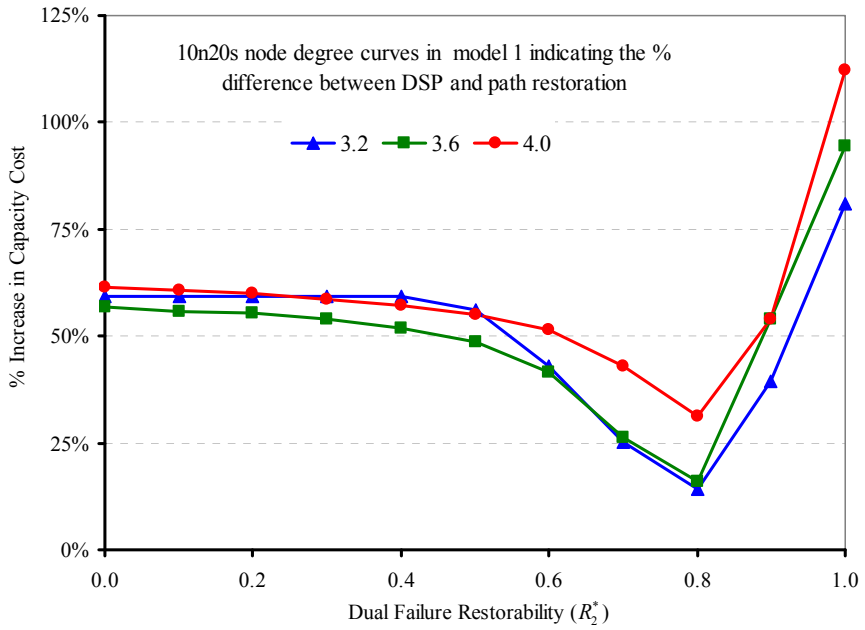

Figure 6.6.6-Percentage increase in dual failure restorability cost required by DSP over path restoration in model 2 of 10n20s network family.

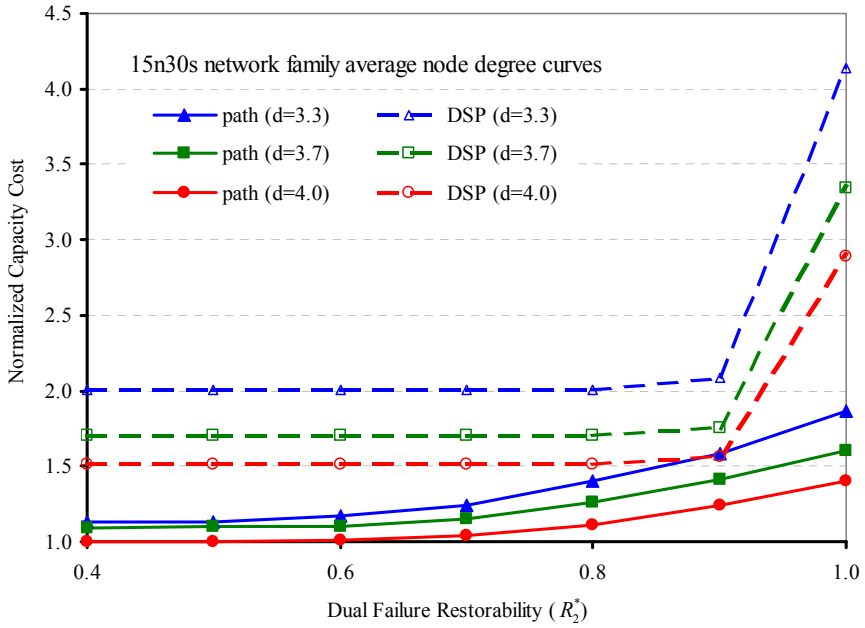

Figure 6.6.7-Comparison of dual failure restorability in model 2 of DSP and path restoration in 15n30s network family.

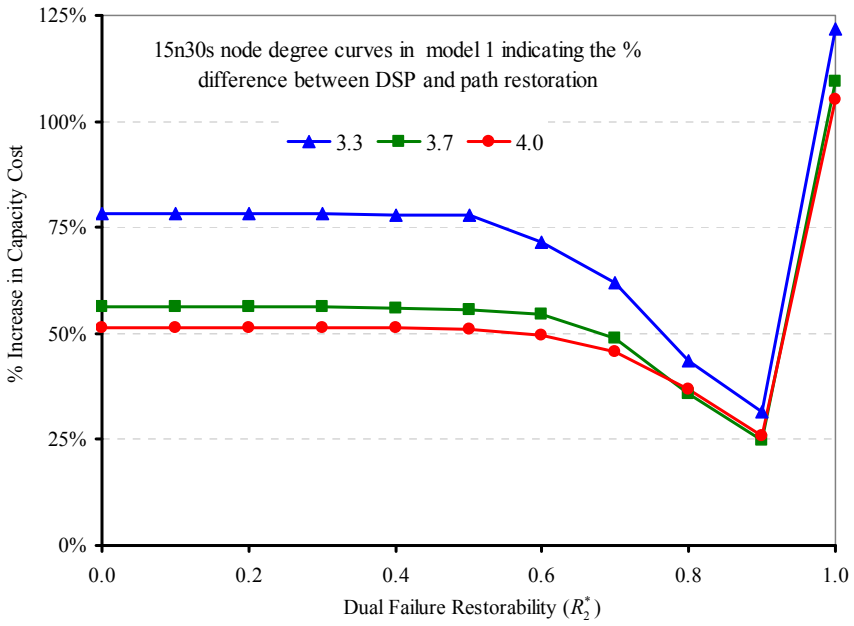

Figure 6.6.8-Percentage increase in dual failure restorability cost required by DSP over path restoration for model 2 of 15n30s network family.

Our findings for model 2 indicate that DSP networks require much higher capacity than path restoration networks to achieve the same level of dual failure restorability for the same network size. In Figure 6.6.8, we see that for the 15n30s network family the maximum percentage increase in total capacity cost required by DSP over path restoration networks approaches 121%, 110%, and 105% for the 3.3, 3.7, and 4.0 $\bar{d}$ networks, respectively, at $R_2^* = 1.0$. In Figure 6.6.6, for the 10n20s network family, the increase in capacity cost required by DSP over path restoration is 112%, 95%, and 81% for the 4.0, 3.6, and 3.2 node degree networks at $R_2^* = 0.1$. Therefore, path restoration performs much better in terms of capacity efficiency in single failure and dual failure restorability than the DSP restoration. We also find that in the 10n20s network family, the 3.2, 3.6, and 4.0 $\bar{d}$ networks require, respectively, at least 61%, 59%, and 57% more capacity for DSP restoration than for path restoration to provide 100% single failure restorability on the same network. Similarly, in the 15n30s network family, 78%, 56%, and 51% more capacity is required by the 3.3, 3.7, and 4.0 $\bar{d}$ connectivities, respectively, for DSP restoration over path restoration to provide 100% single failure restorability.

6.7. Side-by-Side Comparison of Four Survivability Mechanisms

In order to compare the performance in terms of capacity utilization and requirement under dual failure restorability of each of the survivability schemes studied here, we plotted the data generated from each survivability scheme on the same charts with the same scale. Based on models 1 and 2, we compare the restoration mechanisms using four different node degree networks in two network families (10n20s and 15n30s). In order to keep the analysis simple, we use only the 3.2 and 4.0 $\overline{d}$ networks for the 10n20s network family, and 3.3 and 4.0 $\overline{d}$ networks for the 15n30s network family.

6.7.1. Side-by-Side Comparison of Four Survivability Mechanisms Based on Model 1.

Figure 6.7.1 through Figure 6.7.8 describe capacity costs of dual failure restorability for four survivability mechanisms in 10n20s and 15n30s network families based on model 1. Figure 6.7.1 and Figure 6.7.3 plot normalized capacity cost against specified dual failure restorability levels for the 3.2 and 4.0 $\overline{d}$ networks of the 10n20s network family. Figure 6.7.2 and Figure 6.7.4 show the percentage increase in capacity cost of DSP restoration over path restoration against the specified dual restorability levels for the 3.2 and 4.0 $\overline{d}$ networks of the 10n20s network family. Figure 6.7.5 and Figure 6.7.7 plot normalized capacity cost against specified dual failure restorability for the 3.3 and 4.0 $\overline{d}$ networks of the 15n30s network family. Figure 6.7.6 and Figure 6.7.8 show percentage increase in capacity cost of DSP restoration over path restoration against the specified dual restorability levels for the 3.3 and 4.0 $\overline{d}$ networks of the 15n30s network family. From Figure 6.7.2 and Figure 6.7.4 we can see that DSP/Span restoration shows a significant percentage increase in capacity to provide the same level of dual failure restorability as span restoration for the same network. Capacity cost data for the average node degree network curves was generated from dual failure restorability based on model 1 of DSP, span, *p*-cycle and path restorable networks.

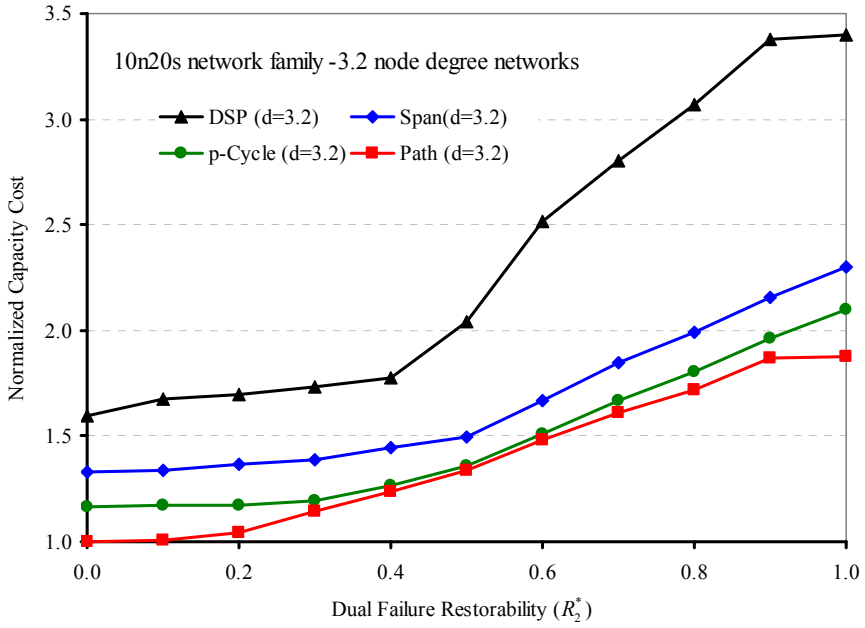

Figure 6.7.1-Comparison of dual failure restorability of model 1 in DSP, span restoration, *p*-cycle, and path restoration in a 10n20s network family with a 3.2 node degree network.

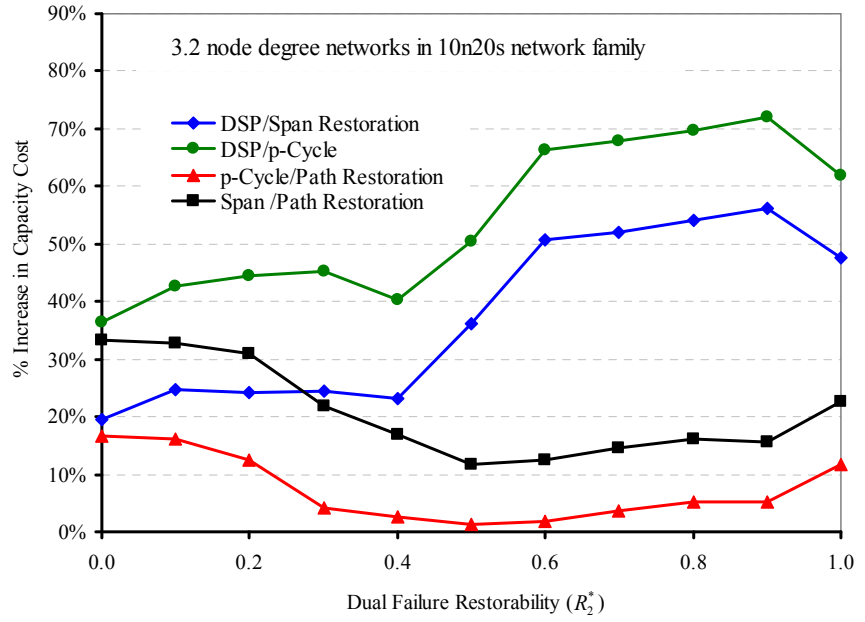

Figure 6.7.2-Percentage increase in dual failure restorability cost required by DSP over path restoration in a 10n20s network family with a 3.2 node degree network (model 1).

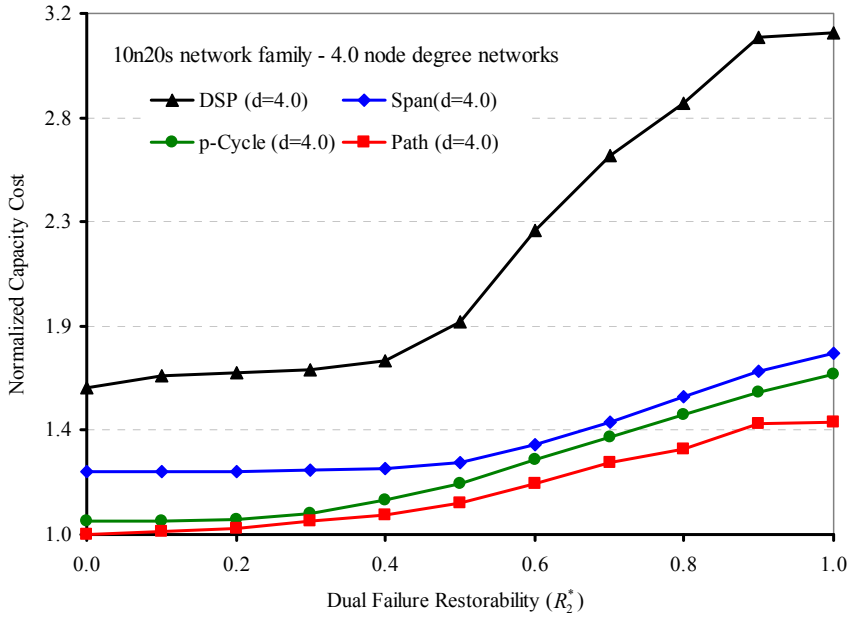

Figure 6.7.3-Comparison of dual failure restorability of model 1 in DSP, span restoration, *p*-cycle, and path restoration in a 10n20s network family with a 4.0 node degree network.

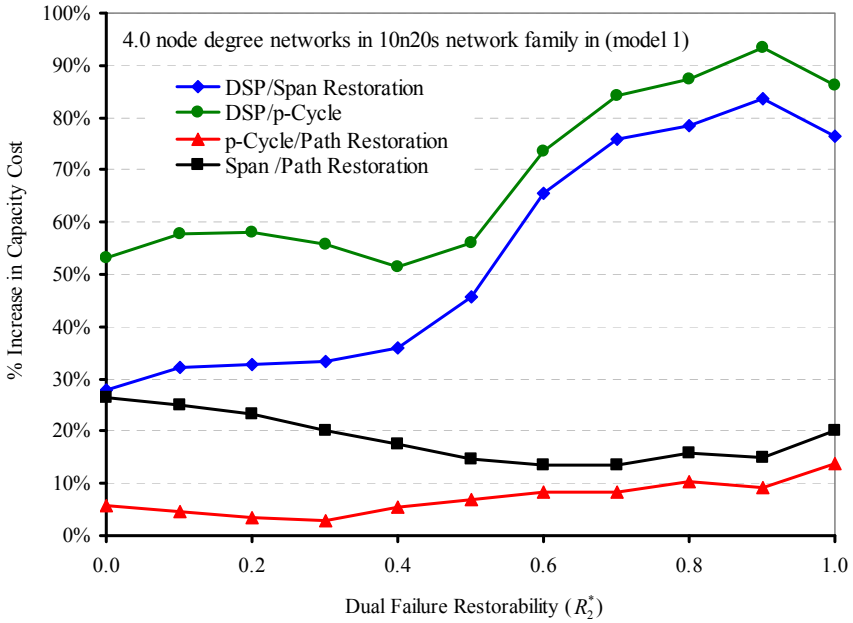

Figure 6.7.4-Percentage increase in dual failure restorability cost required by DSP over path restoration in a 10n20s network family with a 4.0 node degree network (model 1).

As we can see from Figure 6.7.1 and Figure 6.7.3, path restoration network curves achieve the best capacity utilization at all levels of dual failure restorability when compared to DSP, *p*-cycle, and span restoration. Path restoration capacity utilization is followed in order by *p*-cycle, span restoration, and DSP. In

comparing the various network restoration mechanisms relative to one another in Figure 6.7.2 and Figure 6.7.4, the charts show that the largest percentage increase in capacity cost required by one restoration mechanism over others occurs between DSP and span restoration. However, DSP and path restoration appear to have an even larger capacity cost gap than DSP and span restoration or *p*-cycle. Looking at the 4.0 $\bar{d}$ curve in the 10n20s network family (Figure 6.7.4), we find that at $R_2^* = 0.6$, the DSP network requires up to 74% and 66% more capacity cost than *p*-cycle and span restoration, respectively. Similarly, the *p*-cycle requires only 8% more capacity than path restoration to achieve 60% of dual failure restorability (that is, $R_2^* = 0.6$) and span restoration needs about 14% more capacity than path restoration at $R_2^* = 0.6$ to provide an equivalent level of dual failure restorability.

Figure 6.7.5 through Figure 6.7.8 describe capacity costs of dual failure restorability for four survivability mechanisms in 15n30s network families based on model 1. Figure 6.7.5 and Figure 6.7.7 plot the capacity cost versus dual failure restorability of the 3.3 and 4.0 $\bar{d}$ networks of the 15n30s network family. The trends for the survivability mechanisms in Figure 6.7.5 and Figure 6.7.7 are similar to those of Figure 6.7.1 and Figure 6.7.2, respectively. In the larger network sizes, the capacity efficiency of the restoration mechanisms generally improves over the smaller sized networks. Even more significant is the capacity efficiency in path restoration over the other restoration mechanisms. We find that in network curves 3.3 and 4.0 $\bar{d}$ in the 15n30s network family, the capacity cost savings of path restoration over span restoration and *p*-cycles increases by as much as 32% and 27% compared to the 10n20s network family respectively. And the percentage increase in capacity cost of DSP over span restoration and *p*-cycle is reduced by a tiny fraction, approximately 7% and 8%, respectively, compared to the network curves in the 10n20s network family.

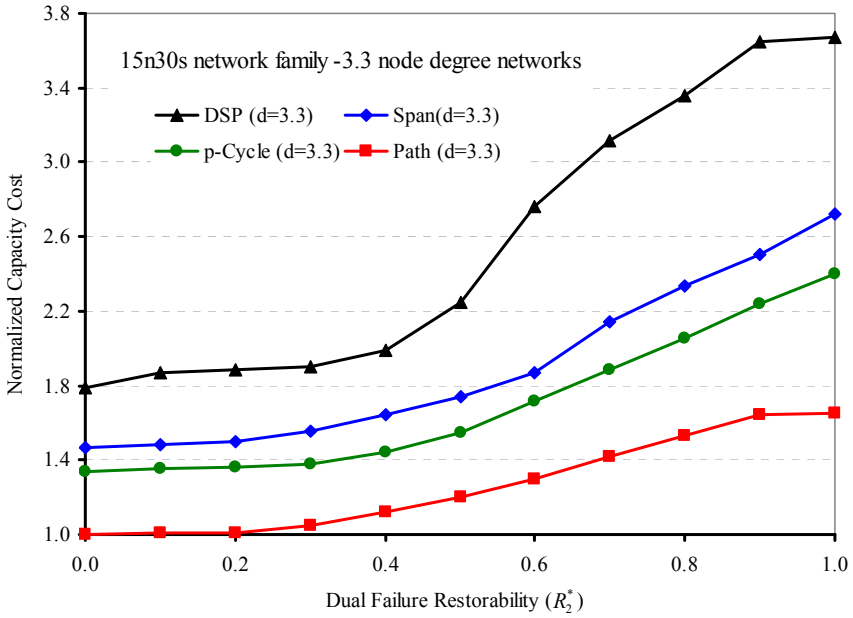

Figure 6.7.5-Comparison of dual failure restorability in model 1 of DSP, span restoration, *p*-cycle, and path restoration in a 15n30s network family with a 3.3 node degree network.

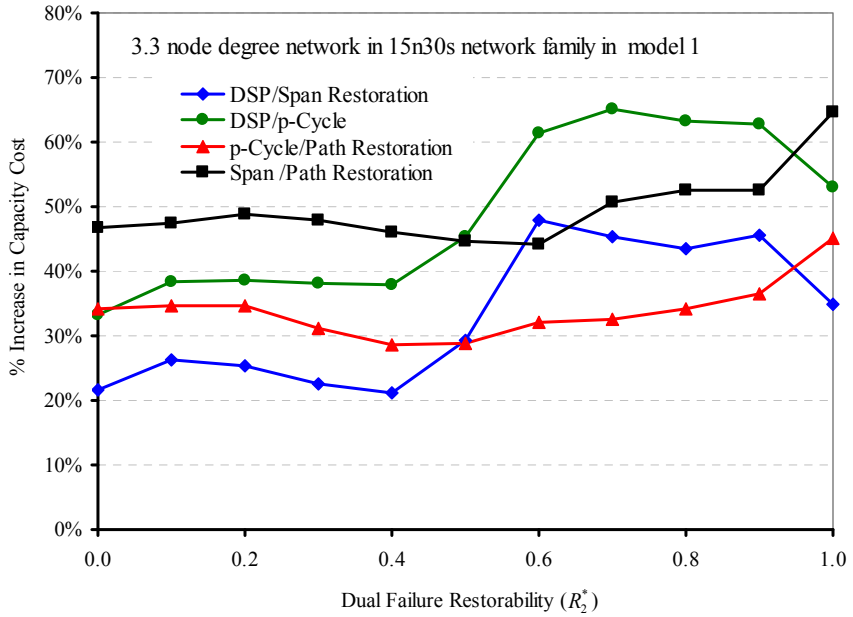

Figure 6.7.6-Percentage increase in dual failure restorability cost required by DSP over path restoration in a 15n30s network family with a 3.3 node degree network (model 1).

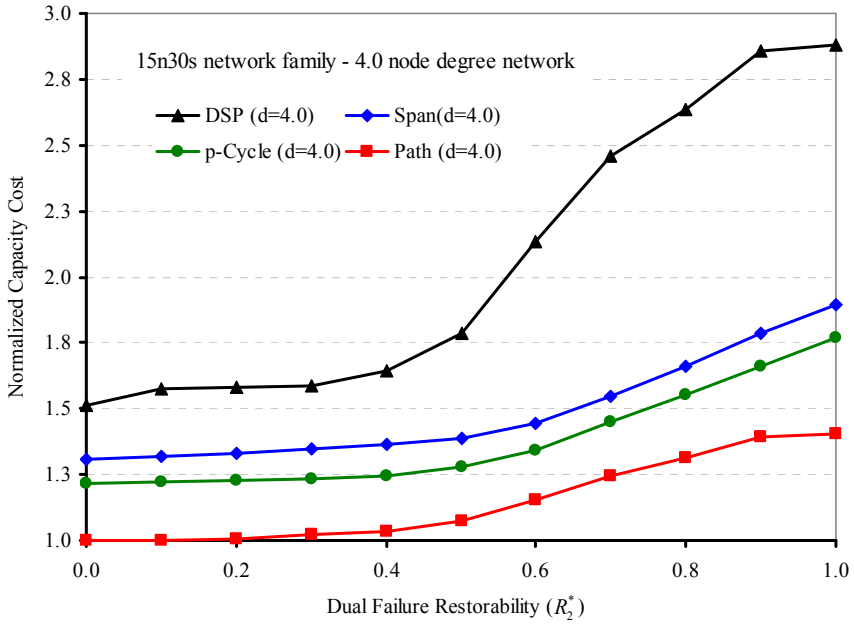

Figure 6.7.7-Comparison of dual failure restorability in model 1 of DSP, span restoration, *p*-cycle, and path restoration in a 15n30s network family with a 4.0 node degree network.

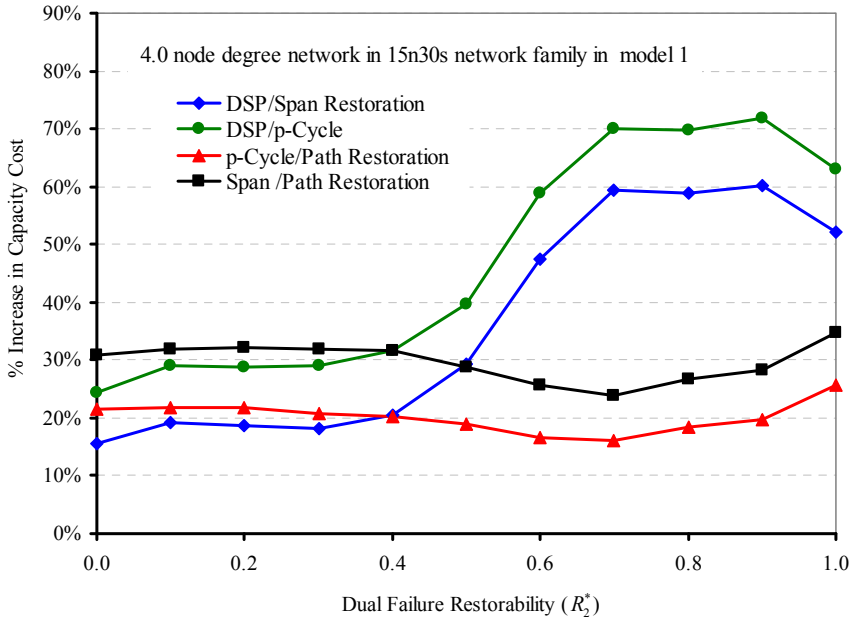

Figure 6.7.8-Percentage increase in dual failure restorability cost required by DSP over path restoration in a 15n30s network family with a 4.0 node degree network (model 1).

Overall, model 1 network design charts show that DSP is the most expensive restoration mechanism among the four studied, followed by span restoration, *p*-cycle, and finally path restoration. The evidence that path restoration is more efficient as illustrated in our results can be validated by the work done in [19] and

can also be validated by looking at the single failure result equivalent to $R_2^* = 0$ herein.

6.7.2. Side-by-Side Comparison of Four Survivability Mechanisms Based on Model 2.

Similar to the comparison made between the restoration mechanisms in the previous section, here we compare the same restoration mechanisms using model 2 of the specified dual failure restorability design. Figure 6.7.9 through Figure 6.7.16 show the capacity cost for dual failure restoration of 10n20s and 15n30s network families based on model 2. Figure 6.7.9 and Figure 6.7.11, plot normalized capacity cost against specified dual failure restorability for 3.2 and 4.0 $\bar{d}$ networks in the 10n20s network family. Figure 6.7.13 and Figure 6.7.15 plot normalized capacity cost against specified dual failure restorability for 3.3 and 4.0 $\bar{d}$ networks in the 15n30s network family. These charts rank the restoration mechanisms in terms of efficiency of capacity investment. Figure 6.7.10, Figure 6.7.12, Figure 6.7.14, and Figure 6.7.16 indicate the percentage increase in total capacity cost of one restoration mechanism over another at various levels of dual failure restorability. For example, in Figure 6.7.10 and Figure 6.7.14, the DSP/span restoration curve indicates the percentage increase in capacity cost over the total capacity cost of span restoration that is required by a DSP network to provide the same level of dual failure restorability on the same network. In other words, DSP networks engender higher capacity cost than span restoration mechanisms to provide the same level of dual failure restorability in equivalent networks. In Figure 6.7.9 and Figure 6.7.11, we see that the capacity cost of path restoration at $R_2^* = 0.6$ through $R_2^* = 0.9$ exceeds the capacity costs of both span restoration and *p*-cycle. This is reflected in Figure 6.7.10 and Figure 6.7.12, where the *p*-cycle/path restoration curve and the span/path restoration curve at $R_2^* = 0.6$ through $R_2^* = 0.9$ are on the negative scale of the *y*-axis. This means that path restoration requires more capacity than span restoration and *p*-cycle at those points to provide the same level of dual failure restorability.

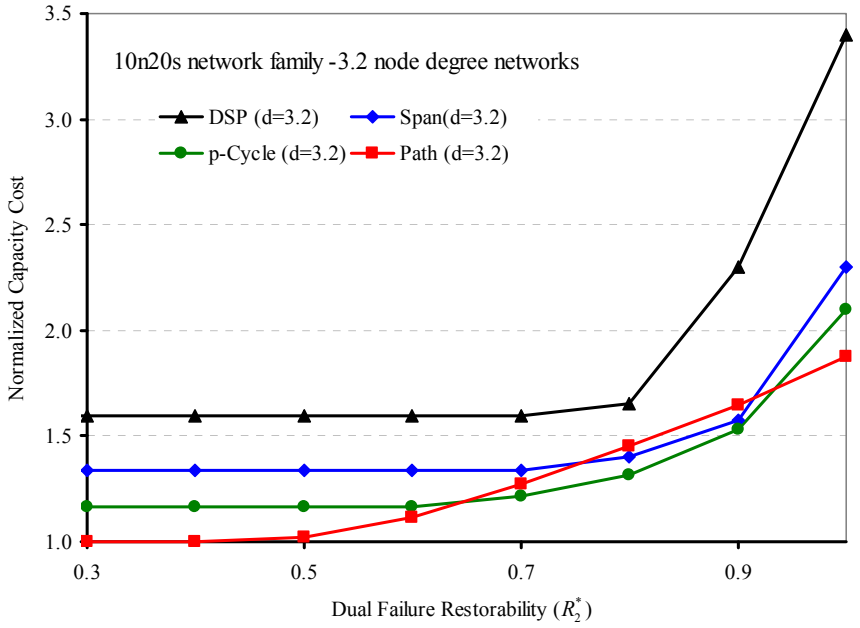

Figure 6.7.9-Comparison of dual failure restorability in model 2 of DSP, span restoration, *p*-cycle, and path restoration in a 10n20s network family with a 3.2 node degree network.

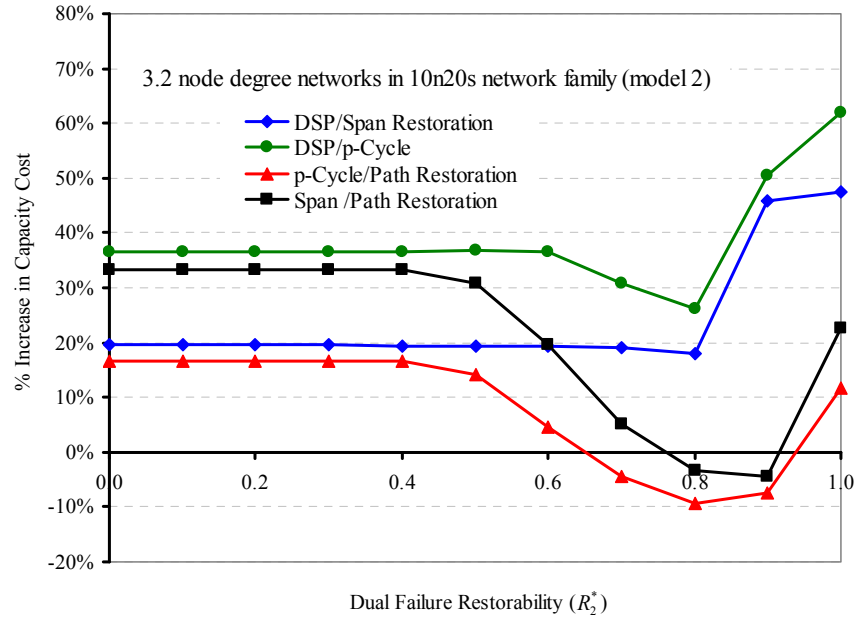

Figure 6.7.10-Percentage increase in dual failure restorability cost required by DSP over *p*-cycle and span restoration in model 2 of a 10n20s network family with a 3.2 node degree network.

Our investigation shows that this effect is seen only in the 10n20s network family and is as a result of limited number of eligible restoration route paths available for path restoration. This limit in eligible routes set therefore constrains the restoration mechanism to select from fewer numbers of eligible routes which

results in higher capacity cost compared to *p*-cycle and span restoration at the various points.

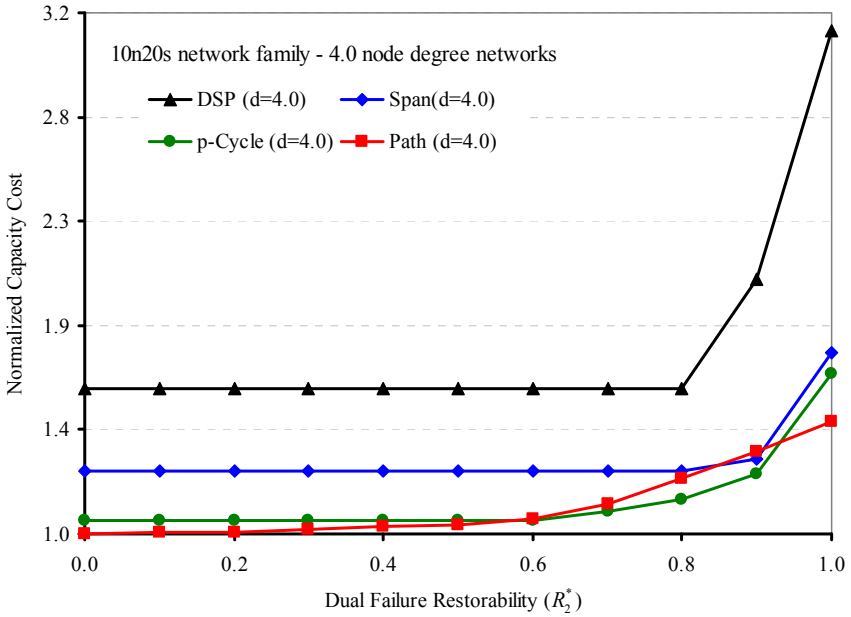

Figure 6.7.11-Comparison of dual failure restorability in model 2 of DSP, span restoration, *p*-cycle, and path restoration in a 10n20s network family with a 4.0 node degree network.

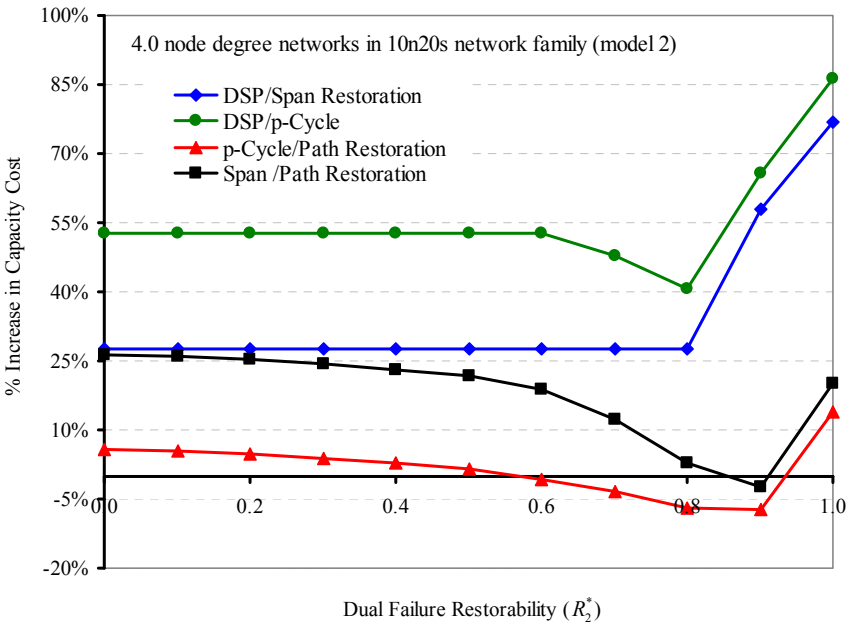

Figure 6.7.12-Percentage increase in dual failure restorability cost required by DSP over *p*-cycle and span restoration in model 2 of a 10n20s network family with a 4.0 node degree network.

The chart Figure 6.7.9 is truncated at $R_2^* = 0.3$ as there is no significant increase in capacity cost between $R_2^* = 0$ and $R_2^* = 0.3$ on the dual failure restorability scale. DSP tops the charts (Figure 6.7.9 and Figure 6.7.11) in the capacity requirement for all levels of dual failure restorability among the other restoration mechanisms, followed by span restoration, *p*-cycle, and path restoration. These trends are similar to those obtained in the analysis based on model 1, where the percentage increase in capacity cost for the DSP networks also ranks higher than *p*-cycle and span restoration. DSP/path restoration and span/*p*-cycle restoration are not represented here as they were discussed in sections 6.6.1 and 6.5.2, respectively. Figure 6.7.10 and Figure 6.7.12 compare the percentage increase in capacity of all four restoration mechanisms to provide the same level of dual failure restorability for 3.2 and 4.0 $\bar{d}$ connectivities, respectively, in the 10n20s network family. Similar charts are shown for the 15n30s network family in Figure 6.7.13 through Figure 6.7.16. These charts compare capacity cost versus dual failure restorability for the four restoration mechanisms for 3.3 and 4.0 $\bar{d}$ networks of the 15n30s network family. From Figure 6.7.13 and Figure 6.7.15 we see that capacity cost versus dual failure restorability for respective connectivities 3.3 and 4.0 $\bar{d}$ tend to follow the same trends in the 15n30s network family as in other networks analysed in this work. The trends for capacity cost increase versus dual failure restorability in Figure 6.7.14 and Figure 6.7.16 for 3.3 and 4.0 $\bar{d}$ networks, respectively, in the 15n30s network family also resemble the relationships shown in other networks studied here.

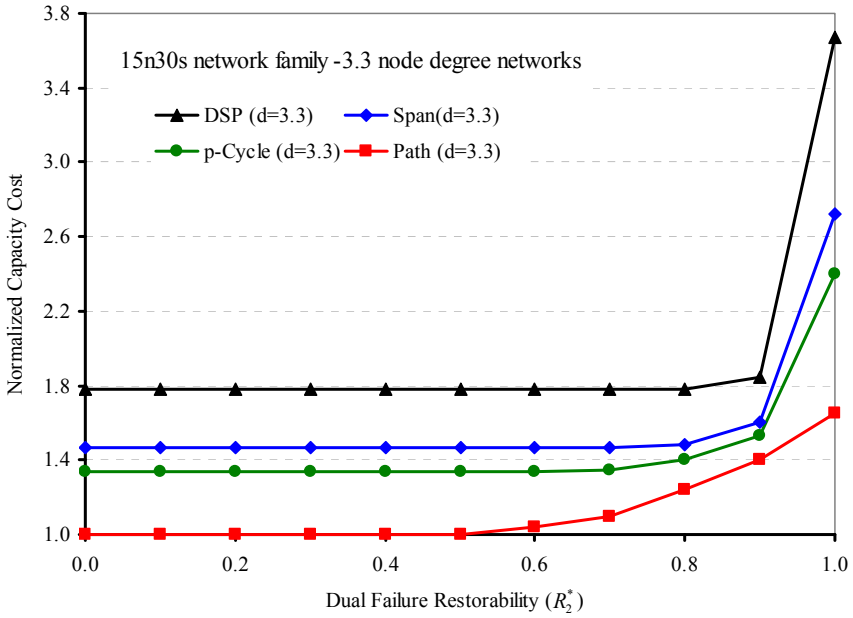

Figure 6.7.13-Comparison of dual failure restorability in model 2 of DSP, span restoration, *p*-cycle, and path restoration in a 15n30s network family with a 3.3 node degree network.

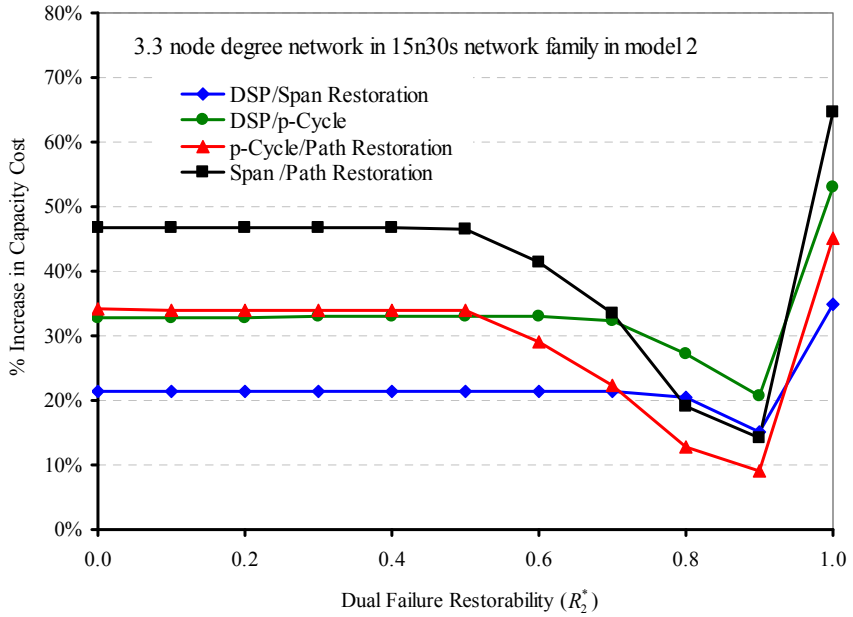

Figure 6.7.14-Percentage increase in dual failure restorability capacity cost required by DSP over *p*-cycle and span restoration in model 2 of a 15n30s network family with a 3.3 node degree network.

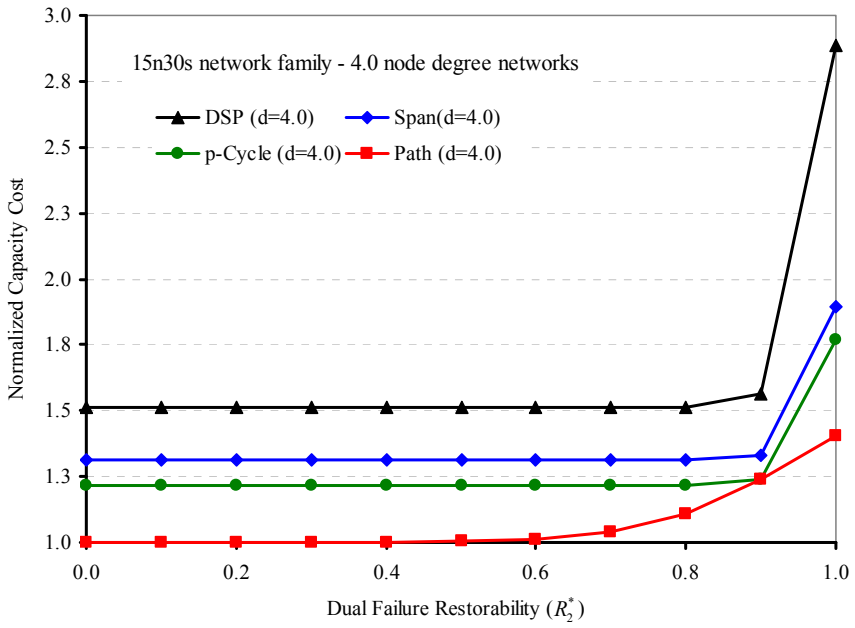

Figure 6.7.15-Comparison of the dual failure restorability in model 2 of DSP, span restoration, *p*-cycle, and path restoration of a 15n30s network family with a 4.0 node degree network.

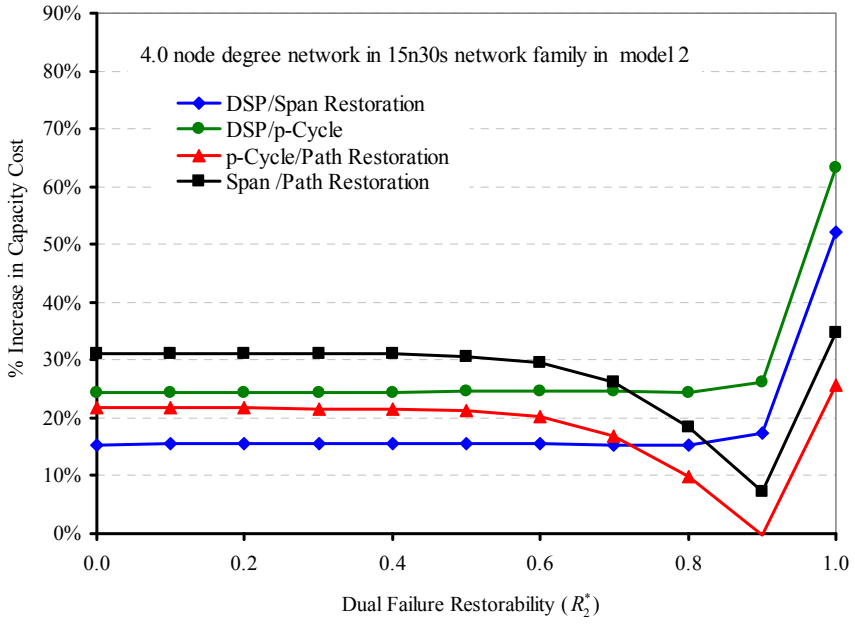

Figure 6.7.16-Percentage increase in dual failure restorability capacity cost required by DSP over *p*-cycle and span restoration in model 2 of a 15n30s network family with a 4.0 node degree network.

Trends for model 2 involving capacity cost versus dual failure restorability in the 15n30s network family are similar to those found in the 10n20s network family, except that the margin of percentage increase in capacity cost is reduced as the network size increases. This is consistent with the findings in model 1 results,

section 6.7.1, where we found that as the network size and connectivity increases capacity cost decreases.

Chapter 7

Concluding Remarks

7. Conclusions

This thesis focuses on developing an efficient method of designing transport networks to withstand dual failure. New ILP design models are formulated to achieve any specified level of dual failure restorability in various restoration mechanisms.

In Chapter 1 we introduced the basic components and the framework of transport networks and discussed briefly the evolution of telecommunication transport networks. And discussed the various types of private networks (LAN, MAN and WAN) and the public networks (Long Haul or Backbone networks) and their functional relationship in terms of demand and signal transmission. Then we defined some of the terms, notations and concepts including graph theory, set theory and mathematical programming that are used in implementing the design models.

In Chapter 2 we discussed the concepts of network survivability and the classifications of network survivability methods into two types; the active *restoration mechanism* and the pre-configured mechanism known as the *protection mechanism*. It introduced the various network architectures and illustrated the basics of these mechanisms including *APS*, *survivable rings*, and others mesh restorable networks such as *span restoration* (SR), *p-cycle*, *path restoration* (PR) and *demand-wise shared protection* (DSP). We also discussed the impact of single failure scenarios on the different survivability mechanisms and how the mechanisms differ with each other in terms of the capacity utilization.

In chapter 3, we discussed the some of the definitions dual failure restorability. We also discussed the various approach used in the formulation of dual failure restorability in the restoration mechanisms mentioned in chapter 2. The chapter

focused on *span restoration* (SR), *p-cycle*, *path restoration* (PR) and *demand-wise shared protection* (DSP). We demonstrated various failure scenarios that can potentially result to an outage in the network. We discussed the mathematical formulations and using ILP methods to develop network design models for each of the survivability scheme studied (including span restoration, *p*-cycle, DSP and path restoration).

In chapter 4 and chapter 5, we discussed the experimental procedure and how the data is collected. We also showed solution data presented in various charts. The solution data are generated from the network problems solved for each of the survivability schemes. The chats show the trend of the total capacity cost for various levels of dual failure restorability on different network sizes. We also show the variations in capacity cost between the different node degree networks in the same network family. The two models developed were compared to one another in various node degrees within the individual network family. We also determined the increase in capacity cost of various levels of dual failure restorability compared to the cost of design for single failure scenario. One of the major findings includes the level of inherent dual failure restorability advantage exhibited by some of this network for single failure restorability design. And as expected, we also find that as the specified dual failure restorability limit approached 100%, a very significant increase in the amount of capacity that is required to protect the network from dual failure scenario. In chapter 6, we performed comparative analysis of the survivability mechanisms and compared them side-by-by for the span-based restoration mechanisms and with the path-based mechanisms. Finally we presented charts that indicate the relative percentage increase in capacity costs of one mechanism over another.

7.1. Main Contributions

The main contributions in this work include:

1). That we developed a number of new dual failure restorability design models for each of the four survivability schemes studied including *p*-cycle, DSP span and path restoration. This new models will enable a network designer to perform

specific dual failure restorability design in the four survivability schemes presented in this thesis.

2). With the results obtained can be used as some benchmark data for future design work to determine total capacity required by each of the network family and connectivity at various levels of specified dual failure restorability. We also performed a comparative analysis of the different restoration mechanisms to determine the capacity efficiency of each scheme relative to another.

3). Other contributions include one refereed journal publication in the *Journal of Optical Networks* (JON) [74], two conference paper publications in the *Proceedings of the IEEE International Conference on Communications* (ICC 2008 and 2009), and two peer symposium publications in *iCORE Alberta ECE Graduate Research Symposium* (AECEGRS 2007 and 2008). We also expect to submit one more conference paper and another in journal publication.

7.1.1. Contributions to Literature

Through the course of this thesis work, we produced the following publications and presentations:

- Peer-reviewed Journal Paper:
  - J. Akpuh and J. Doucette, "Enhanced failure-specific *p*-cycle network dual-failure restorability design and optimization," *OSA Journal of Optical Networking*. vol. 8, no. 1, pp. 1-13, January 2009.
- Peer-reviewed Conference Papers (Archived Literature):
  - J Akpuh, J. Doucette, "Sizing Eligible Route Sets for Restorable Network Design and Optimization," *IEEE International Conference on Communications* (*ICC 2008*), Beijing, China, 19-23 May 2008.
  - J. Akpuh, J. Doucette, "Designing Demand-Wise Shared Protection Networks with Specified Minimum Dual-Failure Restorability," *IEEE International Conference on Communications (ICC 2009)*, Dresden, Germany, 14-18 June 2009.
- Peer-reviewed Conference Papers:

- J. Akpuh, J. Doucette, "Designing *p*-Cycle Networks for Specified Dual-Failure Restorability," *iCORE Alberta ECE Graduate Research Symposium (AECEGRS 2008)*, Edmonton, AB, pp. 24-25, 9 May 2008.

- J. Akpuh, J. Doucette, "Analysis of the Optimality-Runtime Trade-off in Varying Eligible Route Set Sizes in Restorable Network Design and Optimization," *iCORE Alberta ECE Graduate Research Symposium (AECEGRS 2007)*, Edmonton, AB, pp. 19-21, 4 May 2007.

7.2. Limitations and Future Directions

One of the limitations of this work is that we could not use relatively large network sizes for our experiments, and a related limitation is that the number of eligible routes enumerated for each problem may not have been sufficient for the solver to find a near-optimal solution. As the network size and the number of eligible routes increase, the problem complexity (i.e., number of variables and constraints) increases dramatically, as do the solver runtimes, easily in excess of several days per problem. Because of these runtime issues we limited the size of networks in this experiment to an 18-node network family and reduced the size of eligible route sets enumerated for each problem to a manageable size (100 eligible working routes per demand, for instance), so that the problems are solvable in a reasonable time frame. Had we only been interested in solving one or two instances of the problem, these excessive runtimes would not have been a significant issue, but given the fact that we have solved several thousand instances of the problem, we could not accommodate more than several minutes or hours per problem. Future work can explore possible modification to the existing problems so that larger networks and larger eligible route sets can be used to solve these problems without experiencing an exceedingly long runtimes. Some approaches that will help the runtime issue include advanced linear programming methods like *column generation* and meta-heuristic approaches like *genetic algorithms*, *tabu search*, and even *neural networks*.

Another limitation is that the actual cost parameters used in solving our design problems do not include all the cost factors that need to be considered by network operators in real network designs. The incremental costs used in this work are not reality directly proportional to the length and/or the amount of spare capacity

added to the network. In fact, the real situation is quite different, but due to difficulties in obtaining real-world cost data (carriers are very hesitant to provide actual cost data), we and others in the research community often assume that costs are proportional to length for simplicity. Other considerations on cost include capacity modularity and economies of scale, which again, we have not taken in account in our work. Here, we assumed that capacity can be added to a span in any integer amount, but the reality is that capacity typically comes in modular chunks. Further, the cost per unit capacity tends to decrease with larger sized modules due to economies of scale. Future work can be done to introduce some of these cost-related considerations into our problem.

Quite a number of further limitations exist, and we can talk at length about many of them. However, for brevity, we will limit our discussions to a simple list of others:

Our test case network topologies are not real life network topologies, as well as the demand matrices used in various networks sizes

The design, planning, and the assignment of capacity also requires a solid understanding of the nature of the traffic and services that the network carrier intends to transport, what sorts of multi-failure restorability and availability is required, *service level agreements* (SLA's), etc.

Demand patterns in our work are randomly generated, which may not reflect reality very well in some cases

We did not consider over-subscriptions, periodical network growth or planned network expansion

Enhanced dual failure restorability does not necessarily mean improved network availability [87]

We did not consider node failures or other multiple failures of a common cause.

REFERENCES

[1] W. L. Winston, *Operations Research:Applications and Algorithms, 4th Edition*. Thomson Learning, Belmont, CA, 2004.

[2] K. Zhu and B. Mukherjee, "Traffic grooming in an optical WDM mesh network", *IEEE Journal on Selected Areas in Communications*, vol. 20, no. 1, pp. 122-133,January 2002.

[3] S. Thiagarajan and A. K. Somani, "Traffic grooming for survivable WDM mesh networks," in *Proceedings of SPIE,* vol. 4599, pp. 54, August 2001.

[4] M. Pióro, and D. Medhi, *Routing, Flow, and Capacity Design in Communication and Computer Networks*. Morgan Kaufmann Publishers, Amsterdam, 2004.

[5] S. G. Chang and B. Gavish, "Telecommunications network topological design and capacity expansion:Formulations and algorithms," *Telecommunication Systems Journal,* vol. 1, no. 1, pp. 99-131, December 1993.

[6] D. Johnson, G. Brown, S. Beggs, C. Botham, I. Hawker, R. Chng, M. Sinclair and M. O'Mahony, "Distributed restoration strategies in telecommunications networks," *IEEE International Conference on Communications, SUPERCOMM/ICC'94, Conference*, New Orleans, LA,USA, pp. 483-488, May 1994.

[7] A. Hopper, S. Temple and R Williamson, *Local area network design*. Addison-Wesley, Wokingham, England:, 1986.

[8] D. Clark, K. Pogran and D. Reed, "An introduction to local area networks," *Proceedings of the IEEE*, vol. 66, no.11, pp. 1497-1517, November 1978.

[9] G. A. Donahue, *Network Warrior*. O'Reilly Media, Inc., Sebastopol, CA, USA, 2007.

[10] D. Bird and M. Harwood, *Network + Training Guide*. Que Publishing, 2002

[11] M. Conti, L. Lenzini and E. Gregori, *Metropolitan Area Networks*. Springer-Verlag New York, Inc. Secaucus, NJ, USA, 1997.

[12] R. Ramaswami, K. N. Sivarajan, *Optical Networks:A Practical Perspective, Second Edition*. Morgan Kaufmann, Publishers, San Francisco, CA, 1998.

[13] J. E. Flood, *Telecommunication Networks*. Institution of Electrical Engineers, Stevenage, UK, 1996.

[14] D. Fowler, *Virtual private networks: making the right connection*. Morgan Kaufmann, Publishers, San Francisco, CA, 1999.

[15] C. Scott, P. Wolfe and M. Erwin, *Virtual Private Networks*. O'Reilly Media, Inc., Sebastopol, CA, USA, December 1998.

[16] NIIT, A Pradyumnan, N Ravi, *Special Edition Using Optical Networks*. Que, 2001.

[17] M Clouquer, *Availability of services in Mesh Restirable Networks*. Ph.D. Dissertation, University of Alberta, Edmonton, AB, Canada, December 2003.

[18] W. D. Grover, *Mesh-Based Survivable Networks:Options and Strategies for Optical, MPLS, SONET and ATM Networking*. Prentice-Hall PTR, August 2003.

[19] J. Doucette, *Advances on Design and Analysis of Mesh-Restorable Networks*. Ph.D. Dissertation, University of Alberta, Edmonton, AB, Canada, December 2004.

[20] Internet Systems Consortium, Inc. (ISC), "The ISC Domain Survey" accessed May 19, 2009, available on-line: http://ftp.isc.org/www/survey/reports/2008/07/, May 2009.

[21] M. J. Martin, *Understanding the Network: A Practical Guide to Internetworking*. Sam, New Riders Publishing Thousand Oaks, CA, USA, 2000.

[22] P. Jackman and P. Eng, "The evolution of telecommunications," Electrical and Computer Engineering, 2000 Canadian Conference, vol. 2, pp. 990-997, March 2000.

[23] C. G. Omidyar and A. Aldridge, "Introduction to SDH/SONET," *IEEE Communications Magazine*, vol. 31, no. 9, pp. 30-33, September, 1993.

[24] K. Hrbacek and T. J. Jech, *Introduction to Set Theory*. Marcel Dekker Inc., New York Basel, 1978.

[25] A. Shen and N. K. Verschagin, *Basic Set Theory*. vol. 17. Student Mathematical Library, American Mathematical Society, 2002.

[26] F. Hausdorff, *Set Theory*. Chelsea Publishing Company, Incorporated, 2005.

[27] K. Thulasiraman and M. Swamy, *Graphs:Theory and Algorithms*. John Wiley & Sons, Inc. New York, NY, USA, 1992.

[28] J. Bondy and U. Murty, *Graph Theory*. Springer Verlag, 2007.

[29] R. Bhandari, *Survivable Networks:Algorithms for Diverse Routing*. Kluwer Academic Publishers, 1999.

[30] A. Zolfaghari, F. Kaudel, P. Bell and C. San Ramon, "Framework for network survivability performance," *IEEE Journal on Selected Areas in Communications,* vol. 12, no. 1, pp. 46-51, January 1994.

[31] S. Liew, K. Lu and M. Bellcore, "A framework for characterizing disaster-based network survivability," *IEEE Journal on Selected Areas in Communications,* vol. 12, no. 1, pp. 52-58, January 1994.

[32] G. D. Morley, *Analysis and Design of Ring-Based Transport Networks*. Ph.D. Dissertation, University of Alberta, Edmonton, AB, Canada, February 2001.

[33] M. W. Maeda, "Management and Control of Transparent Optical Networks," *IEEE Journal on Selected Areas in Communications*, vol. 16, no. 7, pp. 1005-1023, September 1998.

[34] A. Fumagalli, et al., "Survivable networks based on optimal routing and WDM self-healing rings," *INFOCOM'99. Eighteenth Annual Joint Conference of the IEEE Computer and Communications Societies. Proceedings. IEEE,* vol 2, pp. 726-733, March 1999.

[35] Y. Y. Yang and R. Sankar, "Automatic failure isolation and reconfiguration [ring networks]," Network, IEEE, vol. 7, no. 5, pp. 44-53, September 1993.

[36] T. H. Wu, "Emerging technologies for fibre network survivability," IEEE Communications Magazine, vol. 33, no. 2, pp. 58-74, February 1995.

[37] M. Herzberg, S. J. Bye, A. Utano, "The Hop-Limit Approach for Spare-Capacity Assignment in Survivable Networks," *IEEE/ACM Transactions on Networking*, vol. 3, no. 6, pp. 775-784, December 1995.

[38] W. D. Grover, "Distributed restoration of the transport network in Telecommunications Network Management into the 21st Century," ch. 11, pp. 337-419, S. Aidarous and T. Plevyak, Eds. New York: i*EEE Press, 1994*.

[39] R. R. Iraschko, M. H. MacGregor, W. D. Grover, "Optimal Capacity Placement for Path Restoration in STM or ATM Mesh-Survivable Networks," *IEEE/ACM Transactions on Networking*, vol. 6, no. 3, pp. 325-336, June 1998.

[40] R. R. Iraschko, W. D. Grover, "A Highly Efficient Path-Restoration Protocol for Management of Optical Network Transport Integrity," *IEEE Journal on Selected Areas in Communications*, vol. 18, no. 5, pp. 779-793, May 2000.

[41] A. M. C. A. Koster, A. Zymolka, M. Jäger, R. Hulsermann, and C. Gerlach, "Demand-wise Shared Protection for Meshed Optical Networks," *Design of Reliable Communication Networks* (*DRCN 2003*), Banff, AB, pp. 85-92, 19-22 October 2003.

[42] C. Gruber, A. Koster, A. Zymolka, R. Wessäly, S. Orlowski, "A Computational Study for Demand-wise Shared Protection," *Design of Reliable Communication Networks* (*DRCN 2005*), Island of Ischia (Naples), Italy, October 2005.

[43] B. Jæger, J. Doucette, D. Tipper, *Network Survivability*. Information Assurance: Dependability and Security in Networked Systems, Morgan Kaufman, New York, NY, USA, pp. 81-112, November 2007.

[44] W. D. Grover, J. Doucette, "Design of a Meta-Mesh of Chain Sub-Networks:Enhancing the Attractiveness of Mesh-Restorable WDM Networking on Low Connectivity Graphs," *IEEE Journal on Selected Areas in Communications*, Special Issue on WDM-based Network Architectures, vol. 20, no. 1, pp. 47-61, January, 2002.

[45] A. Kodian, W.D. Grover, "Failure independent path-protecting *p*-cycles:efficient and simple fully pre-connected optical-path protection," *IEEE Journal of Lightwave Technology*, vol. 23, no.10, October 2005.

[46] G. Shen, W. D. Grover, "Extending the *p*-Cycle Concept to Path Segment Protection for Span and Node Failure Recovery," *IEEE Journal on Selected Areas in Communications*, vol. 21, no.8, pp.1306-1319,Oct. 2003.

[47] J. Doucette, W. D. Grover, P. Giese, "Physical-layer *p*-Cycles Adapted for Router-level Node Protection:A Multi-layer Design and Operation Strategy," *IEEE Journal on Selected Areas in Communications*, vol. 25, no. 5, pp. 963-973, June 2007.

[48] H. Sakauchi, Y.Okanoue, S. Hasegawa, "Spare-channel design schemes for self-healing networks," *IEICE Trans*. *Comm*., vol. E75-B, no.7, pp. 624-633, July 1992.

[49] M. Clouqueur, W. D. Grover, "Computational and Design Studies on the Unavailability of Mesh-restorable Networks," *Proceedings of the 2nd international Workshop on Design of Reliable Communication Networks*, Munich, Germany, pp. 181-186, April 2000.

[50] M. Clouqueur, W.D. Grover, "Availability Analysis of Span-restorable Mesh Networks," *IEEE Journal on Selected Areas in Communications: Special Issue on Recent Advances in Fundamentals of Network Management,* vol.20, no. 4, pp. 810-821, May 2002.

[51] M. Clouqueur, W. D. Grover, "Mesh-restorable Networks with Complete Dual Failure Restorability and with Selectively Enhanced Dual Failure Restorability Properties," *Proceedings of the SPIE Optical Networking and Communications Conference* (*OptiComm 2002*), Boston, paper 4874-1, pp. 1-12, July 29-Aug. 2, 2002.

[52] J. Doucette, W. Li, M. Zuo, "Failure-Specific *p*-Cycle Network Dual Failure Restorability Design," *Proceedings of the 6th International Workshop on Design of Reliable Communication Networks*, La Rochelle, France, pp. 1-9, 7-10 October 2007.

[53] M. M. A. Azim, X. Jiang, S. Horiguchi and P. Ho, "Comprehensive Performance Study of Active Restoration-Based Optical Networks under Dual Failure Attacks," *Proceedings of 2005 Fifth International Conference on Information, Communications and Signal Processing*, pp. 1202-1206, September 2005.

[54] M. M. A. Azim, X. Jiang, P. Ho, and S. Horiguchi, "Models of Restoration Probability in WDM Networks Employing Active Restoration", *Journal of Photonic Communications Networks*, vol. 10, No. 2, pp. 141-153, September 2005.

[55] M. M. A. Azim, X. Jiang, P. H. Ho, M. M. R. Khandker and S. Horiguchi, "Active Lightpath Restoration in WDM Networks," *OSA Journal of Optical Networking,* vol.3, no.4, pp.247-260, April 2004.

[56] M. T. Frederick and A. K. Somani, "A Single-Fault Recovery Strategy for Optical Networks using Sub-Graph Routing", *7th IFLP Working Conference on Optical Network Design and Modeling*, Budapest. Hungary, February 2003.

[57] M. Frederick, P. Datta and A. Somani, "Evaluating Dual Failure Restorability in Mesh-restorable WDM optical networks," *Proceedings*. *of 2004 13th International Conference on Computer Communications and Networks*, *ICCCN 2004*, pp. 309-314, 2004.

[58] A. Grue, W. D Grover, B. Forst, D. Onguetou, D. Baloukov, J. Doucette, M. Clouqueur, D. Schupke, "Comparative Study of Fully Pre-Cross-Connected Protection Architectures for Transparent Optical Networks," *Design of Reliable Communication Networks,* (*DRCN 2007*), La Rochelle, France, 7-10 October 2007.

[59] D. A. Schupke, W. D. Grover, M. Clouqueur, "Strategies for Enhanced Dual Failure Restorability with Static or Reconfigurable *p*-Cycle Networks," *IEEE International Conference on Communications* (*ICC 2004*), Paris, France, pp. 1628-1633, June 2004.

[60] A. Kodian and W. D. Grover, "Multiple-quality of Protection Classes including Dual Failure Survivable Services in *p*-Cycle Networks," *Proceedings*. *of 2005 2nd International Conference on Broadband Networks*, vol. 1, pp. 231-240, October 2005.

[61] W Li, J. Doucette and M Zuo, "*p*-Cycle Network Design for Specified Minimum Dual Failure Restorability," *IEEE International Conference on Communications* (*ICC 2007*), pp. 2204-2210, Glasgow, Scotland, June 2007.

[62] A. Raman, Reporter, CNN International News, Cairo, Egypt, "Learn how a massive Internet failure affected several countries" archived, accessed on 18 May, 2009, available online: http://www.cnn.com/2008/LIVING/studentnews/01/31/transcript.fri/index.html, February 1, 2008.

[63] B. Johnson, Technology Correspondent, The Guardian (guardian.co.uk), "Faulty cable blacks out internet for millions" archived, accessed 18 May, 2009, available online: http://www.guardian.co.uk/technology/2008/jan/31/internet.blackout.asia, 31 January 2008.

[64] CANARIE, CA*net 4, " Recent Outage," accessed 10 June 2009, available on-line: http://amidala.canet4.net/network/report.php?type=Outage, 10 June 2009.

[65] W.D. Grover, M.Clouqueur, T. Bach, "Quantifying and Managing the Influence of Maintenance Actions on the Survivability of Mesh-Restorable Networks," *Proceedings* of *17th Annual National Fibre Optic Engineers Conference* (*NFOEC 2001*), pp. 1514-1525, Baltimore, MD, USA, July 2001.

[66] J. Doucette, W. D. Grover, "Capacity Design Studies of Span-Restorable Mesh Networks with Shared-Risk Link Group (SRLG) Effects," *Optical Networking and Communications Conference* (*OptiComm 2002*), Boston, MA, USA, pp. 25-38, July-August 2002.

[67] M. Randall, G. McMahon and S. Sugden, "A Simulated Annealing Approach to Communication Network Design," *Journal of Combinatorial Optimization*, vol. 6, no. 1, pp. 55-65, March 2002.

[68] S. J. Koh and C. Y. Lee, "A tabu search for the survivable fibre optic communication network design," *Journal of Computers and Industrial Engineering*, vol. 28, no 4, pp. 689-700, October 1995.

[69] D. Saha, M. Purkayastha and A. Mukherjee, "An approach to wide area WDM optical network design using genetic algorithm," *Computer*. *Communications*., vol. 22, no. 2, pp. 156-172, January 1999.

[70] H. Sakauchi, Y. Nishimura, S. Hasegawa, "A Self-healing Network with an Economical Spare Channel Assignment," *Proceedings of IEEE Global Telecommunications Conference* (*GlobeCom 1990*), San Diego, CA, vol. 1, pp. 438-441, December 1990.

[71] H. Sakauchi, Y.Okanoue, S. Hasegawa, "Spare-channel Design Schemes for Self-healing Networks," *IEICE Transactions on Communications*, vol. E75-B, no.7, pp. 624-633, July 1992.

[72] B. Venables, W. Grover, M. H. MacGregor, "Two strategies for Spare Capacity Placement (SCP) in Mesh Restorable Networks"*, IEEE International Conference on Communications* (*ICC 1993*), vol.1, pp. 267-271*, Geneva, May 1993*.

[73] M. Herzberg, and S. J. Bye, "An optimal spare-capacity assignment model for survivable networks with hop limits," *Proceedings of IEEE Global Communications Conference* (*GlobeCom 1994*), pp. 1601-1607, San Francisco, CA, December 1994.

[74] J. Akpuh and J. Doucette, "Enhanced failure-specific *p*-cycle network dual-failure restorability design and optimization," *OSA Journal of Optical Networking*. vol. 8, no. 1, pp. 1-13, January 2009.

[75] H. Wang and H. T. Mouftah, "*p*-Cycles in multi-failure network survivability," *Transparent Optical Networks, 2005, Proceedings of 2005 7th International Conference*, vol. 1, pp. 381-384 Vol. 1, 2005.

[76] M. To and P. Neusy, "Unavailability analysis of long-haul networks," *IEEE Journal on Selected Areas in Communications*, vol. 12, no. 1, pp. 100-109, January 1994.

[77] K. Kyandoghere, "Survivability Performance Analysis of Rerouting Strategies in an ATM/VP DCS Survivable Mesh Network," *ACM SIGCOMM Computer Communication Review,* vol. 28, no. 5, pp. 22-49, October 1998.

[78] W. D. Grover, "High Availability Path Design in Ring-based Optical Networks," *IEEE/ACM Transactions on Networking*, vol. 7, no. 4, pp. 558-574, August 1999.

[79] A. Lardies and A. Aguilar, "Planning methodology for SDH + optical networks," *Proceedings of 1st International Workshop Design of Reliable Communication Networks* (*DRCN 1998*), Brugge, Belgium, May 1998.

[80] C. Wynants, Network Synthesis Problems. New York:Kluwer, 2001. Appendix A.

[81] M. Bettin, G. Ferraris, and G. Pignari, "Comparison of protection and restoration schemes for SDH networks," *Proceedings of 1st International Workshop Design of Reliable Communication Networks* (*DRCN 1998*), Brugge, Belgium, May 1998.

[82] J. Akpuh, J. Doucette, "Sizing Eligible Route Sets for Restorable Network Design and Optimization," *Proceedings of IEEE International Conference on Communications* (*ICC 2008*), Beijing, China, 19-23 May 2008.

[83] ILOG, "Introducing NEW ILOG CPLEX 10.0," accessed 14 April 2008, available online:http://www.ilog.com/products/optimization/presentations/cplex10.pdf, 2008

[84] B. Forst, *Analysis and Understanding of Demand-wise Shared Protection*, M.Sc. Thesis, University of Alberta, Edmonton, AB, Canada, 03 December 2008.

[85] G. Dantzig, *Linear Programming and Extensions*, Princeton, New Jersey, Princeton University Press, 1963.

[86] J. Akpuh, J. Doucette, "Designing Demand-Wise Shared Protection Networks with Specified Minimum Dual-Failure Restorability," *Proceedings of IEEE International Conference on Communications* (*ICC 2009*), Dresden, Germany, 14-18 June 2009.

[87] B. Todd, *The Use of Demand-wise Shared Protection in Creating Topology Optimized High Availability Networks*, M.Sc. Thesis, University of Alberta, Edmonton, AB, Canada, 19 November 2009.

APPENDIX A

NETWORK TOPOLOGY

A.1 10n20s Network

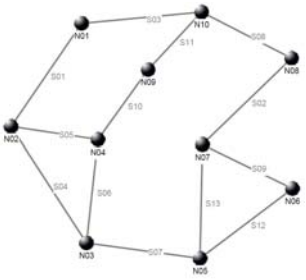

10n20s-13s

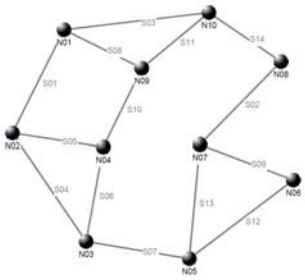

10n20s-14s

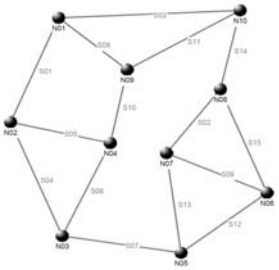

10n20s-15s

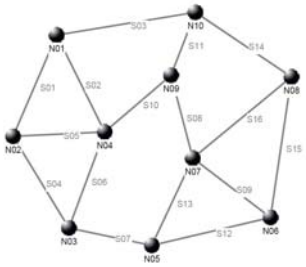

10n20s-16s

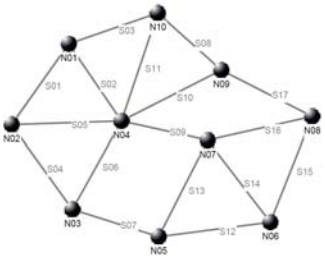

10n20s-17s

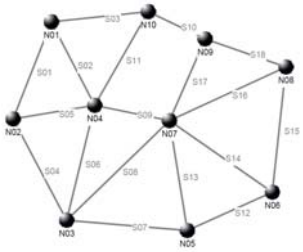

10n20s-18s

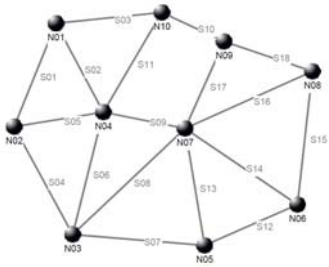

10n20s-19s

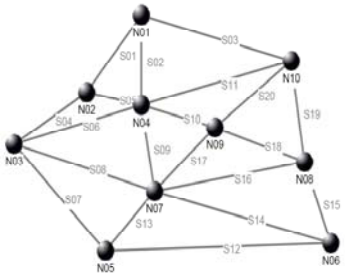

10n20s-20s

A.2 12n24s Network Family

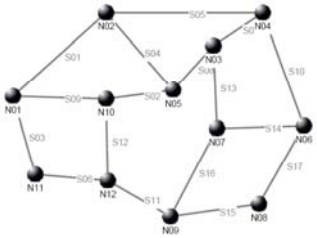

12n24s-17s

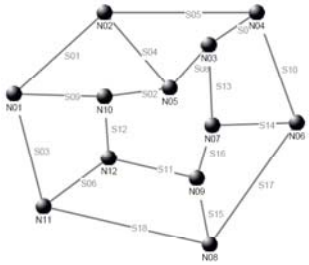

12n24s-18s

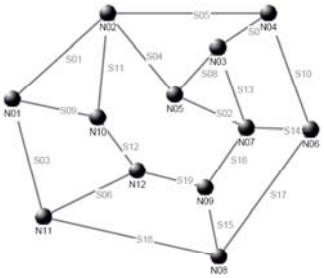

12n24s-19s

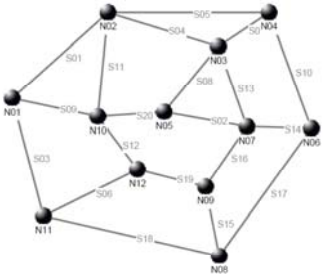

12n24s-20s

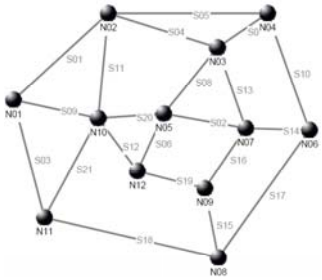

12n24s-21s

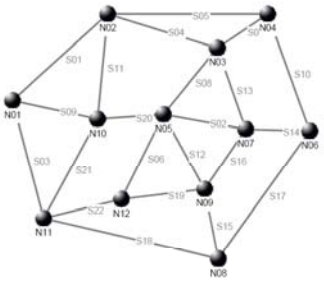

12n24s-22s

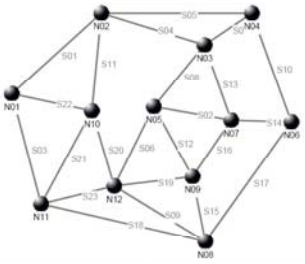

12n24s-23s

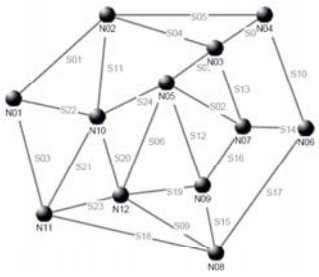

12n24s-24s

A.3 15n30s Network Family

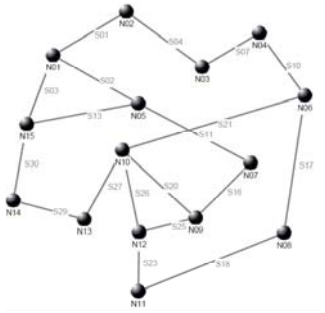

15n30s-19s

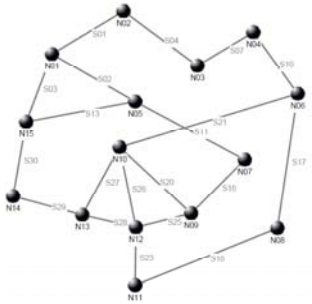

15n30s-20s

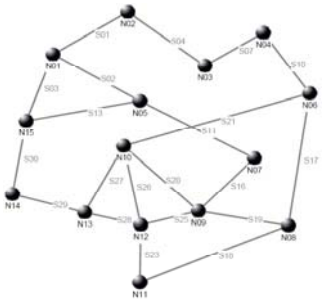

15n30s-21s

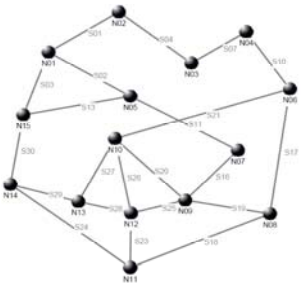

15n30s-22s

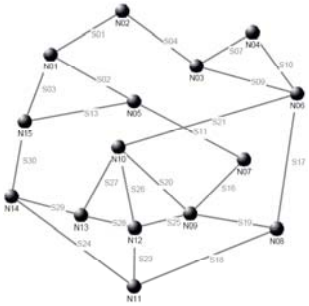

15n30s-23s

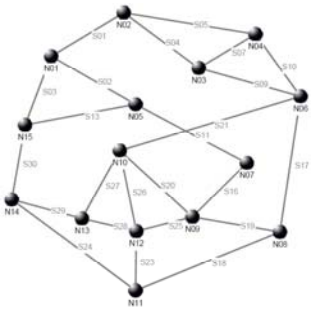

15n30s-24s

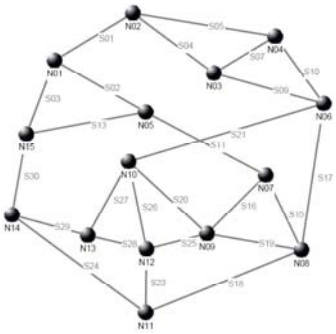

15n30s-25s

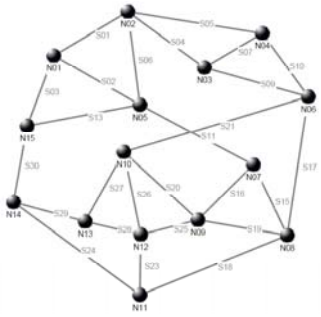

15n30s-26s

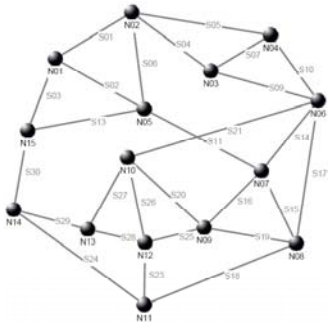

15n30s-27s

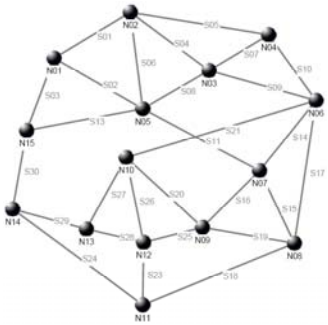

15n30s-28s

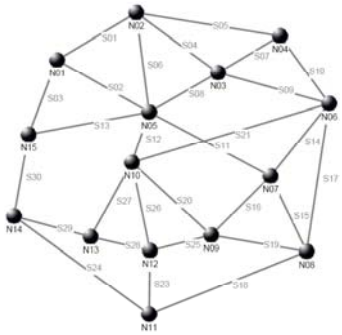

15n30s-29s

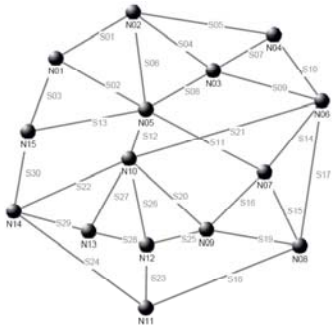

15n30s-30s

A.4 18n36s Network Family

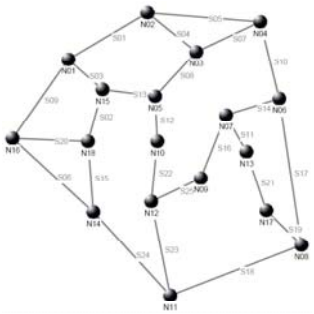

18n36s-25s

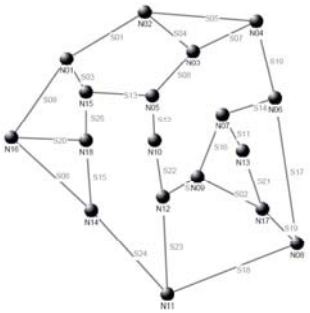

18n36s-26s

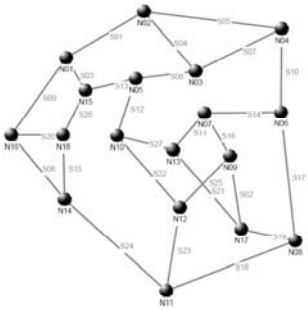

18n36s-27s

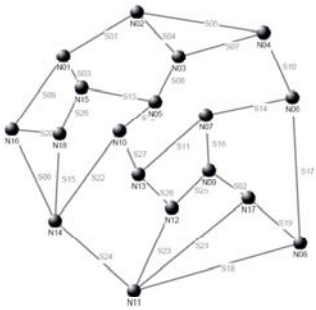

18n36s-28s

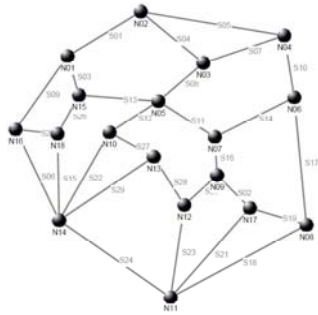

18n36s-29s

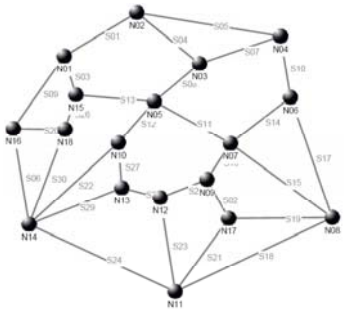

18n36s-30s

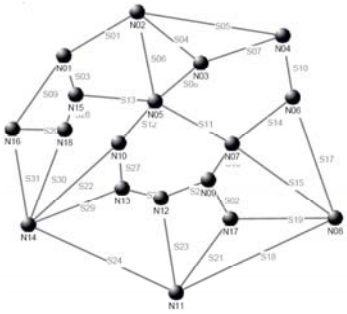

18n36s-31s

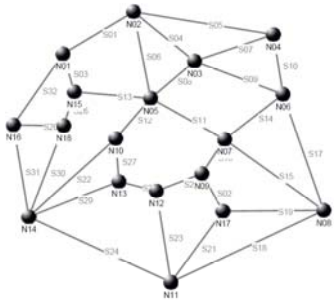

18n36s-32s

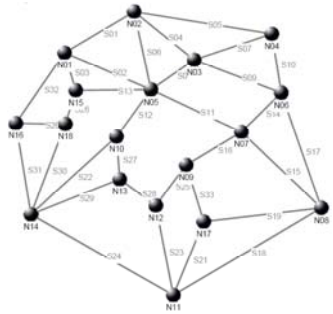

18n36s-33s

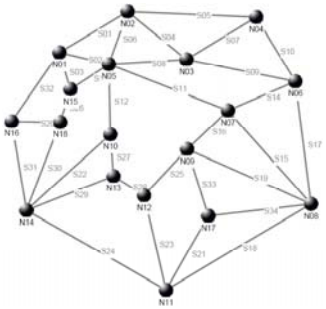

18n36s-34s

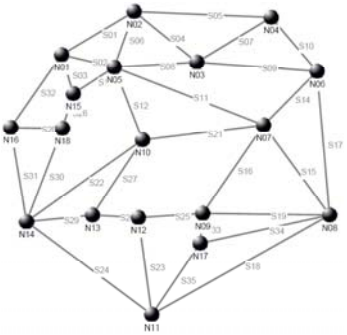

18n36s-35s

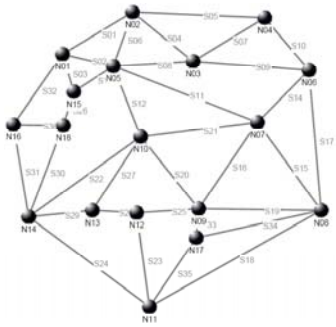

18n36s-36s

APPENDIX B

NETWORK DEMAND DATA

B.1 10n20s Network Family

NAME:10n20s Networks
DATE LAST MODIFIED:Saturday, March 18, 2006 1:50:26 PM MST
MODIFIED BY:MeshBuilder(c)

DEMAND	O	D	NBUNITS	RESTCLASS		HOPLIM	DISTLIM MAXOUTAGE
D01	N01	N02	7	R1	inf	inf	0
D02	N01	N03	9	R1	inf	inf	0
D03	N01	N04	6	R1	inf	inf	0
D04	N01	N05	3	R1	inf	inf	0
D05	N01	N06	5	R1	inf	inf	0
D06	N01	N07	1	R1	inf	inf	0
D07	N01	N08	8	R1	inf	inf	0
D08	N01	N09	1	R1	inf	inf	0
D09	N01	N10	7	R1	inf	inf	0
D10	N02	N03	6	R1	inf	inf	0
D11	N02	N04	7	R1	inf	inf	0
D12	N02	N05	6	R1	inf	inf	0
D13	N02	N06	1	R1	inf	inf	0
D14	N02	N07	3	R1	inf	inf	0
D15	N02	N08	2	R1	inf	inf	0
D16	N02	N09	3	R1	inf	inf	0
D17	N02	N10	2	R1	inf	inf	0
D18	N03	N04	4	R1	inf	inf	0
D19	N03	N05	1	R1	inf	inf	0
D20	N03	N06	5	R1	inf	inf	0
D21	N03	N07	7	R1	inf	inf	0
D22	N03	N08	7	R1	inf	inf	0
D23	N03	N09	10	R1	inf	inf	0
D24	N03	N10	4	R1	inf	inf	0
D25	N04	N05	6	R1	inf	inf	0
D26	N04	N06	1	R1	inf	inf	0
D27	N04	N07	5	R1	inf	inf	0
D28	N04	N08	9	R1	inf	inf	0
D29	N04	N09	2	R1	inf	inf	0
D30	N04	N10	9	R1	inf	inf	0
D31	N05	N06	5	R1	inf	inf	0
D32	N05	N07	8	R1	inf	inf	0
D33	N05	N08	4	R1	inf	inf	0
D34	N05	N09	1	R1	inf	inf	0
D35	N05	N10	10	R1	inf	inf	0
D36	N06	N07	8	R1	inf	inf	0
D37	N06	N08	8	R1	inf	inf	0
D38	N06	N09	5	R1	inf	inf	0
D39	N06	N10	7	R1	inf	inf	0

```
D40   N07   N08   5     R1    inf   inf   0
D41   N07   N09   9     R1    inf   inf   0
D42   N07   N10   8     R1    inf   inf   0
D43   N08   N09   8     R1    inf   inf   0
D44   N08   N10   7     R1    inf   inf   0
D45   N09   N10   5     R1    inf   inf   0
```

B.2 12n24s Network Family

```
NAME:12n24s1
DATE LAST MODIFIED:Wednesday, July 11, 2007 10:55:33 AM MDT
MODIFIED BY:MeshBuilder(c)

DEMAND O    D     NBUNITS     RESTCLASS   HOPLIMDISTLIM
      MAXOUTAGE
D1    N01   N02   8     R1    inf   inf   0
D2    N01   N03   4     R1    inf   inf   0
D3    N01   N04   5     R1    inf   inf   0
D4    N01   N05   6     R1    inf   inf   0
D5    N01   N06   10    R1    inf   inf   0
D6    N01   N07   3     R1    inf   inf   0
D7    N01   N08   9     R1    inf   inf   0
D8    N01   N09   9     R1    inf   inf   0
D9    N01   N10   5     R1    inf   inf   0
D10   N01   N11   10    R1    inf   inf   0
D11   N01   N12   1     R1    inf   inf   0
D12   N02   N03   8     R1    inf   inf   0
D13   N02   N04   2     R1    inf   inf   0
D14   N02   N05   5     R1    inf   inf   0
D15   N02   N06   1     R1    inf   inf   0
D16   N02   N07   6     R1    inf   inf   0
D17   N02   N08   1     R1    inf   inf   0
D18   N02   N09   1     R1    inf   inf   0
D19   N02   N10   3     R1    inf   inf   0
D20   N02   N11   9     R1    inf   inf   0
D21   N02   N12   6     R1    inf   inf   0
D22   N03   N04   2     R1    inf   inf   0
D23   N03   N05   9     R1    inf   inf   0
D24   N03   N06   2     R1    inf   inf   0
D25   N03   N07   3     R1    inf   inf   0
D26   N03   N08   6     R1    inf   inf   0
D27   N03   N09   5     R1    inf   inf   0
D28   N03   N10   9     R1    inf   inf   0
D29   N03   N11   9     R1    inf   inf   0
D30   N03   N12   6     R1    inf   inf   0
D31   N04   N05   3     R1    inf   inf   0
D32   N04   N06   2     R1    inf   inf   0
D33   N04   N07   4     R1    inf   inf   0
D34   N04   N08   7     R1    inf   inf   0
D35   N04   N09   9     R1    inf   inf   0
D36   N04   N10   3     R1    inf   inf   0
D37   N04   N11   5     R1    inf   inf   0
D38   N04   N12   6     R1    inf   inf   0
D39   N05   N06   10    R1    inf   inf   0
D40   N05   N07   7     R1    inf   inf   0
```

```
D41   N05   N08   9     R1    inf   inf   0
D42   N05   N09   6     R1    inf   inf   0
D43   N05   N10   3     R1    inf   inf   0
D44   N05   N11   3     R1    inf   inf   0
D45   N05   N12   1     R1    inf   inf   0
D46   N06   N07   4     R1    inf   inf   0
D47   N06   N08   6     R1    inf   inf   0
D48   N06   N09   4     R1    inf   inf   0
D49   N06   N10   5     R1    inf   inf   0
D50   N06   N11   2     R1    inf   inf   0
D51   N06   N12   5     R1    inf   inf   0
D52   N07   N08   5     R1    inf   inf   0
D53   N07   N09   5     R1    inf   inf   0
D54   N07   N10   7     R1    inf   inf   0
D55   N07   N11   7     R1    inf   inf   0
D56   N07   N12   1     R1    inf   inf   0
D57   N08   N09   2     R1    inf   inf   0
D58   N08   N10   3     R1    inf   inf   0
D59   N08   N11   6     R1    inf   inf   0
D60   N08   N12   8     R1    inf   inf   0
D61   N09   N10   8     R1    inf   inf   0
D62   N09   N11   6     R1    inf   inf   0
D63   N09   N12   8     R1    inf   inf   0
D64   N10   N11   10    R1    inf   inf   0
D65   N10   N12   2     R1    inf   inf   0
D66   N11   N12   5     R1    inf   inf   0
```

B.3 15n30s Network Family

```
NAME:15n30s1
DATE LAST MODIFIED:Wednesday, July 11, 2001 9:42:33 AM MDT
MODIFIED BY:MeshBuilder(c)

DEMAND O    D     NBUNITS     RESTCLASS   HOPLIMDISTLIM
      MAXOUTAGE
D1    N01   N02   8     R1    inf   inf   0
D2    N01   N03   4     R1    inf   inf   0
D3    N01   N04   5     R1    inf   inf   0
D4    N01   N05   6     R1    inf   inf   0
D5    N01   N06   10    R1    inf   inf   0
D6    N01   N07   3     R1    inf   inf   0
D7    N01   N08   9     R1    inf   inf   0
D8    N01   N09   9     R1    inf   inf   0
D9    N01   N10   5     R1    inf   inf   0
D10   N01   N11   10    R1    inf   inf   0
D11   N01   N12   1     R1    inf   inf   0
D12   N01   N13   1     R1    inf   inf   0
D13   N01   N14   4     R1    inf   inf   0
D14   N01   N15   4     R1    inf   inf   0
D15   N02   N03   8     R1    inf   inf   0
D16   N02   N04   2     R1    inf   inf   0
D17   N02   N05   5     R1    inf   inf   0
D18   N02   N06   1     R1    inf   inf   0
D19   N02   N07   6     R1    inf   inf   0
D20   N02   N08   1     R1    inf   inf   0
```

```
D21   N02   N09   1     R1    inf   inf   0
D22   N02   N10   3     R1    inf   inf   0
D23   N02   N11   9     R1    inf   inf   0
D24   N02   N12   6     R1    inf   inf   0
D25   N02   N13   5     R1    inf   inf   0
D26   N02   N14   5     R1    inf   inf   0
D27   N02   N15   7     R1    inf   inf   0
D28   N03   N04   2     R1    inf   inf   0
D29   N03   N05   9     R1    inf   inf   0
D30   N03   N06   2     R1    inf   inf   0
D31   N03   N07   3     R1    inf   inf   0
D32   N03   N08   6     R1    inf   inf   0
D33   N03   N09   5     R1    inf   inf   0
D34   N03   N10   9     R1    inf   inf   0
D35   N03   N11   9     R1    inf   inf   0
D36   N03   N12   6     R1    inf   inf   0
D37   N03   N13   1     R1    inf   inf   0
D38   N03   N14   4     R1    inf   inf   0
D39   N03   N15   2     R1    inf   inf   0
D40   N04   N05   3     R1    inf   inf   0
D41   N04   N06   2     R1    inf   inf   0
D42   N04   N07   4     R1    inf   inf   0
D43   N04   N08   7     R1    inf   inf   0
D44   N04   N09   9     R1    inf   inf   0
D45   N04   N10   3     R1    inf   inf   0
D46   N04   N11   5     R1    inf   inf   0
D47   N04   N12   6     R1    inf   inf   0
D48   N04   N13   4     R1    inf   inf   0
D49   N04   N14   2     R1    inf   inf   0
D50   N04   N15   1     R1    inf   inf   0
D51   N05   N06   10    R1    inf   inf   0
D52   N05   N07   7     R1    inf   inf   0
D53   N05   N08   9     R1    inf   inf   0
D54   N05   N09   6     R1    inf   inf   0
D55   N05   N10   3     R1    inf   inf   0
D56   N05   N11   3     R1    inf   inf   0
D57   N05   N12   1     R1    inf   inf   0
D58   N05   N13   1     R1    inf   inf   0
D59   N05   N14   7     R1    inf   inf   0
D60   N05   N15   3     R1    inf   inf   0
D61   N06   N07   4     R1    inf   inf   0
D62   N06   N08   6     R1    inf   inf   0
D63   N06   N09   4     R1    inf   inf   0
D64   N06   N10   5     R1    inf   inf   0
D65   N06   N11   2     R1    inf   inf   0
D66   N06   N12   5     R1    inf   inf   0
D67   N06   N13   8     R1    inf   inf   0
D68   N06   N14   9     R1    inf   inf   0
D69   N06   N15   3     R1    inf   inf   0
D70   N07   N08   5     R1    inf   inf   0
D71   N07   N09   5     R1    inf   inf   0
D72   N07   N10   7     R1    inf   inf   0
D73   N07   N11   7     R1    inf   inf   0
D74   N07   N12   1     R1    inf   inf   0
D75   N07   N13   9     R1    inf   inf   0
D76   N07   N14   4     R1    inf   inf   0
D77   N07   N15   7     R1    inf   inf   0
```

```
D78   N08   N09   2     R1    inf   inf   0
D79   N08   N10   3     R1    inf   inf   0
D80   N08   N11   6     R1    inf   inf   0
D81   N08   N12   8     R1    inf   inf   0
D82   N08   N13   8     R1    inf   inf   0
D83   N08   N14   2     R1    inf   inf   0
D84   N08   N15   10    R1    inf   inf   0
D85   N09   N10   8     R1    inf   inf   0
D86   N09   N11   6     R1    inf   inf   0
D87   N09   N12   8     R1    inf   inf   0
D88   N09   N13   10    R1    inf   inf   0
D89   N09   N14   1     R1    inf   inf   0
D90   N09   N15   1     R1    inf   inf   0
D91   N10   N11   10    R1    inf   inf   0
D92   N10   N12   2     R1    inf   inf   0
D93   N10   N13   1     R1    inf   inf   0
D94   N10   N14   7     R1    inf   inf   0
D95   N10   N15   1     R1    inf   inf   0
D96   N11   N12   5     R1    inf   inf   0
D97   N11   N13   7     R1    inf   inf   0
D98   N11   N14   1     R1    inf   inf   0
D99   N11   N15   3     R1    inf   inf   0
D100  N12   N13   3     R1    inf   inf   0
D101  N12   N14   5     R1    inf   inf   0
D102  N12   N15   1     R1    inf   inf   0
D103  N13   N14   10    R1    inf   inf   0
D104  N13   N15   3     R1    inf   inf   0
D105  N14   N15   3     R1    inf   inf   0
```

B.4 18n36s Network Family

```
NAME:18n36s1
DATE LAST MODIFIED:Monday, December 11, 2006 6:38:17 PM MST
MODIFIED BY:MeshBuilder(c)

DEMAND O    D     NBUNITS     RESTCLASS   HOPLIMDISTLIM
      MAXOUTAGE
D1    N01   N02   7     R1    inf   inf   0
D2    N01   N03   2     R1    inf   inf   0
D3    N01   N04   1     R1    inf   inf   0
D4    N01   N05   5     R1    inf   inf   0
D5    N01   N06   7     R1    inf   inf   0
D6    N01   N07   9     R1    inf   inf   0
D7    N01   N08   2     R1    inf   inf   0
D8    N01   N09   9     R1    inf   inf   0
D9    N01   N10   2     R1    inf   inf   0
D10   N01   N11   8     R1    inf   inf   0
D11   N01   N12   7     R1    inf   inf   0
D12   N01   N13   8     R1    inf   inf   0
D13   N01   N14   2     R1    inf   inf   0
D14   N01   N15   2     R1    inf   inf   0
D15   N01   N16   7     R1    inf   inf   0
D16   N01   N17   2     R1    inf   inf   0
D17   N01   N18   6     R1    inf   inf   0
D18   N02   N03   9     R1    inf   inf   0
```

D19	N02	N04	9	R1	inf	inf	0
D20	N02	N05	10	R1	inf	inf	0
D21	N02	N06	5	R1	inf	inf	0
D22	N02	N07	6	R1	inf	inf	0
D23	N02	N08	1	R1	inf	inf	0
D24	N02	N09	6	R1	inf	inf	0
D25	N02	N10	8	R1	inf	inf	0
D26	N02	N11	10	R1	inf	inf	0
D27	N02	N12	8	R1	inf	inf	0
D28	N02	N13	1	R1	inf	inf	0
D29	N02	N14	9	R1	inf	inf	0
D30	N02	N15	3	R1	inf	inf	0
D31	N02	N16	7	R1	inf	inf	0
D32	N02	N17	8	R1	inf	inf	0
D33	N02	N18	5	R1	inf	inf	0
D34	N03	N04	5	R1	inf	inf	0
D35	N03	N05	6	R1	inf	inf	0
D36	N03	N06	8	R1	inf	inf	0
D37	N03	N07	7	R1	inf	inf	0
D38	N03	N08	10	R1	inf	inf	0
D39	N03	N09	5	R1	inf	inf	0
D40	N03	N10	1	R1	inf	inf	0
D41	N03	N11	10	R1	inf	inf	0
D42	N03	N12	6	R1	inf	inf	0
D43	N03	N13	6	R1	inf	inf	0
D44	N03	N14	9	R1	inf	inf	0
D45	N03	N15	7	R1	inf	inf	0
D46	N03	N16	10	R1	inf	inf	0
D47	N03	N17	2	R1	inf	inf	0
D48	N03	N18	3	R1	inf	inf	0
D49	N04	N05	10	R1	inf	inf	0
D50	N04	N06	8	R1	inf	inf	0
D51	N04	N07	9	R1	inf	inf	0
D52	N04	N08	2	R1	inf	inf	0
D53	N04	N09	9	R1	inf	inf	0
D54	N04	N10	8	R1	inf	inf	0
D55	N04	N11	9	R1	inf	inf	0
D56	N04	N12	4	R1	inf	inf	0
D57	N04	N13	6	R1	inf	inf	0
D58	N04	N14	10	R1	inf	inf	0
D59	N04	N15	9	R1	inf	inf	0
D60	N04	N16	3	R1	inf	inf	0
D61	N04	N17	1	R1	inf	inf	0
D62	N04	N18	1	R1	inf	inf	0
D63	N05	N06	2	R1	inf	inf	0
D64	N05	N07	6	R1	inf	inf	0
D65	N05	N08	5	R1	inf	inf	0
D66	N05	N09	5	R1	inf	inf	0
D67	N05	N10	2	R1	inf	inf	0
D68	N05	N11	1	R1	inf	inf	0
D69	N05	N12	8	R1	inf	inf	0
D70	N05	N13	5	R1	inf	inf	0
D71	N05	N14	7	R1	inf	inf	0
D72	N05	N15	3	R1	inf	inf	0
D73	N05	N16	5	R1	inf	inf	0
D74	N05	N17	4	R1	inf	inf	0
D75	N05	N18	1	R1	inf	inf	0

D76	N06	N07	1	R1	inf	inf	0
D77	N06	N08	8	R1	inf	inf	0
D78	N06	N09	6	R1	inf	inf	0
D79	N06	N10	2	R1	inf	inf	0
D80	N06	N11	9	R1	inf	inf	0
D81	N06	N12	9	R1	inf	inf	0
D82	N06	N13	9	R1	inf	inf	0
D83	N06	N14	2	R1	inf	inf	0
D84	N06	N15	4	R1	inf	inf	0
D85	N06	N16	8	R1	inf	inf	0
D86	N06	N17	4	R1	inf	inf	0
D87	N06	N18	9	R1	inf	inf	0
D88	N07	N08	9	R1	inf	inf	0
D89	N07	N09	6	R1	inf	inf	0
D90	N07	N10	8	R1	inf	inf	0
D91	N07	N11	9	R1	inf	inf	0
D92	N07	N12	8	R1	inf	inf	0
D93	N07	N13	9	R1	inf	inf	0
D94	N07	N14	5	R1	inf	inf	0
D95	N07	N15	4	R1	inf	inf	0
D96	N07	N16	8	R1	inf	inf	0
D97	N07	N17	8	R1	inf	inf	0
D98	N07	N18	3	R1	inf	inf	0
D99	N08	N09	9	R1	inf	inf	0
D100	N08	N10	4	R1	inf	inf	0
D101	N08	N11	10	R1	inf	inf	0
D102	N08	N12	2	R1	inf	inf	0
D103	N08	N13	5	R1	inf	inf	0
D104	N08	N14	5	R1	inf	inf	0
D105	N08	N15	2	R1	inf	inf	0
D106	N08	N16	6	R1	inf	inf	0
D107	N08	N17	5	R1	inf	inf	0
D108	N08	N18	5	R1	inf	inf	0
D109	N09	N10	3	R1	inf	inf	0
D110	N09	N11	9	R1	inf	inf	0
D111	N09	N12	4	R1	inf	inf	0
D112	N09	N13	7	R1	inf	inf	0
D113	N09	N14	6	R1	inf	inf	0
D114	N09	N15	9	R1	inf	inf	0
D115	N09	N16	3	R1	inf	inf	0
D116	N09	N17	10	R1	inf	inf	0
D117	N09	N18	6	R1	inf	inf	0
D118	N10	N11	8	R1	inf	inf	0
D119	N10	N12	2	R1	inf	inf	0
D120	N10	N13	1	R1	inf	inf	0
D121	N10	N14	7	R1	inf	inf	0
D122	N10	N15	9	R1	inf	inf	0
D123	N10	N16	8	R1	inf	inf	0
D124	N10	N17	3	R1	inf	inf	0
D125	N10	N18	5	R1	inf	inf	0
D126	N11	N12	4	R1	inf	inf	0
D127	N11	N13	5	R1	inf	inf	0
D128	N11	N14	5	R1	inf	inf	0
D129	N11	N15	5	R1	inf	inf	0
D130	N11	N16	8	R1	inf	inf	0
D131	N11	N17	7	R1	inf	inf	0
D132	N11	N18	10	R1	inf	inf	0

```
D133  N12   N13   4     R1    inf   inf   0
D134  N12   N14   7     R1    inf   inf   0
D135  N12   N15   6     R1    inf   inf   0
D136  N12   N16   10    R1    inf   inf   0
D137  N12   N17   5     R1    inf   inf   0
D138  N12   N18   7     R1    inf   inf   0
D139  N13   N14   1     R1    inf   inf   0
D140  N13   N15   2     R1    inf   inf   0
D141  N13   N16   4     R1    inf   inf   0
D142  N13   N17   10    R1    inf   inf   0
D143  N13   N18   5     R1    inf   inf   0
D144  N14   N15   3     R1    inf   inf   0
D145  N14   N16   1     R1    inf   inf   0
D146  N14   N17   5     R1    inf   inf   0
D147  N14   N18   10    R1    inf   inf   0
D148  N15   N16   2     R1    inf   inf   0
D149  N15   N17   1     R1    inf   inf   0
D150  N15   N18   7     R1    inf   inf   0
D151  N16   N17   5     R1    inf   inf   0
D152  N16   N18   3     R1    inf   inf   0
D153  N17   N18   2     R1    inf   inf   0
```

APPENDIX C

AMPL PROGRAMS

The AMPL models presented in this section, "APPENDIX C", including any data and algorithms contained herein are the exclusive property of TRLabs, held on behalf of its sponsors. Except as specifically authorized in writing by TRLabs, users of these models shall keep them confidential and shall protect them in whole or in part from disclosure and dissemination to all third parties.

If any part of these models, including any data and algorithms contained herein, is used in any derivative works or publications, TRLabs shall be duly cited as a reference. TRLabs makes no representation or warranties about the suitability of these models, either express or implied, including but not limited to implied warranties of merchantability, fitness for a particular purpose, or non-infringement. TRLabs shall not be liable for any damages suffered as a result of using, modifying or distributing this model or its derivatives.

```
########################################################################
#                                AMPL PROGRAMS                         #
########################################################################
Some of the original SCP models were written by Dr. John Doucette
in 2001 and are modified for specified dual failure restorability
by Jude Akpuh, December 2007. Copyright (C) 2001 TRLabs, Inc. All
Rights Reserved.

TRLabs
7th Floor
107 116 Street NW
Edmonton, Alberta, Canada
T6G 2V4
+1 780 441-3800
www.trlabs.ca

########################################################################
```

C.1 Span Restoration Model

File name: "span-SCP-R2_v1. mod".

```
# Specified dual failure restorability model for span restorable
# networks with spare capacity placement only.
```

```
# SETS
set SPANS;
set REST_ROUTES{i in SPANS};

# PARAMETERS
param Cost{j in SPANS};
param Work{j in SPANS};
param DeltaRestRoute{i in SPANS, j in SPANS, p in
REST_ROUTES[i]}default 0;
# VARIABLES
var flowrest{i in SPANS, p in REST_ROUTES[i]}>=0 integer,
<=1000000;
var spare{j in SPANS}>=0 integer, <=1000000;
var restorability2{i in SPANS, j in SPANS:i<>j}>=0, <=1.0;
param R2Limit;

# OBJECTIVE FUNCTION

minimize TotalCost:sum{j in SPANS}Cost[j] * (spare[j]+Work[j]);

# CONSTRAINTS

subject to single_failure_restn{i in SPANS}:
sum{p in REST_ROUTES[i]}flowrest[i,p]>=Work[i];
subject to spare_assignment{i in SPANS, j in SPANS, k in SPANS:i<>j
and i<>k and j<>k}:spare[k]>=sum{p in
REST_ROUTES[i]:DeltaRestRoute[i,j,p]<>1}DeltaRestRoute[i,k,p] *
flowrest[i,p]+ sum{p in
REST_ROUTES[j]:DeltaRestRoute[j,i,p]<>1}DeltaRestRoute[j,k,p] *
lowrest[j,p];
subject to dual_fail_constraints{i in SPANS, j in SPANS:i<>j}:
sum{pin
REST_ROUTES[i]:DeltaRestRoute[i,j,p]<>1}flowrest[i,p]>=restorabilit
y2[i,j]* Work[i] ;
subject to ave_dual_failure_restorability2{i in SPANS, j in
SPANS:i<>j}:
restorability2[i,j]>=R2Limit;
```

C.2 *p*-Cycle Restoration Model

File name; "*p*-cycle-SC*P*-R2_v1. mod".

```
# Specified dual failure restorability model for p-cycle restorable
# networks with spare capacity placement only.

# SETS

set SPANS;
set PCYCLES;
set LINKS:={p in PCYCLES, i in SPANS, j in SPANS:i<>j};
set DEMANDS;
set WORK_ROUTES{r in DEMANDS};

# PARAMETERS
param Cost{j in SPANS}default 0;
```

```
param Work{j in SPANS}default 0;
param DemandUnits{r in DEMANDS}default 0;
param Xpi{p in PCYCLES, i in SPANS}default 0;
param pCrossesj{p in PCYCLES, j in SPANS}:=sum{i in SPANS:i=j and
Xpi[p,j]=1}1;
param Wxi{r in DEMANDS,q in WORK_ROUTES[r],i in SPANS}default 0;
param workflow_ij{i in SPANS,j in SPANS:i<>j}:=sum{r in DEMANDS,q
in WORK_ROUTES[r]:Wxi[r,q,i]=1 and Wxi[r,q,j]=1}DemandUnits[r];
param R2Limit;
set PCYCLES_ij{i in SPANS,j in SPANS:i<>j}:={p in
PCYCLES:(Xpi[p,i]=1 and Xpi[p,j]=1)};

# VARIABLES
var p_cycle_usage{p in PCYCLES}>=0 integer, <=10000;
var pij_cycle_usage{(p,i,j) in LINKS:Xpi[p,i]+Xpi[p,j]>=3}>=0
integer, <=10000;
var spare{j in SPANS}>=0 integer, <=10000;
var z1{i in SPANS, j in SPANS:i<>j}>=0, <=Work[i];
var z2{i in SPANS, j in SPANS:i<>j}>=0, <=Work[i];
var restorability2_1{i in SPANS, j in SPANS:i<>j}>=0, <=1;
var restorability2{j in SPANS}>=0, <=1;

# OBJECTIVE FUNCTION

minimize totalcost:sum{j in SPANS}Cost[j] * (spare[j]+ Work[j]);

# CONSTRAINTS

subject to full_restoration{i in SPANS}:
Work[i]<=sum{p in PCYCLES}Xpi[p,i] * p_cycle_usage[p];

subject to spare_capacity_placement{j in SPANS}:
spare[j]=sum{p in PCYCLES}pCrossesj[p,j] * p_cycle_usage[p];

subject to z1_constraint{i in SPANS, j in SPANS:i<>j}:
z1[i,j]<=sum{p in PCYCLES:Xpi[p,i]>=0 and Xpi[p,j]=0}Xpi[p,i] *
p_cycle_usage[p];

subject to z2_constraint1{i in SPANS, j in SPANS:i<>j}:
z2[i,j]<=workflow_ij[i,j];

subject to z2_constraint2{i in SPANS, j in SPANS:i<>j}:
z2[i,j]<=sum{p in PCYCLES_ij[i,j]}p_cycle_usage[p];

subject to one_on_cycle_one_straddling{(p,i,j) in
LINKS:Xpi[p,i]+Xpi[p,j]=3}:
p_cycle_usage[p]>=pij_cycle_usage[p,i,j]+pij_cycle_usage[p,j,i];

subject to two_straddling{(p,i,j) in LINKS:Xpi[p,i]+Xpi[p,j]=4}:
2 *
p_cycle_usage[p]>=pij_cycle_usage[p,i,j]+pij_cycle_usage[p,j,i];

subject to dual_failure_restorability1{i in SPANS, j in
SPANS:j<>i}:restorability2_1[i,j]=(z1[i,j]+z2[i,j]+(sum{p in
PCYCLES:Xpi[p,i]+Xpi[p,j]>=}pij_cycle_usage[p,i,j]))/Work[i];

subject to dual_failure_restorability2{i in SPANS, j in
```

```
SPANS:j<>i}:restorability2_1[i,j]=>R2Limit;
```

C.3 Path Restoration Model

File name: "path-SC*P*-R2_v1. mod".

```
# Specified dual failure restorability model for path restorable
# networks with spare capacity placement only.

# SETS

set SPANS ordered;
set SPAN_PAIRS ={i in SPANS,j in SPANS:i<>j and ord(i) < ord(j)};
set DEMAND_PAIRS;
param span{SPANS}symbolic;
param Cost{j in SPANS};
param DemUnits{r in DEMAND_PAIRS}default 0;

# OTHER SETS AND PARAMETERS

set WORK_ROUTES{r in DEMAND_PAIRS};
set WORK_ROUTE_VECTORS{r in DEMAND_PAIRS, p in
WORK_ROUTES[r]}within {j in SPANS};
param Work_Route_Vectors{r in DEMAND_PAIRS, p in WORK_ROUTES[r], j
in WORK_ROUTE_VECTORS[r,p]}symbolic;
param WorkingPerRoute{r in DEMAND_PAIRS, q in
WORK_ROUTES[r]}default 0;
set DEMANDS_AFFECTED{i in SPANS}
:={r in DEMAND_PAIRS :exists {p in WORK_ROUTES[r], j in
WORK_ROUTE_VECTORS[r,p]}Work_Route_Vectors[r,p,j]=span[i] };
set DEMANDS_AFFECTED2{(i,j) in SPAN_PAIRS}
:={r in DEMAND_PAIRS:exists{p in WORK_ROUTES[r],k in
WORK_ROUTE_VECTORS[r,p]} (Work_Route_Vectors[r,p,k]=span[i] or
Work_Route_Vectors[r,p,k]=span[j])};
set DEMANDS_NOT_AFFECTED2{(i,j) in SPAN_PAIRS}
:=DEMAND_PAIRS diff DEMANDS_AFFECTED2[i,j];
set WORK_ROUTES_AFFECTED{i in SPANS, r in DEMANDS_AFFECTED[i]}
:={p in WORK_ROUTES[r]:exists {j in WORK_ROUTE_VECTORS[r,p]}
Work_Route_Vectors[r,p,j]=span[i]};
set WORK_ROUTES_AFFECTED2{(i,j) in SPAN_PAIRS,r in
DEMANDS_AFFECTED2[i,j]}:={p in WORK_ROUTES[r]:exists{k in
WORK_ROUTE_VECTORS[r,p]}(Work_Route_Vectors[r,p,k]=span[i] or
Work_Route_Vectors[r,p,k]=span[j])};
set WORK_ROUTES_NOT_AFFECTED2{(i,j) in SPAN_PAIRS, r in
DEMANDS_NOT_AFFECTED2[i,j]}:={p in WORK_ROUTES[r]};
param work{j in SPANS}:=sum{r in DEMANDS_AFFECTED[j],q in
WORK_ROUTES_AFFECTED[j,r]}WorkingPerRoute[r,q];
param TotalWorkCost:=sum{j in SPANS}work[j]*Cost[j];
param Stub_release {i in SPANS, r in DEMANDS_AFFECTED[i], j in
SPANS:span[i]<>span[j]} :=sum {p in
WORK_ROUTES_AFFECTED[i,r]:exists {k in
WORK_ROUTE_VECTORS[r,p]}Work_Route_Vectors[r,p,k]=span[j]}
DemUnits[r]/card{WORK_ROUTES[r]}*card{WORK_ROUTES_AFFECTED[i,r]:exi
sts{k in WORK_ROUTE_VECTORS[r,p]}
Work_Route_Vectors[r,p,k]=span[j]};
```

```
param Stub_release2{(i,j) in SPAN_PAIRS, r in
DEMANDS_AFFECTED2[i,j], k in SPANS:j<>k and i<>k}
:=sum{p in WORK_ROUTES_AFFECTED2[i,j,r]:exists {l in
WORK_ROUTE_VECTORS[r,p]}Work_Route_Vectors[r,p,l]=span[k]}
DemUnits[r] / card{WORK_ROUTES[r]}*
card{WORK_ROUTES_AFFECTED2[i,j,r]:exists {l in
WORK_ROUTE_VECTORS[r,p]}Work_Route_Vectors[r,p,l]=span[k]};

# ELIGIBLE ROUTES FOR PATH-LEVEL RESTORATION OF O-D PAIRS

set REST_ROUTES{r in DEMAND_PAIRS};
set REST_ROUTE_VECTORS{r in DEMAND_PAIRS, p in
REST_ROUTES[r]}within {j in SPANS};
param Rest_Route_Vectors{r in DEMAND_PAIRS, p in REST_ROUTES[r], j
in REST_ROUTE_VECTORS[r,p]}symbolic;

# VARIABLES
var rest_flow {i in SPANS, r in DEMANDS_AFFECTED[i], p in
REST_ROUTES[r], q in WORK_ROUTES_AFFECTED[i,r]}>=0 integer,
<=10000;
var rest_flow2{(i,j) in SPAN_PAIRS, r in DEMANDS_AFFECTED2[i,j],q
in WORK_ROUTES_AFFECTED2[i,j,r],p in REST_ROUTES[r]}>=0
integer,<=10000;
var spare{i in SPANS}>=0, <=10000 integer;
var R2_Demands_affected{(i,j) in SPAN_PAIRS,r in
DEMANDS_AFFECTED2[i,j]}>=0, <=1.0000;
var R2_Demands_not_affected{(i,j) in SPAN_PAIRS,r in
DEMANDS_NOT_AFFECTED2[i,j]}>=0, <=1.0000;
var ave_redundancy>=0, <=100000;
param R2Limit;

# OBJECTIVE FUNCTION

minimize TotalCost:sum{i in SPANS}(work[i]+ spare[i])* Cost[i];

# CONSTRAINTS
subject to single_failure_restorability{i in SPANS, r in
DEMANDS_AFFECTED[i], q in WORK_ROUTES_AFFECTED[i,r]}:
sum{p in REST_ROUTES[r]:forall {j in
REST_ROUTE_VECTORS[r,p]}Rest_Route_Vectors[r,p,j]<>span[i]}
rest_flow[i,r,p,q]=WorkingPerRoute[r,q];

subject to spare_capacity_for_single_failure{i in SPANS, j in
SPANS:span[i]<>span[j]}:
spare[j]>=sum {r in DEMANDS_AFFECTED[i], p in REST_ROUTES[r], q in
WORK_ROUTES_AFFECTED[i,r]:
exists {k in
REST_ROUTE_VECTORS[r,p]}Rest_Route_Vectors[r,p,k]=span[j]}rest_flow
[i,r,p,q] -sum {r in DEMANDS_AFFECTED[i]}Stub_release[i,r,j];

subject to spare_capacity_for_dual_failure{(i,j) in SPAN_PAIRS, k
in SPANS:j<>k and i<>k}:spare[k]>=sum{r in DEMANDS_AFFECTED2[i,j],
q in WORK_ROUTES_AFFECTED2[i,j,r], p in REST_ROUTES[r]:forall{l in
REST_ROUTE_VECTORS[r,p], m in
REST_ROUTE_VECTORS[r,p]:m<>l}Rest_Route_Vectors[r,p,l]<>span[i] and
Rest_Route_Vectors[r,p,m]<>span[j] and (exists{n in
REST_ROUTE_VECTORS[r,p]}Rest_Route_Vectors[r,p,n]=span[k])}rest_flo
```

```
w2[i,j,r,q,p] -sum {r in
DEMANDS_AFFECTED2[i,j]}Stub_release2[i,j,r,k];

subject to dual_failure_restorability{(i,j) in SPAN_PAIRS,r in
DEMANDS_AFFECTED2[i,j]}:R2_Demands_affected[i,j,r]<=(sum{q in
WORK_ROUTES_AFFECTED2[i,j,r],p in REST_ROUTES[r]:forall{k in
REST_ROUTE_VECTORS[r,p],l in REST_ROUTE_VECTORS[r,p]:k<>l}
Rest_Route_Vectors[r,p,k]<>span[i] and
Rest_Route_Vectors[r,p,l]<>span[j]}rest_flow2[i,j,r,q,p])/DemUnits[
r];

subject to dual_failure_restorability2{(i,j) in SPAN_PAIRS,r in
DEMANDS_NOT_AFFECTED2[i,j]}:R2_Demands_not_affected[i,j,r]=1;

subject to dual_failure_restorability_limit{(i,j) in SPAN_PAIRS,r
in DEMANDS_AFFECTED2[i,j]}:R2_Demands_affected[i,j,r]>=R2Limit;
```

C.4 DSP Model

File name: "DSP-SC*P*-R2_v1. mod".

```
# Specified dual failure restorability model for DSP restorable
# networks with spare capacity placement only.

# SETS DECLARATION
set SPANS;
set DEMANDS;
set ELIGIBLE_ROUTES{r in DEMANDS};

# PARAMETERS DECLARATION

param Cost{j in SPANS};
param ZetaWorkRoute{i in SPANS,r in DEMANDS,q in
ELIGIBLE_ROUTES[r]}default 0;
param DemandUnits{r in DEMANDS}default 0;
param span{i in SPANS}symbolic:=i;
param R2Limit;
set ELIGIBLE_ROUTE_VECTORS{r in DEMANDS,q in
ELIGIBLE_ROUTES[r]}:={i in SPANS:ZetaWorkRoute[i,r,q]=1};
param RouteCost{r in DEMANDS, q in ELIGIBLE_ROUTES[r]}:=sum{i in
ELIGIBLE_ROUTE_VECTORS[r,q]}Cost[i];
param Eligible_Route_Vectors{r in DEMANDS, p in ELIGIBLE_ROUTES[r],
j in ELIGIBLE_ROUTE_VECTORS[r,p]}symbolic:=span[j];

# VARIABLES DECLARATION

var alpharoute{r in DEMANDS, q in ELIGIBLE_ROUTES[r]}>=0, <=1
integer;
var betaroute{r in DEMANDS, q in ELIGIBLE_ROUTES[r]}>=0, <=1
integer;
var work_flow{r in DEMANDS, q in ELIGIBLE_ROUTES[r]}>=0,
<=DemandUnits[r] integer;
var rest_flow{r in DEMANDS, q in ELIGIBLE_ROUTES[r]}>=0,
<=DemandUnits[r] integer;
```

```
var backup_flow {r in DEMANDS}>=0, <=2*DemandUnits[r] integer;
var restorability2{r in DEMANDS,i in SPANS, j in SPANS:i<>j}>=0,
<=1.0000;

# OBJECTIVE FUNCTION

minimize TotalCost:sum{r in DEMANDS, q in
ELIGIBLE_ROUTES[r]}RouteCost[r,q]* (work_flow[r,q]+rest_flow[r,q]);

# CONSTRAINTS

subject to aroute_disjointness{r in DEMANDS,i in SPANS}:
sum{q in ELIGIBLE_ROUTES[r]}(alpharoute[r,q]+
betaroute[r,q])*ZetaWorkRoute[i,r,q]<=1;

subject to max_two_backup_route{r in DEMANDS}:
sum{q in ELIGIBLE_ROUTES[r]}betaroute[r,q]<=2;

subject to demands_met{r in DEMANDS}:
sum{q in ELIGIBLE_ROUTES[r]}work_flow[r,q]=DemandUnits[r];

subject to working_capacity_assignment{r in DEMANDS,q in
ELIGIBLE_ROUTES[r]}:
work_flow[r,q]<=alpharoute[r,q] * DemandUnits[r];

subject to backup_capacity_assignment{r in DEMANDS,q in
ELIGIBLE_ROUTES[r]}:
rest_flow[r,q]<=betaroute[r,q] * DemandUnits[r];

subject to sufficient_backup_for_working_capacity{r in DEMANDS,q in
ELIGIBLE_ROUTES[r]}:
backup_flow[r]>=work_flow[r,q];

subject to sum_restroutes_for_backup_capacity{r in
DEMANDS}:backup_flow[r]<=sum{q in
ELIGIBLE_ROUTES[r]}rest_flow[r,q];

subject to R2_failure_restorability{r in DEMANDS,i in SPANS,j in
SPANS:i<>j}:
restorability2[r,i,j]<=(sum{p in ELIGIBLE_ROUTES[r]:forall{k in
ELIGIBLE_ROUTE_VECTORS[r,p]}(Eligible_Route_Vectors[r,p,k]<>span[i]
)
and(Eligible_Route_Vectors[r,p,k]<>span[j])}(rest_flow[r,p]+work_fl
ow[r,p]))/DemandUnits[r];

subject to average_restorability{r in DEMANDS,i in SPANS,j in
SPANS:i<>j}:restorability2[r,i,j]>=R2Limit;
```

APPENDIX D

NETWORK CHARTS

D.1 Span Restoration Charts

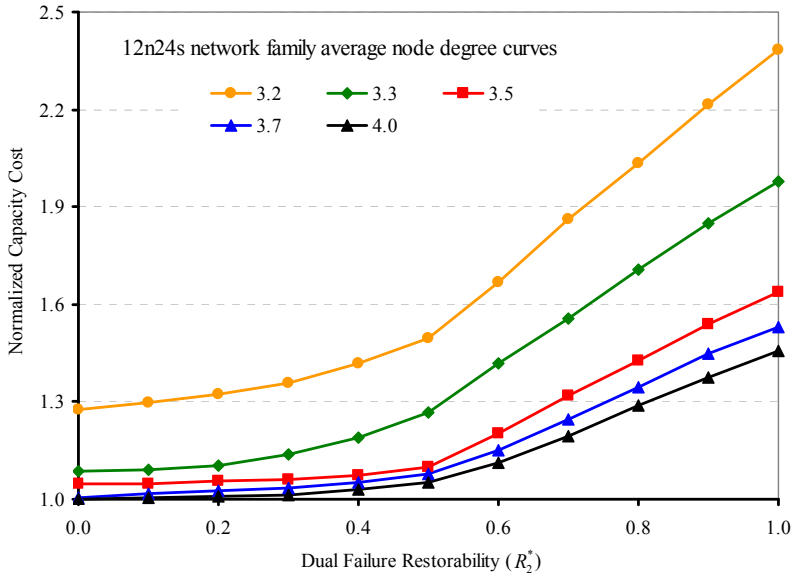

Appendix D.1-Figure 1: Dual failure restorability curves in model 1 of 12n24s span restorable network family.

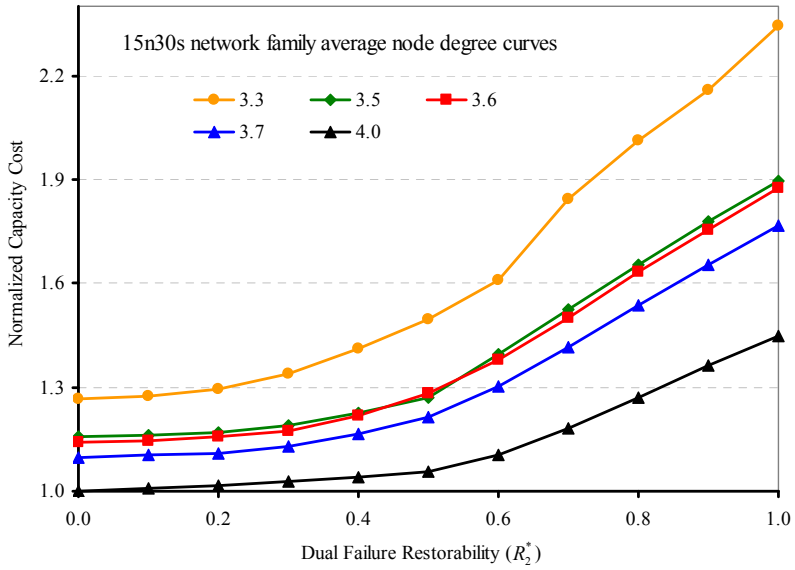

Appendix D.1-Figure 2: Dual failure restorability curves in model 1 of 15n30s span restorable network family.

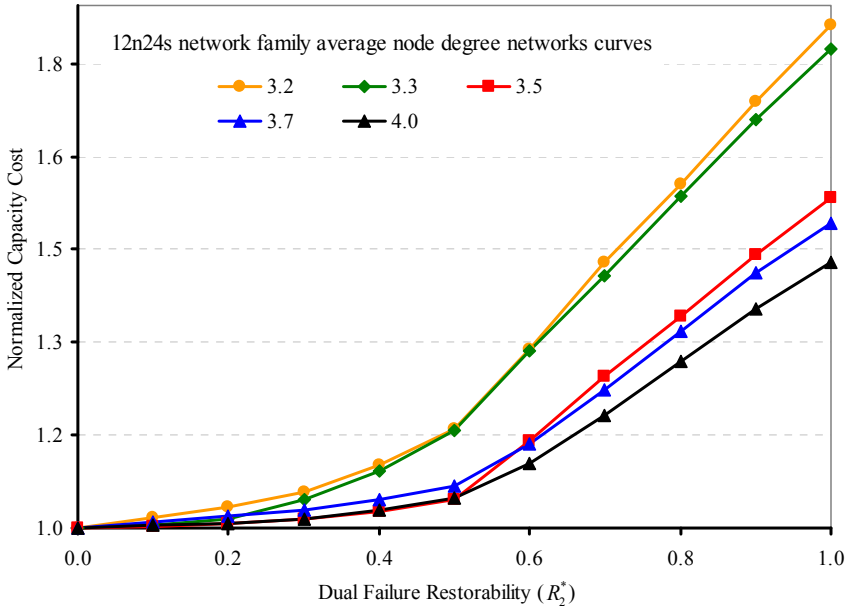

Appendix D.1-Figure 3: Rate of capacity cost increase in 12n24s span restorable network family over specified dual failure restorability limits in model 1.

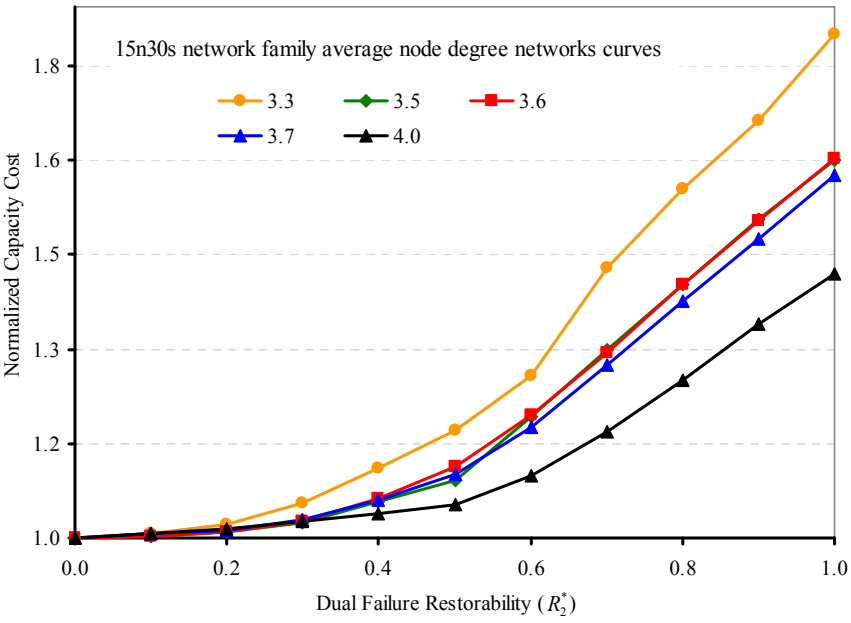

Appendix D.1-Figure 4: Rate of capacity cost increase in 15n30s span restorable network family over specified dual failure restorability limits in model 1.

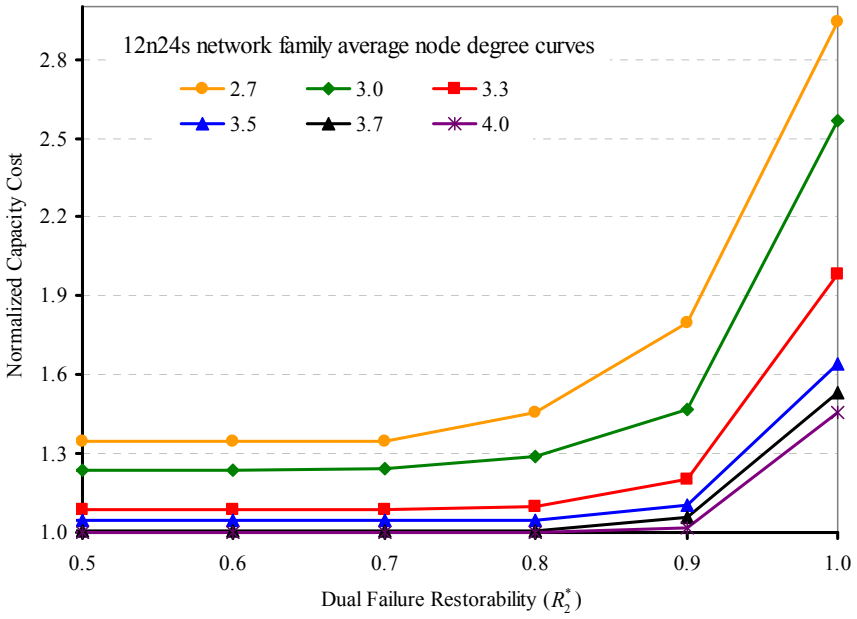

Appendix D.1-Figure 5: Dual failure restorability curves in model 2 of 12n24s span restorable network family.

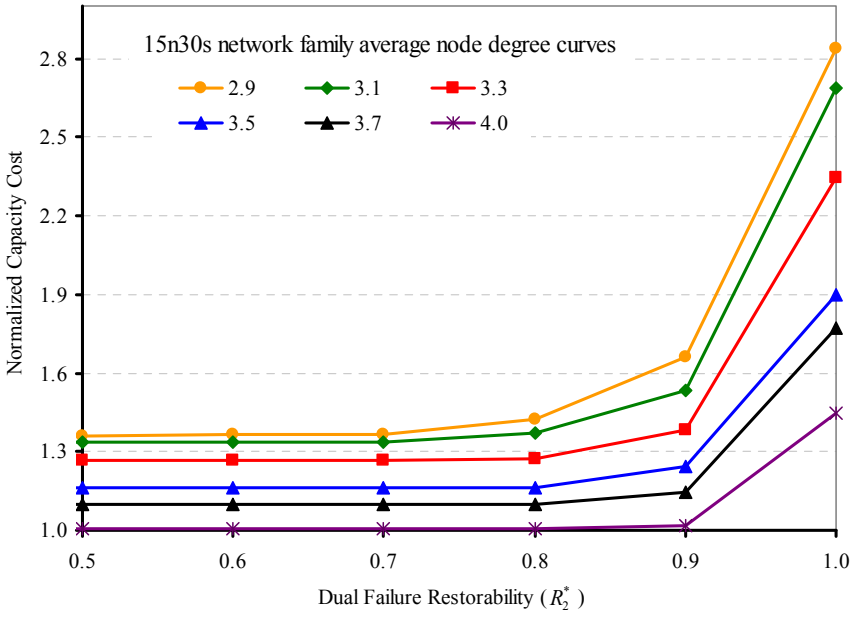

Appendix D.1-Figure 6: Dual failure restorability curves in model 2 of 15n30s span restorable network family.

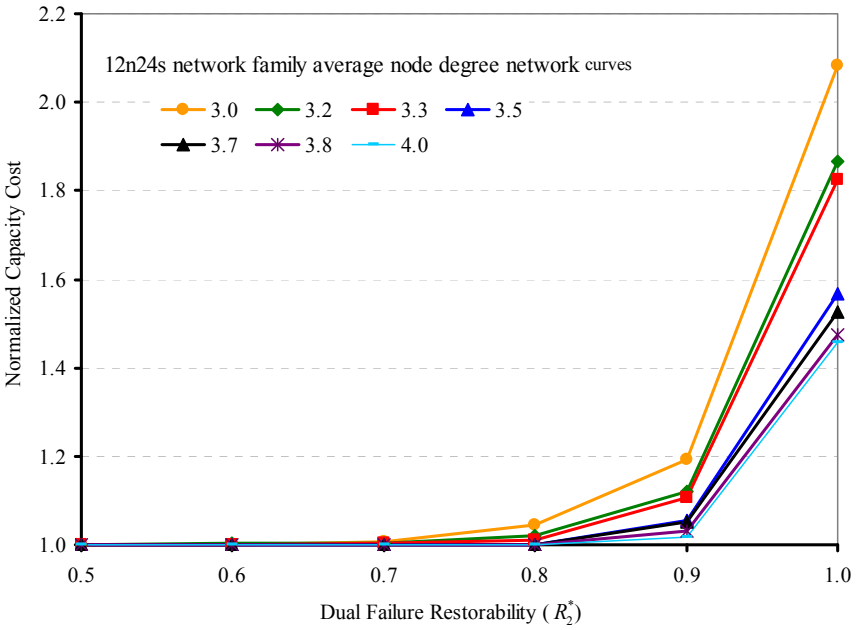

Appendix D.1-Figure 7: Rate of capacity cost increase in 12n24s span restorable network family over specified dual failure restorability limits in model 2.

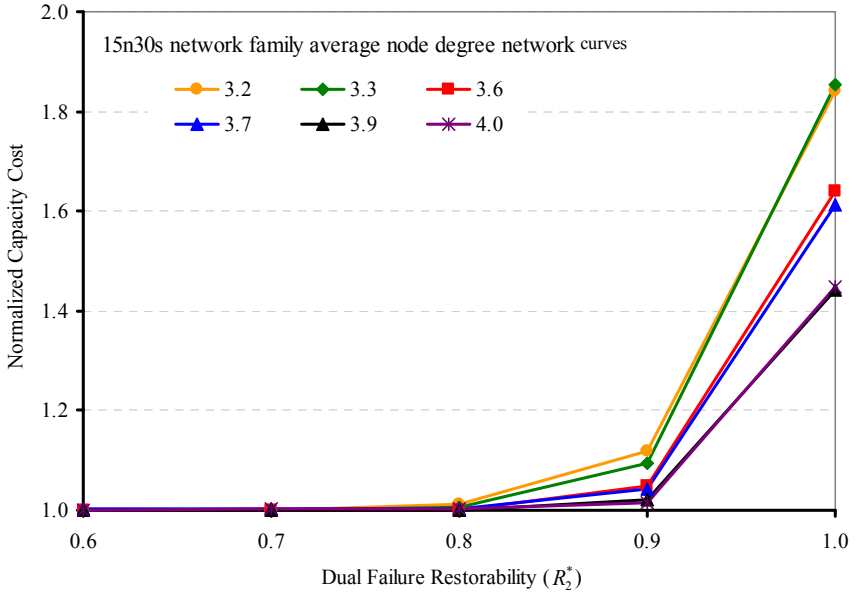

Appendix D.1-Figure 8: Rate of capacity cost increase in 15n30s span restorable network family over specified dual failure restorability limits in model 2.

D.2 *p*-Cycle Restoration

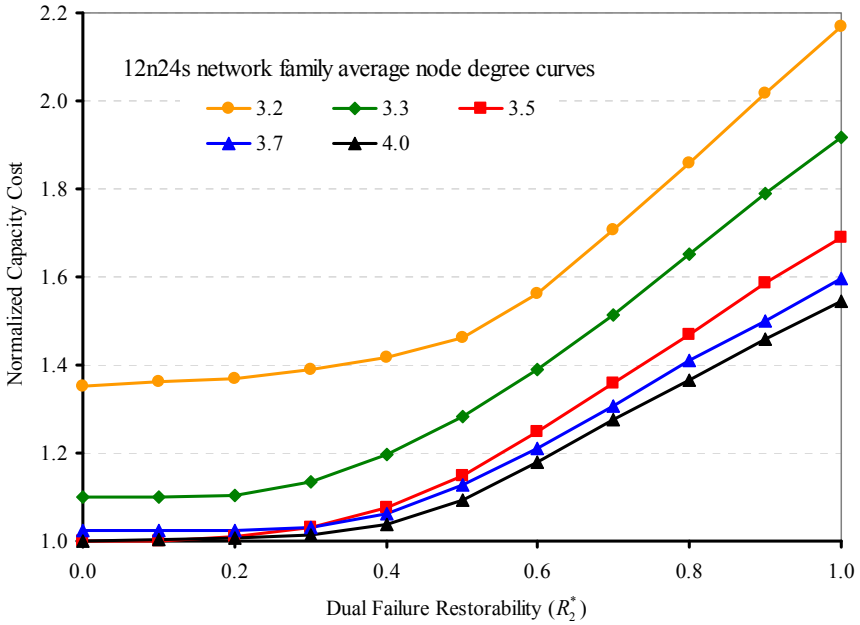

Appendix D.2-Figure 1: Dual failure restorability curves in model 1 of 12n24s *p*-cycle restorable network family.

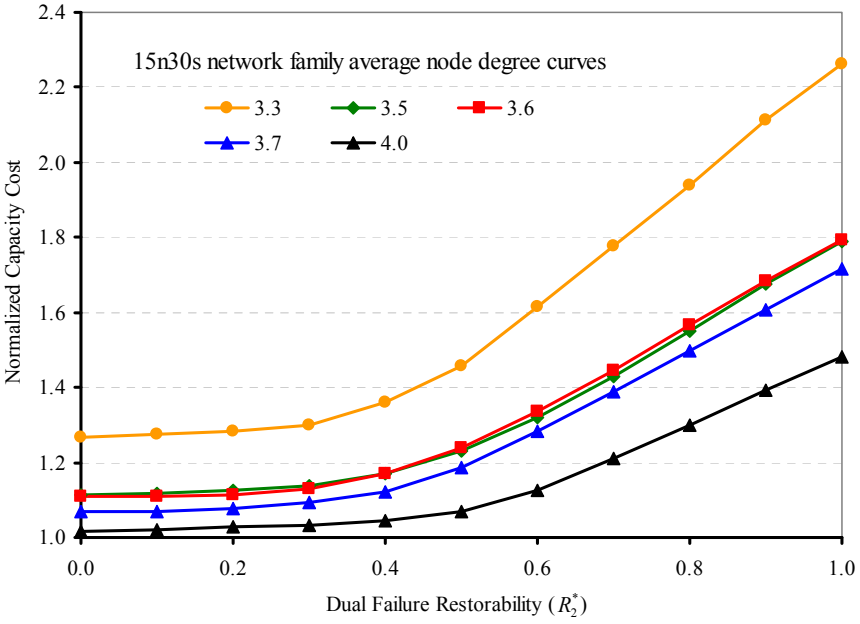

Appendix D.2-Figure 2: Dual failure restorability curves in model 1 of 15n30s p-cycle restorable network family.

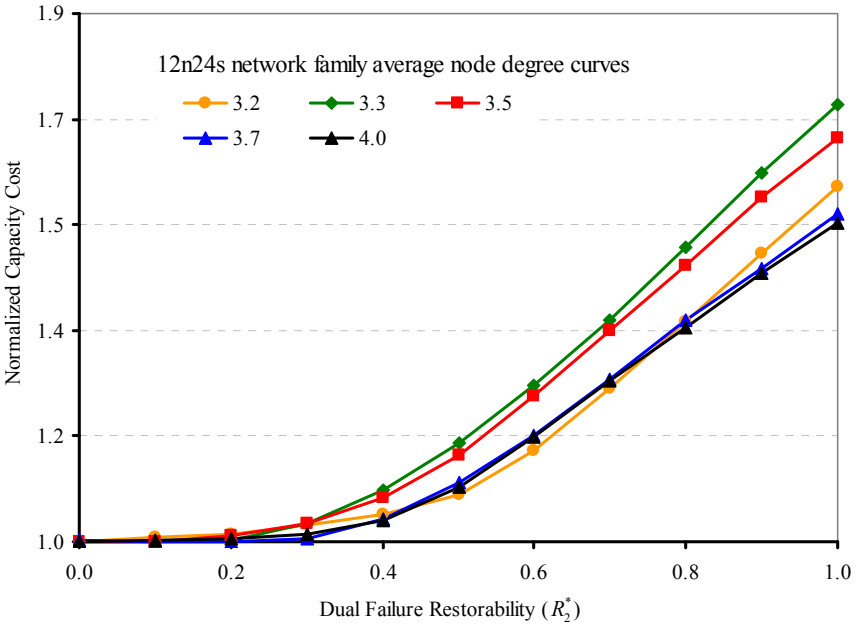

Appendix D.2-Figure 3: Rate of capacity cost increase in 12n24s p-cycle restorable network family over specified dual failure restorability limits in model 1.

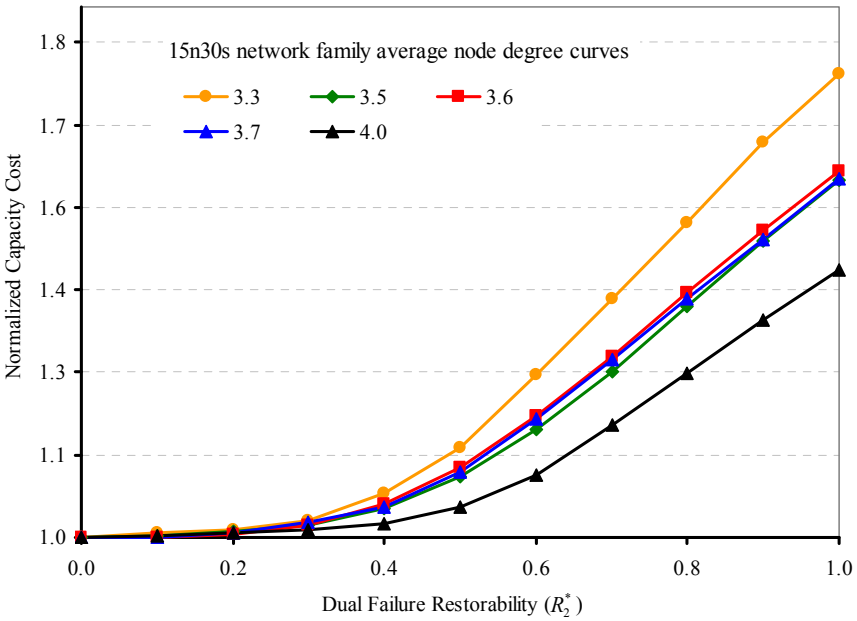

Appendix D.2-Figure 4: Rate of capacity cost increase in 15n30s p-cycle restorable network family over specified dual failure restorability limits in model 1.

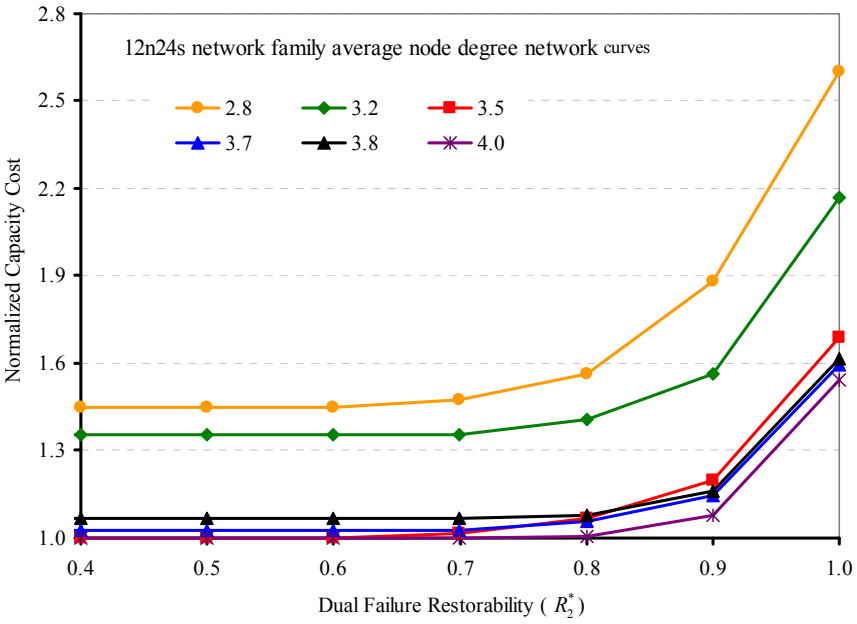

Appendix D.2-Figure 5: Dual failure restorability curves in model 2 of 12n24s *p*-cycle restorable network family.

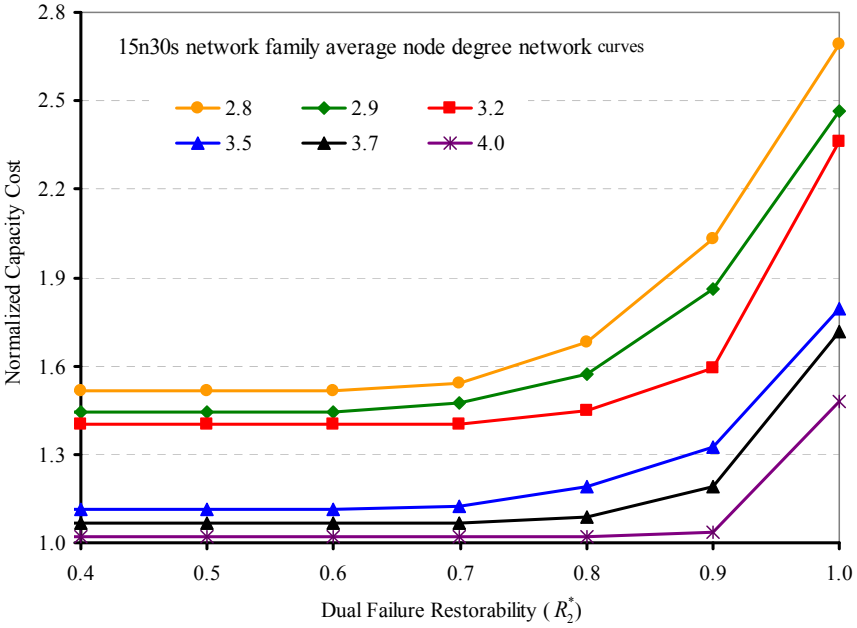

Appendix D.2-Figure 6: Dual failure restorability curves in model 2 of 15n30s *p*-cycle restorable network family.

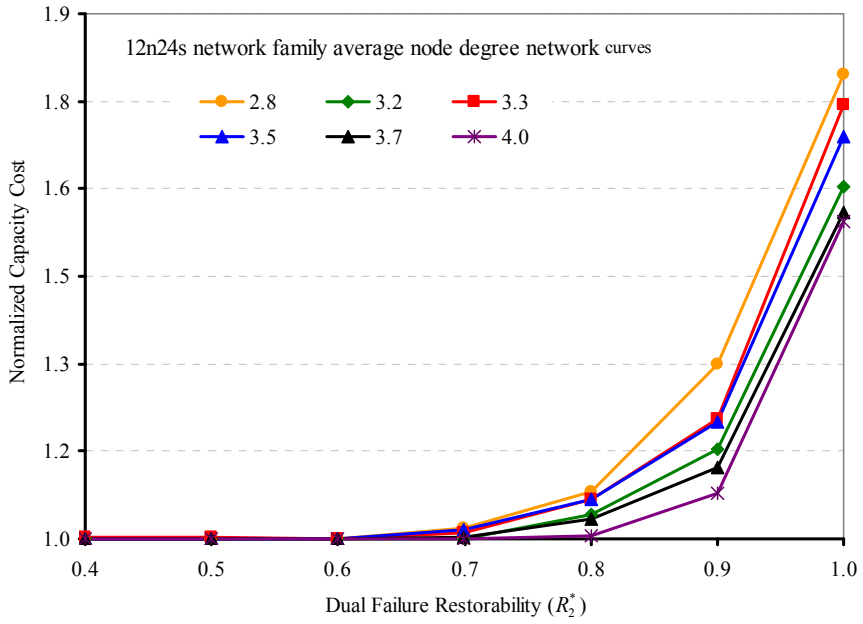

Appendix D.2-Figure 7: Rate of capacity cost increase in 12n24s *p*-cycle restorable network family over specified dual failure restorability limits in model 2.

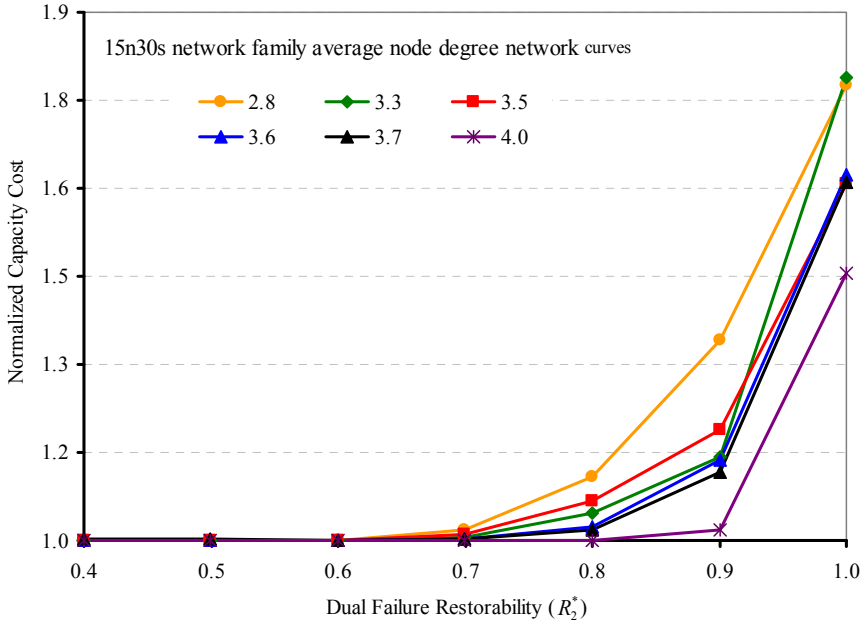

Appendix D.2-Figure 8: Rate of capacity cost increase in 15n30s *p*-cycle restorable network family over specified dual failure restorability limits in model 2.

D.3 Path Restoration

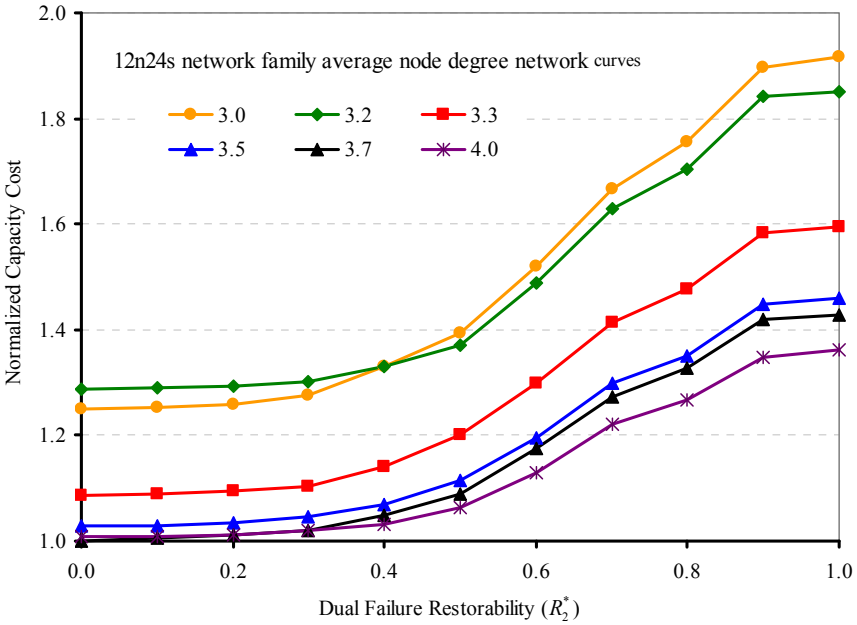

Appendix D.3-Figure 1: Dual failure restorability curves in model 1 of 12n24s path restorable network family.

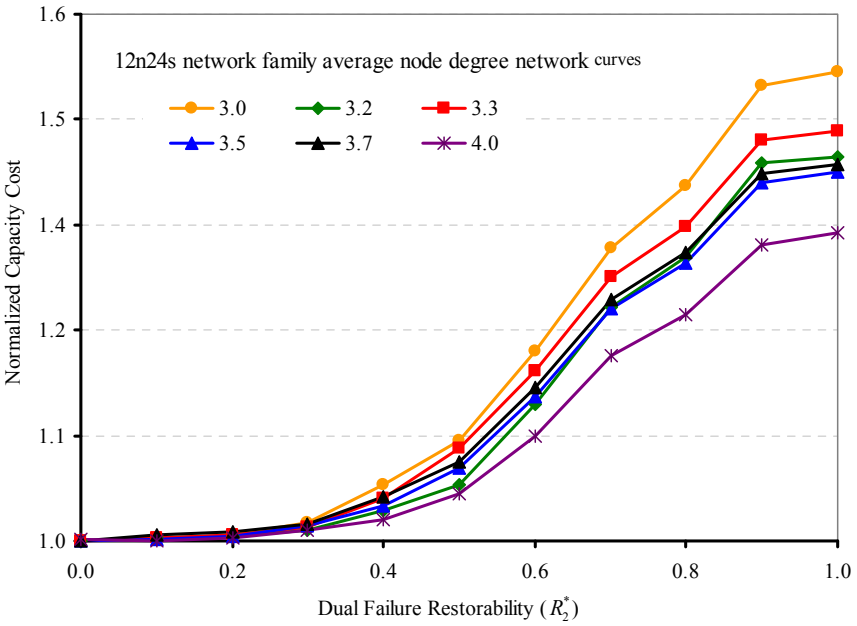

Appendix D.3-Figure 2: Rate of capacity cost increase in 12n24s path restorable network family over specified dual failure restorability limits in model 1.

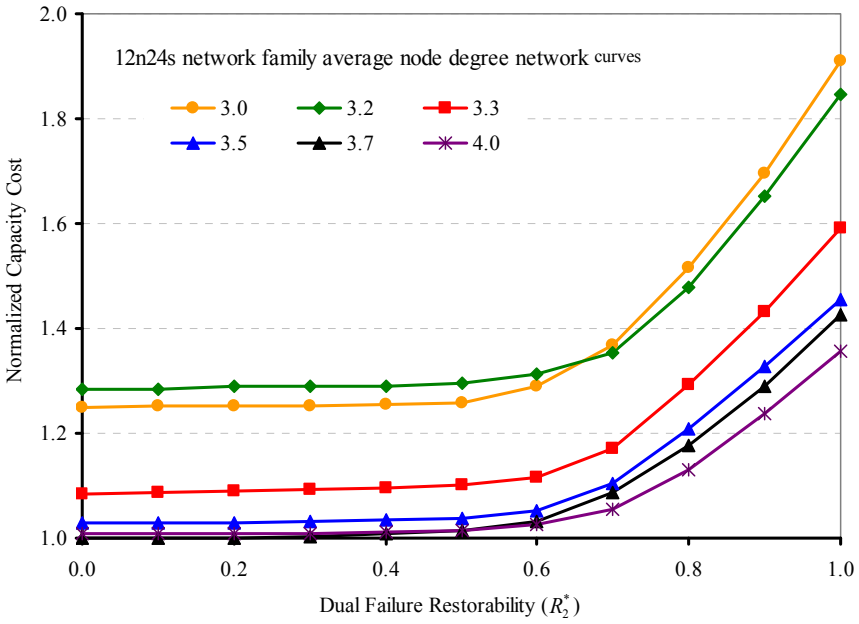

Appendix D.3-Figure 3: Dual failure restorability curves in model 2 of 12n24s path restorable network family.

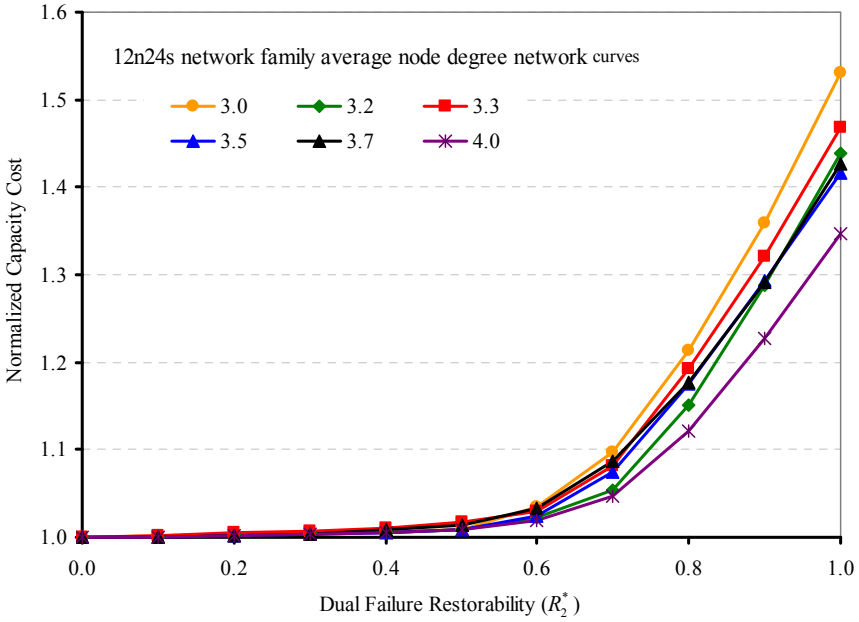

Appendix D.3-Figure 4: Rate of capacity cost increase in 12n24s path restorable network family over specified dual failure restorability limits in model 2.

D.4 Demand-Wise Shared Protection

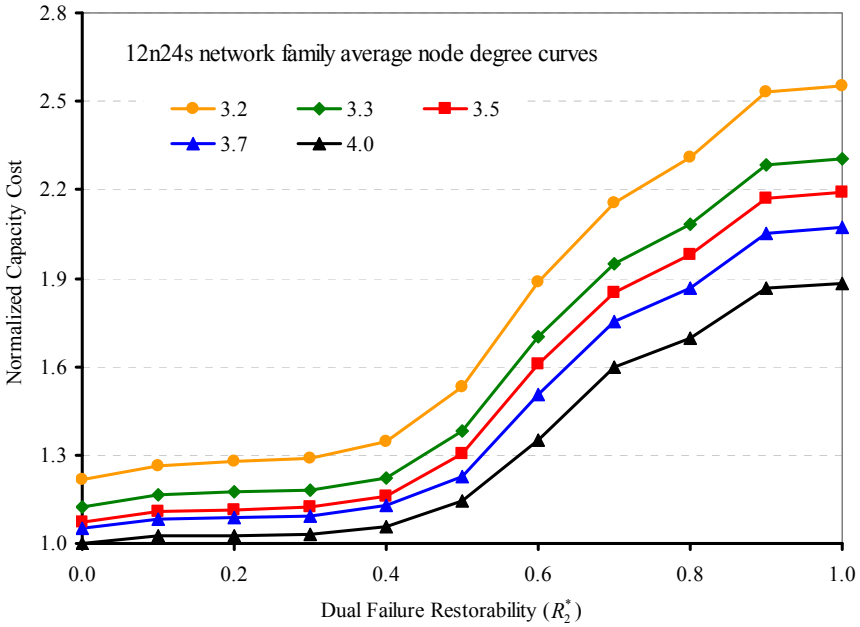

Appendix D.4-Figure 1: Dual failure restorability curves in model 1 of 12n24s DSP restorable network family.

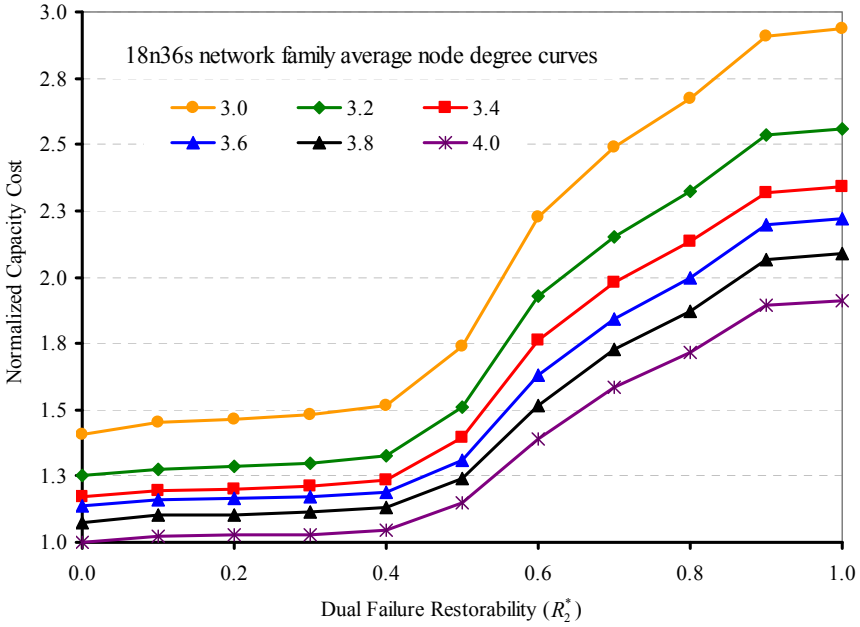

Appendix D.4-Figure 2: Dual failure restorability curves in model 1 of 18n36s DSP restorable network family.

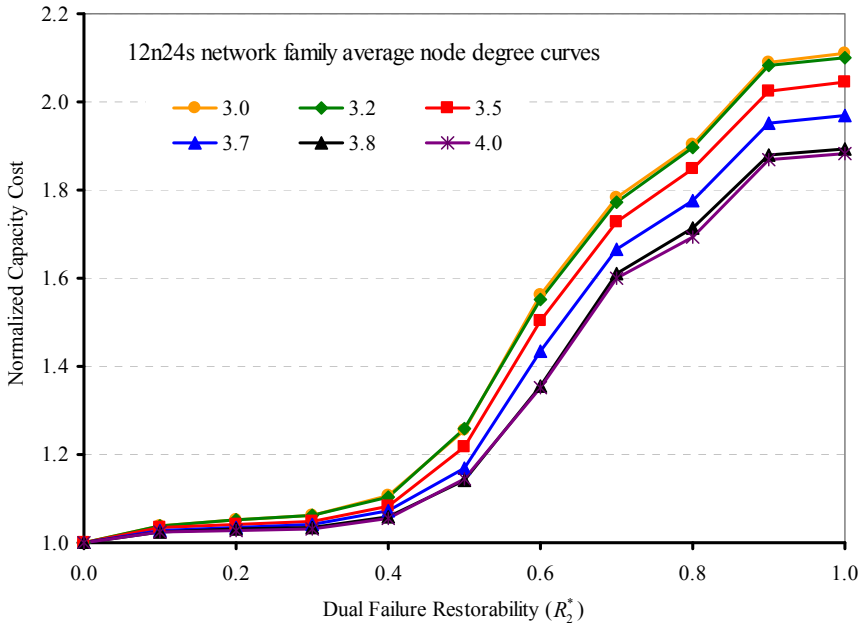

Appendix D.4-Figure 3: Rate of capacity cost increase in 12n24s DSP restorable network family over specified dual failure restorability limits in model 1.

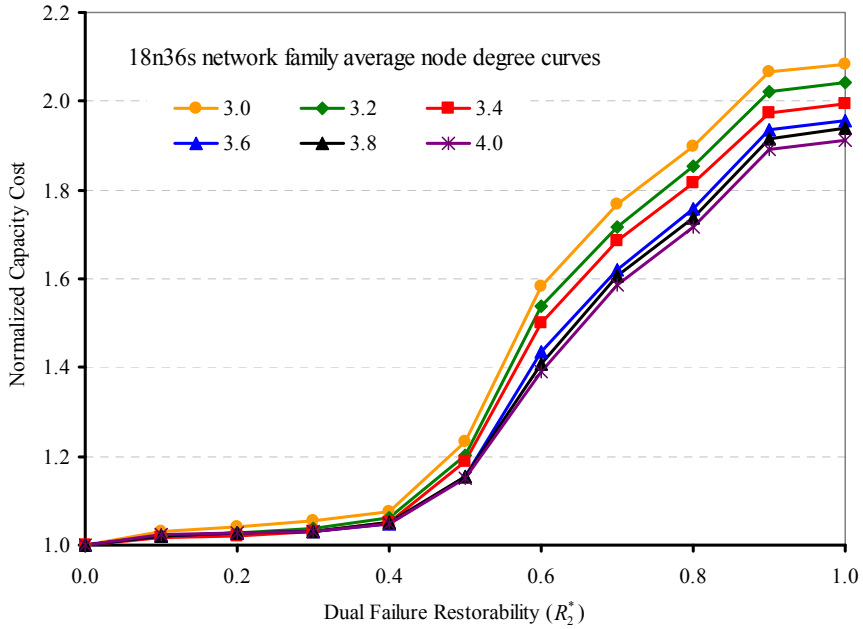

Appendix D.4-Figure 4: Rate of capacity cost increase in 18n36s DSP restorable network family over specified dual failure restorability limits in model 1.

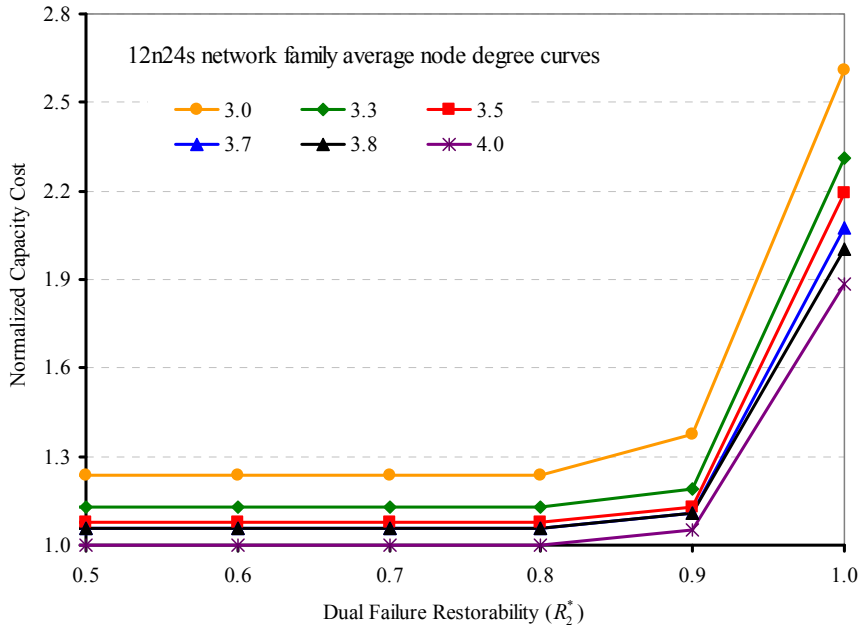

Appendix D.4-Figure 5: Dual failure restorability curves in model 2 of 12n24s DSP restorable network family.

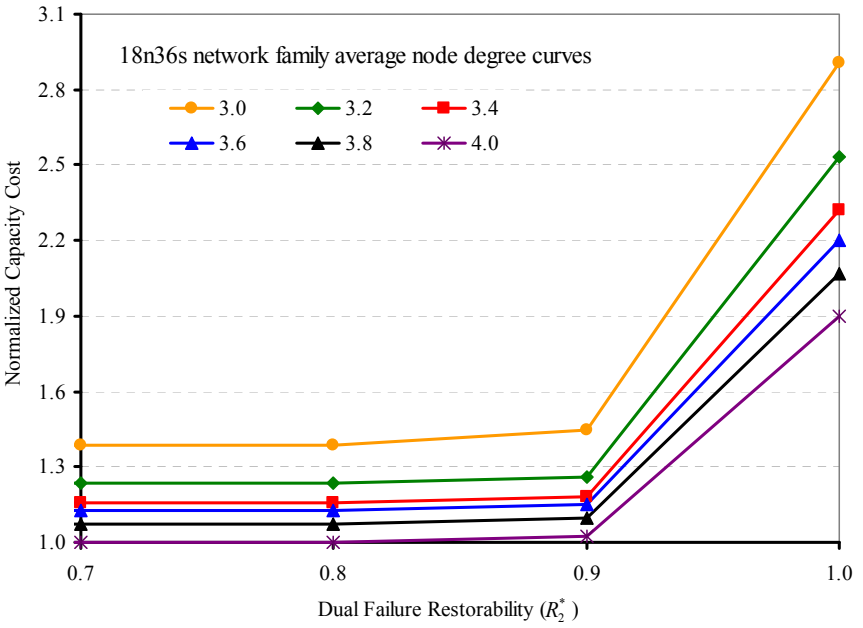

Appendix D.4-Figure 6: Dual failure restorability curves in model 2 of 18n36s DSP restorable network family.

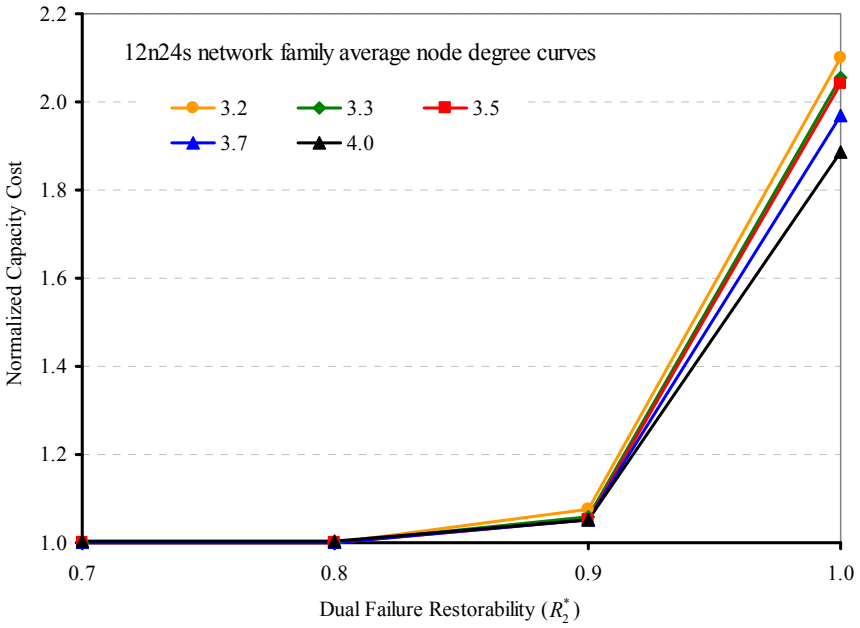

Appendix D.4-Figure 7: Rate of capacity cost increase in 12n24s DSP restorable network family over specified dual failure restorability limits in model 2.

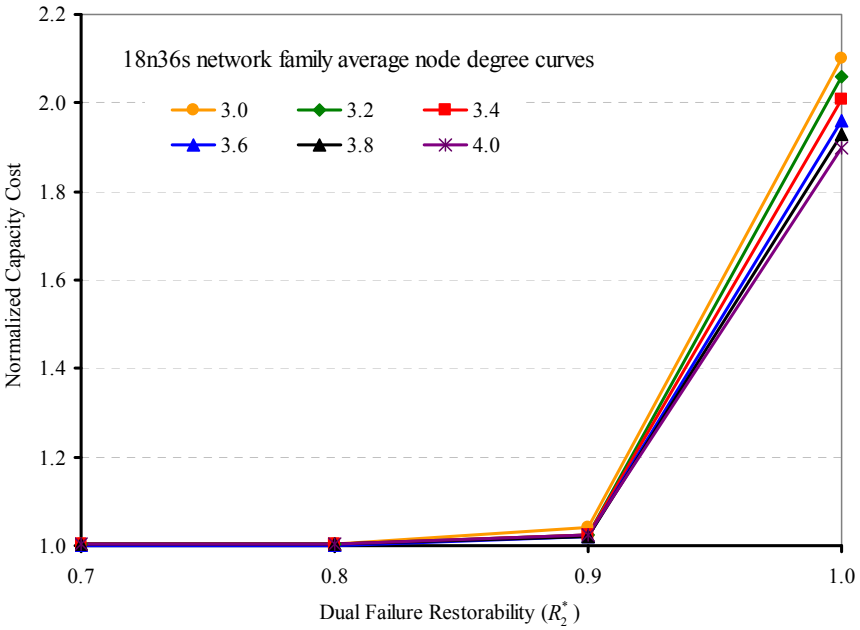

Appendix D.4-Figure 8: Rate of capacity cost increase in 18n36s DSP restorable network family over specified dual failure restorability limits in model 2.